Intercollegiate Faculty of Biotechnology
University of Gdansk and Medical University of Gdansk

PhD thesis

MPharm Katarzyna Dziubek

Dissecting the mechanism and functional landscape of cancer PD1 signalling in osteosarcoma.

Analiza mechanizmu sygnalizacji oraz funkcji receptora PD1 w kostniakomięsaku.

PhD advisor: Prof. Theodore Hupp
PhD assistant advisors: Dr Sachin Kote, Dr Maciej Parys

Thesis submitted to the Board of the Discipline of Biotechnology
of the University of Gdansk in order to be awarded a doctoral degree
in the field of exact and natural sciences in the discipline of biotechnology.
GDANSK 2024

THE UNIVERSITY of EDINBURGH

Funding

This research was funded by the International Research Agenda's Program of the Foundation for Polish Science (MAB/2017/03) and supported by the PRELUDIUM research grant (2022/45/N/NZ1/02699) awarded by the National Science Centre. The generous FNP support also enabled active participation in AACR conference (Atlanta, 2019), while the Mobility Grant awarded by the Polonium Foundation enabled my attendance in Science: Polish Perspectives interdisciplinary scientific meetings in Cambridge (2019) and Oxford (2022). The latter was additionally supported by the UG Doctoral Student Council. The author would also like to acknowledge the National Agency for Academic Exchange (NAWA) for awarding the PROM mobility grant for a research stay at The Roslin Institute (University of Edinburgh, UK). The close collaboration with the institute laid the foundation for the PRELUDIUM project funded by NCN. This project focuses on a comparative study regarding the significance of PD1-intrinsic signalling in human and canine osteosarcoma and serves as a continuation of the presented work.

NARODOWE CENTRUM NAUKI

Abstract

Cancer treatment was revolutionised by immune checkpoint inhibitors (ICIs) targeting the PD1/PDL1 axis, which acts as a brake to the immune system. Despite therapeutic success, some patients do not respond to therapy or rapidly deteriorate due to an unclear mechanism. As reported for several types of tumours, PD1 receptor is not solely expressed on immune cells but also on cancer cells. Moreover, depending on the tumour type, it may act either as a promoter or tumour suppressor and was implicated as a mechanism of resistance to ICIs. The limited response to ICIs was as well reported in osteosarcoma. This study aimed to determine if cancer-PD1 may account for the limited response of osteosarcoma to ICIs and to characterize the functional role of PD1 protein and its interactions in osteosarcoma cells.

Our results demonstrated both surface and intracellular expression of PD1 protein in U2OS osteosarcoma cells. Strikingly, *PDCD1* gene silencing significantly increased cell migration and viability. LC-MS/MS based proteomic analysis revealed that PD1 alterations markedly affected the proteomic landscape of U2OS cells. Large-scale data interpretation tools GO and GSEA strongly indicated that *PDCD1* silencing leads to enrichment of proteins involved in processes such as cell growth, migration, and motility, corresponding to the cellular effects we initially observed. STRING interactome analysis of the most affected proteins revealed they role in mTORC1 signalling, cell and focal adhesion, and increased metastatic potential, implying that cancer-PD1 in osteosarcoma may act as a tumour suppressor.

While PD1 signalling pathway was well characterized in T cells, contradictory results are available regarding its role in cancer, and little is known about cancer-PD1 interactome. Our in-depth PD1 interactome studies performed with LC-MS/MS based proteomics, identified AXL (receptor tyrosine kinase UFO) as a novel PD1 binding partner. The interaction between PD1 and AXL was confirmed with PLA and Western Blotting. Molecular docking studies, used to characterize the interaction, further confirmed protein binding, and indicated that it takes place in their intracellular domains. Aligning with our experimental data, PD1 mutations in tyrosine phosphorylation residues did not abrogate PD1 binding with AXL. However, the *in silico* analysis demonstrated that depending on the mutation, the protein complex was supported by distinct bonds, suggesting varying strength and affinity of the interaction.

In summary, our data report the previously undiscovered functional expression of PD1 protein by osteosarcoma cells and provide valuable insight into the landscape of PD1 downstream signalling. PD1 interactome studies identified a novel interaction between PD1 and AXL. Strikingly, previous reports demonstrated the improved response to PD1/PDL1 ICIs in combination with AXL inhibitors, therefore, our studies may shed new light on the underlying mechanism. However, further studies on cancer-intrinsic PD1 are urgently needed to understand its therapeutic significance to improve safety and efficacy of immunotherapy.

Streszczenie

Terapia nowotworów została zrewolucjonizowana przez inhibitory immunologicznych punktów kontrolnych skierowane przeciwko osi PD1/PDL1, pełniącej rolę hamulca dla układu immunologicznego. Pomimo sukcesu terapeutycznego, niektórzy pacjenci nie reagują na terapię lub ich stan szybko się pogarsza z powodu niezupełnie wiadomego mechanizmu. Badania przeprowadzone w różnych typach nowotworów wykazały, że ekspresja receptora PD1 nie jest obecna wyłącznie na komórkach odpornościowych, ale także na komórkach nowotworowych. Ponadto, w zależności od rodzaju nowotworu, PD1 może działać zarówno jako promotor, jak i supresor wzrostu nowotworu oraz może stanowić mechanizmem oporności na terapię PD1/PDL1. Ograniczona odpowiedź na inhibitory PD1/PDL1 została również zaobserwowana w kostniakomięsaku. Celem tych badań było ustalenie, czy nowotworowy receptor PD1 może być odpowiedzialny za ograniczoną skuteczność inhibitorów PD1/PDL1 w kostniakomięsaku oraz charakteryzacja funkcji PD1 i opisane jego interakcji z innymi białkami w komórkach kostniakomięsaka.

Nasze wyniki wykazały zarówno powierzchniową, jak i wewnątrzkomórkową ekspresję białka PD1 w komórkach U2OS kostniakomięsaka. Wyciszenie genu *PDCD1* znacząco zwiększyło migrację komórek i ich przeżywalność. Analiza proteomiczna techniką LC-MS/MS wykazała, że zmiany w ekspresji PD1 istotnie wpłynęły na proteom komórek U2OS. Narzędzia służące od interpretacji wielkoskalowych danych, GO i GSEA, jednoznacznie pokazały, że wyciszenie *PDCD1* prowadzi do wzrostu poziomu białek zaangażowanych we wzrost komórek, migrację oraz mobilność, co odpowiada efektom, które zaobserwowaliśmy w testach laboratoryjnych. Analiza oddziaływań białek, których poziom najbardziej uległ zmianie przy użyciu bazy danych STRING, wskazała na ich rolę w sygnalizacji mTORC1, adhezji komórkowej oraz przerzutach nowotworowych, sugerując, że nowotworowy PD1 w kostniakomięsaku może działać jako supresor wzrostu nowotworu.

Ścieżka sygnalizacji PD1 została dobrze scharakteryzowana w limfocytach T, jednak rola jaką pełni w nowotworach wciąż podlega dyskusji i nadal niewiele wiadomo o oddziaływaniach białkowych nowotworowego PD1. Badania interaktomu na szeroką skalę, jakie przeprowadziliśmy metodą LC-MS/MS zidentyfikowały dotychczas nieznaną interakcję między PD1 i AXL (receptor kinazy tyrozynowej UFO). Interakcja ta została potwierdzona metodami PLA i Western Blot. Dokowanie molekularne, użyte do scharakteryzowania interakcji, dodatkowo potwierdziło oddziaływanie białkowe i wykazało, że zachodzi ono w domenach wewnątrzkomórkowych obu białek. Zgodnie z naszymi danymi eksperymentalnymi, mutacje w resztach tyrozynowych PD1 podlegających fosforylacji nie przerwały wiązania PD1 z AXL. Jednak analiza *in silico* wykazała, że w zależności

od mutacji, kompleks białkowy podtrzymywany był przez inne typy wiązań, sugerując zróżnicowaną siłę i powinowactwo kompleksu.

Podsumowując, nasze badania opisują uprzednio nieznane funkcje białka PD1 przez komórki kostniakomięsaka oraz stanowią źródło informacji o szlaku sygnalizacji PD1 w komórkach nowotworowych. Ponadto, analiza odziaływań białkowych PD1 zidentyfikowała nową interakcję pomiędzy PD1 a AXL. W świetle badań naukowych i klinicznych, które wykazały lepszą odpowiedź na inhibitory PD1/PDL1 w połączeniu z inhibitorami AXL, nasze wyniki mogą rzucać nowe światło na leżący u podstaw tej odpowiedzi mechanizm. Niemniej jednak, dalsze prace nad znaczeniem nowotworowego receptora PD1 są niezbędne, aby zrozumieć jego znaczenie terapeutyczne i poprawić bezpieczeństwo i skuteczność immunoterapii.

Acknowledgements

I would like to express my sincere gratitude to those who have played key roles in the completion of this PhD thesis. They made it possible by offering expertise, support, and encouragement. For that, I am truly grateful.

I want to thank my supervisors. Prof. Ted Hupp for the inspiring idea behind this project, I am grateful for his visionary guidance. Despite my initial scepticism, it turned out to be my personal undertaking, which I would like to continue in the future.

I extend my thanks to Dr Maciej Parys, for his unlimited confidence in the potential of this project. Also, for his guidance, an easy-going attitude and addressing difficulties with constructive perspective.

I would like to thank my co-supervisor, Dr Sachin Kote, for offering support during the most critical moments of doubt and for his efforts to achieve the best outcome of this work.

My special thanks to Dr Jakub Faktor for dedicating numerous hours to plan, execute and analyse with me the mass spectrometry data. His openness to my ideas and theories has been invaluable, also for his insightful comments both during the experimental part and during the preparation of this work. This project would not have been possible without his expertise.

I want to thank our collaborator, Dr Kiran Bharat Lokhande, for performing the molecular modelling and molecular dynamics simulations. His work improved the quality of this study and will surely help with our future works on dissecting the importance of our discoveries.

I thank Prof. Natalia Marek-Trzonkowska, for supporting my scientific activities and her optimism and strong belief that I would one day make a significant discovery.

Also, to Ines Papak and Dr Elzbieta Chrusciel, for their expertise in flow cytometry.

I am truly grateful to my husband, Krzysztof Dziubek, whose unwavering support, understanding, and shared moments of both doubt and excitement have been a source of strength throughout this journey.

Also, to my parents, for fostering an environment that allowed me to pursue my career ambitions. Although they cannot witness this moment, I am confident they would have been immensely proud.

My sincere gratitude to my former mentors, Dr Courtney and Christopher Sansam, for providing me with the opportunity to undertake a traineeship in their laboratory at OMRF (Oklahoma City, USA; 2015-2016). Also, for their patience, gained knowledge and broadened horizons. The year I spent in Oklahoma City perhaps remains my biggest adventure thus far.

Not to mention Dr Mohamed Albed Alhnan, the supervisor of my Erasmus+ exchange at the University of Central Lancashire, (UK, 2013); for creating opportunities that have significantly contributed to my academic and professional growth. I still owe him a lot.

Moreover, I want to express my appreciation to Prof. Pawel Szymanski, for initiating my interest in research and encouraging me to engage in activities abroad.

Also, to Ms Alicja Jaros, my high school chemistry teacher, whose humour and positive attitude made the subject enjoyable and inspired my early interest in science.

Finally, I am grateful to Magdalena Pilch and Mikolaj Kocikowski for their support when the PhD student life was most challenging. I wish them both success at the next stages of their careers.

Table of contents

Abbreviations

4E-BP1	4E binding protein 1
ADAP	adhesion and degranulation-promoting adaptor protein
AKT1S1	proline-rich AKT1 substrate 1
ALCAM	activated leukocyte cell adhesion molecule
AP-1	activator protein 1
APC	antigen presenting cell
ATGL	adipose triglyceride lipase
AXL	tyrosine-protein kinase receptor UFO
Bcl-10	B-cell lymphoma/leukaemia 10
BLAST	Basic Local Alignment Search Tool
CAR-T	chimeric antigen receptor T-cell therapy
CD	cluster of differentiation
CDK2	cyclin-dependent kinase 2
c-Fos	proto-oncogene c-Fos
CPT1A	carnitine palmitoyltransferase 1A
CRAC	Calcium release-activated calcium channel protein 1
c-Rel	REL proto-oncogene
c-Src	cellular tyrosine kinase
CTGF	connective tissue growth factor
CTLA-4	cytotoxic T-lymphocyte associated protein 4
CTP1A	carnitine palmitoyltransferase 1A
CYR6	cysteine-rich angiogenic inducer 6
DAG	diacylglycerol
DAPI	4',6-diamidino-2-phenylindole
DCs	dendritic cells
DDA	data dependent acquisition
DIA	data independent acquisition
E2F	transcription factor E2F
ECD	extracellular domain
ECM	extracellular matrix
EGFR	epithelial growth factor receptor
eIF4E	eukaryotic translation initiation factor 4E
Elk	domain-containing protein Elk
EMT	epithelial to mesenchymal transition
ER	endoplasmic reticulum
ERK	extracellular signal-regulated kinases
EXC	extracellular domain
FAK	Focal adhesion kinase
FAs	focal adhesions
FAS	tumour necrosis factor receptor superfamily member 6
FBS	foetal bovine serum
FBXO38	F-box only protein 38
FDA	Food and Drug Administration
Fyn	tyrosine-protein kinase Fyn
Gads	GRB2-related adapter protein 2
GAS6	Growth arrest-specific protein 6
GDP	guanosine diphosphate

GO	gene ontology
Grb2	growth factor receptor-bound protein 2
GRP1	Glycine-rich RNA-binding protein 1
GSEA	gene set enrichment analysis
GTP	guanosine triphosphate
HER2	human epidermal growth factor receptor 2
HPD	hyperprogressive disease
HRP	horseradish peroxidase
ICB	immune checkpoint blockade
ICD	intracellular domain
ICIs	immune checkpoint inhibitors
IFN	interferon
IGF	insulin-like growth factor
IgG	immunoglobulin G
IKK	IκB kinase complex formation
IL-2	interleukin 2
IL-3	interleukin 3
IL-4	interleukin 4
IP3	inositol trisphosphate
IP3R1	inositol 1,4,5-trisphosphate receptor type 1
IRF8	interferon regulatory factor 8
ITIM	immunoreceptor tyrosine-based inhibitory motif
Itk	interleukin-2-inducible T-cell kinase
ITSM	immunoreceptor tyrosine-based switch motif
IκB	IkappaB kinase
JAK	Janus kinase
JNK	c-Jun N-terminal kinase
Ki67	proliferation marker protein Ki-67
Lag-3	lymphocyte-activation gene 3,
LAMTOR	late endosomal/lysosomal adaptor and MAPK and mTOR activator
LAT	linker for activation of T cells
Lck	lymphocyte-specific protein tyrosine kinase
LC-MS	liquid chromatography – mass spectrometry
LKB1 - AMPK	liver kinase B1 - AMP-activated protein kinase
MALT1	mucosa-associated lymphoid tissue lymphoma translocation protein 1
MAPK	mitogen-activated protein kinase
MCAM	melanoma cell adhesion molecule
MD	molecular dynamics
MDM	murine double minute gene
MEK	MEKK1 mitogen-activated protein kinase kinase
MERTK	tyrosine-protein kinase Mer
MHC	major histocompatibility complex
mTOR	mammalian (recently mechanistic) target of rapamycin
mTORC1	mammalian (recently mechanistic) target of rapamycin complex 1
MUC18	mucin 18
NFκB	nuclear factor kappa B
NKs	natural killer cells
NSCLC	non-small cell lung cancer
OE	overexpression

ORR	objective response rate
OS	osteosarcoma
$p27^{Kip}$	cyclin-dependent kinase inhibitor
p38	p38 MAP Kinase
p53	tumour protein P53
p85	regulatory PI3K subunit
PBS	phosphate buffered saline
PD1	programmed cell death protein 1
PDGF	platelet-derived growth factor
PDK1	phosphoinositide-dependent kinase 1
PDL1	programmed cell death ligand 1
PDL2	programmed cell death ligand 1
PI3K	phosphatidylinositol 3-kinase
PIP2	phosphatidylinositol 4,5-bisphosphate
PIR	pirin
PKC	protein kinase C
PKCθ	protein kinase C-θ
PLA	proximity ligation assay
PLC	phospholipase C
PLCγ1	phospholipase C γ1 isoform
PRAS40	proline-rich AKT1 substrate 1
PSAT	phosphoserine aminotransferase
PTEN	phosphatase and tensin homolog deleted on chromosome ten
PTMs	post-translational modifications
PTPN11	protein tyrosine phosphatase non-receptor type 11
Rac	Ras-related C3 botulinum toxin substrate
Raf	rapidly accelerated fibrosarcoma
Ras	rat sarcoma virus
Rb	retinoblastoma protein
RBPs	RNA binding proteins
Rheb	Ras homolog enriched in brain
RMSD	Root Mean Square Deviation
RPS6	ribosomal protein S6
RT	room temperature
RTK	receptor tyrosine kinase
RT-qPCR	reverse transcription - quantitative polymerase chain reaction
S6K1	ribosomal protein S6 protein kinase 1
SCF^{Skp2}	Skp1-cullin 1-F-box S-phase kinase-associated protein 2
SDS-PAGE	sodium dodecyl sulphate polyacrylamide gel electrophoresis
SERC	phosphoserine aminotransferase
SHP1	Src homology 1 domain – containing phosphotyrosine phosphatase 1
SHP2	Src homology 2 domain – containing phosphotyrosine phosphatase 2
SKP2	S-phase kinase-associated protein 2
SLP-76	SH2-domain-containing leukocyte protein of 76 kDa
SOS	Ras/Rho guanine nucleotide exchange factor 2
Src	proto-oncogene tyrosine-protein kinase Src
SRX1	sulfiredoxin
STAT	signal transducer and activator of transcription
Syk	spleen tyrosine kinase

TAMs	tumour associated macrophages
TCR	T cell receptor
TFA	trifluoroacetic acid
TGFα	tumour growth factor α
TIGIT	T cell immunoreceptor with Ig and ITIM domains
TILs	tumour infiltrating lymphocytes
Tim-3	T-cell immunoglobulin mucin receptor 3
TME	tumour microenvironment
TNF	tumour necrosis factor
TSC1/2	tuberous sclerosis proteins 1 and 2
TSP-1	thrombospondin 1
TYRO3	Tyrosine-protein kinase receptor TYRO3
VAV1	Vav 1 oncogene
VEGF-A	vascular endothelial growth factor A
VEGFR	vascular endothelial growth factor receptor
WT	wild-type
ZAP-70	ʒ-associated protein of 70kDa

Units

µg	microgram
µl	microlitre
µm	micrometre
µs	microsecond
Å	angstrom
fs	femtosecond
kDa	kilodalton
M	molar
mg	milligram
ml	millilitre
mm	millimetre
mM	millimolar
ng	nanogram
nl	nanolitre
ppm	parts per million
ps	picosecond
UI	international unit

1. Introduction

1.1 PD1 receptor: from gene discovery to protein functional description

The *PDCD1* gene encoding programmed cell death protein 1 (PD1) was first described in 1992 as a gene expressed in response to induced programmed cell death in T cell hybridoma. It was classified as a novel member of the immunoglobulin like gene superfamily (Ishida et al. 1992). Back then, PD1 protein size was predicted as ~30kDa, but soon after PD1 monoclonal antibody was developed, PD1 protein was described as a 50-55kDa membrane protein which is highly glycosylated and mostly present on activated T and B cells (Agata et al. 1996).

Further studies conducted in mice, revealed that PD1 deficiency leads to lupus-like autoimmune diseases (Nishimura, Honjo, and Minato 2000), suggesting its regulatory role in modulating the immune response rather that directly inducing apoptosis. Currently, PD1 is widely recognized as an immune checkpoint receptor, which plays a critical role in regulating the immune response. PD1 acts by favouring the immune tolerance and protecting from autoimmunity (Francisco, Sage, and Sharpe 2010). This mechanism is targeted by cancer immunotherapies, which aim at stimulation of cytotoxic T cells to defeat cancer, which were previously inhibited by the excessive PD1 signalling (Okazaki and Honjo 2007; Zamani et al. 2016; Topalian, Drake, and Pardoll 2012; Tumeh et al. 2014). In 2018, James P. Allison and Tasuku Honjo were awarded the Noble Prize in Physiology or Medicine "for their discovery of cancer therapy by inhibition of negative immune regulation" revealing the mechanism for CTLA-4 and PD1, respectively.

1.2 The role of immune checkpoint receptors

The immune system homeostasis is critical for successful defence from microbes and early elimination of cancer cells. Simultaneously, it is crucial for preserving self-tolerance and protecting from the autoimmune response (Schönrich and Raftery 2019; Okazaki and Honjo 2007; Patsoukis, Wang, et al. 2020; Riley 2009; Nishimura et al. 1999). To achieve this, the T cell activation is a tightly controlled process. On one hand, self-reactive T lymphocytes are eliminated in the thymus, the process called central tolerance. However, some autoreactive cells may still

escape this step (Kappler, Roehm, and Marrack 1987; Wartewig et al. 2017; Ahn et al. 2018). As a result, additional self-protective mechanisms evolved to maintain T cell tolerance in the periphery. This includes inhibitory receptors, which usually cause dephosphorylation, in other words inactivation, of key proteins essential for immune activation. Alternatively, the regulatory mechanisms operate through E3 ubiquitination and subsequent proteasomal degradation of the signalling molecules involved in T cell activation (Bonnevier, Zhang, and Mueller 2005; Gavali et al. 2021). The inhibitory receptors signalling can either prevent T cell activation upon antigen recognition like CTLA-4 or, like PD1, modulate the activity of lymphocytes, which had already undergone activation. Therefore, both CTLA-4 and PD1 play a role of the immune checkpoints (Parry et al. 2005; Safaeifard et al. 2022).

1.2.1.1 PD1: expression and activation by PDL1

While CTLA-4 regulates T cell response during activation in secondary lymphoid organs, such as lymph nodes, PD1 receptor dampens the activity of T cells, which were already activated and predominantly happens in the peripheral tissues (Parry et al. 2005; Callahan and Wolchok 2013). PD1 receptor is activated upon binding by its ligands PDL1 and PDL2, whereas PDL1 is far more common and better described. PDL1 is expressed not only by immune cells but also by various types of tissues such as pancreatic islets, endothelium, lungs, and placenta (Okazaki and Honjo 2007; Francisco, Sage, and Sharpe 2010; Butte et al. 2007). This mechanism directly protects tissues from the autoimmune response. Apart from self-tolerance, the role of PD1/PDL1 axis is to protect from an excessive damage of the surrounding tissues during inflammation and chronic infections (Kao et al. 2011; Brown et al. 2010).

However, PD1/PDL1 axis not always acts in our favour and is exploited by multiple cancer types in which the malignant cells can express PDL1. Persistent PD1 signalling in the tumour microenvironment leads to T cell functional exhaustion and inability to defeat cancer (Bengsch et al. 2016; Blank et al. 2019). Therefore, PD1 is often called a negative regulator of immune response during infections, autoimmune response as well as in cancer (Nishimura et al. 1999). Currently available PD1/PDL1

immunotherapies utilize monoclonal blocking antibodies to target the interaction between the PD1 receptor and its ligand (Tumeh et al. 2014).

1.2.2 CTLA-4

As first suggested in 1970 and further explained in 1999, T cell activation is a two-step process. It was discovered that T cell receptor (TCR) ligation by MHC II peptides presented by DCs is not sufficient to induce the activation of naïve T cells (P. A. Bretscher 1999; P. Bretscher and Cohn 1970). This mechanism ensures the maintenance of immune tolerance in the periphery. The second signal required for T cell activation comes from the interaction between the costimulatory molecules CD28 and CD80/86 expressed on T cells and APCs, respectively. CTLA-4, by competing with CD28 for binding to CD80/86, tightly controls the costimulatory signalling during T cell activation (Krummel and Allison 1995; Tivol et al. 1995). CTLA-4 is generally expressed at low levels, but high affinity to CD80/86 makes it a preferred target over CD28 (Sansom 2000). Lack of the costimulatory signal results in T cell anergy and unresponsiveness to further antigen challenge. Targeting CTLA-4 with blocking monoclonal antibodies was the first form of immune checkpoint inhibition used for cancer treatment (Pandey et al. 2022; Seidel, Otsuka, and Kabashima 2018; Rowshanravan, Halliday, and Sansom 2018).

1.3 The role of PD1 in T cell exhaustion

T cell activation is a complex process involving a dynamic interplay between multiple costimulatory and inhibitory factors. The outcome of activation depends on which type of signal outweighs its counterpart. Following activation, T cells upregulate inhibitory receptors, including PD1, as a control mechanism protecting from self-antigen response or tissue damage during long-term infection. However, persistent antigen stimulation of effector T cells observed in chronic viral infections or cancer leads to increased expression of inhibitory receptors (Pauken and Wherry 2015). This includes not only PD1, but also many other proteins such as CTLA-4, Lag-3, Tim-3, CD244/2B4, CD160 or TIGIT. Ultimately, the prolonged inhibitory signalling results in the state of T cell functional exhaustion characterized by impaired secretion of cytokines such as IL-2, IFN-γ or TNFα and decreased proliferative capacity, comprised cytolytic activity and degranulation. In this state, T cells are no longer

capable of clearing the infection or killing tumour cells effectively (Rota et al. 2018; Bengsch et al. 2016).

Interestingly, the exhaustion of T cells can be reversed by PD1 blockade. Exhausted T cells become reinvigorated, but the question of which cells exactly and to what extent respond to PD1 inhibition is still under debate. This likely depends on factors such as the level of PD1 expression and the stage of exhaustion, but the exact mechanism of T cell reinvigoration remains incompletely understood (Y. T. Chan et al. 2022). Considering that PD1 ligand (PDL1) is not only expressed by immune cells and healthy tissues but also by cancer cells, accounts for one of the fundamental mechanisms of cancer immune evasion leading to T cell functional exhaustion and became a key target for cancer immunotherapy (Blank et al. 2019; Xia et al. 2019).

1.4 PD1 as a target for immunotherapy: PD1/PDL1 blocking antibodies

Ipilimumab, the first immune checkpoint inhibitor (ICI) targeting the CTLA-4 receptor, was approved by the FDA in 2011 for the treatment of metastatic melanoma (Lipson and Drake 2011). Also, as soon as the significance of the PD1/PDL1 axis in cancer was better understood, efforts to develop monoclonal blocking antibodies for this pathway started. Successfully, in 2014 the first PD1 inhibitor, pembrolizumab, was approved by the FDA (Pandey et al. 2022; Q. Wu et al. 2022; Garon et al. 2015).

Recommendations for the implementation of ICIs include assessment of PDL1 expression by the tumour, which is regarded as a good indicator to predict the response to immunotherapy. Over the years, it became a standard medical procedure before therapy implementation (Alexander et al. 2016; Hodi et al. 2016; Sul et al. 2016). Currently, there are three FDA-approved PDL1 monoclonal blocking antibodies: atezolizumab, durvalumab, and avelumab in addition to three PD1 monoclonal blocking antibodies: pembrolizumab, nivolumab, and cemiplimab (Twomey and Zhang 2021). These immune checkpoint inhibitors cause relatively mild adverse effects in comparison to CTLA-4 blocking antibodies and incomparably less severe in contrast to chemotherapy (Weber et al. 2015; Brahmer et al. 2012).

The first clinical recommendation for PD1/PDL1 inhibitors was advanced-stage or unresectable melanoma. Currently, the recommendations are much broader. Depending on the specific antibody, they now encompass a wide range of malignancies, including lymphomas and solid tumours such as NSCLC, head and neck squamous cell carcinoma, Hodgkin lymphoma, renal or urothelial carcinoma and many others (Gong et al. 2018; Majidpoor and Mortezaee 2021).

Initially, ICIs were used as monotherapeutics. However, much better efficacy is observed when they are combined with chemotherapy or a combination of chemotherapy and additional monoclonal antibody targeting, for example EGFR (bevacizumab) or VEGFR (lenvatinib) and many more (Lee, Kim, and Ha 2022; Andersson et al. 2018). The introduction of PD1/PDL1 blocking agents in cancer treatment has undeniably revolutionized approach to the therapy. Nevertheless, the response to these treatments varies among different cancer types and individual patients, while the underlying mechanism is not yet fully comprehended (Kocikowski, Dziubek, and Parys 2020; Camelliti et al. 2020).

1.5 PD1 role in hyperprogressive disease

The objective response rate (ORR) for ICIs typically ranges from 15% to 70%, depending on the patient and tumour type (S. Chen et al. 2021). However, a vast number of patients still do not benefit from the therapy or even show rapid cancer progression following the treatment with PD1/PDL1 monoclonal antibodies (Arasanz et al. 2021). This phenomenon is called hyperprogressive disease (HPD) and was reported shortly after clinical trials evaluating PD1/PDL1 blocking antibodies started (Chubachi et al. 2016).

In some patients, following the first evaluation upon drug administration, the tumour can increase two times or more compared to the pre-treatment assessment (Brower 2016; P. Shen et al. 2021). Importantly, HPD must be distinguished from pseudoprogression, as the latter describes a temporary state in which the observed tumour growth does not indicate cancer progression. In fact, it arises from inflammation and TILs recruitment to the tumour microenvironment (Hodi et al. 2016). Despite many years has passed since PD1/PDL1 inhibitors were first used in clinical

trials, there is still no clarity in the mechanism causing hyperprogression (Camelliti et al. 2020). Nevertheless, several hypotheses were proposed as possible causes of HPD and selected are discussed below.

1.5.1 Cancer-intrinsic PD1 signalling

Initially, the PD1 receptor was described as an immune checkpoint expressed exclusively on immune cells, where it acts as a brake protecting from excessive immune activation. This, together with cancer cells' ability to express PDL1, led to the development of therapeutic PD1/PDL1 monoclonal blocking antibodies. The mechanism behind ICB efficacy relies on the functional reinvigoration of cytotoxic T cells and their gain of function to eliminate cancer cells. Strikingly, in parallel with the first FDA approval of PD1/PDL1 immune checkpoint blockade for cancer treatment, expression of PD1 receptor was identified in cancer cells (Schatton et al. 2010). Only later was the blockade of cancer PD1 linked to the development of hyperprogressive disease in NSCLC patients, suggesting that in some cases, tumour-intrinsic PD1 may be the mechanism of resistance to ICIs (Du et al. 2018). This could be a game changer in our understanding of the mechanism underlying PD1/PDL1 blockade, determining the safety of immunotherapy.

Considering that PD1 blocking antibodies affect multiple immune cell populations, it became evident that HPD can be caused by multiple factors, suggesting the need for combinatorial therapies rather than a single agent approach (Kocikowski, Dziubek, and Parys 2020). However, the role of cancer-intrinsic PD1 is still debatable and contradictory reports are available regarding whether it acts as a tumour suppressor or tumour promoter (Denis et al. 2020). Therefore, it must be further clarified to determine the safety of PD1 ICB and to further improve the therapeutic outcomes (Camelliti et al. 2020).

1.6 Hyperprogressive disease: beyond cancer-intrinsic PD1

1.6.1 Clonal selection

Apart from NSCLC cases, immunotherapy is frequently not the first line of treatment (Bie et al. 2022). In fact, many patients receiving immunotherapy were already pre-treated with chemotherapy but with poor results. In such cases, it can be assumed

that tumour cells have undergone clonal selection, favouring the survival of the most aggressive cells, which already escaped the immune surveillance. Therefore, the immunotherapy, which aims to restore the natural immune response, simply will not prove effective not to mention the burden of chemotherapy to the immune system, which could lead to its compromised efficacy (Baldwin et al. 2022; Gutwillig et al. 2022; Trajanoski et al. 2020).

1.6.2 Immunosuppressive PD1$^+$ T regulatory cells

It is crucial to consider that PD1 receptor is not only expressed on CD4$^+$ and CD8$^+$ but also on T regulatory cells (Bardhan, Anagnostou, and Boussiotis 2016). While the biggest benefit of immunotherapy implementation lies in reinvigorating the CD8$^+$ T cells, the effects on other cell populations must as well be considered. As a matter of fact, based on a study in advanced gastric patients, HPD was reported in 10% of the patients treated with PD1/PDL1 immune checkpoint inhibitors (Kamada et al. 2019). Within the tumour infiltrate of all examined patients, highly suppressive FoxP3^{high}CD45RA$^-$CD4$^+$ T cells (effector Treg cells) expressing PD1 receptor were identified. Interestingly, only those patients who developed HPD had significantly increased proliferative (Ki67$^+$) effector Treg cells, opposed to the group that responded to treatment and whose Ki67$^+$ Tregs were decreased. Both *in vitro* and *in vivo* studies confirmed that PD1 blockade on highly suppressive T regulatory cells facilitates their proliferation and suppressive capability, suggesting its role in hyperprogression (Kamada et al. 2019; Kang et al. 2022).

1.6.3 Tumour associated macrophages (TAM)

The role of macrophages in hyperprogression upon ICB primarily arises from the binding of PD1 blocking antibodies by FCγRs expressed on these macrophages, therefore diminishing the activity of ICIs (Dahan et al. 2015; Russo et al. 2019). However, the role of macrophages in cancer is very complex. They are acknowledged as early-stage tumour promoters, which facilitate tumour progression, exert negative effects on the response to ICB and are associated with poor prognosis.

Macrophage activation can be categorized into two types: classically activated M1 macrophages, involved in the phagocytosis of microbes, and M2 macrophages, which arise from an alternative activation pathway. While M2 macrophages

are generally involved in tissue repair, then in cancer, they support the pro-inflammatory environment known to facilitate tumorigenesis. Moreover, TAMs release growth factors and cytokines, which further promote cancer cell proliferation, migration, and ability to metastasize (Xiang et al. 2021; X. Chen et al. 2019). In a study evaluating 152 NSCLC patients treated with nivolumab, up to 26% of patients were diagnosed with hyperprogression. Interestingly, immunohistochemistry analysis of tumour samples revealed that the major difference between patients who developed HPD and those who did not, was that the former had significantly more M2-like $CD163^{+}CD33^{+}PDL1^{+}$ macrophages in the TME. Murine studies revealed that HPD did not developed when Fc depleted antibody was administered. This suggest that Fcγ receptor binding the therapeutic antibodies may be critical for the development of HPD in patients treated with PD1/PDL1 monoclonal blocking antibodies (Russo et al. 2019).

Nivolumab is an IgG4 isotype antibody with limited ability to bind Fcγ activating receptors to minimize IgG-mediated $PD1^{+}$ immune cell toxicity. However, as an IgG4, nivolumab still can bind FcγIIB inhibitory receptors, which was proposed as the reason for the attenuated immune response. Although, it is possible that other Fc receptors may as well bind the therapeutic antibodies to some extent, predicting the exact effects would be challenging (Russo et al. 2019).

1.6.4 Association of MDM2/MDM4 amplification and EGFR mutations

Alternatively, in the study conducted by Kato et al. (2017), which enrolled more than 150 participants, all patients with *MDM2/MDM4* amplifications developed HPD (Kato et al. 2017). MDM2/MDM4 are well-known p53 inhibitors, often amplified in cancer. It was hypothesized that PD1 blockade-induced production of IFNγ, stimulated JAK-STAT activation and led to increased expression of interferon regulatory factor IRF8. IRF8 is a transcription factor, which directly promotes transcription of the *MDM2* gene, causing even stronger inhibition of p53 (Zhou et al. 2009).

Moreover, Kato et al. (2017) pointed to EGFR aberrations as an alternative driver for HPD. EGFR was reported to correlate with increased expression of immune checkpoint molecules, promoting cancer immune escape (Camelliti et al. 2020; Akbay et al. 2013; Azuma et al. 2014; Concha-Benavente et al. 2016; Kato et al. 2017).

1.7 Dual role of PD1 cancer-intrinsic signalling

In recent years, a growing body of evidence suggested the significance of cancer-expressed PD1 in cancers such as melanoma, NSCLS, bone and tissue sarcomas, thyroid or ovarian cancer, and hepatocellular carcinoma (Kleffel et al. 2015; Liotti et al. 2021; Du et al. 2018; Zhi et al. 2022; Yuting Zhang et al. 2021; Rotolo et al. 2023; Torabi et al. 2017; Hui Li et al. 2017; Gan et al. 2022). Nevertheless, conflicting reports exist regarding the role and mechanism of tumour-intrinsic PD1 implying both pro-tumorigenic and tumour suppressor functions (Hudson et al. 2020).

1.7.1 PD1 as a tumour promoter

Expression of PDL1, along with high mutational burden and presence of immune infiltrates in the tumour microenvironment are widely regarded as prognostic markers indicating a positive response to immune checkpoint inhibitors (F. Yang et al. 2022; Hanxiao Li, van der Merwe, and Sivakumar 2022). However, PD1/PDL1 blockade demonstrated beneficial outcomes even in patients with less immunogenic tumours (Herbst et al. 2014; Brahmer et al. 2012). This, in addition to the therapeutic success of PD1/PDL1 blockade in patients unresponsive to CTLA-4 blockade (targeting an alternative immune checkpoint receptor) suggest that besides T cell reinvigoration, there may be an additional immune system-independent mechanism involved in response to PD1/PDL1 monoclonal blocking antibodies (Majidpoor and Mortezaee 2021; Weber et al. 2015).

Strikingly, in 2010 Schatton et al. first reported cancer-expressed PD1 and its association with cancer stem-like characteristics of melanoma cancer cells. Subsequent studies conducted using clinical samples as well as melanoma cell lines, demonstrated that PD1-positive melanoma cancer cells exhibited pro-tumorigenic capabilities (Schatton et al. 2010). These results were validated both *in vitro* and in murine studies, which confirmed enhanced tumour growth in cells overexpressing PD1. Conversely, both PD1 knockdown and antibody-mediated inhibition of PD1 suppressed tumour growth. Notably, these effects were independent of adaptive immunity, given that the *in vivo* studies were conducted in severely immunocompromised mice (Schatton et al. 2010; 2008).

Further works demonstrated cancer PD1 mediated activation of mTOR pathway indicated as increased phosphorylation of mTORC1 downstream effector S6 ribosomal protein. Importantly, these effects were dependent on PD1 ligation with PDL1. Moreover, PD1 downstream signalling was propagated through ITSM (immunoreceptor tyrosine-based switch motif) and ITIM (immunoreceptor tyrosine-based inhibitory motif) as mutations interfering with phosphorylation sites of these motifs abrogated melanoma PD1 intrinsic signalling (Kleffel et al. 2015).

A more recent report identified an additional pro-tumorigenic function of cancer PD1 in glioblastoma. Interestingly, PD1 expression was once again detected in brain tumour–initiating cells exhibiting stem cell-like properties. Further analysis revealed that the tumour-promoting effects of PD1 were not dependent on PDL1, but instead involved the activation of NFκB pathway. However, the activation still required SHP2 recruitment to PD1 intracellular motifs followed by SHP2 phosphorylation (Álvarez-Viejo, Menéndez-Menéndez, and Otero-Hernández 2015; Mirzaei et al. 2021).

Supporting information was published regarding NSCLS, where PD1 was not only associated with cancer cell stemness but also with PD1-mediated chemoresistance to cisplatin treatment. Although PD1 expression was indeed upregulated in response to cisplatin, mice studies revealed that cisplatin sensitivity could be restored upon PD1 blockade with nivolumab and ultimately resulted in a favourable response (Rotolo et al. 2023). Moreover, PD1 was implied as a potential target to overcome resistance to BRAF/MEK inhibitors in melanoma (Sanlorenzo et al. 2018).

An alternative mechanism for tumour-expressed PD1 as a tumour promoter was proposed in pancreatic cancer. PD1 was linked to the upregulation of cysteine-rich angiogenic inducer 61 (CYR61, CCN1) and connective tissue growth factor (CTGF, CCN2) through the Hippo pathway. Both CYR61 and CTGF may affect cell proliferation, migration, apoptosis, or senescence, playing an important role in supporting cancer development. Noteworthy, combining CYR6/CTGF inhibitors with PD1 monoclonal antibodies resulted in a synergistic inhibition of pancreatic cancer cells *in vitro* (Pu et al. 2019).

1.7.2 PD1 as a tumour suppressor

In addition to multiple reports demonstrating that cancer-intrinsic PD1 has pro-tumorigenic effects, several reports suggest the opposite. A case report published by Du et al. in 2018 described rapid progression of the disease in NSCLC patient treated with PD1 blocking antibodies. Both *in vitro* and *in vivo* validation revealed PD1 tumour suppressor properties (Du et al. 2018).

Further studies on cancer-expressed PD1, revealed its role in the inhibition of AKT and ERK1/2 pathways (likewise in T cells), while no stimulation of mTOR pathway signalling was reported both in NSCLC and colon cancer models. Strikingly, tumour progression was observed upon treatment with both PD1 (nivolumab) or PDL1 (atezolizumab) blocking antibodies, suggesting the requirement for PDL1 ligation to PD1 (X. Wang et al. 2020; Ieranò et al. 2022).

Additional works on cancer intrinsic PD1 in colon cancer model revealed that PD1 promotes apoptosis as determined by annexin staining. Cancer PD1 was proposed as a potential mechanism of hyperprogressive disease and failure, or even rapid relapse observed in some patients undergoing immunotherapy (X. Wang et al. 2020).

Considering the contradictory implications regarding the role of cancer-intrinsic PD1, further works are required to reevaluate the safety and maximize the efficacy of PD1/PDL1 blockade in patients with tumours expressing PD1 receptor (Zha et al. 2021; Long et al. 2022).

1.8 Osteosarcoma

1.8.1 Incidence

Osteosarcoma (OS) is the most common type of bone cancer in humans, predominantly affecting children and young adults. While the 5-year survival rate for patients who have not developed metastasis is 60-70%, it dramatically decreases to less than 20% in the metastatic disease (Saraf, Fenger, and Roberts 2017; Rastogi et al. 2018; Zenan Wang et al. 2019). Regrettably, the majority of patients manifest micrometastases in the lungs at the time of diagnosis (X. Zhao et al. 2021). Despite rapid progress in treatment approaches observed for other types of cancer, osteosarcoma patients still follow the therapeutic regimen introduced more than 30 years ago. It is based on surgical resection of the tumour followed by chemotherapy with methotrexate, cisplatin, doxorubicin or ifosfamide (Piperno-Neumann et al. 2016; Ya Zhang et al. 2018).

While a decrease of nearly 50% is observed in cancer-related mortality among children with other forms of cancer, no substantial decrease was observed in children suffering from osteosarcoma (Jemal et al. 2017). The lack of therapeutic advancement in osteosarcoma treatment is partially attributed to the relatively low incidence of the disease. It accounts for approximately 1% of cancer related deaths each year (Cancer Research UK, 2017-2019). The limited incidence, together with heterogeneity across patients made osteosarcoma studies difficult and contributed to incomplete understanding of the disease (Jemal et al. 2017).

1.8.2 Immunotherapy in osteosarcoma

Considering the great success of immunotherapy implementation in cancer treatment, clinical trials employed PD1/PDL1 blocking antibodies for the treatment of osteosarcoma but with unsatisfactory effects (Z. Zhang et al. 2022; Boye et al. 2021; Tawbi et al. 2017; Y. Lu et al. 2022; Le Cesne et al. 2019).

In SARC028 clinical trial (number NCT03013127), which enrolled 12 patients with unresectable, relapsed osteosarcoma, no patients demonstrated clinical benefit at 18 weeks of pembrolizumab treatment and the trial was terminated before reaching stage 2 (Tawbi et al. 2017). Patients did not develop serious grade 3 or 4 adverse

events nor drug-related deaths. Notably, PDL1 was expressed in 1 out of 11 patient tumour samples, which was coming from the patient with partial response to the therapy. PD1 expression was not evaluated (Tawbi et al. 2017). Similarly, the limited response to pembrolizumab treatment in combination with cyclophosphamide was observed in PEMBROSARC study enrolling 17 patients (Le Cesne et al. 2019). 15 patients were assessed after 6 months; only 1 patient demonstrated partial response, while 2 patients were progression-free, however no correlation with PDL1 expression was observed this time (Le Cesne et al. 2019). No evaluation of cancer-PD1 expression was performed in either of those studies.

Several mechanisms were proposed to explain poor outcomes of ICIs in the treatment of osteosarcoma. First of all, similarly to other cancer types, the tumour microenvironment of OS is characterized by the presence of immunosuppressive immune cell populations, including M2 macrophages, T regulatory cells or myeloid derived tumour suppressor cells, creating unfavourable environment for cytotoxic T cells (Simpson et al. 2017; Koirala et al. 2016).

Moreover, ICB has the most favourable outcomes in malignancies such as melanoma or NSCLC, which are considered as hot tumours due to high mutational burden and immune infiltrate (Bonaventura et al. 2019; Galon and Bruni 2019; Majidpoor and Mortezaee 2021; Maleki Vareki 2018). Conversely, osteosarcoma is regarded as a cold tumour, characterized by reduced immunogenicity and limited infiltration by immune cells (de Azevedo et al. 2020). Nevertheless, some works characterizing the expression of immune checkpoints in OS confirmed PDL1 expression by the tumour cells, suggesting a potential efficacy of PD1/PDL1 inhibition (J. K. Shen et al. 2014; Na, Kim, and Park 2012; Han et al. 2019; Hashimoto, Nishimura, and Akagi 2020).

Given the lack the explanation for the ultimate effect of PD1 signalling in cancer and its significance for immunotherapy implementation, it is tempting to hypothesize that tumour intrinsic PD1 expression may be a contributing factor to unsatisfactory outcomes of immunotherapy in OS patients. Thereby, a full understanding of the osteosarcoma PD1 intrinsic signalling is crucial, as targeting cancer-PD1-

associated mechanisms may enhance the efficacy of immunotherapy in patients suffering from this type of cancer.

1.9 T cell activation: a key to the significance of PD1 signalling

PD1 is an inhibitory receptor for activated T cells, which inhibits the TCR (T cell receptor) signalling (Tumeh et al. 2014). Therefore, to fully understand the molecular mechanism and cellular effects of the PD1 pathway, it is crucial to understand the molecular signalling triggered upon antigen recognition by the TCR.

1.9.1 T cell activation

Antigen recognition and signal transduction initiated by the TCR is regarded as one of the most advanced signalling mechanisms in the human body. Its complexity is necessary to ensure that non-self-antigens induce an immune response without compromising the tolerance to self-antigens (Wong et al. 2017). The TCR does not function as a single protein, but like many other immune receptors, creates a TCR multiprotein complex in which all components play a role in inducing a T cell response (Courtney, Lo, and Weiss 2018). The short cytosolic tail of the T cell receptor itself lacks intrinsic catalytic activity. Therefore, signal transduction is ensured by the other complex components – the transmembrane proteins with cytosolic immunoreceptor tyrosine-based activation motifs (ITAMs) (Shah et al. 2021).

1.9.2 The structure of the TCR complex

The TCR complex is composed of the T cell receptor heterodimer, ζ chain protein homodimer and two heterodimers of CD3 proteins: CD3γε and CD3εδ. Each chain of CD3 protein contains a single ITAM in its intracellular tail, while the ζ chain protein encompasses three ITAMs on each cytosolic chain (Appleman and Boussiotis 2003; Roncagalli et al. 2010). It gives a total of 10 ITAMs that can undergo phosphorylation during T cell activation (**Figure 1**). The number of phosphorylated motifs is associated with the strength and duration of the antigen binding to the TCR, which regulates the strength and character of the T cell response (F. Wei et al. 2013).

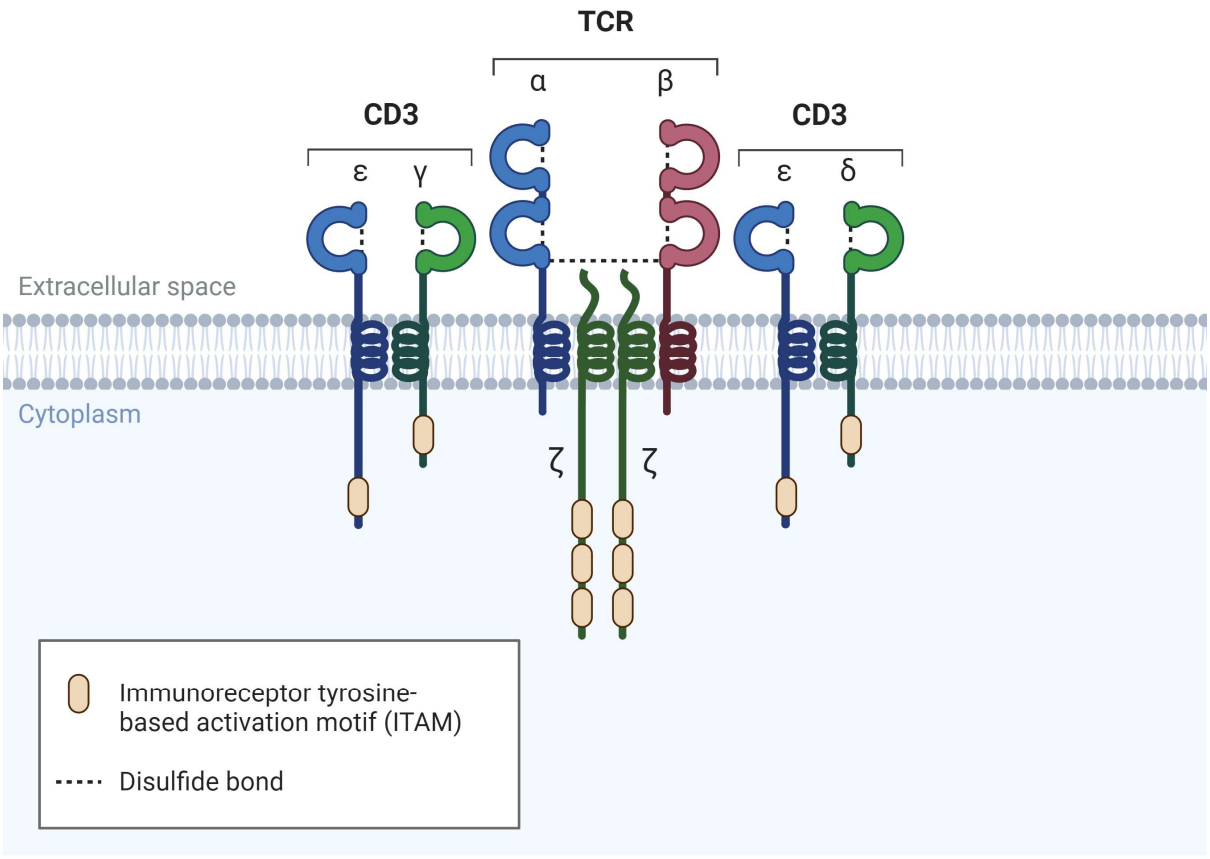

Figure 1 Schematic overview of the structure of the T cell receptor complex. Figure created with BioRender.com.

1.9.3 Initiation of the TCR signal transduction

T cell activation transforms resting cells into highly proliferative secretory cells, causing major signalling remodelling (Frauwirth and Thompson 2004). Following the recognition of an antigen presented by the MHC complex on an APC cell, the TCR undergoes conformational changes and forms clusters with other components of the TCR complex (Nurieva et al. 2006; Shah et al. 2021). At this stage, TCR signalling is further enhanced by T cell coreceptors recruited to the site of antigen recognition. Depending on the type of T cell being activated, two types of coreceptors are involved: CD4, which recognizes MHC II and CD8, which binds to MHC I (Artyomov et al. 2010). CD4 and CD8 are not a part of the TCR complex, but they facilitate TCR-antigen recognition. Importantly, these molecules drive the very first ITAMs phosphorylation step upon TCR activation (Gaud, Lesourne, and Love 2018).

The cytoplasmatic tails of both CD4 and CD8 associate with Lck (or Fyn alternatively), which is a Src family kinase (Laird and Hayes 2010). Subsequently, Lck phosphorylates tyrosine residues of ITAMs located on CD3 and ʒ proteins, which are required for further signal transduction (Wartewig and Ruland 2019; Chatterjee et al. 2013).

In the following step, the Syk family kinase ZAP-70 is recruited to the phosphorylated ITAMs of ʒ chains. ZAP-70 binds to them through its SH2 domains and undergoes phosphorylated by Lck, which is still in proximity, facilitating the reaction. Phosphorylated ZAP-70 can function as a tyrosine kinase itself. Interestingly, to achieve full activation, ZAP-70 must reach a certain threshold of activity, which is acquired when multiple ZAP-70 molecules bind to multiple ITAMs of the TCR complex proteins - CD3 and ʒ molecules (Chatterjee et al. 2013). Subsequently, ZAP-70 phosphorylates LAT protein, which serves as a scaffold due to the presence of multiple tyrosine residues in its cytoplasmatic tail (Sheppard et al. 2004). Proteins recruited to LAT can bind to the phosphorylated tyrosines either directly or indirectly, forming a complex known as LAT signalosome. The direct interactors are PLC-γ1, GRB2, and GADs, which further recruit the following to the LAT signalosome: SLP-76, ADAP, and VAV1 (Gaud, Lesourne, and Love 2018; C. Liu et al. 2020). Essentially, the LAT signalosome functions as a hub for the activation of TCR signalling effector pathways (for reference, please check **Figure 2**).

1.10 TCR effector pathways: MAPK, PLCγ and calcium signalling

The downstream signalling of TCR majorly results in the activation of transcription factors, which in turn drive the expression of proteins essential for T cell activation and differentiation. This process is facilitated by the activation of key signalling cascades, including, PLCγ1, MAPK and calcium signalling (Shah et al. 2021; Barnes et al. 2015).

1.10.1 PLCγ1

PLCγ1, a phospholipase component of the LAT signalosome, plays a role of a downstream effector for activation of transcription factors essential for T cell activation. Following antigen recognition, PLCγ1 becomes phosphorylated by both ZAP-70 and Itk (recruited to LAT signalosome but bound indirectly) (Strazza

et al. 2021; Hinz et al. 2014). Subsequently, the plasma membrane protein PIP2 serves as a substrate for PLCγ1 and is enzymatically hydrolysed to DAG and IP3. Both DAG and IP3 are second messenger molecules regulating numerous downstream pathways (Garçon et al. 2008; Shyer, Flavell, and Bailis 2020). The schematic overview of the signalling events is illustrated in **Figure 2**. IP3 further

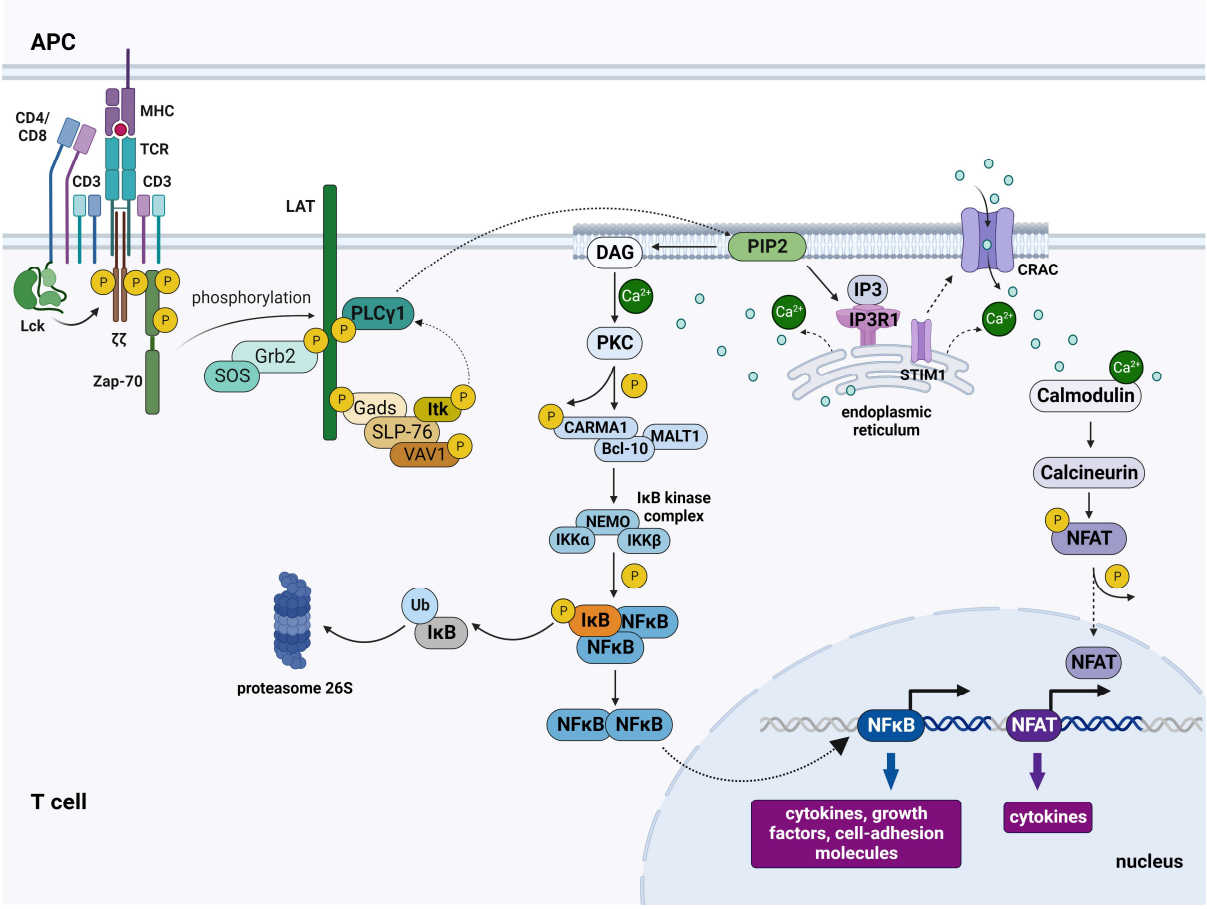

Figure 2 Schematic overview of the PLCγ1 signalling cascade. Upon activation, PLCγ1 generates the secondary messenger molecules IP3 and DAG, which triggers a cascade of signalling events. Ultimately, the activate NFAT and NFκB transcription factors, which promote expression of cytokine genes, cell adhesion molecules, growth factors and apoptosis regulating genes. Figure created with BioRender.com.

migrates to the endoplasmic reticulum (ER). There, it binds to its receptor IP3R1, resulting in calcium release from the endoplasmic storage into the cytoplasm (DeSouza et al. 2007). The decrease of calcium level in the ER causes the opening of membrane calcium channels (CRAC), leading to the extracellular influx of the calcium ions into the cytosol (Shah et al. 2021). Free cytosolic calcium ions can further propagate the signalling, majorly by binding to a calcium dependent protein –

calmodulin (Gaud, Lesourne, and Love 2018). It is a regulatory protein with the ability to activate downstream enzymes such as calcineurin. Calcineurin, in turn, controls the activity of numerous transcription factors, including those critical for T cell activation and differentiation, for example NFAT (Hogan 2017; Oestreich et al. 2008). Mechanistically, calcineurin dephosphorylates NFAT in the cytoplasm, what is required for its migration to the nucleus, where it binds to DNA. NFAT controls the transcription of multiple genes encoding proteins driving the T cell activation, for example IL-2, IL-4, or TNF (Barnes et al. 2015).

The second product of PLCγ1 mediated hydrolysis of PIP2 is DAG (Appleman and Boussiotis 2003). Together with free calcium ions released upon IP3 signalling, DAG induces conformational changes in the various isoforms of PKC kinase. One of them, PKCθ is a critical component of the immunological synapse controlling the downstream activation of NFκB transcription factor (Gaud, Lesourne, and Love 2018). NFκB is a group of closely related proteins, including DNA binders: p50 and p52 along with DNA transactivators: RelA, RelB and c-Rel (Visekruna, Volkov, and Steinhoff 2012; Atsaves et al. 2019).

In the steady state, NFκB proteins form inactive heterodimers bound to NFκB inhibitors (IκB) and are present in the cytosol (Visekruna, Volkov, and Steinhoff 2012). The release of NFκB dimers happens upon phosphorylation of IκB and their subsequent ubiquitin-mediated degradation. The phosphorylation of IκB, necessary for NFκB activation, is initiated by IκB kinase complex formation (IKK) (Sakthivel, Gereke, and Bruder 2012; Barnes et al. 2015). IKK is formed upon a cascade of signalling events starting from calcium-dependent activation of PKC by DAG. PKC further phosphorylates CARMA1, which along with Bcl-10 and scaffolded MALT1, form a complex, which facilitates formation of the IKK complex (Visekruna, Volkov, and Steinhoff 2012; Huang and August 2015). In other words, the IKK mediated IκB degradation activates the NFκB pathway, which is critical for transcription of genes encoding cytokines, growth factors or proteins regulating apoptosis.

1.10.2 MAPK

The mitogen-activated protein kinase (MAPK) signalling pathway acts via distinct activation patterns. Eventually, these signalling networks (illustrated in **Figure 3**) lead

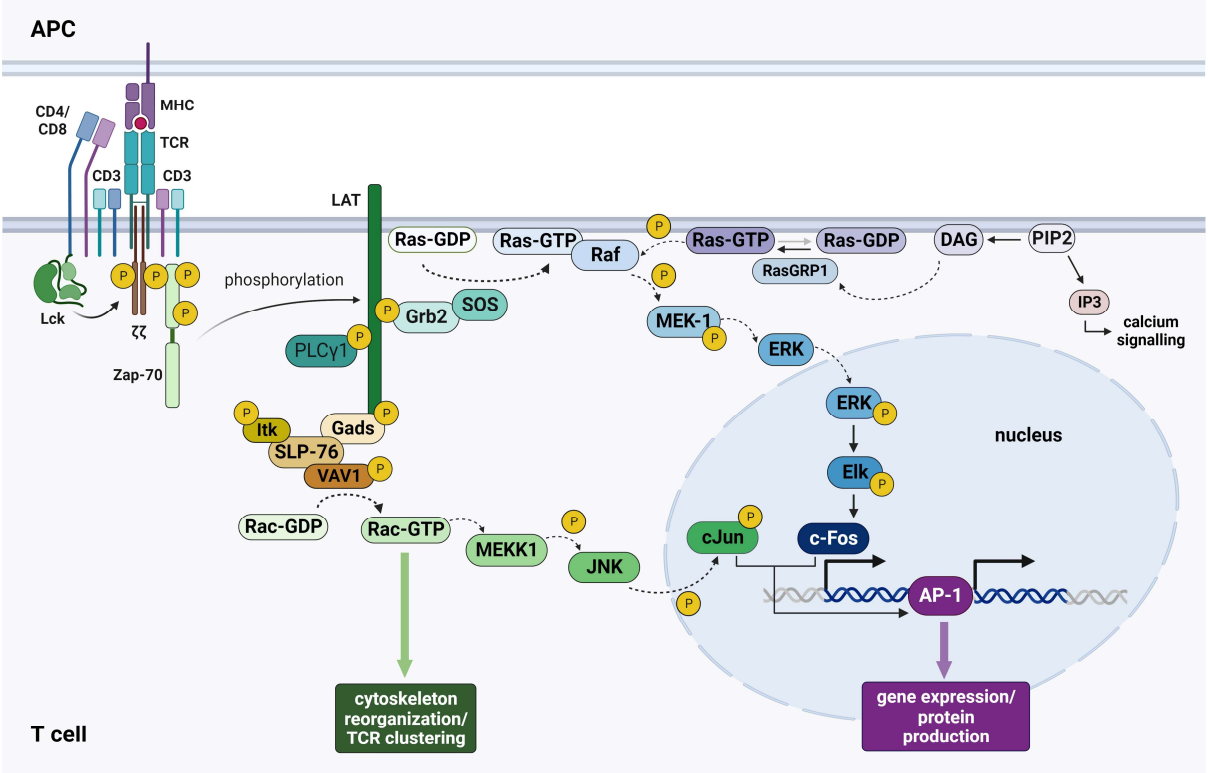

Figure 3 Schematic overview of the MAP kinase signalling cascade demonstrating JNK and ERK1/2 activation patterns. A detailed description provided in the main text. Figure created with BioRender.com.

to the synthesis of an AP-1 protein components, an essential transcription factor involved in the activation of T cells (Atsaves et al. 2019; Yukawa et al. 2020).

One way of the MAPK cascade activation is mediated by Ras signalling. Ras is a small G protein, active in the GTP bound form and becomes inactivated upon GTP hydrolysis to GDP. Following T cell activation, LAT phosphorylation facilitates docking of Grb2 and further recruitment of SOS protein (Roose et al. 2005). The latter promotes conversion of GDP to GTP and subsequent activation of Ras protein. Alternatively, RasGTP can be generated under control of RasGRP1 molecule, which is recruited by a second messenger molecule DAG. It is worth noting, that DAG is generated following the activation of PLCγ1, acting as an intersecting point between these two pathways (Roose et al. 2005).

Subsequently, RasGTP triggers MAPK signalling cascade through consecutive phosphorylation steps of Raf, MEK-1 and ERK1/2. Once phosphorylated, ERK1/2 translocates to the nucleus, mobilizes Elk, ultimately activating c-Fos, which is an integral component of AP-1 transcription factor (Yukawa et al. 2020; Gazon et al. 2018).

Simultaneously, an alternative MAPK signalling cascade occurs, leading to c-Jun activation, which together with c-Fos, form AP-1 transcription factor. This type of MAP kinase signalling cascade employs another small GTP binding protein called Rac. Rac becomes activated through the exchange of GDP for GTP coordinated by VAV1 (Shah et al. 2021; Gaud, Lesourne, and Love 2018). VAV1 binds to LAT signalosome via Gads and SLP-76. It transforms inactive Rac-GDP to active Rac-GTP, initiating the MAPK signalling cascade through MEKK1 an JNK. JNK in turn phosphorylates c-Jun in the nucleus, which then becomes a complement for c-Fos protein. Together, they form AP-1 transcription factor, which regulates expression of genes essential for cellular growth and survival (Atsaves et al. 2019; Roose et al. 2005). Alternatively, the third type of MAPK signalling, besides ERK and JNK intermediates, acts through p38 signalling.

The ultimate outcome of MAPK signalling is the transcription of genes essential for T cell activation and differentiation. However, the specific effects exerted by ERK1/2, JNK or p38 may differ depending on whether the T cell is naïve, or antigen-experienced (Adachi and Davisa 2011).

1.10.3 LAT independent signalling - PI3K/Akt/mTOR

While the majority of signalling events following the TCR activation is mediated by ZAP-70, some crucial pathways become stimulated independently of ZAP-70 protein. Such pathways include PI3K/Akt/mTOR signalling, a fundamental regulator of pro survival signals, cell cycle progression and T cell differentiation (Garçon et al. 2008). The schematic overview of PI3K/Akt/mTOR pathway cascade upon TCR activation is illustrated in **Figure 4**.

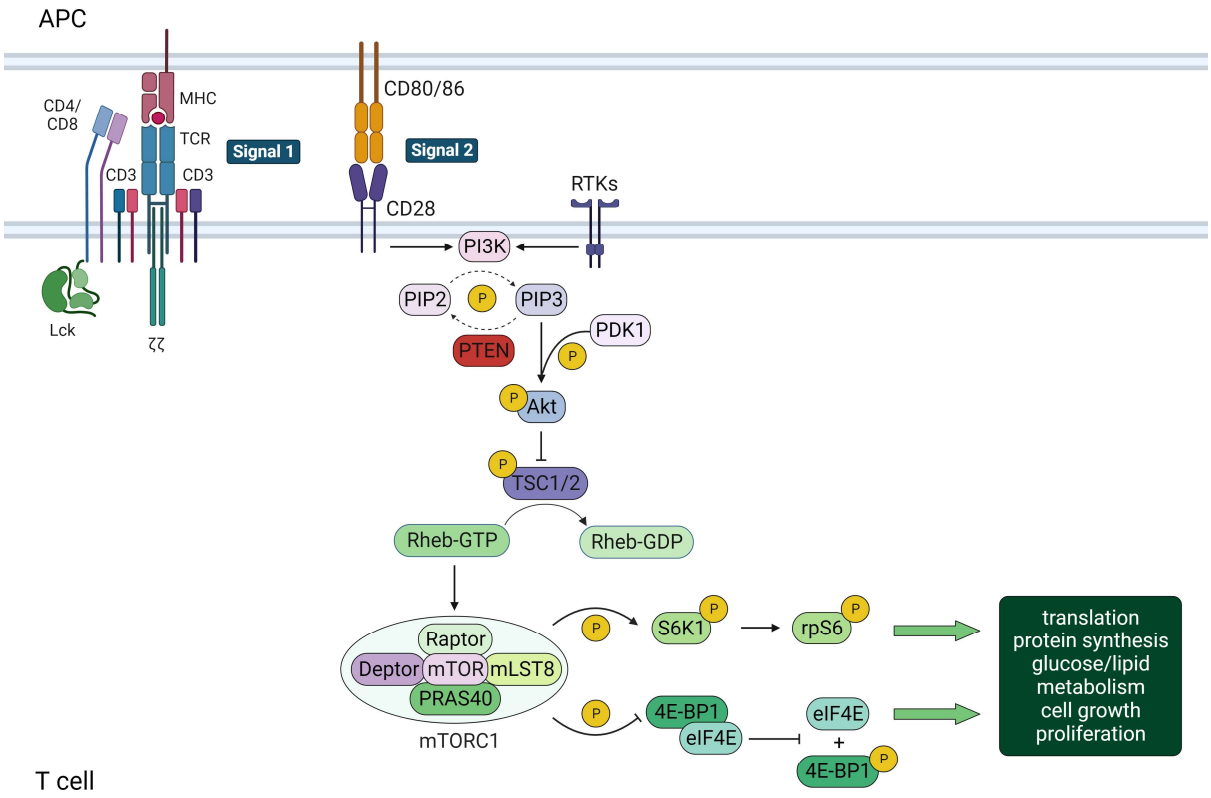

Figure 4 Schematic overview of the PI3K/Akt/mTOR signalling events. mTOR pathway activation upon TCR signalling is triggered independently of LAT signalosome but upon PI3K binding to the CD28 costimulatory receptor. Ultimately, the PI3K/Akt/mTOR signalling cascade promotes cellular, growth, proliferation, survival, and modifications in cellular metabolism. A detailed description of the signalling cascade is provided in the accompanying text. Figure created with BioRender.com.

The signalling cascade starts upon PI3K kinase activation following binding to CD28 receptor (Garçon et al. 2008). Subsequently, PI3K phosphorylates PIP2 localized on the cytosolic side of plasma membrane and generates PIP3. Several tyrosine kinases require PIP3 for their activity, such as Itk or PDK1. While Itk is required for the activation of transcription factors crucial for T cell activation, PDK1 propagates Akt signalling (Rogel et al. 2017). Phosphorylation of Akt directly suppresses the GTPase activity of TSC1/2, which controls the hydrolysis of RhebGTP. RhebGTP is a GTP-binding protein, playing a crucial role in activating mTORC1 signalling and its downstream effectors S6K1 and 4E-BP1 (Y. Li et al. 2004; Inoki et al. 2002). Subsequently, S6K1 phosphorylates ribosomal protein S6, while phosphorylation of 4E-BP1 causes the release of eIF4E, which promotes protein synthesis (Y. Li et al. 2004; Megat and Price 2018). Ultimately, the mTORC1 pathway signalling

results in the increase of protein production, metabolism222, stimulation of cell growth and proliferation (Waickman and Powell 2012; Herrero-Sánchez et al. 2016).

1.11 PD1 pathway

The recognition of an antigen by the TCR is followed by multiple signalling events as well as the physical formation of the immune synapse. Simultaneously, all components involved in the TCR signalling are recruited to the site of antigen recognition and are in proximity. This comprises costimulatory molecules such as CD8 or CD28 and coinhibitory receptors like CTLA-4 and PD1 (Garçon et al. 2008). Therefore, the outcome of the T cell antigen challenge is an interplay between stimulatory and inhibitory signals coming from intra- and extracellular environment and often relies on the negative feedback loops. Importantly, the presence or absence of specific costimulatory or inhibitory molecules determines the employment of certain proteins for activation of pathways with opposing functions (Nurieva et al. 2006; Attanasio and Wherry 2016).

For example, Lck and Fyn, members of the Src family tyrosine kinases, play dual roles in mediating T cell activation and PD1 signalling - two pathways with opposing effects. A key event in the activation is the formation of the immune synapse, which is partially supported by CD4/CD8 stabilization of the TCR - antigen binding. The intracellular domain of CD8 receptor stably associates with the Lck kinase, which initiates the early phosphorylation evens of the TCR signalling. As outlined in the previous paragraph, Lck kinase propagates T cell activation by phosphorylation of ITAMs localized in the cytosolic domain of the TCR complex (Laird and Hayes 2010; Chatterjee et al. 2013). Recently, it was demonstrated that Lck can also phosphorylate the tyrosine residues Y223 in ITIM (Immunoreceptor Tyrosine-based Inhibition Motif) and Y248 in ITSM (Immunoreceptor Tyrosine-based Switch Motif) of PD1 immune checkpoint receptor. Ultimately, apart from propagating the activation of TCR signalling, Lck and Fyn are crucial for the activation of PD1 pathway, which dampens the T cell activation (Hui et al. 2017; Chatterjee et al. 2013; Bardhan, Anagnostou, and Boussiotis 2016).

In T cells, PD1 becomes phosphorylated only upon engagement by its ligands PDL1 or PDL2. It was demonstrated that Y248 tyrosine phosphorylation in the ITSM motif of PD1 is crucial for the downstream recruitment of SH2 domain-containing tyrosine phosphatases, mostly SHP-2 (PTPN11) and to lesser extend SHP-1 (Rota et al. 2018). Y248 phosphorylation of PD1 followed by the recruitment of SHP-2 was proven crucial to mediate the inhibitory effects of PD1 on T cells and was linked to impaired cytokine synthesis and T cell functional exhaustion (Bardhan et al. 2019; Patsoukis, Duke-Cohan, et al. 2020).

Mechanistically, when recruited to PD1, SHP-2 drives the dephosphorylation of proteins involved in the activation of T cells. This effectively abrogates the stimulatory signalling (depicted in **Figure 5**), making SHP-2 a key downstream

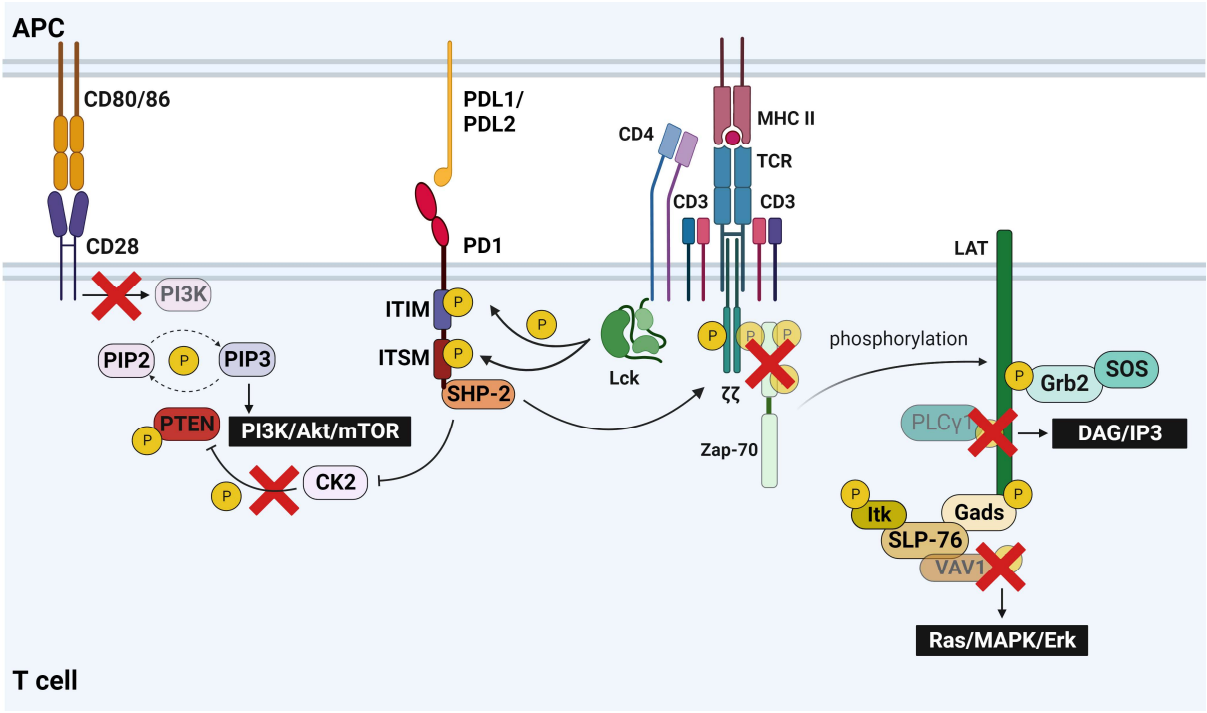

Figure 5 PD1 signalling cascade in T cells. PD1 engagement by is ligand PDL1 abrogates signalling cascades downstream the TCR and CD28 receptors and inhibits Ras/MAPK/Erk; DAG/IP3 and PI3K/Akt/mTOR signalling cascades. Figure created with BioRender.com.

effector of PD1 signalling pathway (Strazza et al. 2021). SHP-2 was demonstrated to preferentially dephosphorylate CD28 receptor over other proteins, therefore abrogating PI3K/Akt/mTOR activation. Additionally, to a considerably lesser extent, SHP-2 targets CD3 and ʒ phosphorylation sites along with other TCR downstream

effectors such as ZAP-70, or PLCγ and VAV, which are members of LAT signalosome. Ultimately, it attenuates Ras/MAPK/Erk pathway and calcium signalling (Marasco et al. 2020).

Therefore, SHP-2 acts as a downstream effector of PD1 pathway, inhibiting pathways crucial for T cell activation, differentiation, growth, and survival. Additionally, PD1 signalling facilitates the activity of PTEN molecule, which is a phosphatase dephosphorylating PIP3 to PIP2 (Peng et al. 2016). Through this indirect mechanism, PD1 activation further abrogates PIP3 mediated Akt signalling. PTEN activity is regulated through PD1-mediated inhibition of CK2 kinase. CK2 kinase acts as an inhibitor of PTEN by maintaining its phosphorylated state and blocks PTEN ability to carry out the dephosphorylation of PIP3 to PIP2 (Patsoukis et al. 2013; Torres and Pulido 2001).

1.12 Downstream effects of PD1 signalling in T cells

Understanding the complex mechanism of TCR downstream signalling and how it is abrogated by PD1 activation, reveals that the PI3K/Akt/mTOR and Ras/MAPK/Erk pathways are particularly impacted. Considering that these signalling cascades play the central role in T cell activation, differentiation, proliferation, and survival, it becomes evident that multiple fundamental processes become altered upon activation of PD1 pathway.

1.12.1 Cell cycle

Naïve T cells reside in the G0 phase of the cell cycle and their entry into G1 and S- phase progression happens only when a cascade of molecular events is triggered. These events heavily rely on PI3K/Akt and Ras/MEK/ERK signalling, antigen recognition, CD28 co-stimulation and subsequent IL-2 production (Da and Ly 2021). Cell cycle is a tightly controlled process, which requires multiple factors such as cyclins, cyclin dependent kinases (CDKs) and their inhibitors. Specific cyclins govern distinct steps of the cell cycle, for example cyclin G1 is associated with entry into G1, cyclin E with late G1 and cyclin A is characteristic of the S-phase (Chang et al. 2003). Cyclins activity strictly relies on the complexes with their specific kinases and can be abrogated by their dedicated inhibitors. However, cyclin kinase inhibitors can be removed through E3 ligase ubiquitination, a process releasing cyclin-

dependent kinases and restoring the activity of cyclin-CDK holoenzymes (Choudhury et al. 2017; Patsoukis, Sari, and Boussiotis 2012).

Modifications of CDKs inhibitors partially account for PD1-mediated inhibition of the cell cycle in activated lymphocytes. It was indicated that by modulating Akt signalling, PD1 supresses transcription of the *SKP2* gene encoding an integral part of the SCF^{Skp2} ligase, which controls $p27^{kip}$ degradation (Spruck and Strohmaier 2002; Choudhury et al. 2017). $p27^{kip}$ is a cyclin-dependent kinase inhibitor of cyclin A-CDK2 and cyclin E-CDK2 complexes. Upon $p27^{kip}$ proteasomal degradation, cyclin-CDKs complexes restore their functional activity and ability to drive cell cycle progression (Patsoukis, Sari, and Boussiotis 2012). Thus, by diminishing the activity of the SCF^{Skp2} ligase, PD1 modulates cyclin-CDKs activity and prevents entry into G_1 phase (Patsoukis et al. 2012; Tsvetkov et al. 1999; Timmerbeul et al. 2006).

Alternatively, but again through PI3K/Akt/mTOR axis, cell cycle progression can be controlled by PD1-mediated suppression of mTORC1 signalling. S6K, the downstream effector of mTORC1, most probably activates E2F activity (Patsoukis et al. 2012). E2F is a group of key transcription factors responsible for the expression of proteins required for cell cycle progression and entry into the S-phase (Patsoukis, Sari, and Boussiotis 2012). E2F is naturally supressed by Rb and related proteins. However, the suppressive effect of Rb may be overcome by its hyperphosphorylation driven by cyclin D–CDK4 or cyclin D-CDK6 complexes, which are activated in response to Akt signalling (Weinberg 1995). Consequently, Rb decouples from E2F, enabling E2F-mediated transcription of genes encoding proteins crucial for S-phase progression, such as cyclin E and cyclin A (Patsoukis et al. 2012). Therefore, by inhibiting the PI3K/Akt pathway and affecting various factors controlled by this axis, PD1 alters cell cycle progression through G1 and S-phase. **Figure 6** provides a schematic summary of the mechanisms involved in cell cycle control by PD1 pathway.

Moreover, cell cycle progression in activated T cells may be additionally controlled by Ras/MEK/ERK pathway, however selective mutation, and inhibition studies

demonstrated that PI3K/Akt pathway appears to be indispensable for the full inhibitory effect of PD1 signalling (Patsoukis et al. 2012).

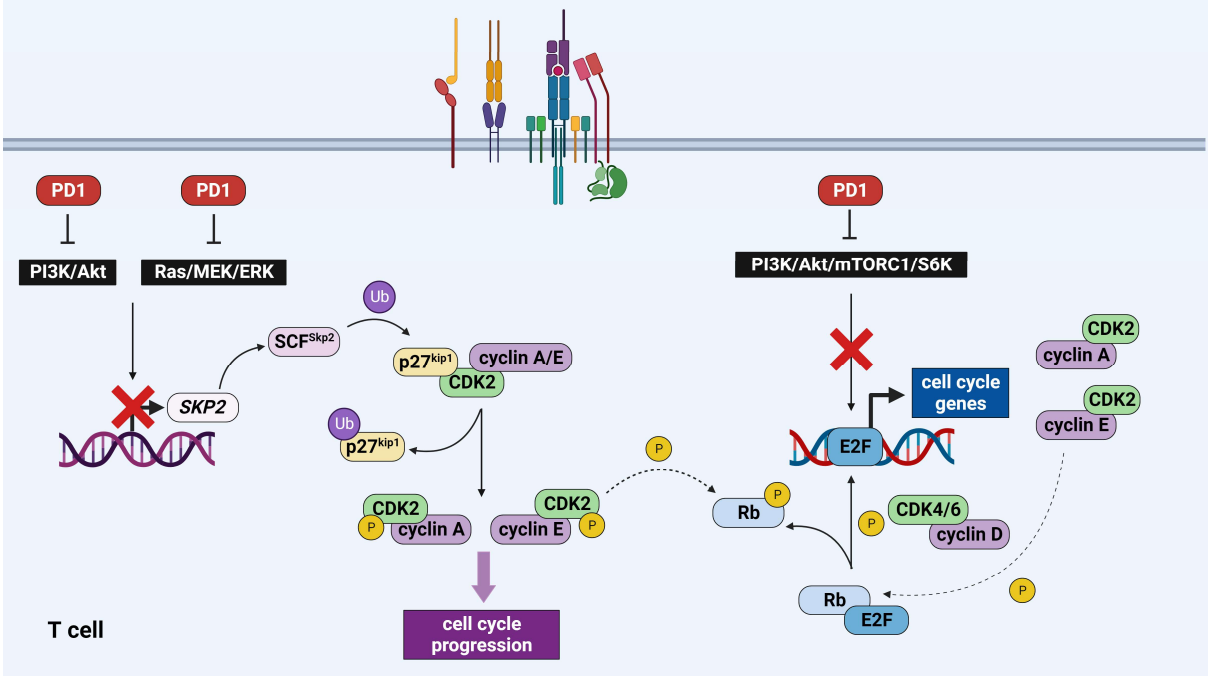

Figure 6 Schematic summary of PD1-mediated cell cycle control in T cells. PD1 supress cell cycle progression by affecting PI3K/Akt and Ras/MEK/ERK signalling, followed by modulation of cyclin-CDK activity. Inhibition of the most important effector mechanism was denoted with a **red X**. For a detailed description of the signalling cascade, refer to the main text. Figure created with BioRender.com.

1.12.2 Glucose metabolism

The T cell activation reshapes cellular metabolism to meet elevated energetic demands and is associated with increased glucose uptake to produce energy and building blocks for macromolecules. This can be achieved by either increased expression of glucose transporters or metabolic reprogramming (Frauwirth and Thompson 2004).

Glucose uptake in T cells is regulated by PI3K/Akt pathway in response to the CD28 costimulatory receptor signalling. This leads to increased membrane expression of glucose transporter Glut1, therefore facilitating glucose uptake by the cells (Frauwirth et al. 2002; Shyer, Flavell, and Bailis 2020; Barthel et al. 1999). Additionally, the Akt pathway was reported to upregulate the expression of hexokinase 2, which is a critical enzyme for intracellular glucose phosphorylation and its subsequent entry into the glycolytic cycle (Rathmell et al. 2003).

Resting naïve T cells primarily rely on mitochondrial oxidative phosphorylation to generate ATP. However, upon activation, T cells switch to aerobic glycolysis, even in the presence of sufficient oxygen levels and functional mitochondria (Liberti and Locasale 2016). During glycolysis, the energy can only be generated from glucose, whereas oxidative phosphorylation can utilize various macromolecules such as amino acids or lipids. In rapidly growing cells, amino acids and lipids serve as building blocks for nucleic acids and proteins rather than as a source of energy. Thus, switching to glycolysis preserves these molecules, while glucose metabolism is utilized to produce energy (Vaupel and Multhoff 2021). Considering PI3K/Akt pathway as the core regulator of T cell glucose metabolism, this process becomes naturally affected upon PD1 signalling. PD1 disrupts the PI3K/Akt pathway, therefore limits glucose uptake and glycolytic rate, both by inhibiting CD28 signalling and by increasing PTEN activity, as described earlier (Peng et al. 2016; Torres and Pulido 2001).

Although PD1 signalling hinders T cell metabolic reprogramming towards oxidative glycolysis, these cells remain metabolically active. In CD4+ cells, PD1 signalling is associated with increased expression of adipose triglyceride lipase (ATGL) and CPT1A. ATGL mediates triglyceride hydrolysis, while CTP1A is a crucial enzyme involved in fatty acid ß-oxidation (FAO). Notably, in memory T cells FAO facilitates their long-term survival. It was hypothesized that FAO may enable exhausted T cells to persist over time, despite experiencing continuous PD1 inhibitory signalling. It was proposed, that by displaying this memory cells-like phenotype and sustained metabolic activity, T cells may become reinvigorated upon immune checkpoint blockade. (Pearce et al. 2009; Patsoukis et al. 2015; Chatterjee et al. 2013) Overall, in the context of chronic infections and cancer, prolonged PD1 signalling affects glucose metabolism reprogramming and contributes to T cell functional exhaustion.

In summary, the PD1 signalling pathway and the downstream cellular effects are well described in T cells. However, only scarce reports are available describing the PD1 pathway in cancer, while some propose it as a mechanism of resistance to immunotherapy. Considering the contradictory results regarding the significance

of cancer-intrinsic signalling and its impact on immunotherapy, further studies on cancer-expressed PD1 are urgently needed. Better understanding of the molecular mechanisms underlying PD1 signalling in cancer will not only improve our knowledge but also holds the potential for novel targeted cancer treatments.

2. Materials and methods

2.1 Cell culture

U2OS human osteosarcoma cell line was obtained from Elabscience, cat. CL-0236. The cells were cultured in modified McCoy's 5A medium (Gibco, cat. 16600082) supplemented with 10% heat inactivated FBS (Gibco, cat.10500064) and 100UI/ml Penicillin-Streptomycin (Gibco, cat. 15140122) in the humidified atmosphere supplemented with 5% CO_2 at 37°C.

2.2 Attractene transfection of U2OS cells with plasmid vectors

200000 cells were seeded per well of a 6-well plate 24 hours prior to the transfection. The transfection was performed using Attractene transfection reagent (Qiagen, cat. 301005) and either empty vector control or PD1 WT, PD1 Y223F or PD1 Y248 pcDNA 3.1 plasmid vector. Following the manufacturer's protocol and the initially optimized transfection conditions, 1.8µg of plasmid DNA was diluted with supplement free media to 100µl. Then, 6.75µl of Attractene transfection reagent was added and incubated for 15 minutes at RT to allow complex formation. Transfection complexes were added dropwise to the cells grown in 2.5ml of cell culture media. Subsequently, for transient transfection, the cells were cultured for 48 hours and collected for experiments. To create stable cell lines, the cells were incubated for 24 hours before replacing the media to the antibiotic selection media. PD1 vectors encoded the neomycin resistance gene, and successfully transfected cells were selected by 2-week incubation in 400µg/ml Geneticin (Roche, cat. G418-RO) selection media. Empty vector control plasmid encoded hygromycin B phosphotransferase gene, and stably transfected cells were selected for 2 weeks in 100µg/ml Hygromycin B (Gibco™, cat. 10687010) media.

2.3 siRNA mediated PD1 knockdown in U2OS cells

Three different *Silencer*® Select pre-designed siRNA oligonucleotides were purchased from Life Technologies LTD. Arbitrary names were assigned to each construct for simplicity. The names, catalogue numbers and sequences are listed in **Table 1**.

Table 1 Sense and antisense sequences of siPD1 oligonucleotides used for PD1 interference.

Label	ID	Sense sequence (5'→3')	Antisense sequence (3'→5')
siPD1 #1	s10171	GCUUCGUGCUAAACUGGUAtt	UACCAGUUUAGCACGAAGCtc
siPD1 #2	s10172	GGGCGUGACUUCCACAUGAtt	UCAUGUGGAAGUCACGCCCgt
siPD1 #3	s226730	ACAGGACUCAUGUCUCAAUtt	AUUGAGACAUGAGUCCUGUgg
negative control	cat. AM4611	-	-

Following the manufacturers guidelines, the cells were seeded 24 hours prior to the transfection. On the day of transfection, 10μM dilution of silencing RNA targeting *PDCD1* or non-targeting siRNA negative control were prepared in OptiMEM (Gibco™, cat. 31985070) and mixed with Lipofectamine® RNAiMAX transfection reagent (Invitrogen™, cat. 13778100). Number of cells seeded for experiments and volumes of reagents depended on the scale of an experiment; 3000 cells and 0.3μl of Lipofectamine per well of a 96-well plate and 200000 cells and 7.5μl of Lipofectamine per well of a 6-well plate. The cells were incubated for 48 hours on 6-well plates to be used for Western Blot, flow cytometry, scratch assay, and proteomic analysis. Experiments performed on 96-well plates were incubated for 96 hours and were used to perform cell viability assays.

2.4 Protein isolation for Western Blot

Prior to protein isolation, cells were washed two times with PBS and lysed directly on a cell culture plate with ice-cold CelLytic™ M lysis buffer (Sigma-Aldrich, cat. C2978) supplemented with appropriate amount of protease inhibitor cocktails (Sigma-Aldrich, cat. P8340-1ML). Lysates were gently mixed on ice for 20 minutes and centrifuged for 15 minutes at 14,000x*g* at 4°C. Protein concentration in the supernatant was quantified by Bradford assay. Lysates were mixed with 4X reducing sample buffer and samples were denatured by boiling for 5 minutes at 95°C.

2.5 Immunoblotting

Protein lysates or samples obtained through pull-down were resolved by 8% SDS-PAGE using standardized protein amounts of 20-50µg per well. The resolved proteins were then transferred onto a nitrocellulose blotting membrane (Amersham Protran®, cat. 10600004) using Trans-Blot® Turbo™ Transfer System (Bio-Rad). Subsequently, membranes were blocked overnight in 5% non-fat milk in 0.1% Tween 20 Phosphate buffered saline (PBS) at 4°C. Next, membranes were washed three times with 0.1% PBST and incubated overnight at 4°C with one of the following antibodies diluted in 2% blocking buffer: anti-PD1 UltraMAB™ dilution 1:500 (clone UMAB199, OriGene, cat. UM800091 or anti-AXL dilution 1:1000 (clone C89E7, Cell Signalling, cat. #8661). Restore Plus Western Blot Stripping Buffer (Thermo Scientific™, cat. 46430) was used when membrane reprobing with 1:10000 dilution of anti-ß-actin (abcam, cat. ab6276) was performed. Following primary antibody incubation, membranes were washed three times with PBST and incubated for 1 hour at RT with HRP-conjugated secondary antibodies: goat anti-rabbit, dilution 1:10000 (abcam, cat. ab97051) or rabbit anti-mouse, dilution 1:5000 (abcam, cat. ab6728). Finally, membranes were washed three more times with PBST, visualized by ECL substrate (Westar Antares, CYANAGEN, cat. XLS142,0250) and ChemiDoc imaging system (Bio-Rad).

2.6 Flow cytometry

Cells were dissociated from cell culture plates, then 1,000,000 of cells were aliquoted into flow cytometry tubes and centrifuged for 5 minutes at 1500rpm. Cell pellets were washed with PBS and centrifuged for 5 minutes at 1500rpm. Cells were stained for the surface expression of PD1 with 5µl of PE-Cy7 conjugated anti-PD1 antibody (clone MIH4, Invitrogen, cat. 25-9969-42) for 30 minutes at RT, protected from light and washed two times with PBS. Cells were fixed-permeabilized for 30 minutes using eBioscience™ Foxp3/Transcription Factor Fixation/Permeabilization Concentrate and Diluent (Invitrogen, cat. 00-5521-00) and washed with Perm-Wash working solution. It was followed by intracellular staining of PD1 protein with 5µl of APC conjugated anti-PD1 antibody (clone MIH4, Invitrogen, cat. 17-9969-42) for 30 minutes at RT, protected from light. The cells were washed twice with Perm-Wash working solution by 5-minute centrifugation at 1500rpm. Cell pellets were resuspended in 500µl

of PBS and analysed with BD FACSAria II cell sorter (BD Biosciences). Results were analysed with FlowJo v10.8.1 flow cytometry analysis software (BD Biosciences).

2.7 Analysis of *PDCD1* gene expression by RT-qPCR

2.7.1 RNA isolation

Total RNA was isolated from approximately 1,000,000 of cells following the manufacturer protocol for RNeasy mini kit (Qiagen, cat. 74104). During isolation, an additional step of DNA digestion was applied using RNase-Free DNase Set (Qiagen, cat. 79254) following the manufacturer instructions.

2.7.2 cDNA generation

Reverse transcription was performed with High-Capacity cDNA Reverse Transcription Kit (Applied Biosystems™, cat. 4368814), using 10µl of previously isolated RNA. 0.5µl of RNaseOUT™ (Invitrogen™,cat. 10777019) per sample was used instead of 1µl of RNase inhibitor recommended in the manufacturer protocol. The remaining volume was topped up to 20µl with nuclease-free water. The reaction was conducted accordingly to the kit instructions in ProFlex PCR System thermal cycler (Applied Biosystems™ by Life Technologies).

2.7.3 RT-qPCR

Subsequently, the quantitative real-time PCR analysis of *PDCD1* expression was performed with TaqMan Gene Expression assay following the manufacturer instructions. cDNA was diluted 50x and approximately 400ng (1µl) of cDNA template was used per 20µl reaction of TaqMan® Gene Expression Assay. Subsequently, 10µl of 2X TaqMan® Master Mix II with UNG (cat. 4304437, Applied Biosystems™) were mixed with 1µl of *PDCD1* Hs01550088_m1 TaqMan™ Gene Expression Assay (FAM, ThermoFisher Scientific, cat. 4331182). *GAPDH* was used as a housekeeping gene control, which expression was measured with Hs02758991_g1 TaqMan® TaqMan™ Gene Expression Assay (FAM, ThermoFisher Scientific, cat. 4331182). All reactions were performed in technical triplicates for each biological replicate using Rotor-Gene Q real-time cycler (Qiagen). Relative quantitative analysis was performed using $2^{-\Delta\Delta Ct}$ method based on the Ct values obtained from thermal cycler Rotor-Gene Q Series Software version 2.3.1. The statistical significance of the fold change

expression of *PDCD1* transcript levels was calculated and visualized in GraphPad Prism version 9.1.1.

2.8 Scratch assay

200,000 cells were seeded per well of a 6-well plate and incubated for 48 hours prior to the experiment to reach full confluency. On the day of experiment, a scratch on monolayer culture of cells was made with a p200 pipette tip, the cells were washed with PBS to remove cell debris and fresh media was applied. The cells were imaged immediately at 0 hour and then every several hours tracking the same imaging area after 6, 12, 24 and 32 hours. Images were acquired at 40X magnification using Opta-Tech MW50 bright field microscope. Wound area was calculated by analysing images at a given timepoint using an Image J wound healing size tool plugin. Detailed description of the assay protocol was described by Liang et al., 2007 (Liang, Park, and Guan 2007).

2.9 Cell viability assay

100µl of plating media was used to seed 3000 cells per well of a 96-well opaque-walled plate. After 24 hours, media was replaced in PD1 OE stable cell lines, while U2OS wild-type cells were transfected with siRNA constructs. The cells were further cultured for additional 96 hours. Cellular viability was assessed by measuring ATP as an indicator of metabolically active (viable) cells using CellTiter-Glo® assay (Promega, cat. G7571). The assay was performed following the manufacturer protocol. Briefly, on the last day of the experiment, CellTiter-Glo® Buffer and CellTiter-Glo® Substrate were thawed and equilibrated to room temperature. Then, the substrate was reconstituted in the buffer. Meanwhile, the cells were removed from the cell culture incubator and equilibrated to room temperature for 30 minutes. Subsequently, 100µl of CellTiter-Glo® reagent per well was added to the cells and mixed for 2 minutes on an orbital shaker to lyse the cells. Next, plates were incubated for 10 minutes at room temperature to stabilize luminescent signal. Results were obtained by measuring luminescent signal as an indicator of cell viability using Thermo Scientific™ Varioskan™ LUX multimode microplate reader. Further data analysis and statistical calculations were performed with GraphPad Prism version 9.1.1.

2.10 Liquid chromatography – mass spectrometry analysis

2.10.1 Sample processing

Cells were washed two times with ice-cold PBS and scraped off from cell culture dishes and pelleted by two centrifugations with PBS at 4°C, 1500rpm, 5 minutes each time. Pellets were snap-frozen and kept at -80°C until further processing. Then, samples were lysed in 8M urea buffer (in 0.1M Tris, pH=8.5) mixed with protease inhibitors (Roche, cat. 11836170001), vortexed briefly and incubated for 30 minutes on ice with gentle swinging. It was followed by 10-minute sonication on ice. Then, samples were snap-frozen and thawed three times and transferred to -80°C freezer overnight. Next day, samples were thawed and centrifuged at 8°C for 30 minutes at 13,300x*g*. Supernatant was transferred to new tubes and protein concentration was determined using BCA assay (ThermoFisher Scientific, cat. 23225).

2.10.2 Peptide generation through FASP

Peptides were generated following a modified filter-aided sample preparation (FASP) protocol described by Wisniewski et al. (Wiśniewski et al. 2009). In brief, 200µl of urea buffer was applied onto Microcon Ultracel-10 spin filter column with 10 kDa cutoff (Millipore, cat. MRCPRT010), followed by loading approximately 100µg of protein lysate per column. Specimens were mixed by pipetting up and down and centrifuged at 20°C, 17000x*g* for 30 minutes. In the following step, protein reduction was performed by adding 100µl of urea buffer and 20µl of 100mM Tris (2-carboxyethyl) phosphine hydrochloride (Merck, cat. C4706) and incubating for 30 minutes at 37°C with agitation at 600rpm. Then, samples were centrifuged for 20 minutes at 17000x*g*. Subsequently, for protein alkylation, 100µl of urea buffer and 20µl of 300mM iodoacetamide were applied onto columns and mixed for 1 minute at 20°C, 600rpm. Next, samples were incubated for 20 minutes at room temperature, protected from light, and centrifuged at 17000x*g* for 20 minutes. For pull-down samples processing, three additional washes with 100µl of urea buffer were applied at this point. For a complete removal of the detergent from the columns' wall samples were vortexed briefly and centrifuged for 30 minutes at 17000x*g*. Subsequently, columns were washed three times with 100µl of 100mM ammonium bicarbonate and centrifuged for 20 minutes at 17000x*g* each time. For protein digestion, 100µl of 50mM ammonium bicarbonate and 3µl of 1µg/µl trypsin solution were added

onto each column and incubated overnight at 37°C in a humidity chamber. On the following day, peptides were eluted into fresh collecting tubes by 15 minutes centrifugation at 17000x*g*. To increase peptide yield, second elution step was applied with 50µl of 0.5M sodium chloride and 15 minutes centrifugation at 17000x*g*.

2.10.3 Peptide desalting

MicroSpin C18 columns (Harvard Apparatus, cat. 744601) were used to desalt tryptic peptides following a modified protocol initially described by Bouchal et al. (2009) (Bouchal et al. 2009). Briefly, columns were conditioned three times with 200µl of ACN (acetonitrile) with 0.1% FA (formic acid) each time followed by 2-minute centrifugation at 200rpm. Then, columns were equilibrated with 200µl of water with 0.1% FA and centrifuged for 2 minutes at 300rpm. Subsequently, the slurry was hydrated with 200µl of water with 0.1% FA for 15 minutes and centrifuged for 2 minutes at 300rpm. Peptides were transferred onto hydrated columns and centrifuged for 2 minutes at 500rpm. Next, samples were washed three times with 200µl of water with 0.1% FA and centrifuged for 2 minutes at 500rpm each time. Then, C18 columns were transferred into fresh collecting tubes and peptides were eluted with 200µl of 50% ACN with 0.1% FA and additionally two more times with 80% ACN with 0.1% FA, all centrifugation steps were performed for 2 minutes at 500rpm. Finally, all specimens were dried by vacuum centrifugation using Eppendorf™ Concentrator Plus system (Eppendorf) for approximately 3 hours at 30°C in VC-AQ mode. Dried peptides were stored at -80°C until LC-MS/MS analysis.

2.10.4 Liquid chromatography-mass spectrometry (LC-MS/MS) analysis

The dried samples were dissolved in 30µl of the loading buffer containing 0.08%(v/v) trifluoroacetic acid (TFA), 2.5%(v/v) ACN in water, vortexed thoroughly and sonicated for 5 minutes to be completely dissolved. Subsequently, 220nm and 280nm absorbance of the samples was measured using Life Real micro UV-Vis spectrophotometer to normalize peptide concentrations in all samples. A mix of iRT (indexed Retention Time) calibration peptides (Biognosys, cat. Ki-3002-1) was added to each sample. Next, 6 µl (approximately 1µg) of peptides were injected into and separated using UltiMate™ 3000 RSLCnano System (ThermoFisher Scientific) coupled with Orbitrap ExplorisTM 480 mass spectrometer (ThermoFisher Scientific). The analysis included three biological replicates, while each sample was subjected

to three technical replicate measurements. Upon injection, peptides were trapped and concentrated on PepMap™ Neo Trap C18 cartridge with 300µm inner diameter, 5mm length, packed with 100Å pore size 5µm particles. (ThermoFisher Scientific, cat. 174500). Next, at 300nl/min flow rate, peptides were separated on Acclaim™ PepMap™ RSLC 100 C18 reverse phase analytical column, 75µm inner diameter, 250mm length, packed with 100Å pore size 2µm particles (ThermoFisher Scientific, cat. 164941). The analytical column equilibration was performed for 10 minutes with 2.5 to 97.5 ratio of solvent B (0.1% (v/v) TFA in ACN) to A (0.1% (v/v) TFA in H_2O), respectively. For peptide separation, a 90-minute gradient increase of solution B from 2.5% to 40% was used. It was followed by 2-minute gradient increase of solvent B, reaching 99**%,** then column equilibration was performed after each run with 2.5% solvent B for 8 minutes. Peptides eluted from the analytical column were ionized with Nanospray Flex Ion Source. Next, the ions entered Orbitrap Exploris 480 mass spectrometer operating in a high voltage (2500V) resolution positive ion mode. The temperature of the ion transfer tube was set to 250°C and the data was acquired both in DDA and DIA modes. For the MS1 in DDA mode, the Orbitrap Resolution was set to 120000, scan range 350-1200*m/z*, AGC (automatic gain control) in custom mode and normalized AGC target of 300%, while the maximum injection time was in auto mode. To prevent repeated analysis of the same precursor ion, dynamic exclusion mode was set to custom mode, exclusion was made after one time and 20 seconds duration time, mass tolerance was set to 10ppm. Precursor ion selection for higher-energy C-trap dissociation (HCD) and MS2 scan was based on the precursor charge state set between +2 and +6 and intensity threshold higher than 5.0e3. MS2 was set to perform 15 fragmentation scans. In MS2 scan properties, *m/z* isolation window was set as 2, HCD collision energy 30% with maximum injection time of 40ms and Orbitrap resolution of 15000. In the data-independent acquisition (DIA) mode and the full-scan analysis Orbitrap resolution was 60000, *m/z* scan range was set between 350 and 1450, AGC in custom mode, AGC target set to 300% and maximum injection time was 100ms. In the DIA scan parameters *m/z* precursor mass range was set between 350 and 1100, DIA window type to auto and its mode as *m/z* range; *m/z* isolation window was set to 12 and *m/z* window overlap to 1, HCD collision energy was 30% and in normalized mode, Orbitrap resolution 3000, AGC in custom mode and normalized AGC target set to 1000%. Maximum injection time

and scan range were in auto mode, and microscan was set to 1. Data acquisition was performed by Dr Jakub Faktor and Dr Artur Pirog.

2.10.5 Spectral library and MS data analysis

The raw DDA Mass Spectrometry data was searched with FragPipe (v15.0) against human proteome database downloaded from UniProt (closed search). The database was accessed on 14 October 2021, and encompassed a total number of 78120 entries, comprising 20371 SwissProt reviewed entries and 57749 TrEMBL unreviewed entries. Additionally, sequences for the recombinant PD1 protein (listed in the “plasmid vectors” section) and iRT peptide (Biognosys, cat. Ki-3002-1) sequences were manually incorporated into the database. Subsequently, equal number of reverse and common contaminant protein sequences were generated in FragPipe and added to the search database. In the search settings, protein digestion was specified to trypsin enzymatic cleavage. Precursor mass tolerance was set to ±8ppm and fragment mass tolerance to 10ppm. Fixed modifications comprised carbamidomethylation of cysteine residues and variable modifications included methionine oxidization and N-terminal acetylation. Other settings were maintained at their default. Trans Proteomic-Pipeline (TPP 6.0.0) (Deutsch et al. 2010) tools including PeptideProphet (Keller et al. 2002) and iProphet (Shteynberg et al. 2011) were utilized for further analysis of the pep.XML search files and recalculation of their iprobabilities. Next steps of the analysis were performed in Skyline-daily (64-bit, 20.1.9.234) where the recalculated iprobability files were used to build a spectral library stored in .blib format. The iprobability cut-off score was set to 0.99 and library used in the previous step for FragPipe search was used to match the remaining peptides to their precursors. Peptides matching multiple proteins were excluded from the spectral library. The spectral library was required to extract peptides intensities from DIA files and perform the quantitative analysis, which utilized tryptic peptides of length between 2 to 60 amino acids. Filters used for peptides transition settings included precursor charges from +1 to +5, ion types y and b; and the product ion charges +1 or +2. Ion mass tolerance was set to 0.05*m/z*, and only the peptides with minimum 3 transition product ions were considered for the analysis. If multiple product ions were detected, then 6 most intense were chosen for the quantitation. In the full-scan settings, DIA was set as the acquisition method and Orbitrap as the mass

analyser with resolving power 30000 at 200*m/z*. Retention time filter was set to 7 minutes of MS/MS IDs. The target transitions were refined by adding the corresponding number of reverse decoy transitions. Subsequently, raw DIA data were imported into Skyline-daily, and both the target peptides and decoys were used to train the mProphet scoring model. This step allowed to refine the peak group boundaries and obtain their mProphet q values (Reiter et al. 2011). The results were exported including all dependencies so they could be used for further analysis (Choi et al. 2014).

2.10.6 Statistical analysis and data visualization

Data exported from Skyline-daily were used for further processing in *MSstats 4.0.1.* R package (version 2022.12.0). First, the data was filtered out for any truncated or false positive peak groups with q-value > 0.01 (FDR<1%). Next, the data was annotated, and peak group intensities were transformed to log2 scale and quantile normalized. Further analysis was performed using sums of protein intensities. *MSstats* group comparison function of mixed-effect models was implemented for the pairwise relative comparison of protein abundance across all experimental conditions. The adjustment of p-values was performed with Benjamini-Hochberg method. Custom Python 3.9.13 scripts were employed to annotate protein abundance comparisons. The gene set enrichment analysis was performed using *gseGO* function within clusterProfiler 4.0 package (T. Wu et al. 2021). The resulting analysis of GO pathways were visualized by implementing Enrichment Map for enrichment result of over-representation test or gene set enrichment analysis emapplot and ridgeplot functions. The above-listed steps of statistical analysis were performed by Dr Jakub Faktor, while the following was done independently. Protein interacting network was analysed and visualised using STRING database: http://string-db.org (Szklarczyk et al. 2014). Unique and overlapping proteins significantly changed in the experiments were plotted with Deep-Venn diagrams (Hulsen 2022).

2.11 Pull-down assay

For one biological replicate, the cells were directly lysed on two 80% confluent 15cm cell culture dishes using 500µl of ice-cold Pierce IP lysis buffer per plate (Thermo Scientific™, cat. 87787) containing protease inhibitor cocktail (Roche, cat. 11697498001). Cell lysates were incubated on ice for 25 minutes applying gentle

swinging and centrifuged for 20 minutes at 14000x*g* at 4°C. Total protein concentration in the supernatant was measured using Pierce™ BCA Protein Assay Kit (Thermo Scientific™, cat. 23227) and 2mg of total protein lysate was used for the pull-down experiment. Following the manufacturer protocol, 60µl of 5% suspension of MagStrep "type3" XT magnetic beads (IBA-Lifesciences, cat. 2-1613-002) were equilibrated in the wash buffer (IBA-Lifesciences, cat. 2-1003-100) and added to the cell lysate. Samples were incubated for 1 hour at 4°C with gentle rotation. Lysates were placed in a magnetic separator, PD1-bound proteins were washed three times and eluted in 75µl of 1X reducing Laemmli buffer by boiling each sample for 2 minutes at 95°C. Eluted samples were further used for LC-MS/MS or Western Blot analysis.

2.12 Alexa Fluor™ 488 Tyramide SuperBoost™ staining

800,000 cells were seeded on 18mm cover slips in a 6-well plate, 24 hours prior to staining. Next day, cells were rinsed two times with PBS, fixed with 4% paraformaldehyde for 15 minutes, washed three times with PBS and permeabilized with 0.1% Triton X-100 for 10 minutes. Slides were blocked with 10% goat serum for 1 hour. In the next steps, staining was performed following the manufacturer protocol using the reagents included in Tyramide SuperBoost™ Kit with Alexa Fluor™ 488 (Invitrogen™, cat. B40941). Briefly, endogenous peroxidase activity was inhibited by incubation with 3% hydrogen peroxidase (Component C2) for 1 hour at RT. Slides were washed and rinsed three times with PBS at RT, 5 minutes each time, then blocked for 1 hour with bocking buffer (Component A). Cells were stained with anti-PD1 primary antibody UltraMAB™ (clone UMAB199, OriGene, cat. UM800091) diluted 1:100 in the blocking buffer (Component A) for 1 hour at RT. Next, samples were washed three times with PBS, 10 minutes each wash. Subsequently, samples were incubated for 7 minutes at RT with 100µl of a tyramide working solution, which was prepared accordingly to the protocol. The reaction was stopped by 10-minute incubation with 100µl of Reaction Stop Reagent, followed by three 10-minute washes with PBS. Samples were mounted using ProLong™ Diamond Antifade Mountant with DAPI (Invitrogen™, cat. P36966) and left overnight protected from light to dry. Specimens were stored at 4°C until imaging, which was performed with Olympus Fluoview FV3000 confocal laser scanning microscope

using 63x oil immersion lens. All images were acquired using the same settings for laser power, voltage, and gain.

2.13 Confocal microscopy

800,000 cells were seeded on 18mm cover slips in a 6-well plate. On the next day, cells were rinsed two times with PBS, fixed with 4% paraformaldehyde for 15 minutes, washed three times with PBS and permeabilized with 0.1% Triton X-100 for 10 minutes. Slides were blocked with 10% goat serum for 1 hour, followed by 1 hour staining with 100µl of primary antibodies diluted in 0.1% goat serum as follows: anti-PD1 dilution 1:100 (clone J121, Invitrogen, cat. 14-2798-82); anti-AXL dilution 1:200 (clone C89E7, Cell Signalling, cat. #8661). Slides were washed five times with 0.1% PBST and incubated for 1 hour with 100µl of 1:500 dilution of Alexa Fluor™ 488 (Invitrogen, cat. A32723) and Alexa Fluor™ 647 (Invitrogen, cat. A32733) secondary antibodies. From that point all steps were carried out in the dark. Slides were again washed five times with PBST for 2 minutes, mounted using ProLong™ Diamond Antifade Mountant with DAPI (Invitrogen™, cat. P36966) and left overnight protected from light to dry. Specimens were stored at 4°C until imaging, which was performed with Olympus Fluoview FV3000 confocal laser scanning microscope using 63X oil immersion lens. All images were acquired using the same settings for laser power, voltage, and gain.

2.14 Proximity ligation assay

250,000 cells were seeded on 10mm diameter round cover slips in 6-well plates 48 hours before the experiment. Cells were rinsed two times with PBS, fixed with 4% paraformaldehyde for 15 minutes, washed three times with PBS and permeabilized with 0.1% Triton X-100 for 10 minutes. Following manufacturer protocol, slides were blocked for 1 hour with 1 drop of Duolink® Blocking Solution at 37°C. Primary antibodies were diluted in the Duolink® Antibody Diluent preparing 1:100 dilution of anti-PD1 (clone J121, Invitrogen, cat. 14-2798-82) and 1:200 dilution of anti-AXL (clone C89E7, Cell Signalling, cat. #8661). Slides were incubated for 1 hour at RT with 30µl of antibodies dilutions, then washed three times with wash buffer A (Sigma-Aldrich, cat. DUO82046), 5 minutes each wash. Slides were incubated with PLUS and MINUS probes for 1 hour at 37°C and washed three times with wash buffer A, 5 minutes each wash. It was followed by 30-minute incubation with

ligase at 37°C, two washes in buffer, 5 minutes each wash. Then, polymerase containing amplification solution was applied onto slides, which were incubated for 100 minutes at 37°C. Slides were washed two times with wash buffer B (Sigma-Aldrich, cat. DUO82048), 10 minutes each wash, followed by additional 10-minute wash with ten times diluted wash buffer B. Slides were mounted with 8µl of Duolink® PLA Mounting Medium with DAPI and left overnight at 4°C before imaging. The imaging was performed with Olympus Fluoview FV3000 confocal laser scanning microscope using 63X oil immersion lens. All images were acquired using the same settings for laser power, voltage, and gain.

2.15 Plasmid vectors

The transfection grade pcDNA 3.1 (+) vectors with neomycin resistance gene encoding *PDCD1* were purchased from Thermo Scientific. Vectors encoded either WT PD1 protein or one of the two mutants in which tyrosine phosphorylation sites (Y223 and Y248) were mutated to phenylalanine. Constructs were designed to encode PD1 protein tagged with only Twin-Strep-tag or Twin-Strep-tag and V5 tag either on their C-terminal or N-terminal ends. The tags were separated with GGGGS linkers. The full amino acid sequences are shown below, with the full-length protein amino acid sequence written in black and the tag sequence in blue, with mutation sites highlighted in fuchsia.

C-terminus-V5-Twin-Strep-tags

WT PD1

MQIPQAPWPVVWAVLQLGWRPGWFLDSPDRPWNPPTFSPALLVVTEGDNATFTC
SFSNTSESFVLNWYRMSPSNQTDKLAAFPEDRSQPGQDCRFRVTQLPNGRDFHM
SVVRARRNDSGTYLCGAISLAPKAQIKESLRAELRVTERRAEVPTAHPSPSPRPAG
QFQTLVVGVVGGLLGSLVLLVWVLAVICSRAARGTIGARRTGQPLKEDPSAVPVFS
VDYGELDFQWREKTPEPPVPCVPEQTEYATIVFPSGMGTSSPARRGSADGPRSA
QPLRPEDGHCSWPLGGGGSGGGGSGGGGSGKPIPNPLLGLDSTGGGGSGGGG
SGGGGSSAWSHPQFEKGGGSGGGSGGSAWSHPQFEK

Y223F PD1

MQIPQAPWPVVWAVLQLGWRPGWFLDSPDRPWNPPTFSPALLVVTEGDNATFTC
SFSNTSESFVLNWYRMSPSNQTDKLAAFPEDRSQPGQDCRFRVTQLPNGRDFHM
SVVRARRNDSGTYLCGAISLAPKAQIKESLRAELRVTERRAEVPTAHPSPSPRPAG

QFQTLVVGVVGGLLGSLVLLVWVLAVICSRAARGTIGARRTGQPLKEDPSAVPVFS
VDFGELDFQWREKTPEPPVPCVPEQTEYATIVFPSGMGTSSPARRGSADGPRSAQ
PLRPEDGHCSWPLGGGGSGGGGSGGGGSGKPIPNPLLGLDSTGGGGSGGGGS
GGGGSSAWSHPQFEKGGGSGGGSGGSAWSHPQFEK

Y248F PD1

MQIPQAPWPVVWAVLQLGWRPGWFLDSPDRPWNPPTFSPALLVVTEGDNATFTC
SFSNTSESFVLNWYRMSPSNQTDKLAAFPEDRSQPGQDCRFRVTQLPNGRDFHM
SVVRARRNDSGTYLCGAISLAPKAQIKESLRAELRVTERRAEVPTAHPSPSPRPAG
QFQTLVVGVVGGLLGSLVLLVWVLAVICSRAARGTIGARRTGQPLKEDPSAVPVFS
VDYGELDFQWREKTPEPPVPCVPEQTEFATIVFPSGMGTSSPARRGSADGPRSAQ
PLRPEDGHCSWPLGGGGSGGGGSGGGGSGKPIPNPLLGLDSTGGGGSGGGGS
GGGGSSAWSHPQFEKGGGSGGGSGGSAWSHPQFEK

C-terminus-Twin-Strep-tags

WT PD1

MQIPQAPWPVVWAVLQLGWRPGWFLDSPDRPWNPPTFSPALLVVTEGDNATFTC
SFSNTSESFVLNWYRMSPSNQTDKLAAFPEDRSQPGQDCRFRVTQLPNGRDFHM
SVVRARRNDSGTYLCGAISLAPKAQIKESLRAELRVTERRAEVPTAHPSPSPRPAG
QFQTLVVGVVGGLLGSLVLLVWVLAVICSRAARGTIGARRTGQPLKEDPSAVPVFS
VDYGELDFQWREKTPEPPVPCVPEQTEYATIVFPSGMGTSSPARRGSADGPRSA
QPLRPEDGHCSWPLGGGGSGGGGSGGGGSSAWSHPQFEKGGGSGGGSGGGSA
WSHPQFEK

N-terminus-V5-Twin-Strep-tags

WT PD1

MSAWSHPQFEKGGGSGGGSGGSAWSHPQFEKGGGGSGGGGSGGGGSGKPIP
NPLLGLDSTGGGGSGGGGSGGGGSMQIPQAPWPVVWAVLQLGWRPGWFLDSP
DRPWNPPTFSPALLVVTEGDNATFTCSFSNTSESFVLNWYRMSPSNQTDKLAAFP
EDRSQPGQDCRFRVTQLPNGRDFHMSVVRARRNDSGTYLCGAISLAPKAQIKESL
RAELRVTERRAEVPTAHPSPSPRPAGQFQTLVVGVVGGLLGSLVLLVWVLAVICSR
AARGTIGARRTGQPLKEDPSAVPVFSVDYGELDFQWREKTPEPPVPCVPEQTEYA
TIVFPSGMGTSSPARRGSADGPRSAQPLRPEDGHCSWPL

N-terminus-Twin-Strep-tags

WT PD1

MSAWSHPQFEKGGGSGGGSGGSAWSHPQFEKGGGGSGGGGSGGGGSMQIPQ
APWPVVWAVLQLGWRPGWFLDSPDRPWNPPTFSPALLVVTEGDNATFTCSFSNT
SESFVLNWYRMSPSNQTDKLAAFPEDRSQPGQDCRFRVTQLPNGRDFHMSVVRA
RRNDSGTYLCGAISLAPKAQIKESLRAELRVTERRAEVPTAHPSPSPRPAGQFQTL
VVGVVGGLLGSLVLLVWVLAVICSRAARGTIGARRTGQPLKEDPSAVPVFSVDYGE
LDFQWREKTPEPPVPCVPEQTEYATIVFPSGMGTSSPARRGSADGPRSAQPLRPE
DGHCSWPL

2.16 Molecular modelling and molecular dynamics studies

2.16.1 Sequence retrieval, Robetta and protein structure modelling

Due to lack of the full crystal structures of PD1 and AXL proteins in Protein Data Bank (PDB), the structure modelling approach had to be implemented to predict protein structures. The PDB crystal structure of the extracellular domain of PD1 at 1.70Å resolution was downloaded from PDB, ID: 6K0Y, while input sequences for the intracellular domain of PD1 (PD1-ICD), the extracellular domain of AXL (AXL-ECD) and the intracellular domain of AXL (AXL-ICD) were obtained from UniProt database. The UniProt IDs for the retrieved sequences were as follows: Q15116 for PD1-ICD, P30530 for AXL-ECD and AXL-ICD. Subsequently, the structural models for AXL-ECD, AXL-ICD, and PD1-ICD were generated with the ab-initio modelling approach using the ROBETTA Baker server. Specifically, the RoseTTAFold method was implemented, which is the default option provided by the server and is based on deep learning techniques (Baek et al. 2021). RoseTTAFold method demonstrates superior performance in protein structure modelling compared to other available methods on the ROBETTA Baker server (http://robetta.bakerlab.org) (Baek et al. 2021). Therefore, the RoseTTAFold method allowed to obtain accurate and reliable structural models for AXL-ECD, AXL-ICD, and PD1-ICD, despite the unavailability of their full crystal structures.

2.16.2 Long-scale full atomistic MD simulation

D. E. Shaw's Desmond software was utilized to perform all-atom molecular dynamics (MD) simulations lasting 2μs (Yan et al. 2020). The goal of these simulations

was to investigate the binding potency or strength of the programmed cell death protein 1 (PD1) intracellular domain (ICD) and extracellular domain (ECD) with the AXL intracellular domain (ICD) and extracellular domain (ECD). To create the simulation systems, all the complexes were placed in a solvated cubic box with dimensions of 10Å, and periodic boundary conditions were applied. For solvation, the TIP3P water model was employed. Additionally, the total charges of the system were neutralized by including counter ions. Before the MD simulation, an energy minimization step was conducted using the steepest descent method while employing the OPLS 2005 force field. During the initial 400ps of the simulation, all systems underwent linear heating in the NVT ensemble, gradually increasing the temperature from 0 to 300K, where N denotes the number of atoms, V represents the volume, and T signifies the temperature. The system was then equilibrated using an NPT ensemble, operating at a pressure of 1 bar and a temperature of 300K. To control the system's temperature, the Noose-Hoover chain thermostat method was employed, while the Martyna-Tobias-Klein barostat method with an isotropic coupling style was utilized to regulate the system's pressure. The equations of motion were integrated using the leap-frog approach with a time step of 2fs. Additionally, a cutoff radius of 9.0Å was set for the coulomb short-range interactions. (Bowers et al. 2006) During the 2μs of MD simulations, a total of 20,000 frames were captured for each of the complexes. Following the production run, trajectory analysis was conducted to evaluate the structural changes that occurred during the simulation. The analysis involved calculating the Root Mean Square Deviation (RMSD).

2.17 Macromolecular Docking using HDOCK

The macromolecular docking of protein structures and prediction of their binding complexes and binding affinities was performed using HDOCK online server for blind docking (http://hdock.phys.hust.edu.cn/). HDOCK predicts the intermolecular interactions at the interface of two proteins in binding complexes through a hybrid algorithm (Baek et al. 2021). It generated ten top binding complexes along with their corresponding binding affinity scores. Those results were used to assess the potential interactions and binding strengths between AXL and PD1, specifically the extracellular domain (ECD) and intracellular domain (ICD) of both receptors. The resulting protein-

protein complexes were downloaded and subjected to analysis of their intermolecular interaction patterns using the Schrodinger's Maestro software.

3. Aims

Recently, PD1/PDL1 immune checkpoint blockade has revolutionized cancer treatment approach. This type of treatment targets an inhibitory receptor on T cells, liberating them from the functional exhaustion and restoring their capability to combat cancer cells (Topalian, Drake, and Pardoll 2012; J. Liu et al. 2021). Therefore, there was considerable optimism regarding implementation of ICB for treatment of rare and refractory malignancies, such as osteosarcoma (Saraf, Fenger, and Roberts 2017).

Despite remarkable success observed in some patients, a significant number still do not benefit from immunotherapy or experience rapid clinical deterioration (Denis et al. 2020). Following the discovery of the cancer-expressed PD1, the intrinsic signalling of PD1 was proposed as a potential mechanism of resistance to immunotherapy and a cause of the unfavourable outcomes reported in these patients (Du et al. 2018; Kocikowski, Dziubek, and Parys 2020). To date, tumour-PD1 expression was identified in various types of cancer. No such data is available regarding PD1 expression in osteosarcoma but at the same time efficacy of PD1/PDL1 blockade in osteosarcoma patients was proven disappointing (Z. Zhang et al. 2022; Boye et al. 2021). Therefore, it is still uncertain whether tumour-expressed PD1 could be the reason for the immunotherapy ineffectiveness in osteosarcoma patients.

Research questions and hypotheses addressing the gaps in current knowledge:

1. **To characterize the expression and significance of PD1 protein in osteosarcoma cells.**
2. **To reveal the molecular mechanisms of cancer-intrinsic PD1.**
3. **To characterize cancer-intrinsic PD1 interactome.**
4. **To predict the mechanism of the identified interaction.**

4. Results: PD1 functional studies

4.1 Characterization of PD1 expression in osteosarcoma cells

To validate the rationale of our hypothesis, it was essential to test if PD1 is indeed expressed by osteosarcoma cells, what we initially confirmed by Western Blotting (**Figure 7**). The migration pattern indicated by SDS-PAGE revealed two bands

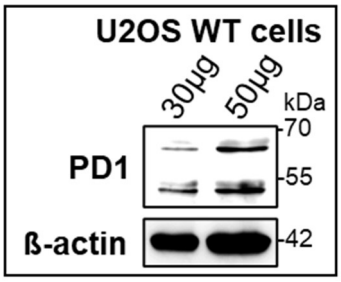

Figure 7 Western Blot analysis confirms PD1 expression in osteosarcoma cells. Western Blot analysis revealed the presence of PD1 expression in U2OS cells, detected as two bands around 55kDa and 70kDa. ß-actin was used as a loading control.

detected at ~55kDa and ~70kDa, whereas the predicted molecular weight of PD1 is 32kDa. This observation suggests the potential presence of posttranslational modifications representing distinct isoforms of the protein. In fact, 55kDa molecular weight was previously described as heavily glycosylated, functionally active PD1, supporting the specificity of our results (C. W. Li et al. 2016; Sun et al. 2020).

However, there is a lack of information regarding the modifications associated with 70kDa isoform, despite being reported as PD1 specific signal in a study utilizing multiple monoclonal antibodies for protein detection demonstrated in **Figure 8** (Y. Chen et al. 2010). We presumed that such shift is too large to represent PD1 phosphorylation. Moreover, preservation of protein phosphorylation requires an addition of phosphatase inhibitors to the lysis buffer, therefore could not be detected.

In fact, 70kDa molecular weight may indicate an even higher degree of glycosylation, which could be experimentally validated by treatment with Peptide-N-Glycosidase F. Alternatively, 70kDa might represent PD1 dimerization via disulfide bonds. Theoretically, these dimers could potentially re-establish despite reducing conditions

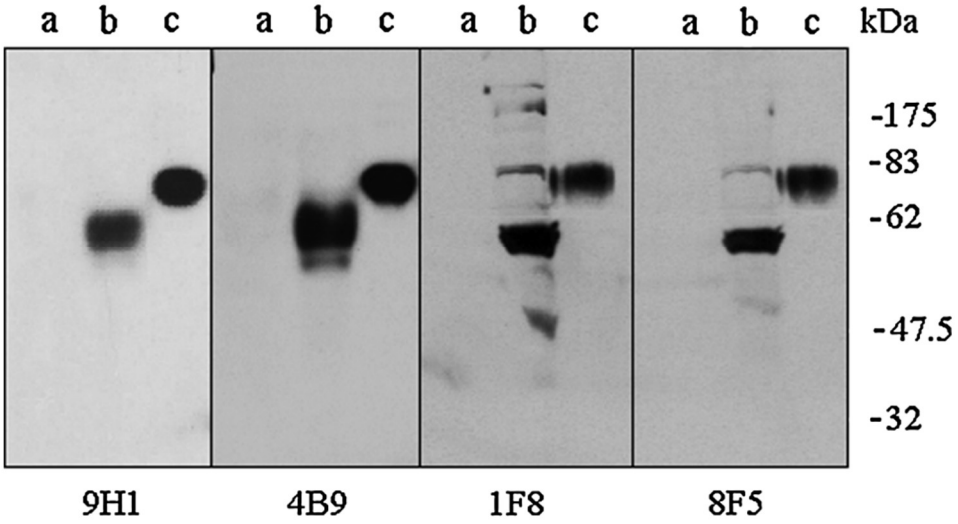

Figure 8 Western blot analysis of the specific anti-human PD-1 MAbs. a=L929 negative control, cells, b=PD1 overexpressing L929 cells, c=commercial recombinant PD1 Ig protein. and L929=PD1. Cells were lysed by RIPA, and the lysates were loaded to SDS-PAGE and transferred onto the nitrocellulose membranes. The membranes were probed with the anti-PD-1 MAbs for 1 hour at room temperature followed by HRP-goat anti-mouse IgG. Adopted from Y. Chen et al. (2010), DOI: 10.1089=hyb.2009.0091.

of the experiment (Müller and Winter 2017). However, unlike other type I transmembrane glycoproteins such as CTLA-4 or CD28, PD1 lacks the analogous cysteine residues required for covalent bond formation. Therefore, PD1 cannot form such homodimers (X. Zhang et al. 2003; Ikemizu et al. 2000; Patsoukis, Wang, et al. 2020).

Alternatively, the signal we observed could be attributed to PD1 ubiquitination, which was previously reported by Meng et al. (2018) as a mechanism regulating PD1 degradation in T cells (Meng et al. 2018; Serman and Gack 2019). They observed that upon internalization, PD1 receptor becomes polyubiquitinated by E3 ubiquitin ligase FBXO38 and undergoes degradation by the proteasome. Considering that ubiquitin has the molecular weight of approximately 8.5kDa, two molecules of ubiquitin added to the glycosylated PD1 would explain the origin of 70kDa band. However, the experimental validation is required to confirm any of the above speculations.

Additionally, we observed that an optimal protein loading of 50µg per lane of a polyacrylamide gel was necessary, indicating low expression of PD1 in U2OS cells. This was corroborated by our immunofluorescent staining results, where PD1 detection was unsuccessful using a general staining protocol. PD1 was only visualized after implementation of Alexa Fluor™ 488 Tyramide SuperBoost™ staining, designed to amplify fluorescent signal for the detection of low-abundance proteins. Additionally, microscopy imaging revealed that PD1 is expressed in the cytoplasm and does not localize specifically to the membrane as could be expected (**Figure 9**).

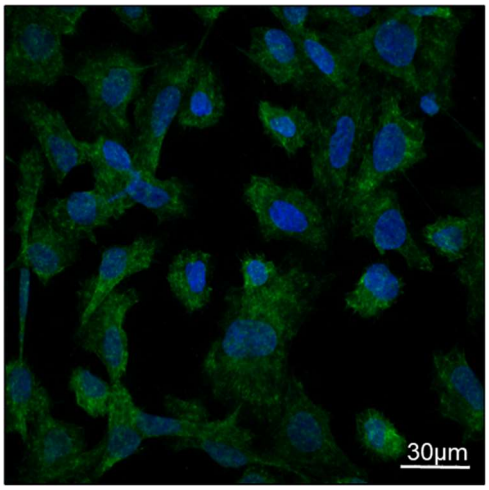

Figure 9 Immunofluorescence analysis confirms low level of PD1 expression in osteosarcoma. PD1 expression demonstrated by immunofluorescence staining performed with Alexa Fluor™ 488 Tyramide SuperBoost™. The image was acquired with Olympus Fluoview FV3000 confocal microscope, using 63X objective with oil immersion. Nuclei were stained with DAPI.

4.2 U2OS cells express PD1 both intra- and extracellularly.

Knowing that PD1 does not localize specifically to the cellular membrane, we performed flow cytometry analysis to precisely assess both surface and intracellular expression of PD1 in U2OS cells (**Figure 10A and B**). Data from four independent experiments demonstrated that nearly 100% of the cells expressed PD1 intracellularly, while surface PD1 expression averaged 3.9% (**Figure 10C**). This level of surface PD1 expression corresponds to cancer-PD1 expression observed in melanoma patients (depending on a study, 3%, ±0.7%, n=15 or 8.7% ± 1.5%, n=8) or detected in NSCLC cell lines (4%, ±0.3, n=12) (Schatton et al. 2010; Kleffel et al. 2015; Rotolo et al. 2023).

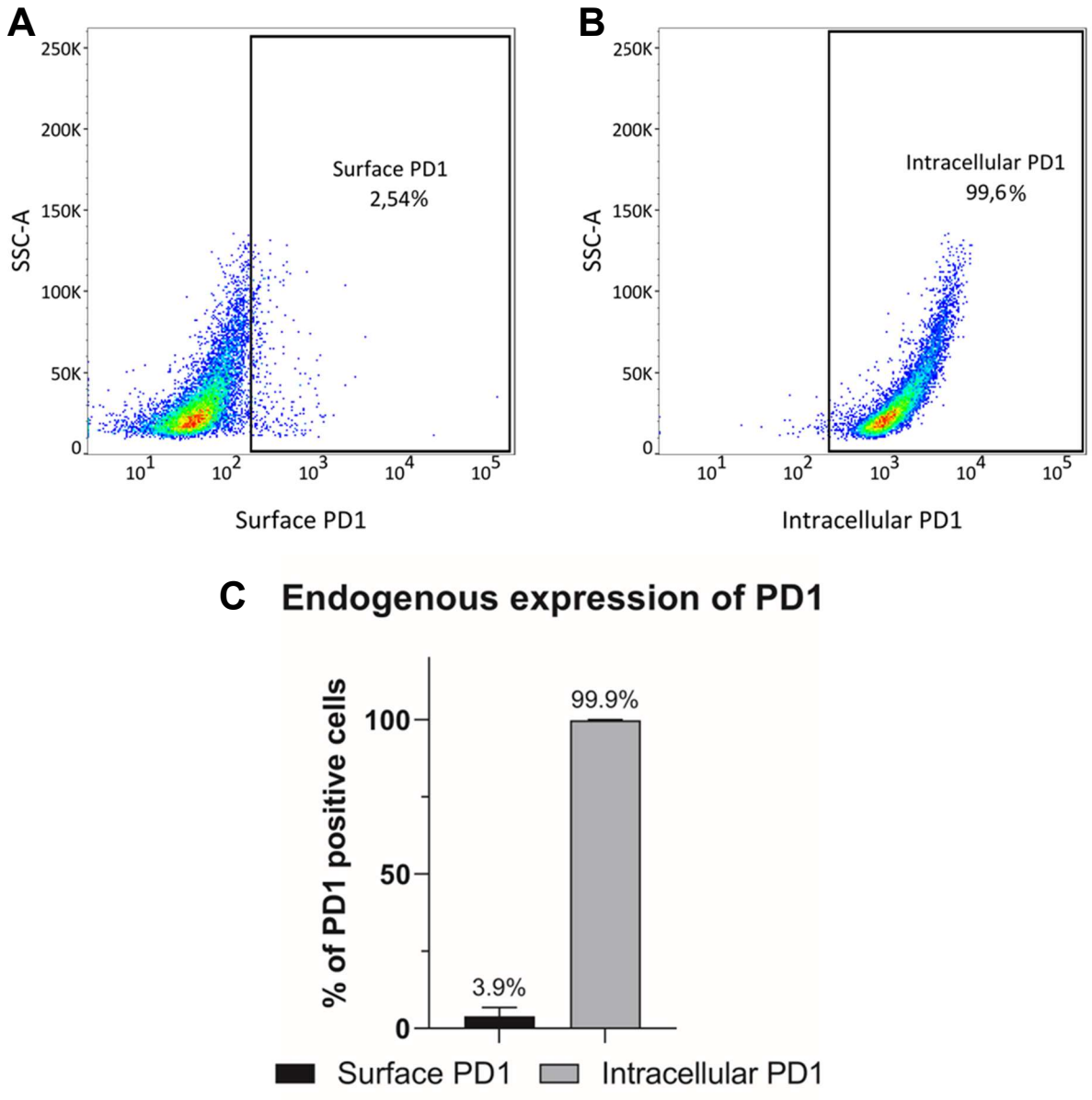

Figure 10 PD1 protein is endogenously expressed by U2OS cells, both on the surface and intracellularly. A) Flow cytometry analysis revealed spontaneous expression of both surface and **B)** intracellular PD1 in nearly all U2OS cells (more than 99%). A and B show data from a representative experiment, which was repeated four times. **C)** Demonstrates the mean percentage of the surface and intracellular expression of PD1 calculated from four independent flow cytometry experiments. Error bars display SD, the graph was created in GraphPad Prism software, version 9.1.1. Raw flow cytometry data was analysed with FlowJo version 10.8.1.

4.3 siRNA-mediated *PDCD1* silencing significantly reduces its transcript levels.

To study the functional effects of PD1 expression and consequences of PD1 depletion in U2OS cells, we employed siRNA technology. First, we evaluated the efficacy of three distinct Silencer Select siRNAs for *PDCD1* gene silencing. To select the most efficient siRNA oligonucleotide and determine the optimal time of treatment, we performed RT-qPCR analysis at 24-, 48-, and 72-hours post-transfection and calculated relative *PDCD1* transcript levels (**Figure 11A-C**). A non-targeting siRNA was used as a negative control for the transfection. For simplification, we assigned arbitrary names to the oligonucleotides: siPD1 #1, siPD1 #2 and siPD1 #3.

We observed that siPD1 #2 and siPD1 #3 significantly reduced *PDCD1* gene expression after 24 hours, whereas siPD1 #1 significantly reduced transcript levels after 48 hours. Following 72 hours post-transfection, reduced *PDCD1* transcripts persisted for siPD1 #2 and #3, while siPD1 #1 demonstrated a slight increase in transcript levels. Thereby, we determined 48 hours as the optimal time point for experiments requiring siRNA-mediated knockdown.

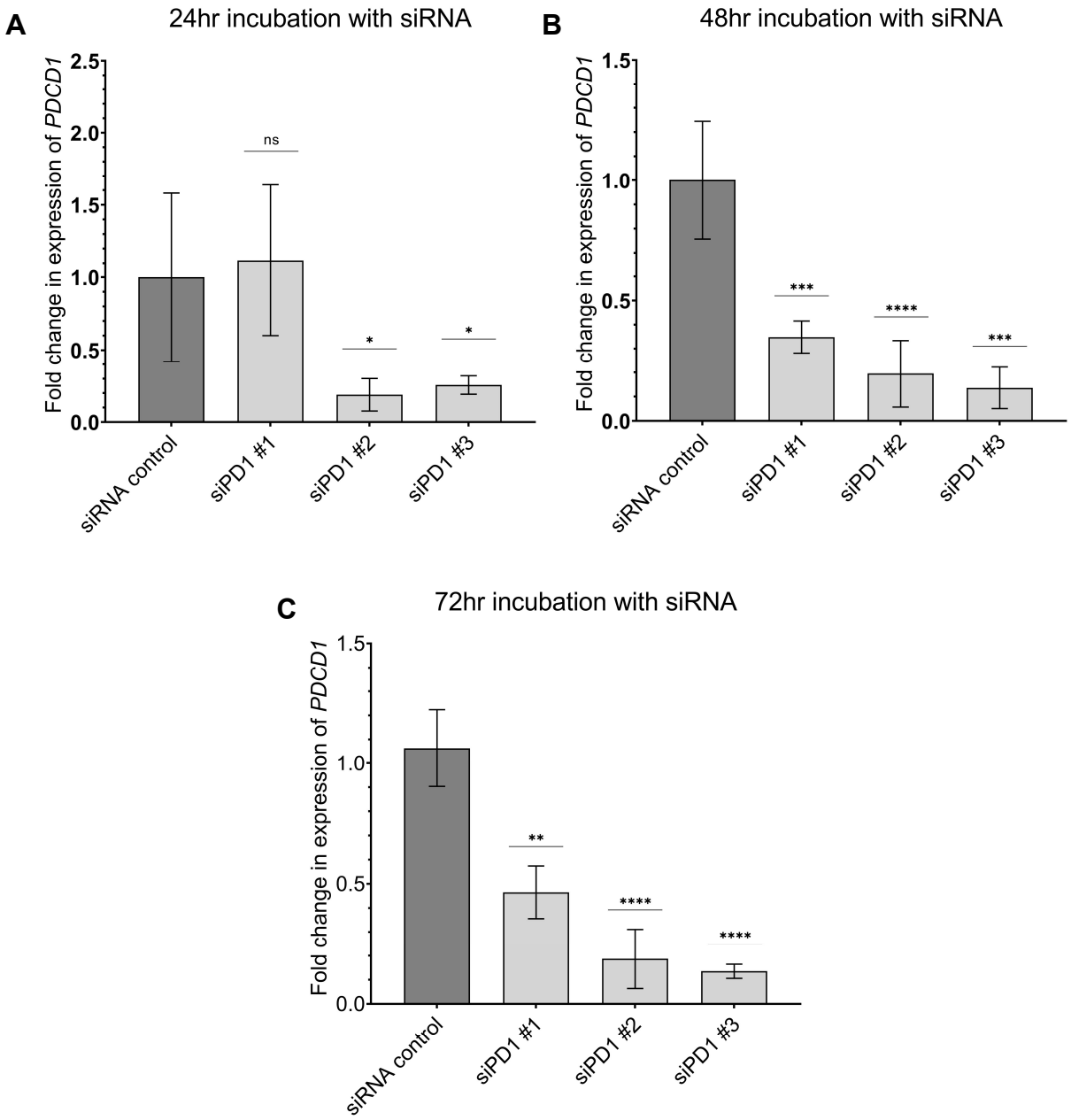

Figure 11 Fold change expression of *PDCD1* gene transcripts measured by RT-qPCR confirms reduction of *PDCD1* transcript levels upon siRNA treatment. Samples were collected at various timepoints **A)** 24 hours, **B)** 48 hours and **C)** 72 hours following the transfection with siRNA negative control and with siRNA targeting *PDCD1* transcripts. The expression of *PDCD1* was assessed using RT-qPCR analysis. Gene expression levels were normalized to *GAPDH*. Relative quantitative levels of the gene transcripts were determined using 2−ΔΔCt method. The dataset exhibited a non-normal distribution; therefore, the statistical significance was assessed using the unpaired Mann-Whitney test at a 95% confidence level. The comparison was made between the siRNA control and a single siPD1 condition. All error bars represent mean ± SD. The asterisks are used to indicate the corresponding p-values: (*) P ≤ 0.05; (**) P ≤ 0.01; (***) P ≤ 0.001; (****) P ≤ 0.0001, (ns) not significant.

4.4 *PDCD1* silencing perturbs equilibrium of PD1 protein in U2OS cells.

We demonstrated that siRNA technology has proven successful in reducing *PDCD1* gene transcript levels. However, to confirm whether it translates to protein expression, we employed Western Blot analysis (**Figure 12A**).

Immunoblotting indicated that depending on PD1 PTMs silencing led to contrasting expression patterns. As previously mentioned, Western Blot migration pattern for PD1 comprises two bands detected at 55 and 70kDa. However, following signal quantification (**Figure 12B**), a decrease in protein expression was observed exclusively in the lower molecular weight band (55kDa), while 70kDa isoform became slightly upregulated.

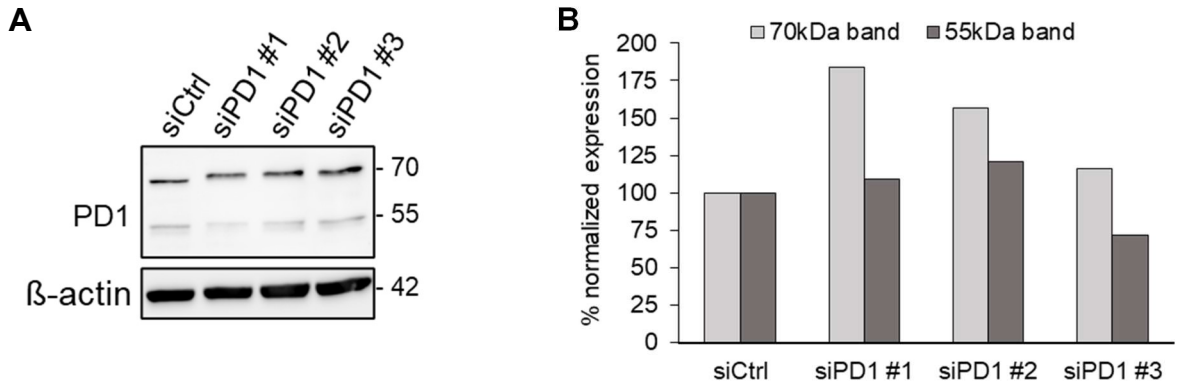

Figure 12 Immunoblotting of PD1 expression upon *PDCD1* silencing A) PD1 runs as two bands detected at 55kDa and 70kDa. ß-actin was used as loading control. **B)** Western Blot quantitation of two bands detected for PD1 protein. Quantification of each lane by separate measurement of 55kDa and 70kDa bands was performed in ImageJ using gel analysis plugin. Quantified signal was normalized to the corresponding B-actin measurement. The figure demonstrates data from a representative experiment.

Next, we performed flow cytometry to examine whether these two bands may correspond to the surface and intracellular expression of PD1. Apart from a minor shift in intracellular expression of PD1 upon treatment with siPD1 #1, no visible change in protein expression was observed for other conditions neither on the surface nor intracellularly. This suggests that immunoblotting pattern of PD1 expression does not reflect the extra- and intracellular expression of PD1 (**Figure 13A and B**).

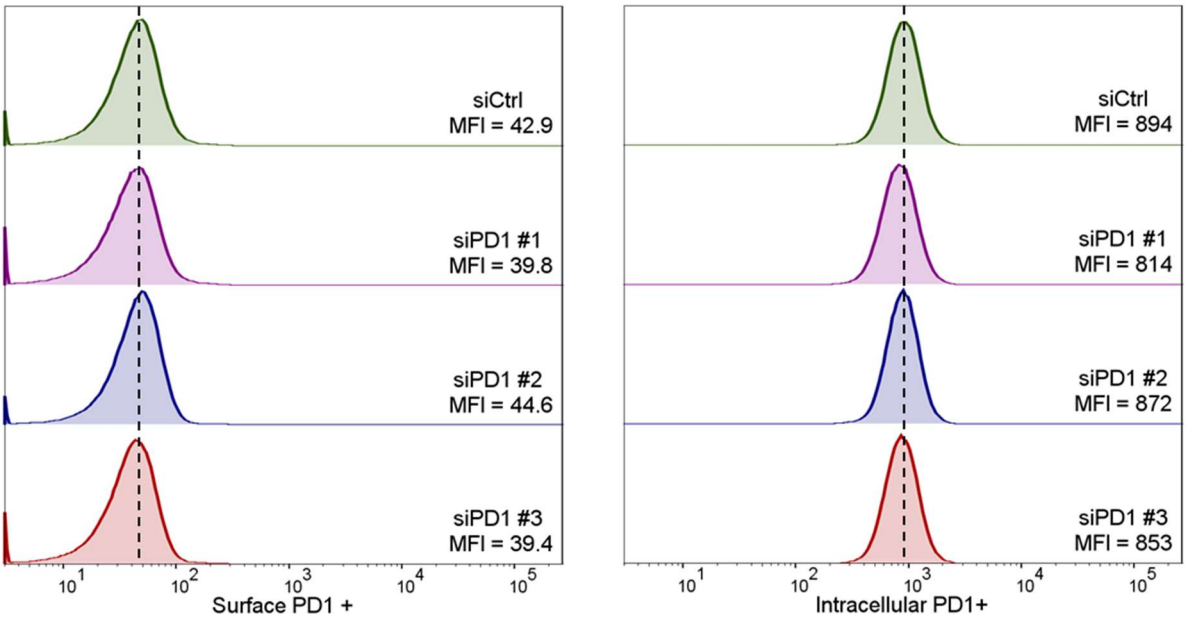

Figure 13 Flow cytometry analysis does not indicate reduction of A) extracellular or B) intracellular expression of PD1 upon *PDCD1* silencing. PD1 expression was measured 48 hours after transfection. The figure shows a representative experiment which was repeated three times, MFI values are plotted together with histograms. Due to low percentage of surface PD1 positive cells, 1,000,000 of cells was recorded per sample for improved accuracy.

Apart from distinguishing between the surface and intracellular expression of a protein, flow cytometry analysis has no capacity to discriminate between protein isoforms if they are detected by the same antibody. Therefore, flow cytometry data may not be fully representative in our experiment as Western Blotting demonstrated downregulation in the expression of 55kDa isoform upon treatment with siPD1, while increase in 70kDa. This shift in PD1 equilibrium simply cannot be detected by flow cytometry measurement when it does not result from the imbalance in the surface vs intracellular protein expression.

The observed decrease in 55kDa molecular weight PD1 expression most likely represents glycosylated PD1, which was reported as functional and crucial for PD1 signal transduction in T cells (Sun et al. 2020). We speculate, that PD1 glycosylation in cancer cells plays equally important role and is required for exerting PD1 function, however it must be experimentally validated.

Moreover, 70kDa may represent a highly stable form of PD1, which is not degraded but accumulates over time. As suggested in the previous paragraph, the 70kDa band

may illustrate the ubiquitinated pool of PD1 protein targeted for degradation by the proteasome (Gavali et al. 2021; Meng et al. 2018). Therefore, our data could illustrate the accumulation of soon-to-be-degraded protein. Our results demonstrate that we shifted the balance between two isoforms of PD1 expressed in U2OS cells. In fact, siPD1 treatment of U2OS cells leads to perturbed expression of PD1 isoforms, therefore it is more accurate to claim that by *PDCD1* silencing with siRNA, we perturbed the equilibrium of PD1 protein in the cells.

Regarding PD1 stability, to our knowledge, only one experimental report describes PD1 turnover, which estimated PD1 half-life to be ≥ 49.5 hours. Such long protein half-life may suggest that utilizing transient transfection for PD1 knockdown may not be the optimal. Likely, implementation of shRNA or CRISPR-Cas9 techniques, which allow to control protein expression for long period of time, would result in more efficient *PDCD1* knockdown (Lassman et al. 2021).

4.5 *PDCD1* knockdown impacts migration and viability of U2OS cells.

Next, we assessed the biological consequences of *PDCD1* silencing in U2OS cells. We implemented RNAi in experiments characterizing viability and migratory properties of cells to indicate changes in their malignant capabilities in response to disruptions in PD1 expression. Cell migration was evaluated by a scratch assay, which is considered as a simple and reproducible method for assessing cell migratory properties (Liang, Park, and Guan 2007).

U2OS cells were transfected with either siCtrl, siPD1 #1, siPD1 #2 or siPD1 #3. After 48 hours, when the cells reached full confluency, a scratch was made on the cell monolayer (0-hour time point). Subsequently, we monitored wound closure over the next 32 hours, imaging cells with a brightfield microscope at 0-, 6-, 12-, 24- and 32-hour intervals (**Figure 14A**). We observed that treatment with siPD1 #1 and siPD1 #3 significantly enhanced cell motility, resulting in faster wound closure compared to the control, while this effect was more prominent for siDP1 #1. Conversely, cells treated with siPD1 #2 initially exhibited a slower wound closure rate, followed by extensive cell death and inability to migrate observed after 24 hours (**Figure 14B**).

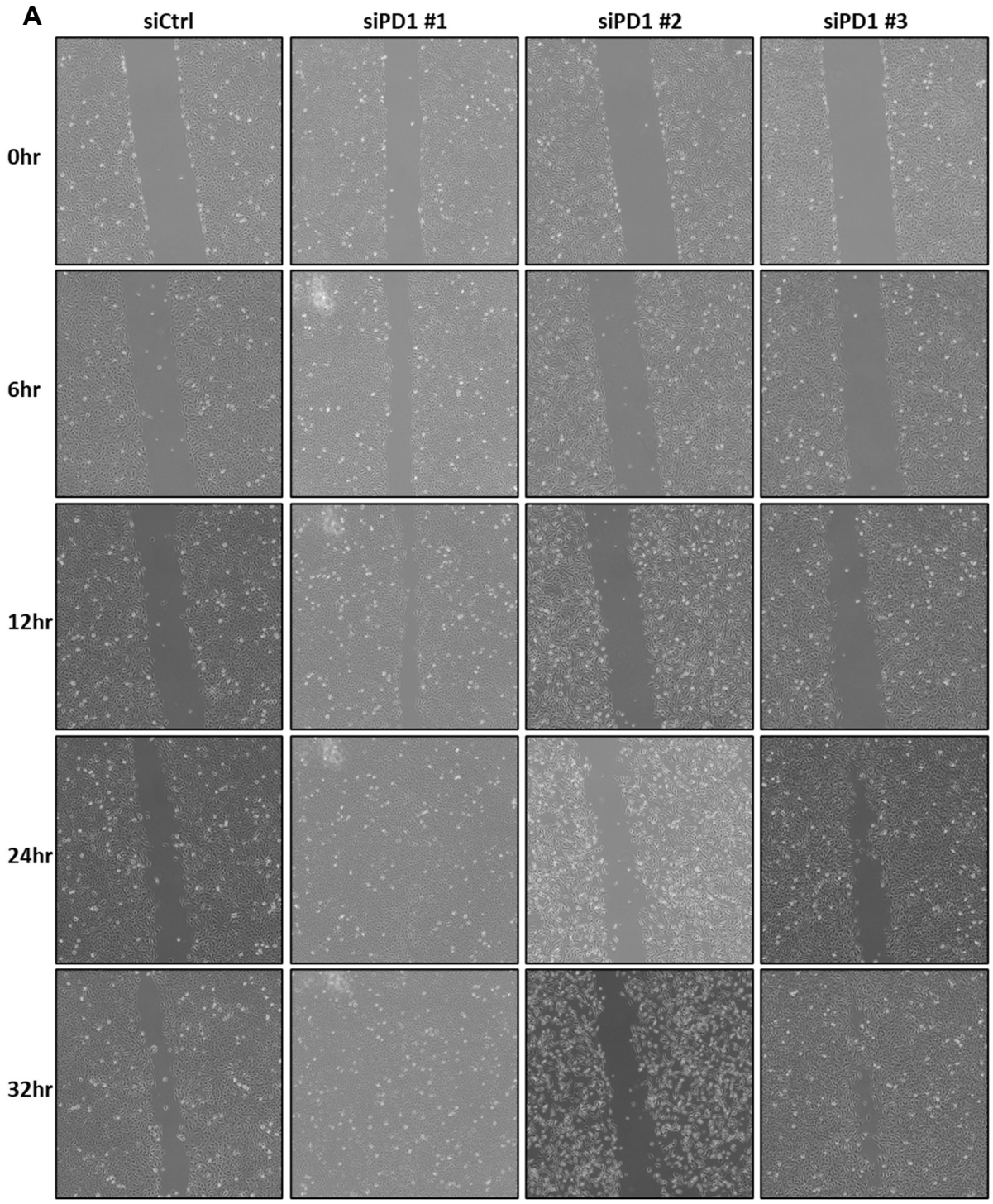

Figure 14 *PDCD1* silencing impacts cell migration as demonstrated by the scratch assay.
A) shows representative bright-field microscope images taken at 0 hour (when the scratch was made, 48 hours after transfection) and subsequently after 6, 12, 24 and 32 hours. Images were acquired at 40X magnification using Opta-Tech MW50 bright field microscope. **B)** graph summarizing scratch assay data from three independent experiments performed in duplicates. Wound area was calculated by analysing images at a given time point using the Image J wound healing size tool plugin. The area

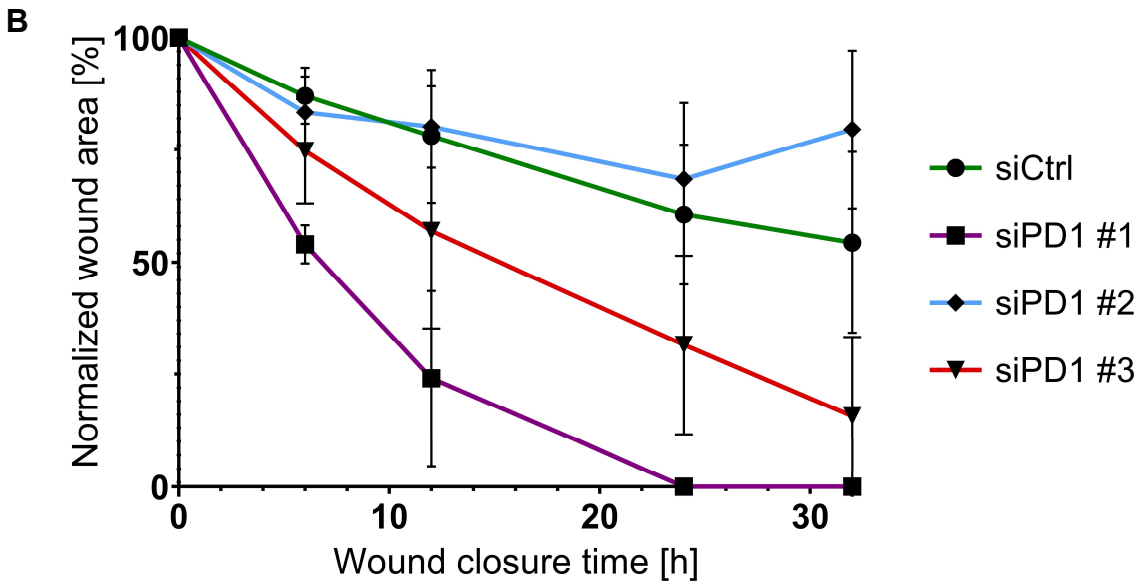

was normalized to a percentage of the initial scratch area, where 100% refers to wound area at 0 hour, whereas 0% represents total closure of the wound. Error bars represent the ± mean area of the scratch calculated based on all technical and biological replicates.

Additionally, we evaluated how disrupted PD1 equilibrium impacts U2OS cells viability. We employed CellTiter-Glo® viability assay measuring ATP levels in the cells, what directly corresponds to the number of viable cells in the sample. The experiment revealed that *PDCD1* silencing in cells treated with siPD1 #1 and siPD1 #3 resulted in improved cell viability and accelerated cell growth compared to the control conditions. Correspondingly, the effect was more pronounced for siPD1 #1, for which we observed the highest reduction of PD1 expression. In accordance with the scratch assay findings, cells treated with siPD1 #2 displayed significantly diminished viability than the control (**Figure 15**).

To understand the contradictory results observed in cell-based assays, we considered several hypotheses. We first considered if variations in siRNAs binding sites might be responsible for these discrepancies. The mechanism of siRNA-mediated post-transcriptional gene silencing is based on siRNA binding to mRNA, either in its coding or 3' untranslated region (3' UTR). While both approaches were reported to silence genes with equal efficiency, their mechanisms of gene silencing differ (Lai, Chen, and Au 2013).

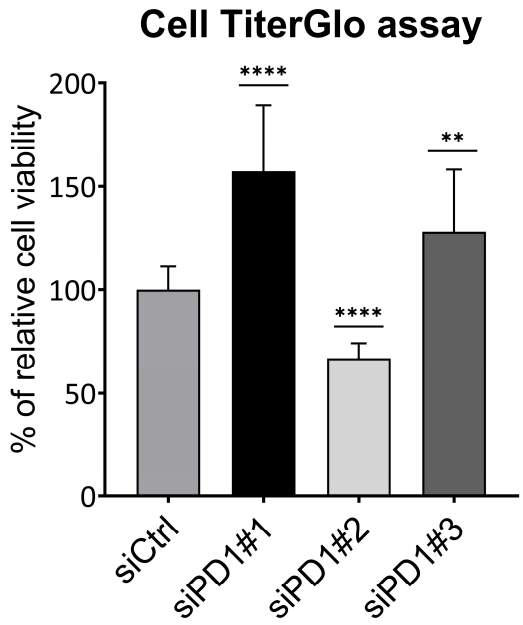

Figure 15 *PDCD1* gene silencing with various oligos differently affects cell viability. Cell TiterGlo® cell viability assay was performed 96 hours post-transfection. The graph and statistical analysis were performed in GraphPad Prism software, version 9.1.1. The dataset exhibited a non-normal distribution, therefore statistical significance was assessed using the unpaired Mann-Whitney test at a 95% confidence level. The comparison was made between the siRNA control and a single siPD1 condition. The error bars indicate standard deviation (SD). The asterisks indicate the corresponding p-values: (*) P ≤ 0.05; (**) P ≤ 0.01; (***) P ≤ 0.001; (****) P ≤ 0.0001.

When siRNA specifically recognizes the coding region of mRNA, it prevents ribosome binding or leads to mRNA degradation without affecting the translation process. Even though no coding potential is associated with 3' UTR, it harbours regulatory functions by controlling mRNA stability, localization, and translation. These processes are governed by RNA binding proteins (RBPs) or other RNAs, primarily miRNAs. We aimed to verify if the opposite effects on cells could be attributed to the oligonucleotide binding to 3'UTR.

By analysing the nucleotide sequence of *PDCD1* mRNA, we identified the binding sites for all siPD1 oligonucleotides. *PDCD1* gene comprises 5 exons and we found that siPD1 #1 and siPD1 #2 recognize fragments in the coding region of exon 2, while siPD1 #3 binds to the 3'UTR of exon 5 (**Figure 16**). We observed that although siPD1 #1 and siPD1 #2 bind to the coding region of exon 2, they exert the opposing effects in U2OS cells. Conversely, siPD1 #3, despite binding to 3'UTR, promotes cell

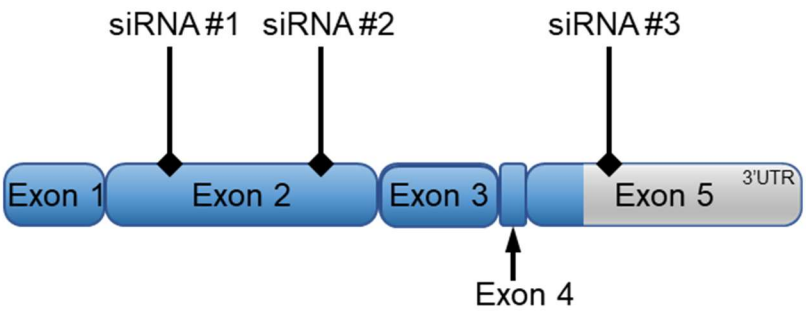

Figure 16 Schematic overview of PD1 siRNAs binding sites to PD1 mRNA transcripts, which were used for *PDCD1* knockdown in U2OS cells. siPD1 #1 and siPD1 #2 target two different regions of exon 2 and siPD1 #3 binds in untranslated region of exon 5 of *PDCD1* mRNA.

migration and viability similarly to siPD1 #1. This implies that differences in siRNAs binding sites do not account for the contradictory effects of our experiments.

Then, we explored the possibility that the opposing effects of siPD1 treatment could be linked to alternative splicing of *PDCD1* and selective targeting of PD1 isoforms by the oligonucleotides. Only scarce reports are available regarding PD1 isoforms and their functions. Aside from the full-length protein, several PD1 variants were identified, including PD1Δex2, PD1Δex3, PD1Δex2,3 and PD1Δex2,3,4 and are illustrated in **Figure 17** (Nielsen et al. 2005; Ponce de León et al. 2021). We established that, although siPD1 #1 and siPD1 #2 induce dramatically different effect in the cells, they both bind to exon 2 of *PDCD1*. Therefore, for our hypothesis to hold, siPD1 #2 would need to selectively recognise the isoform not targeted by siPD1 #1. It would only be correct if there were an isoform with truncation in 5' region of exon 2, within the binding site for siPD1 #1. To date, no such isoform has been identified, making this explanation invalid.

Finally, we considered the possibility of off-target effects as the reason for substantial differences following siRNA treatment. We employed Nucleotide Basic Local Alignment Search Tool (BLAST) to search for sequence similarities between nucleotides used in our experiments and the human genome. The results did not show a complete alignment with any other gene. However, we cannot exclude that partial similarity may be sufficient to induce gene interference as no specific threshold has been determined.

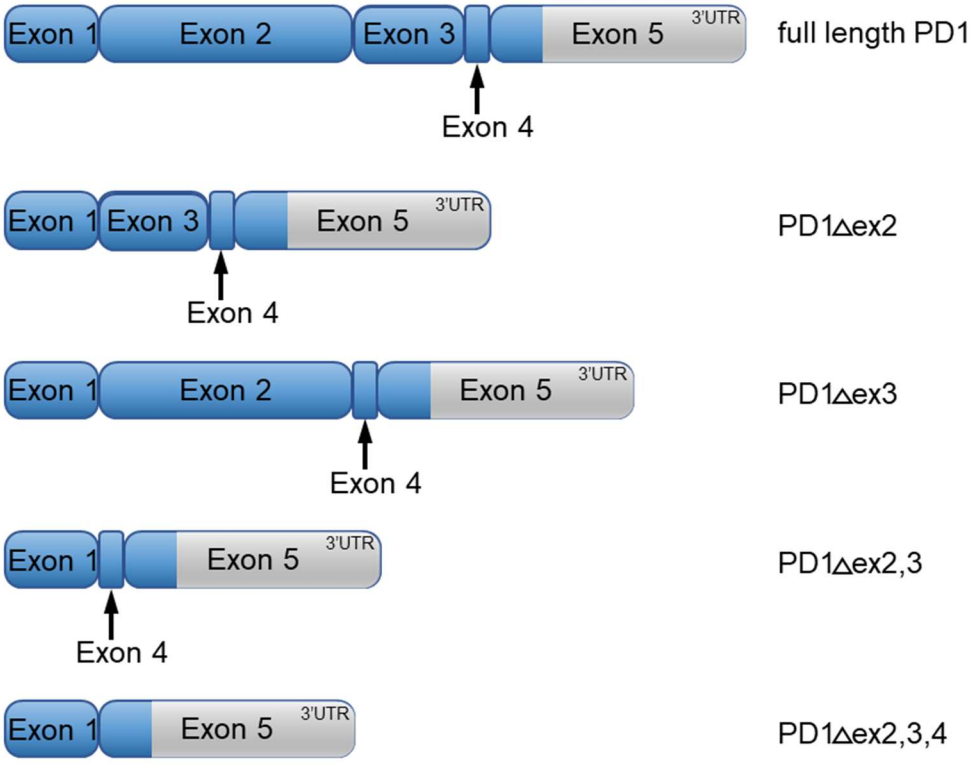

Figure 17 Alternative splice variants of *PDCD1*.

While Silencer Select technology, which we used for siRNA mediated *PDCD1* knockdown, ensures maximal gene silencing efficiency with minimal off-target effects, it can still induce non-specific response (Patel et al. 2009). Therefore, employing multiple siRNAs is advisable to isolate gene-specific effects. It is plausible that, apart from targeting *PDCD1*, siPD1 #2 may non-specifically impact a gene essential for cellular viability or involved in fundamental cellular processes. Therefore, we hypothesized that the off-target effect associated with siPD1 #2 is the most likely explanation for our contradictory results. At the same time, we assumed that effects observed for siPD1 #1 and siPD1 #3 represent the actual role of *PDCD1* knockdown in osteosarcoma cells.

4.6 Perturbed equilibrium of PD1 induces changes in the cellular proteome.

Determination of the ultimate consequences of PD1 intrinsic-signalling in U2OS cells appeared challenging due to inconsistency in cellular responses to siPD1. Thus, to dissect effects specific to PD1 disruptions, while eliminating potential off-target effects, we employed LC-MS/MS technology and analysed protein alterations shared across all siPD1s. Our analysis demonstrated that perturbed equilibrium of PD1 had the capacity to induce changes at the proteomic level, emphasizing

the significance of PD1 signalling in U2OS cells (**Figure 18**). To determine the impact

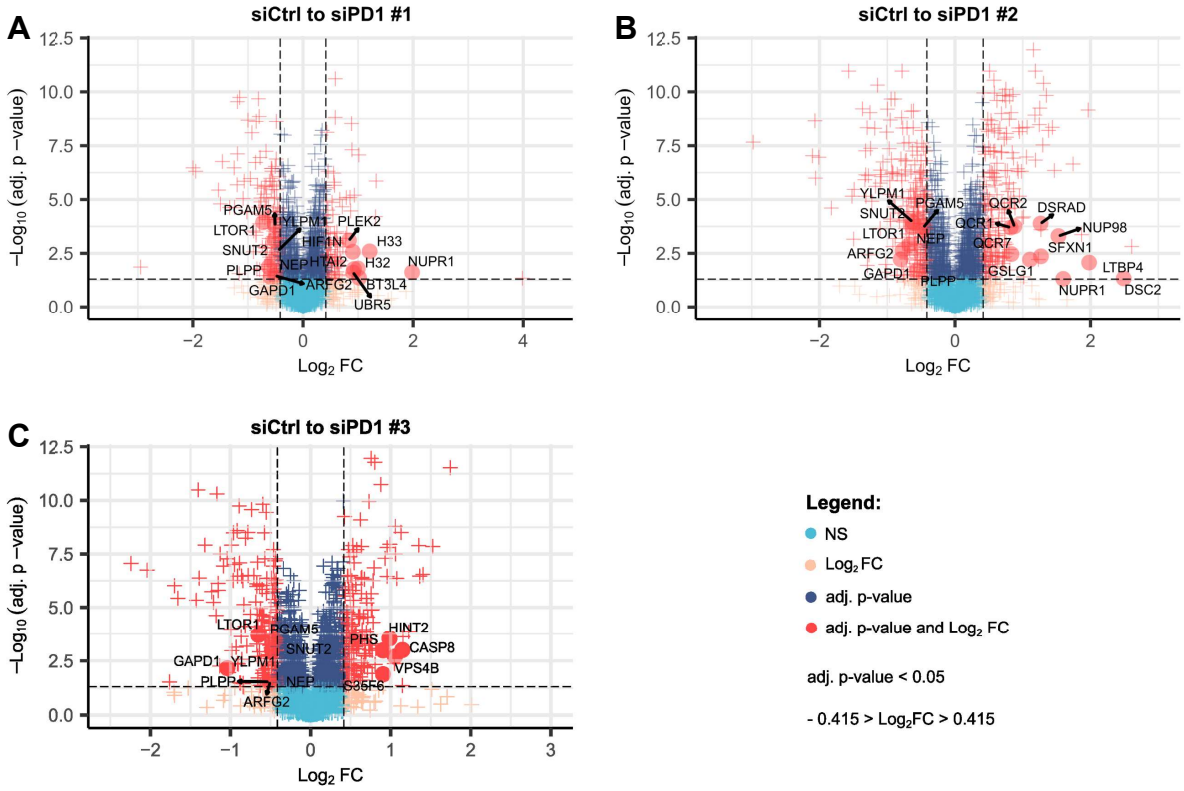

Figure 18. *PDCD1* knockdown induces changes in the global proteome of U2OS cells. All constructs **A)** siPD1 #1, **B)** siPD1 #2 and **C)** siPD1 #3 were used independently for *PDCD1* silencing and changes in protein expression between control and knockdown conditions were analysed. The cut-off of adjusted p-value was set to less than 0.05, what represents proteins with statistically significant difference in abundance between the control and siPD1 treatment. -0.415 > Log2FC > 0.415 (0.75>FC>1.33; FC=fold change) was arbitrary set as significantly different protein level between the control and PD1 knockdown samples. Proteins meeting the criteria for both, the adj. p value and Log2FC are represented by pink marks. Navy blue represents proteins with adj. p-value less than 0.05 but with no significant change in the protein abundance between the control and siRNA treated samples. All hits below the dashed line failed to meet the requirements for adjusted p-value, thus the statistical significance. The cut-offs were indicated by the dashed lines. Chosen proteins, common for all conditions were annotated in volcano plots. Log2FC < -0.415 represents the proteins, which were upregulated upon *PDCD1* knockdown, while Log2FC > 0.415 corresponds to those, which were downregulated upon siPD1 treatment. The graphs were prepared by Dr Jakub Faktor.

of proteomic alterations, we applied statistical criteria by setting the adjusted p value threshold to be less than 0.05. This value describes the significance of alterations of protein abundance resulting from *PDCD1* silencing. Of those, for further analysis we chose the proteins with fold change abundance of at least 1.33 for upregulated

proteins and below 0.75 for downregulated proteins. Such small changes in protein levels were considered as significant due to high quality of sample preparation. **Figure 19** demonstrates that only minor adjustments were required for proteomics data

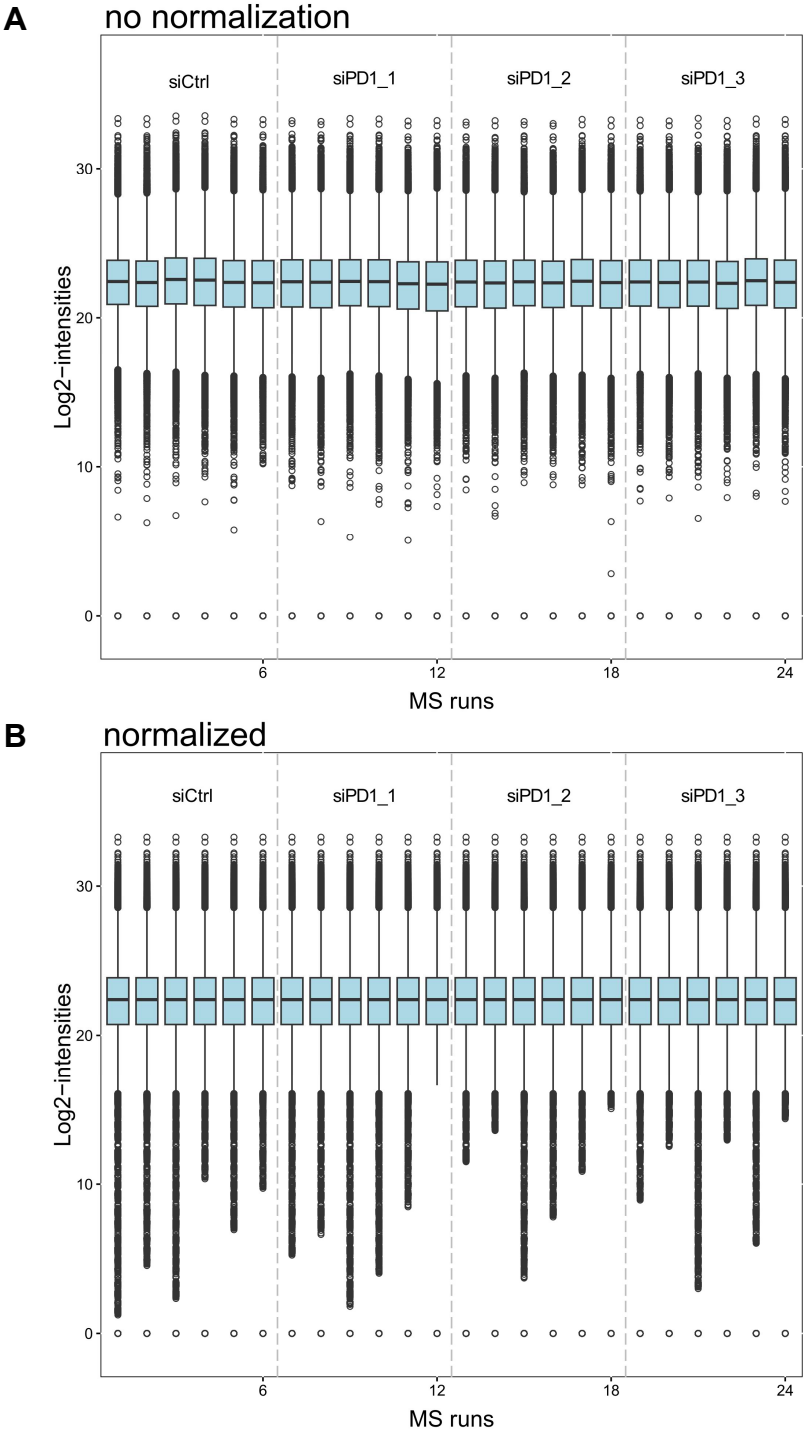

Figure 19 Box plots representing quality control of samples prepared for LC-MS/MS proteomic analysis. **A)** box plot displaying the distribution of proteins detected in both biological and technical replicates before data normalization; **B)** the same dataset after application of data normalization techniques, revealing only minor impact of normalization on protein distribution.

normalization. Thus, even small differences could be confidently regarded as significant. This suggests that the variations in protein abundance observed between the control and siPD1 treated samples arise from the actual changes in the protein levels.

4.7 *PDCD1* knockdown causes enrichment of processes crucial in cancer.

For deeper understanding of PD1-dependent proteomic alterations, hits identified in the global proteome analysis were subjected to the GO and GSEA tools (Gene Ontology and Gene Set Enrichment Analysis, respectively). Notably, in all conditions, disruptions in PD1 equilibrium were associated with the positive regulation of MAPK cascade. In T lymphocytes, PD1 receptor signalling negatively regulates MAPK cascade through LAT-signalosome (detailed description in the introduction chapter). Therefore, it could be anticipated that treatment with siPD1 would have the opposite effect. Our results, which demonstrate increased MAPK signalling upon treatment with siPD1, align with the established effects of PD1 signalling in immune cells (Patsoukis, Wang, et al. 2020). As demonstrated by the **Figure 20A-C** in the comparison between siCtrl and siPD1 samples, the analysis demonstrated negative (below zero) enrichment distribution of positive MAPK signalling, meaning that positive regulation of MAPK pathway was enhanced upon *PDCD1* knockdown, while was diminished when compared to the control. This suggests that, on the molecular level, PD1 may play a similar function in the osteosarcoma cells as it does in T cells. Furthermore, enrichment of MAPK signalling across all constructs tested may be considered as a positive control of *PDCD1* knockdown and supports the reliability of GO/GSEA analysis.

Apart from MAPK signalling, functional enrichment analysis for samples treated with siPD1 #1 and siPD1 #3 encompassed cell adhesion, migration, and motility. These processes are critical for cancer development and progression and were reflected by our biological data. Also, the analysis revealed that siPD1 treatment leads to enrichment of molecules regulating cellular growth, migration, and metabolism of macromolecules. As described in the previous chapter, it is known that activation of PD1 signalling in T cells diminishes cellular growth, proliferation, and survival. It happens by abrogating PI3K/AKT driven activation of CDKs and mTOR pathway

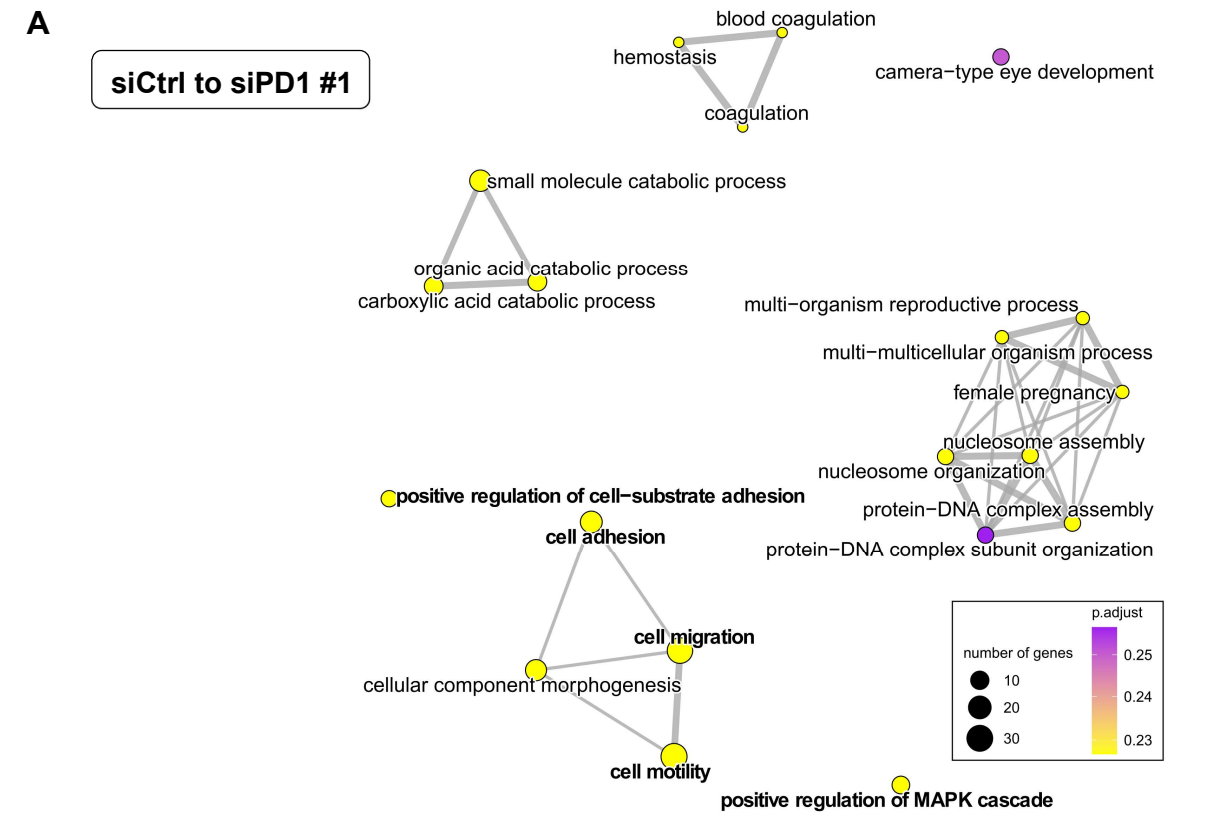

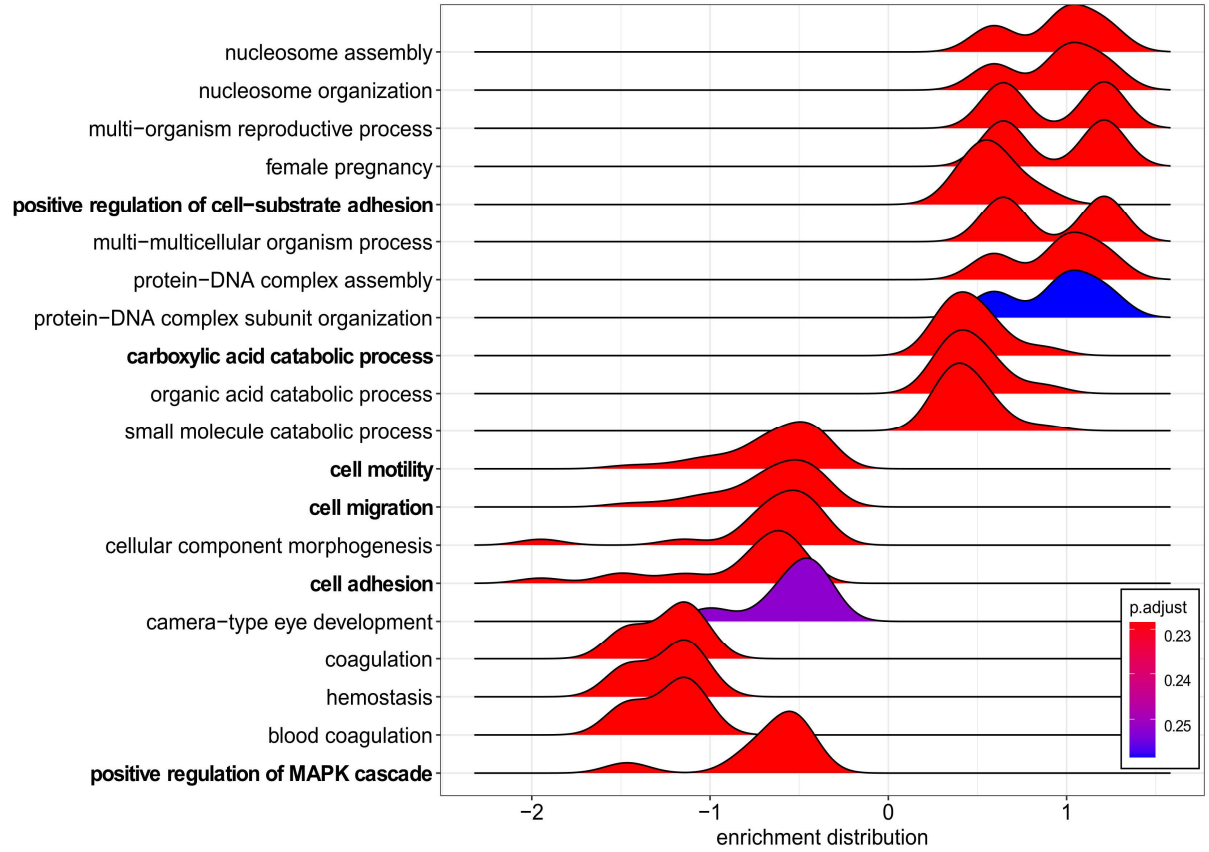

Figure 20 GSEA and GO analysis of biological processes affected by treatment with *PDCD1* targeting siRNAs. The analysis was performed for each siPD1 treatment **A)** siPD1 #1, **B)** siPD1 #2, **C)** siPD1 #3 with proteins identified in LC-MS/MS analysis, which met statistical criteria (adj. p value

B

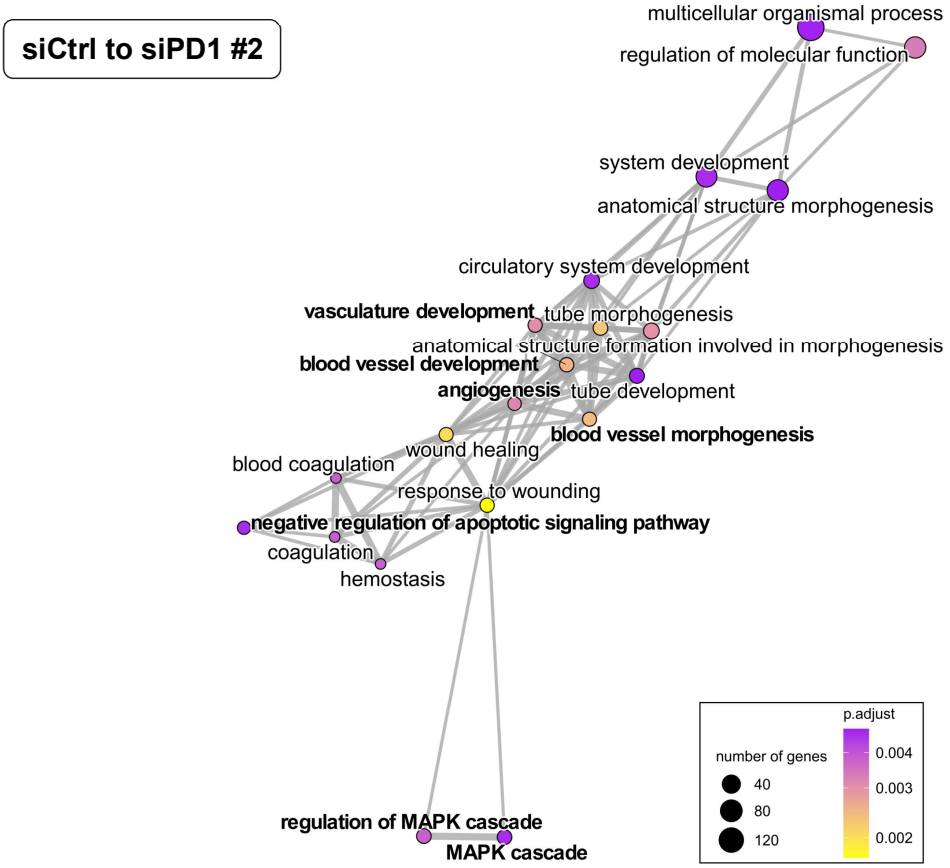

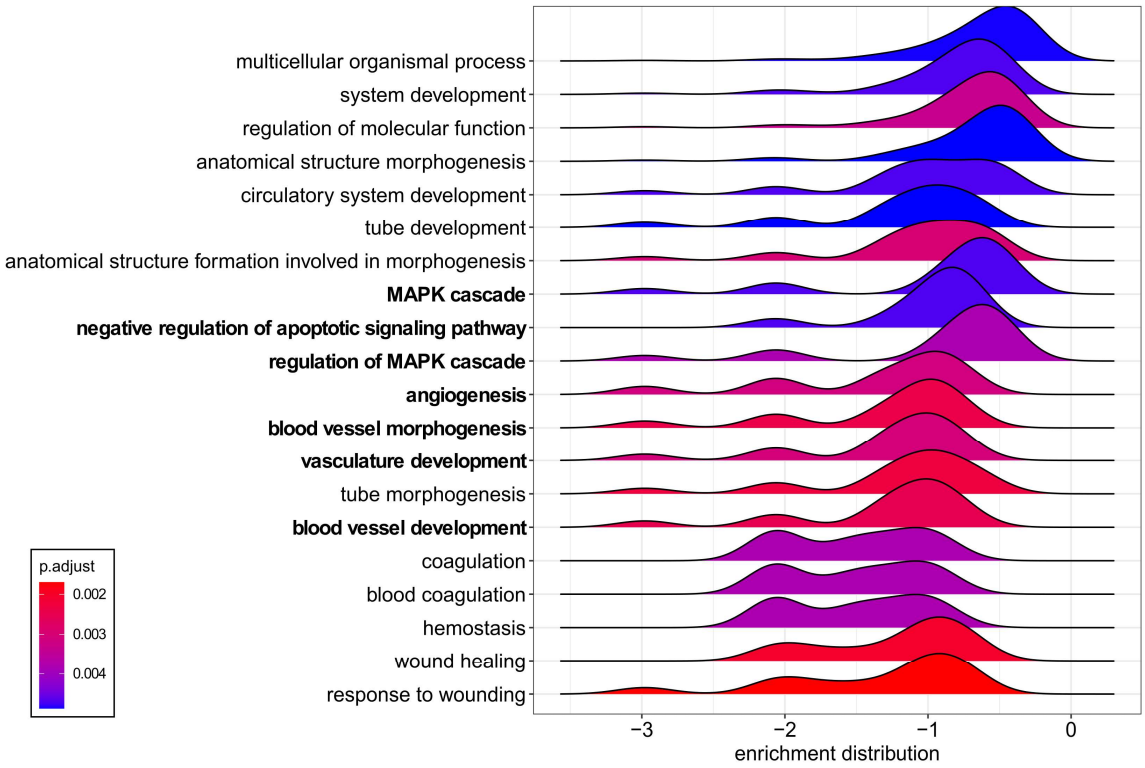

< 0.05). The legends of adj. p value correspond to the significance of the enrichment analysis and not to the significance of protein identification and quantification by the LC-MS/MS. Enrichment distribution describes whether a given term was negatively (<0) or positively (>0) regulated in control

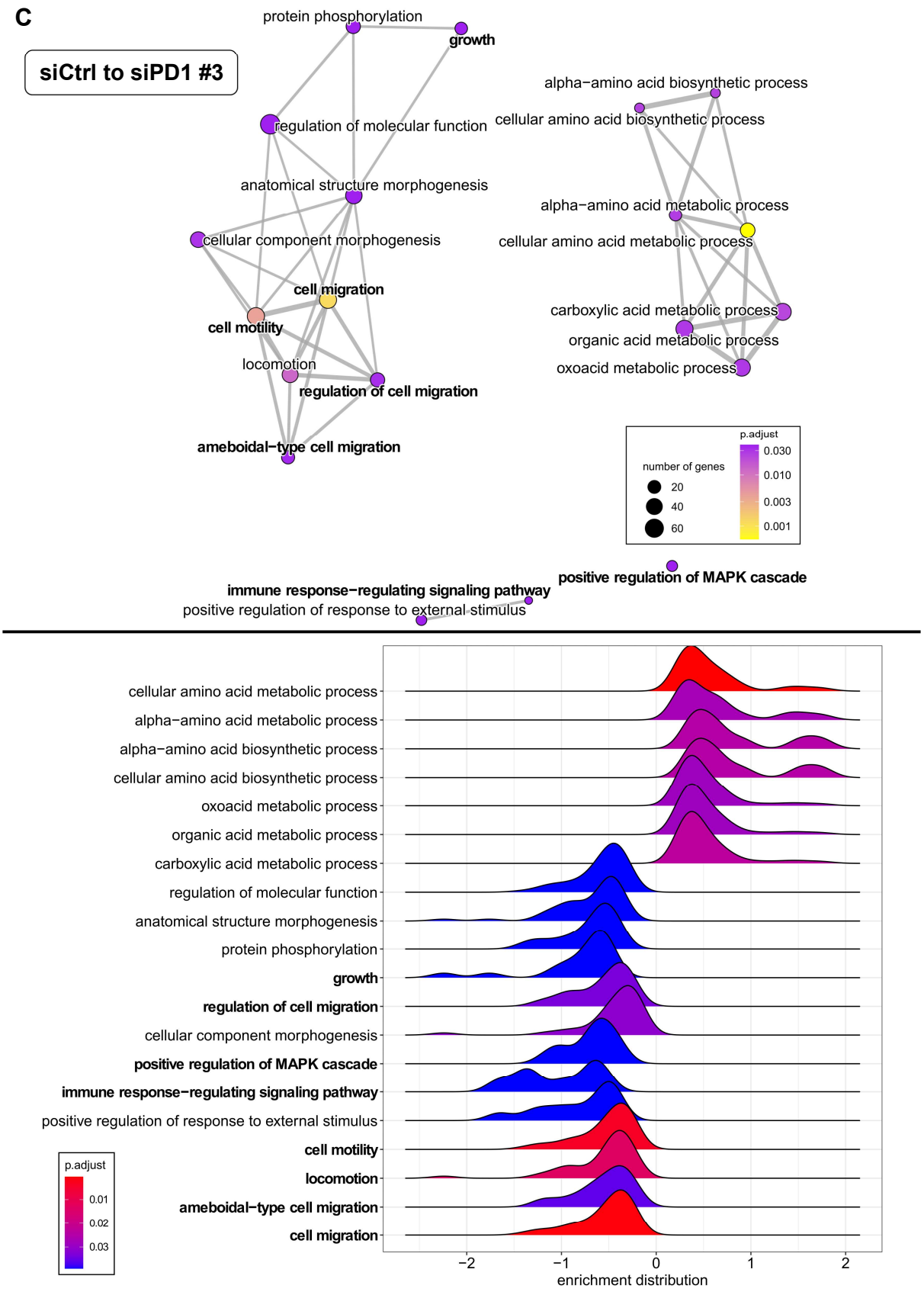

compared to *PDCD1* knockdown. For example, the enrichment distribution for cell motility is <0, thus it is down-regulated in control, while upregulated upon siPD1 treatment. The functional enrichment analysis and graphs were kindly prepared by Dr Jakub Faktor.

signalling. At the same time PI3K/AKT repression is controlled by PTEN. Therefore, by activating PTEN, PD1 indirectly controls PI3K/AKT mediated regulation of cell cycle and survival.

While most of the biological processes identified by GO/GSEA analysis are closely associated with cancer, some, less relevant such as blood coagulation, also emerge. This can be attributed to the fact that certain proteins are involved in multiple signalling networks of distinct functions. Moreover, the significance of PD1 extends beyond cancer and was reported in non-cancer related conditions, including neuro-degenerative diseases, neurotransmission, or pain (Zilong Wang et al. 2020; J. Zhao et al. 2021; G. Chen et al. 2017; K. Wang et al. 2020).

4.8 Defining the proteins commonly regulated across all siPD1s.

GO/GSEA analysis provided a comprehensive overview of processes affected by perturbed equilibrium of PD1 in U2OS cells. It demonstrated that MAPK signalling, cell adhesion, migration, motility, and cell growth are the key processes altered by *PDCD1* silencing. However, major discrepancies in cell response emerged among the oligonucleotides employed for RNA interference. Therefore, to dissect the exact PD1 effects at molecular level and eliminate non-specific outcomes, we performed a comparative analysis of our proteomic data to pinpoint the single protein alterations shared across all conditions.

Searching for similarities in alterations of the protein abundance, we observed that 59 proteins were consistently upregulated in response to siPD1 treatment across all constructs tested (**Figure 21A**) (Hulsen 2022). At the same time, among the downregulated proteins 5 were common for all conditions (**Figure 21B**), all proteins are listed in **Table 2 and 3**. Notably, PD1 was not detected in this experiment, likely due the low abundance of PD1, which we also observed in immunofluorescence staining or Western Blot analysis. Additionally, structural features of PD1 may cause poor ionization, therefore impacting protein detection by mass spectrometer. Alternatively, heavy glycosylation previously reported for PD1, may be an additional obstacle for peptide fragmentation and subsequent detection (Sun et al. 2020). Therefore, by using alternative experiments, we confirmed that

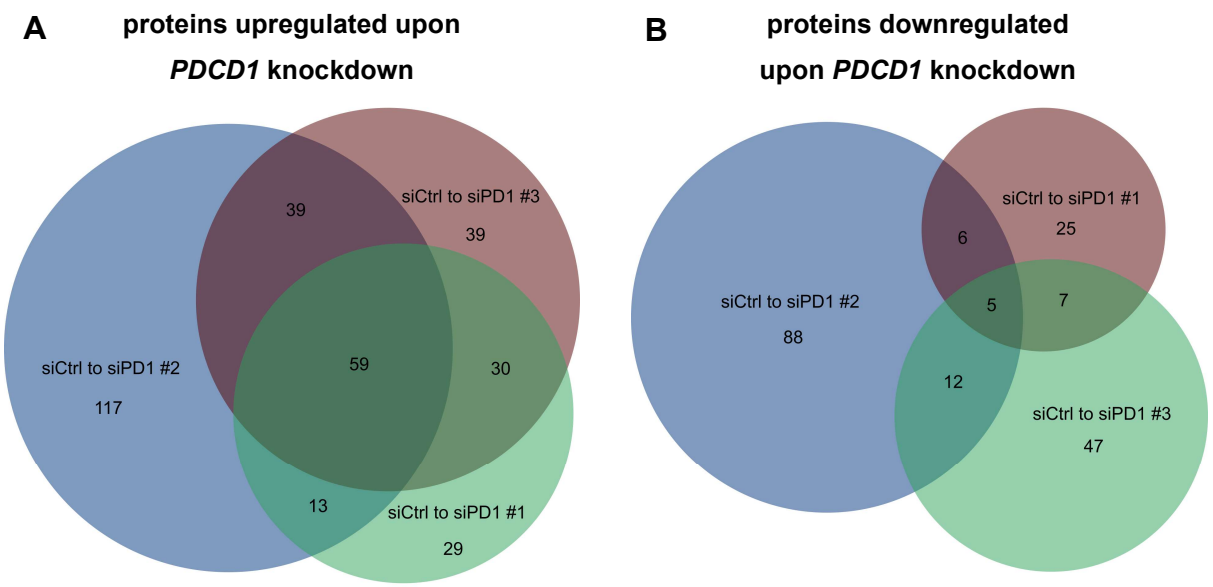

Figure 21 Deep-Venn diagrams demonstrating the number of proteins identified by LC-MS/MS analysis, which were either common or unique across all conditions. **A)** displays proteins significantly upregulated upon perturbed equilibrium of PD1, **B)** demonstrates the number of proteins downregulated upon siRNA treatment. The diagrams represent proteins with adjusted p value cutoff < 0.05 and 0.75 > fold change > 1.5 in comparison to control conditions.

siPD1 treatment disrupts the equilibrium of PD1, ensuring the reliability of our proteomic data.

Table 2 Proteins significantly downregulated (fold change < 0.75) in U2OS cells upon *PDCD1* knockdown identified by the global proteome analysis.

		Proteins downregulated upon PD1 silencing
No.	Protein	Full name
1	**ASNS**	Asparagine synthetase (glutamine-hydrolyzing)
2	**SERC**	Phosphoserine aminotransferase
3	**SQSTM**	Sequestosome-1
4	**PIR**	Pirin
5	**SRXN1**	Sulfiredoxin-1

Table 3 List of proteins significantly upregulated (fold change > 1.5) in response to perturbed equilibrium of PD1 protein.

		Proteins upregulated upon PD1 silencing
No.	Protein	Full name
1	**AGFG1**	Arf-GAP domain and FG repeat-containing protein 1
2	**AKAP12**	A-kinase anchor protein 12
3	**AKT1S1**	Proline-rich AKT1 substrate 1
4	**ALCAM**	CD166 antigen
5	**ALYREF**	THO complex subunit 4
6	**ARFGAP2**	ADP-ribosylation factor GTPase-activating protein 2
7	**ATXN2**	Ataxin-2
8	**CLASP1**	CLIP-associating protein 1
9	**CLIC4**	Chloride intracellular channel protein 4
10	**CSK**	Tyrosine-protein kinase CSK
11	**DNAJB1**	Dnaj heat shock protein family (hsp40) member b1
12	**DNAJC7**	DnaJ homolog subfamily C member 7
13	**EIF5B**	Eukaryotic translation initiation factor 5B
14	**FDFT1**	Squalene synthase
15	**GAPVD1**	GTPase-activating protein and VPS9 domain-containing protein 1
16	**GLO1**	Lactoylglutathione lyase
17	**HNRNPD**	Heterogeneous nuclear ribonucleoprotein a/b/d
18	**HNRNPUL1**	Heterogeneous nuclear ribonucleoprotein U-like protein 1
19	**HNRNPUL2**	Heterogeneous nuclear ribonucleoprotein U like 2
20	**IQGAP1**	Iq motif containing gtpase activating protein 1
21	**KDELC2**	KDEL motif-containing protein 2
22	**LAMTOR1**	Late endosomal/lysosomal adaptor, mapk and mtor activator 1
23	**LAMTOR2**	Ragulator complex protein LAMTOR2
24	**LAMTOR3**	Late endosomal/lysosomal adaptor, mapk and mtor activator 3
25	**LMAN2**	Vesicular integral-membrane protein VIP36
26	**LRRC20**	Leucine-rich repeat-containing protein 20
27	**LSM14A**	LSM14A, mRNA processing body assembly factor
28	**LUZP1**	Leucine zipper protein 1
29	**MCAM**	Cell surface glycoprotein MUC18
30	**MME**	Membrane metalloendopeptidase
31	**MTPN**	Myotrophin
32	**NELFB**	Negative elongation factor B
33	**PDXP**	Pyridoxal phosphate phosphatase
34	**PGAM5**	Pgam family member 5, mitochondrial serine/threonine protein phosphatase
35	**PNN**	Pinin
36	**PPP1R14B**	Protein phosphatase 1 regulatory subunit 14B
37	**PRKAR1A**	cAMP-dependent protein kinase type I-alpha regulatory subunit
38	**PRMT5**	Protein arginine N-methyltransferase 5
39	**QKI**	Qki, kh domain containing rna binding
40	**RAB14**	Ras-related protein Rab-14
41	**RAP2B**	Ras-related protein Rap-2b
42	**RBP1**	Retinol-binding protein 1
43	**RDX**	Radixin
44	**RRM2B**	Ribonucleotide reductase regulatory tp53 inducible subunit m2b
45	**SEC24B**	Protein transport protein Sec24B
46	**SGTA**	Small glutamine-rich tetratricopeptide repeat-containing protein alpha
47	**THBS1**	Thrombospondin-1
48	**TLN1**	Talin-1
49	**TOMM34**	Mitochondrial import receptor subunit TOM34
50	**TRIO**	Triple functional domain protein
51	**UBL7**	Ubiquitin-like protein 7
52	**UGP2**	UTP-glucose-1-phosphate uridylyltransferase
53	**USP15**	Ubiquitin carboxyl-terminal hydrolase 15
54	**USP39**	U4/U6.U5 tri-snRNP-associated protein 2
55	**WDR6**	WD repeat-containing protein 6
56	**WDR77**	Methylosome protein 50
57	**YES1**	Yes proto-oncogene 1, src family tyrosine kinase
58	**YLPM1**	YLP motif-containing protein 1
59	**YWHAH**	14-3-3 protein eta

4.9 Dissecting the molecular effects of perturbations in PD1 equilibrium.

In the next step, we examined if the 59 upregulated and 5 downregulated proteins, shared across samples are interconnected. We employed STRING database to search for known and predicted protein-protein interactions among these proteins. The analysis illustrated that the vast majority of the proteins commonly modulated form a signalling network (**Figure 22**). Furthermore, to explore their potential mechanistical connection to PD1 pathway, the PD1 protein was added manually to the dataset. We observed that PD1 was indeed a part of this network. Moreover, the analysis indicated that proteins creating the interacting network are majorly phosphoproteins. Presence of multiple phosphoproteins may indicate alterations in signalling pathways, cell cycle regulation or stress response (Bartholomew M. Shefton 1998). Thereby, it could be assumed that perturbed PD1 equilibrium in U2OS cells plays a role in modification of vital cellular processes. In fact, STRING analysis revealed that mTORC1-mediated signalling, MAPK2 and MAPK activation and energy dependent regulation of mTOR by LKB1-AMPK are the top three significantly enriched reactome pathways (**Table 4**). These pathways play a crucial role in regulating cellular metabolism, growth, proliferation, and response to growth factors. This correlates with our *in vitro* experiments, demonstrating *PDCD1*-knockdown-dependent alterations in cellular viability and migration. Moreover, GO/GSEA analysis, conducted for each condition independently, consistently indicated that regardless of the siPD1 used for silencing, MAPK signalling was augmented in all conditions. Altogether, suggesting that PD1 may play a critical role not only in T cells, but also in cancer cells.

Table 4 Functional enrichment of the proteins commonly identified across all treatment conditions with siPD1. Table generated in STRING database.

	Reactome Pathways			
pathway	*description*	*count in network*	*strength*	*false discovery rate*
HSA-166208	mTORC1-mediated signalling	4 of 23	1.75	0.0014
HSA-5674135	MAP2K and MAPK activation	5 of 40	1.61	0.00054
HSA-380972	Energy dependent regulation of mTOR by LKB1-AMPK	3 of 29	1.53	0.0458
HSA-6802952	Signaling by BRAF and RAF fusions	4 of 65	1.3	0.0255
HSA-5628897	TP53 Regulates Metabolic Genes	5 of 87	1.27	0.0065
HSA-3700989	Transcriptional Regulation by TP53	7 of 363	0.8	0.0458

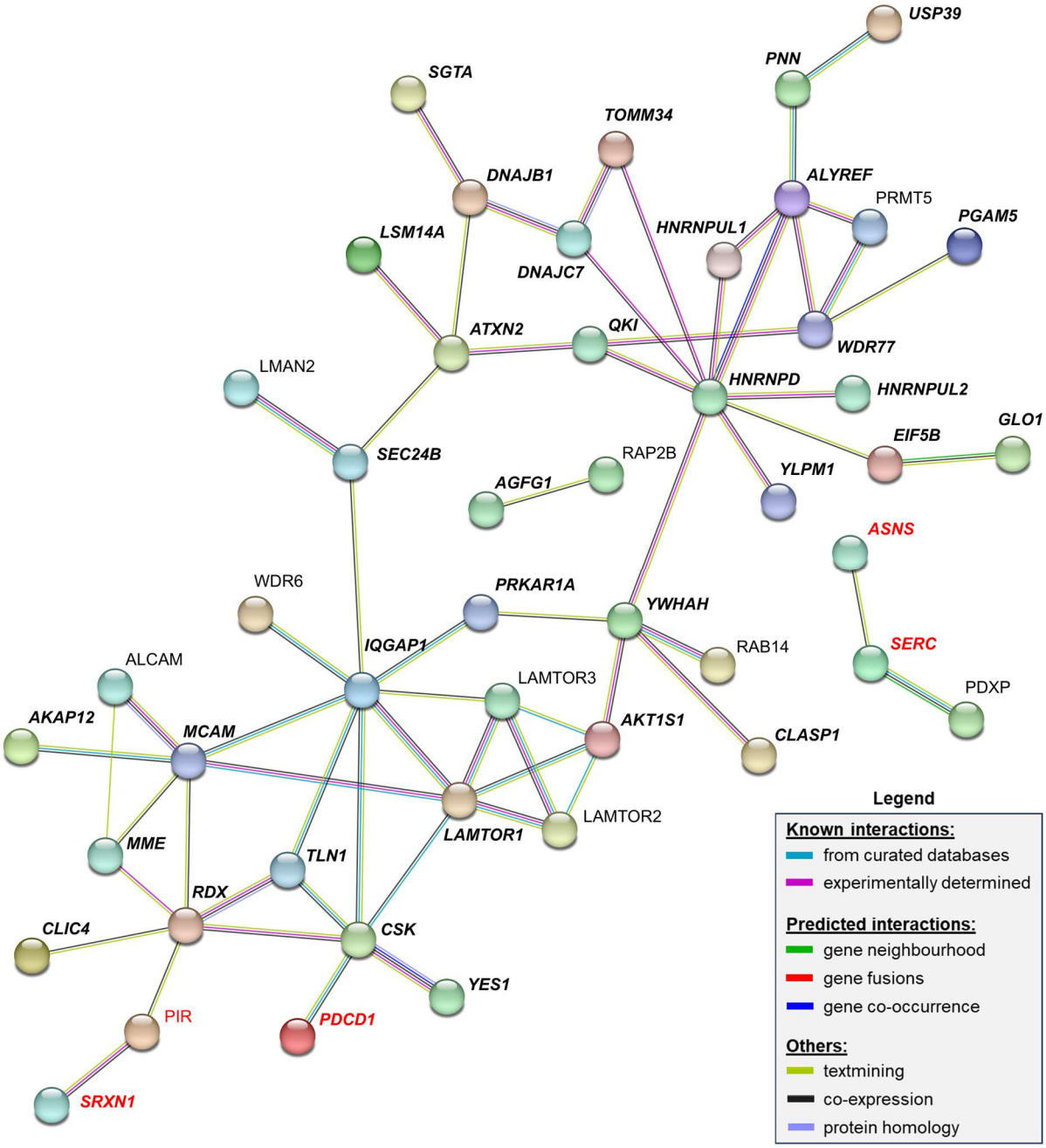

Figure 22 Interacting network of the significantly impacted proteins identified in proteomic analysis. Signalling network created in STRING database (https://string-db.org) with significantly upregulated and downregulated proteins in response to siPD1 treatment. The plot includes proteins which met the criteria of adj. p value < 0.05; 0.75 > fold change > 1.5. PD1 protein was added manually to demonstrate the link between PD1 and identified proteins. Upregulated proteins are denoted with black font, while downregulated are marked in red font. Phosphoproteins are indicated with ***bold italics***.

4.10 Discussion: downstream effects of PD1 signalling in osteosarcoma cells

Immune checkpoints discovery and their targeting in various malignancies revolutionized cancer treatment approach. It initiated extensive studies on the development of PD1/PDL1 immune checkpoint inhibitors and their implementation in cancer immunotherapy. However, somewhat less attention was dedicated to in-depth understanding of PD1 molecular mechanisms in immune cells, while only scarce reports highlight cancer-intrinsic PD1 signalling. Of those, it is still unclear whether tumour intrinsic PD1 acts as a tumour suppressor or a tumour promoter. Given that only some patients respond to immunotherapy, while others rapidly progress in response to ICB, it becomes evident that we may lack full understanding of PD1-PDL1 axis. For example, no beneficial effects of clinical trials with PD1/PDL1 blockade were reported in osteosarcoma patients and several mechanisms such as poor immune infiltrate or low tumour immunogenicity were proposed to justify the failure of immunotherapy in osteosarcoma patients (Boye et al. 2021; Le Cesne et al. 2019). However, some reports suggested cancer PD1 intrinsic signalling as one of the reasons why some tumours are refractory to immunotherapy. Therefore, in our studies we implemented human osteosarcoma cellular model to determine the importance and molecular mechanisms of cancer PD1 in this type of tumour.

Detailed discussion regarding complex and unclear nature of some results obtained for *PDCD1* silencing in osteosarcoma cells was provided along with the data for clarity. To summarize, we demonstrated that PD1 is spontaneously expressed by human osteosarcoma cells at the low level. The average of 4% of cells expressed PD1 on the surface, however the intracellular expression of PD1 was detected in almost all the cells. Such level of cancer-expressed PD1 on the surface corresponds to the previous studies reporting 3% to 9% PD1 positive cells, while intracellular expression of PD1 was not described in those reports (Schatton et al. 2010; Kleffel et al. 2015; Rotolo et al. 2023).

Moreover, our observations suggested that PD1 protein could be post-translationally modified what was observed as PD1 migration at 55kDa and 70kDa molecular weight detected by Western Blot analysis. Based on previous reports, we hypothesized that

55kDa represented heavily glycosylated PD1, which was described as the active form required for effective signalling in T cells (C. W. Li et al. 2016; Sun et al. 2020).

However, no public data is available in regard to the second post-translationally modified form that we detected as 70kDa molecular weight, which was previously reported as specific for PD1 protein and detected by various monoclonal antibodies (Y. Chen et al. 2010). We considered a number of possible PTMs, however most of them could be easily excluded. First, detection of certain PTMs require special conditions, which must be applied in order to protect them from degradation during cell lysis or due to reducing conditions, for example phosphorylation or SUMOylation. Apart from that, protein palmitoylation adds a mass too small to a protein to be visualized. Finally, PD1 dimerization through disulfide bonds was reported as infeasible. Alternatively, PD1 could be glycosylated on even higher level than 55kDa. Based on the molecular weight, we presumed that likely it corresponds to PD1 ubiquitination. Polyubiquitination of PD1 by FBXO38 ubiquitin ligase was demonstrated to control PD1 surface expression on immune cells (Meng et al. 2018). Additionally, it was proven essential to maintain anti-tumour activity of T cells, presumably by preventing PDL1 ligation and T cell exhaustion (Gavali et al. 2021; Bonnevier, Zhang, and Mueller 2005; Meng et al. 2018). However, no information regarding how ubiquitination affects cancer PD1 signalling, nor protein detection was described and requires further experimental validation.

To investigate the function of PD1 in U2OS cells we implemented the siRNA technology. Experiments were performed with three different oligonucleotides targeting *PDCD1* mRNA. RT-qPCR analysis confirmed reduction of *PDCD1* transcript levels 48 and 72 hours upon transfection for all siPD1s. SDS-PAGE analysis demonstrated changes in the migration pattern of PD1 protein exhibited as reduction in PD1 expression, but only for 55kDa molecular weight. Strikingly, the expression of the higher molecular weight representing the unidentified PD1 PTM was slightly increased. Simultaneously, flow cytometry analysis did not reveal substantial changes in PD1 expression, either on the membrane nor intracellularly. Therefore, we hypothesized that siPD1 treatment of U2OS cells in fact perturbs the equilibrium of PD1 protein in U2OS cells.

Next, we examined the impact of the perturbed equilibrium of PD1 on U2OS cell migration and viability. All experiments were performed using all three siPD1s. Treatment of the cells with siPD1 #1 and #3 significantly enhanced cellular migration and viability. This suggest that when in equilibrium, PD1 may as a tumour suppressor, likewise in NSCLC and colon cancer (Du et al. 2018; X. Wang et al. 2020; Ieranò et al. 2022) but in contrast to tumour promoter role in melanoma, glioblastoma or pancreatic cancer (Mirzaei et al. 2021; Kleffel et al. 2015; Pu et al. 2019).

Surprisingly, siPD1 #2 caused the opposite cellular effect exhibited as limited cellular migration and proliferation. We reasoned that the contradictory results of our studies most probably result from the off-target effect caused by the siRNA used in our experiments. Dangerously, these unpredicted binding to the unknown target could take place in parallel to targeting PD1, impacting the observed silencing effects. Moreover, if a single siRNA was used, these unspecific effects would be impossible to identify. It is tempting to consider, that this issue could partially account for contradictory results described in cancer-PD1 reports, especially those implementing si/shRNA technology. Non-specific binding of siRNAs to additional targets is a prevalent concern. Thus, it is recommended to implement more than one oligonucleotide in any analysis for improved accuracy.

To further understand molecular consequences of altered expression of PD1, we performed LC-MS/MS analysis of the global proteome of U2OS cells induced by *PDCD1* knockdown. Once again, the experiment was performed for all silencing conditions. We observed that siPD1 treatment clearly induces changes in the global proteome of U2OS cells, emphasizing the significance of cancer PD1 signalling. Proteins with either increased or decreased abundance compared to the control conditions were subjected to Gene Ontology (GO) and Gene Set Enrichment Analysis (GSEA). In all datasets positive regulation of MAPK signalling was annotated as the response to *PDCD1* knockdown. Abrogation of MAPK signalling is a known effect of PD1 activation in T cells, therefore we considered this result as a validation of PD1 manipulations in the cells. Additionally, the data pointed to changes in motility, migration, and adhesion. Therefore, together with increased MAPK signalling, this data corresponds to cellular effect observed upon treatment with siPD1 #1 and #3.

Subsequently, to better understand which proteins and corresponding pathways were directly affected, we considered data similarities across all conditions. We postulated that through the evaluation of proteins commonly impacted following siPD1s treatment, we could observe the proteomic reaction to the altered PD1 equilibrium in U2OS cells. Concurrently, we aimed to exclude any unintended effects of siRNAs. Consequently, we identified significant reduction in the abundance of 5 proteins, with a minimum fold change of 0.75. Conversely, the increased abundance (fold change more than 1.5) was observed in 59 proteins, all of which exhibited statistical significance. Next, we implemented STRING database to investigate potential mechanistical connections at a single protein level to explore any correlation. Although PD1 was not detected in the LC-MS/MS analysis, most likely due to technical constraints, we manually incorporated it into the network. As a result, the majority of these proteins formed a comprehensive protein-protein interaction network, suggesting their close interconnections. Finally, we considered the implications of these alterations in protein abundance and their potential connection to PD1 signalling. Below, we provide a comprehensive discussion regarding selected findings.

Although predominantly, there is no direct link reported in the literature between PD1 and the LC-MS/MS identified proteins, these correlations may remain undiscovered. Cancer-intrinsic PD1 has not been extensively studied, and there may still me be gaps regarding the interacting network of the proteins we detected in our analysis. However, our results provide a solid foundation for further studies deciphering the PD1 interacting network in cancer cells. Additionally, similar mechanisms can be shared by immune cells, and our data hold the potential to significantly expand the existing knowledge of PD1 signalling. Recognizing the correlation between PD1 and other cancer-related proteins may have therapeutic potential and could be implemented in combinatory therapy against cancer. Therefore, we analysed how PDCD1 silencing affects osteosarcoma signalling and summarized the most important observations below.

4.10.1 The role of proteins upregulated upon *PDCD1* silencing

4.10.1.1 Perturbations in PD1 expression alter mTORC1 signalling.

Our LC-MS/MS analysis identified several proteins involved in mTORC1 pathway signalling, including the Ragulator complex proteins/Late Endosomal (Lysosomal) Adaptor, MAPK, and mTOR Activator (LAMTOR1; LAMTOR2; LAMTOR3) and proline-rich AKT1 substrate 1 (AKT1S1).

mTORC1 signalling is a vital pathway controlling protein and lipid synthesis but also purine and ribosome production, process indispensable in rapidly growing and metabolically active cells (Takahara et al. 2020). LAMTOR proteins are pivotal for the activation of mTOR complex 1 (mTORC1) in response to amino acid sensing. To become activated, mTORC1 must translocate from the cytosol to late endosomal/lysosomal membranes, where it is anchored by a complex formed between RAG GTPases and Ragulator (LAMTOR) proteins. Interestingly, the LAMTOR complex is where mTORC1 and MAPK signalling intersect (de Araujo et al. 2013; Manifava et al. 2016).

In T cells, PD1 indirectly constrains mTOR pathway signalling by modulating PI3K/Akt signalling in T cells. The association between cancer PD1 and mTORC1 was previously reported by Kleffel et al. (2015). That study indicated that unlike in T cells, cancer-PD1 increased the activation of mTORC1 effector molecule - ribosomal protein S6 (RPS6) (Kleffel et al. 2015). Notably, the results demonstrated that RPS6 activation was independent of the upstream PI3K signalling, suggesting the role of an alternative mTORC1 activation. Conversely to PD1 role in melanoma, our study suggested that the mTOR signalling in osteosarcoma may be repressed by PD1, similarly to the role of PD1 in T cells, however the upstream mechanism for mTORC1 activation upon *PCDC1* silencing remains unclear.

In addition to molecules facilitating the activation of mTOR signalling, we identified increased abundance of AKT1S1, which plays a regulatory function for mTORC1 activity. Upon phosphorylation by AKT and mTORC1 itself, AKT1S1 dissociates from mTORC1, facilitating its activation. Following the release and phosphorylation,

AKT1S1 binds to 14-3-3 proteins, maintaining the mTORC1 activity. Interestingly, increased abundance of 14-3-3 eta in response *PDCD1* knockdown was also detected in our analysis. 14-3-3 proteins coordinate vital cellular processes such as apoptosis, cell cycle and transcriptional regulation and were implicated in cancer, neurodegenerative diseases, diabetes, or metabolic disorders (Nascimento et al. 2010; Wiza, Nascimento, and Ouwens 2012; Pennington et al. 2018).

Detection of multiple components of mTOR pathway signalling and crucial regulatory proteins in the cell demonstrates the significance of PD1 in osteosarcoma cells. While the experimental validation of the presented data is necessary, this study offers valuable insights into further directions to study cancer PD1.

4.10.1.2 The link between PD1, cell adhesion and metastatic potential

ALCAM

ALCAM (CD166) is a glycoprotein also known as Activated Leukocyte Cell Adhesion Molecule. In the context of cancer, ALCAM as a cell adhesion molecule, facilitates cell to cell interactions and interactions between cells and the extracellular matrix. A growing body of evidence implicates CD166 importance in cancer metastasis as it promotes cancer cell binding to endothelial cells (Ferragut et al. 2021). Previous reports indicated that the increased expression of ALCAM by tumour cells has been associated with poor prognosis and shorter overall survival in multiple types of cancer, including osteosarcoma (D. K. Kim et al. 2020; Ferragut et al. 2021). Interestingly, preliminary studies indicated a therapeutic potential of anti-CD166/4-1BB CAR T-cell adoptive therapy in cellular model of osteosarcoma or colorectal cancer. (Y. Wang et al. 2019; He et al. 2023)

To our knowledge, PD1 has not yet been linked to cell adhesion. However, cancer-intrinsic PD1 expression has been previously associated with malignant melanoma and brain tumour-initiating cells (Schatton et al. 2008; Mirzaei et al. 2021), while CD166 was recently identified as a marker for cancer stem cells (Kalantari et al. 2022; Brinkhof et al. 2020). Bearing this in mind, the increased abundance of ALCAM in response to perturbed equilibrium of PD1 could suggest that PD1 may indirectly impact the stemness of osteosarcoma cells. Our data indicates that CD166 expression

conversely correlates to PD1 expression in osteosarcoma cells and siPD1 treated cells exhibit faster migration as indicated by the wound healing assay. Therefore, we see the effect opposite to the observations made in melanoma and glioblastoma. The role of cancer-intrinsic PD1 was already demonstrated to significantly differ depending on the tumour type. In fact, studies conducted in melanoma and glioblastoma indicated that cancer-PD1 acts as a tumour promoter, while our data strongly suggest tumour suppressive role in osteosarcoma. Therefore, it can be assumed that apart from PD1, more molecules may play the opposite functions depending on the type of malignancy. Further studies are necessary to validate the correlation between CD166 and PD1 and to explore whether cancer-PD1 could be associated with cancer stemness. Additionally, determining if cancer-intrinsic PD1 blockade with therapeutic monoclonal antibodies results in the same effect observed for *PDCD1* gene knockdown, could elucidate the role of cancer-PD1 in hyperprogression and ICB resistance.

MUC18

Apart from CD166, we observed that perturbed equilibrium of PD1 increased the abundance of MUC18 (CD146). MUC18 is a member of the mucin family, which comprises heavily glycosylated large proteins predominantly involved in the formation of the mucus barrier. However, CD146 is also expressed by endothelial cells at the intercellular cell junctions in the vascular system (Anfosso et al. 2000). Like other mucins, MUC18 it is aberrantly expressed in cancer, supporting the disease progression and metastasis. Initially identified as melanoma adhesion molecule (MCAM), MUC18 is well-documented to be associated with poor prognosis and increased metastatic potential (Lehmann, Riethmuller, and Johnsont 1989). Additionally, MUC18 is also expressed by osteosarcoma cells, and mouse studies demonstrated that inhibition of MUC18 significantly decreased osteosarcoma metastasis to the lungs (Mcgary et al. 2003). Consequently, the previously unknown association between MUC18 and PD1 that we observed may contribute a deeper understanding of the biological role of PD1 receptor in cancer cells.

4.10.1.3 PD1 links to focal adhesion, cancer progression and metastasis

Talin-1

In addition to alterations observed in cell adhesion molecules, enhanced metastatic potential could result from the modifications of focal adhesions (FAs). FAs comprise a complex of proteins, which sense mechanical signals coming from extracellular environment and convert them into intracellular signalling at the molecular level (Gregg 2021). Our proteomics analysis indicated that *PDCD1* knockdown in U2OS cells increased the abundance of talin-1. It is a crucial component of the focal adhesion complex involved in the outside-in communication between cells and extracellular matrix (ECM) (Daniel E Shumer 2017). Adhesion of cells to the ECM is indispensable for any multicellular organism and is majorly mediated by integrins. Integrins comprise a group of transmembrane receptors, which determine cell fate, participate in the regulation of cell survival, proliferation, and cell cycle but also in tissue development and repair (Danen and Sonnenberg 2003; Guo and Giancotti 2004). Failure of integrin binding to ECM leads to apoptosis. Integrins become activated by binding of an adaptor protein talin to their cytoplasmatic tails, what enables the interaction between integrins with actin cytoskeleton and formation of focal adhesions. Due to the structural properties, talin plays a central role in mechanotransduction governed by FAs (Y. Zhao, Lykov, and Tzeng 2022; P. Tang et al. 2007). Talin controls integrin downstream signalling cascade, and together with paxillin facilitate recruitment of SFKs (including Yes) and focal adhesion kinase (FAK) to integrins (Parsons and Parsons 2004; Guo and Giancotti 2004). In fact, talin controls integrin downstream signalling cascade, which converges with RTK signalling, therefore intersects with ERK and PI3K/AKT/mTOR signalling. Downstream effectors of integrins and ERK signalling, c-Jun and c-Fos respectively, lead to activation of AP-1 transcription factor. AP-1 promotes expression of genes vital for cell proliferation, migration, and invasion. Talin was reported to be a key player in ECM independent cell growth, facilitating carcinogenesis. Consequently, Dysregulation of RTKs and integrin signalling plays a critical role in cancer progression and metastasis (F. Lu et al. 2022).

Moreover, talin participates in the formation of the immunological synapse, facilitating contact between T cells and APCs and is involved in the maintenance of T regulatory

cells (Toomer 2016). Interestingly, AP-1 is one of the core downstream effectors during T cell activation, which becomes abrogated by PD1/PDL1 signalling, a mechanism linking the above-mentioned signalling events. Interestingly, our results additionally indicated increased abundance of radixin, which is a cytoskeletal protein implicated to activate integrins in talin-independent manner. Considering established associations among proteins identified in our proteomic analysis, this study gains additional corroborative evidence, but further studies are urgently needed to closely explore the links between these proteins (P. Tang et al. 2007). Taken together, the enhanced motility of U2OS cells, along with abundance of CAM molecules observed upon siPD1 treatment suggest that PD1 may impact metastatic properties of osteosarcoma cells.

4.10.1.4 C-terminal Src kinase (CSK)

Apart from that, the LC-MS/MS analysis indicated that perturbed expression of PD1 caused increased abundance of CSK and Yes1 proteins. CSK is a negative regulator of the SRC family of tyrosine kinases (SFKs), the proteins acting as upstream activators of PI3K/AK, MAPK/ERK and STAT3 pathways, which play crucial role in anti-apoptotic, pro-survival and growth signalling (S. Zhu et al. 2023). Therefore, by abrogating MAPK or PI3K/AKT signalosome, CSK is regarded as a pro-apoptotic factor. Additionally, it is involved in the regulation of cell survival, proliferation, and cytoskeletal organisation (Fortner et al. 2022). CSK executes its function by phosphorylation of C-terminal tyrosine residues of SFKs, a family comprising nine members: ubiquitously expressed Fyn, Src, Yes and Yrk; but also, Blk, Fgr, Hck, Lck and Lyn, which are predominantly expressed in differentiated cells (S. Zhu et al. 2023). Interestingly, Lck and Fyn play a critical role in TCR downstream signalling during T cell activation, a step inhibited upon PD1 activation (Laird and Hayes 2010; Chatterjee et al. 2013).

Yes1 and CSK proteins play the opposing functions as Yes is one of the SFKs targeted by CSK. Perhaps, it can be hypothesized that the mutual increase of these two proteins in our experiments is a result of a feedback signalling. It was previously reported that a feedback loop between CSK and SFKs exists in response to hyperactivation of the latter (Jiang et al. 2006). Possibly, a similar mechanism may

be present in our model. On the other hand, CSK seems to inhibit similar molecular targets as PD1 does, such as PI3K/Akt or MAPK signalling. Therefore, it is tempting to speculate that CSK signalling could maintain homeostasis when PD1 signalling becomes disturbed. Nevertheless, none such studies were conducted, and it remains pure speculation.

Collectively, the data demonstrates that perturbations in PD1 expression in human osteosarcoma cells resulting from *PDCD1* knockdown modulate major signalling events in these cells. These alterations comprise mTORC1 pathway, focal and cell adhesion but also Src kinase signalling. Consequently, leading to accelerated cancer cell growth and enhanced ability to migrate. Therefore, cancer PD1 signalling may play an important role in cancer metastasis and most probably acts as a tumour suppressor in osteosarcoma cells. However, further experimental works must be conducted to validate our initial observations.

4.10.2 The role of proteins downregulated upon *PDCD1* silencing

4.10.2.1 Phosphoserine aminotransferase - SERC (PSAT1)

The LC-MS/MS analysis indicated the phosphoserine aminotransferase (SERC, PSAT1) as one of the few proteins downregulated in response to *PDCD1* silencing. SERC is an enzyme that controls serine biosynthesis - a critical amino acid required for the synthesis of nucleotides, other amino acids, and cell membranes. Therefore, SERC plays an important role in cellular metabolism and is particularly significant for rapidly dividing cells, such as malignant cells (Yiqun Zhang et al. 2020; H. Wang et al. 2020; Y. Yang et al. 2015; Gao et al. 2017). Increased expression of SERC was reported in several types of cancer such as triple negative breast cancer, NSCLC or colon cancer and was associated with drug resistance and increased metastatic potential of the cells (Liao et al. 2016; Qian et al. 2017; Vié et al. 2008; Y. C. Chan et al. 2020). Despite decreased abundance of SERC upon *PDCD1* siRNA interference, U2OS cells proliferate and migrate faster than the control, while reports regarding SARC role in cancer cells would suggest otherwise. Nevertheless, cell signalling is a tremendously complex and finely controlled process in which the feedback loops maintain the signalling homeostasis. Therefore, when multiple

proteins are analysed, it is likely to observe ambiguous outcomes perhaps as a result of feedback mechanisms. Yet, the more we learn about the signalling events in the cells, the higher the chances are for the effective multivalent cancer therapeutic approach.

4.10.2.2 Implications of PD1 role in the oxidative stress response

Sulfiredoxin-1 and pirin

By regulating the activity of antioxidant proteins (peroxiredoxins), SRXN1 protects cells from damaging consequences of reactive oxygen species (ROS). Increased rate of ROS production is associated with rapid cell growth and high rate of metabolism like in cancer cells. High levels of SRXN1 were associated with increased proliferative potential in several types of cancer. Therefore, targeting proteins protecting cells from oxidative stress can be a potential strategy to preferentially target cancer cells, which already have high levels of toxic ROS (Perillo et al. 2020; H. Kim et al. 2015). SRXN1 expression is regulated by AP-1 - a transcription factor, which is activated upon T cell activation but becomes abrogated upon PD1/PDL1 signalling. One could expect that if PD1 pathway in cancer cells resembles PD1 axis in immune cells, then *PDCD1* silencing should act as an “inhibitor” of its downstream effects, resulting in increased expression of AP-1 targets, while our results demonstrate the opposite (Yukawa et al. 2020; Q. Wei et al. 2008; Atsaves et al. 2019).

Another oxidative stress-related protein downregulated upon *PDCD1* silencing was pirin (PIR), an oxidative stress sensor and iron-dependent transcriptional co-regulator of NF-κB pathway (F. Liu et al. 2013; Perez-Dominguez et al. 2021). PIR was linked to cell-cycle control, EMT and was associated with more malignant phenotype of cancer cells. Therefore, decreased abundance of PIR as the effect of perturbations in PD1 expression does not correspond to the observed cellular effect of increased cell viability and migration. Together, we can speculate that although cancer-intrinsic PD1 in osteosarcoma cells may supress mTOR signalling, control cell and focal adhesion, then it could potentially improve oxidative stress response. However further studies are necessary to determine cancer-PD1 function in broader context.

Altogether, our results demonstrated that PD1 protein is expressed by human osteosarcoma cells, while the *in vitro* studies indicated that cancer-intrinsic PD1 in osteosarcoma could act as a tumour promoter. Moreover, the proteomic studies provided a comprehensive description of the molecular foundations of PD1 pathway signalling in osteosarcoma cells and should be further explored in the future.

5. Results: identification of PD1 protein-protein interactions

Determining the role of cancer-intrinsic PD1 is absolutely vital for safety of immunotherapy and improvement of its efficacy. Should the necessity arise to modify cancer-intrinsic PD1 signalling for future clinical implementation, it is crucial to identify PD1 interactors as potential targets for the therapy. Simultaneously, elucidating PD1 signalling network is still equally important for better understanding of PD1 function in cancer cells. Although, some downstream effects of cancer-intrinsic PD1 signalling have been described, the underlying mechanism is not fully understood. Therefore, the second objective of my research studies aimed at identification of PD1 interacting partners.

5.1 The experimental setup used to identify PD1 interacting proteins

We adapted a high-throughput screening protocol to identify PD1 interactions. First, using a plasmid system, we overexpressed the recombinant PD1 protein in U2OS cells and next we performed a pull-down experiment. Presuming that the pull-down isolated proteins interact with PD1, we processed the samples, performed LC-MS/MS and computational analysis. Finally, we validated the interactions between PD1 and selected proteins using independent molecular biology methods such as Western Blot and Proximity Ligation Assay (**Figure 23**).

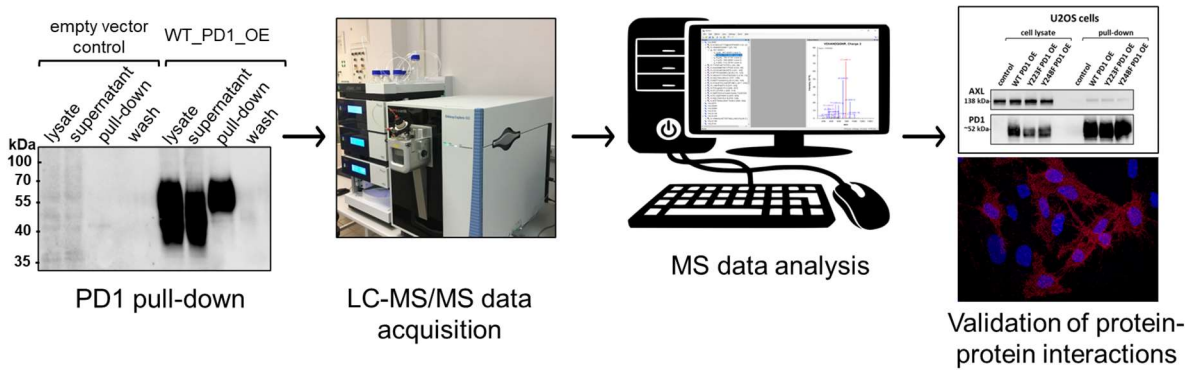

Figure 23 Schematic illustration of the workflow implemented in the study to identify PD1 interacting partners.

5.2 Implementation of recombinant PD1 protein for pull-down experiment.

Unlike antibody-dependent coimmunoprecipitation approach, the pull-down assay is an in vitro method, which utilizes a tagged bait protein. In this technique, a gentle

affinity purification method is employed to isolate both the bait protein and its interacting partners referred to as the prey (**Figure 24**). Subsequent

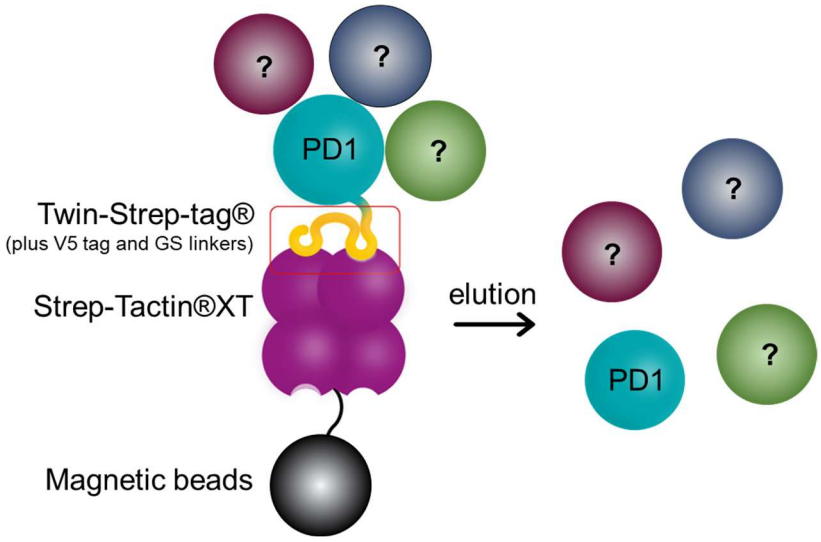

Figure 24 Schematic illustration of the key steps of a pull-down experiment. To be used as a bait protein, PD1 was tagged with Twin-Strep-tag®. Recombinant PD1 was subsequently overexpressed in U2OS cells, which were lysed under gentle conditions to preserve protein-protein interactions. The undisrupted complex formed by the bait and prey proteins was isolated by exploiting the interaction between Twin-Strep-tag® of PD1 and Strep-Tactin®XT immobilied on magnetic beads. Noteworthy, the interaction between the Twin-Strep-tag® and Strep-Tactin®XT employs one of the strongest covalent bonds existing between biotin and streptavidin. In our setup, both components were chemically modified to increase their affinity and stability even further. In the final step of the experiment proteins were eluted with SDS buffer under reducing conditions. Protein identification and quantification was performed using LC-MS/MS approach followed bioinformatic analysis.

identification of isolated proteins can be achieved through LC-MS/MS analysis.

Given the necessity to use a recombinant protein, along with the low abundance of endogenous PD1, we employed a plasmid system for PD1 overexpression. First, we assessed the optimal approach to tag PD1, aiming to minimize any interference with protein expression, stability, and protein-protein interactions. We tested distinct combinations of PD1 modifications, including either a single Twin-Strep-tag® or Twin-Strep-tag® with V5 tag. Moreover, these modifications were inserted either at the C-terminus or N-terminus of PD1 protein.

Western Blot analysis revealed that C-terminally tagged recombinant PD1 was highly overexpressed and detected at a molecular weight of 55kDa, suggesting that

it undergoes glycosylation. However, the introduction of the N-terminal tag resulted in the complete absence of PD1 overexpression at this height (**Figure 25**). Simultaneously, both protein types were weakly overexpressed in their unmodified

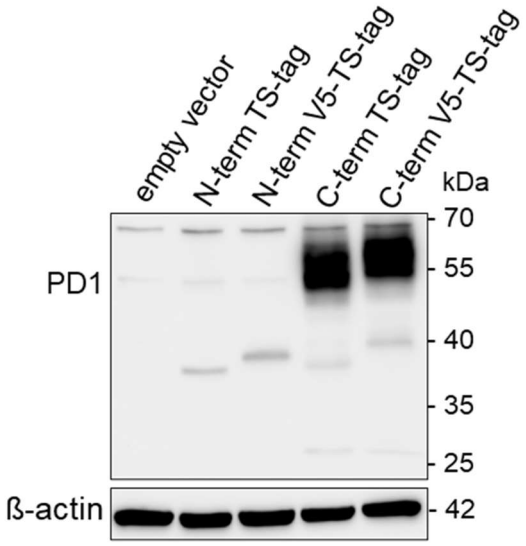

Figure 25 Western blot analysis demonstrating the impact of N-terminal and C-terminal tagging of PD1 protein overexpression in U2OS cells. TS=Twin-Strep-tag®

form detected at the predicted height of approximately 32 kDa.

Alterations in the expression of recombinant proteins tagged at the N-terminus are a well-established phenomenon. It is often attributed to steric hindrance obstructing the access of ribosomes to the start codon of mRNA, making translation impossible. Similarly, steric hindrance caused by the tag may obstruct attachment of glycan groups to the protein. Alternatively, the N-terminus frequently contains the target peptide sequence determining protein localization. Therefore, certain N-tags may alter proper transport of a protein to its target cellular localization, potentially leading to protein degradation, explaining our observations.

Moreover, in both types of modifications, we observed a slight shift in protein size. The lower (non-glycosylated) band exhibited a shift from 32kDa to 38kDa for a single tag and 40kDa for a dual tag, respectively. Similar changes were detected in the 55kDa band present in C-terminally tagged PD1. The increase in protein size directly results from the tag insertion. Notably, PD1 overexpressing cells did not exhibit an elevation in the expression of the 70kDa band. We hypothesized that the recombinant PD1 protein may lack the posttranslational modifications represented by 70kDa band

(detailed description of possible modifications in the previous chapter). PD1 specificity of the 70kDa isoform was previously reported in a study characterizing various hybridoma PD1 monoclonal antibodies, therefore we did not consider it as unspecific, please check Figure 8 for reference (Y. Chen et al. 2010).

Given that C-terminal tags enabled the expression of all PD1 protein forms, we selected them for subsequent experiments. Additionally, we used the protein with two tags for more flexibility. If additional staining of the recombinant PD1 protein needed to be performed, it could be accomplished with readily available anti-V5 tag antibodies.

5.3 Introduction of p-tyrosine mutations for targeted PD1 interactome studies

To perform the experiment on a larger scale, as required for LC-MS/MS analysis, we generated stable cell lines overexpressing either the wild-type PD1 protein or one of its mutants. Mutations were introduced at the Y223 and Y248 tyrosine phosphorylation sites through substitution with phenylalanine, further referred to as Y223F and Y248F mutants, respectively (**Figure 26**). As demonstrated in T cells, the phosphorylation of these two tyrosine residues, particularly Y248, plays a crucial role in downstream PD1 signalling upon PDL1 activation (Bu et al. 2021; Okazaki et al. 2001; Bardhan et al. 2019). By incorporating PD1 mutants into our study,

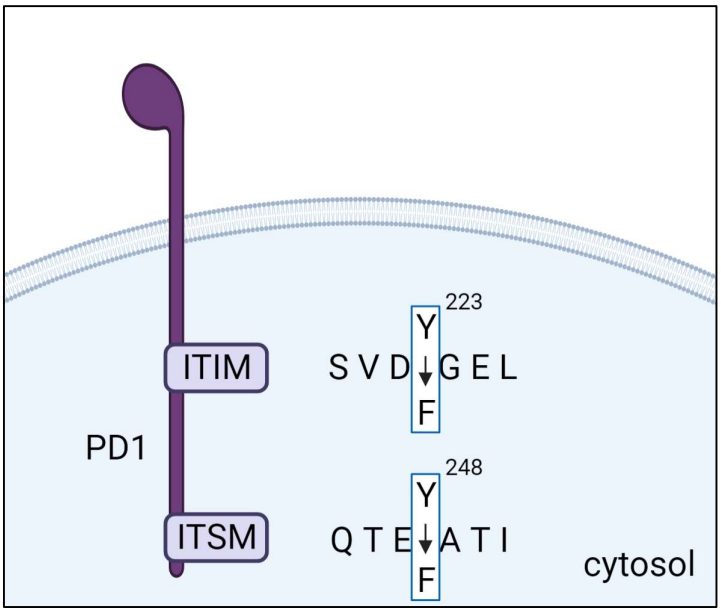

Figure 26 Schematic overview of mutations introduced in PD1 protein.

we aimed to discover new interacting partners for PD1 and explore whether their binding depends on PD1 phosphorylation.

Following transfection and antibiotic selection, stable overexpression of PD1 protein in U2OS cells was confirmed with Western Blot analysis. The expression pattern closely resembled our prior observations, demonstrating a strong signal at 55kDa with no change at 70kDa (**Figure 27**).

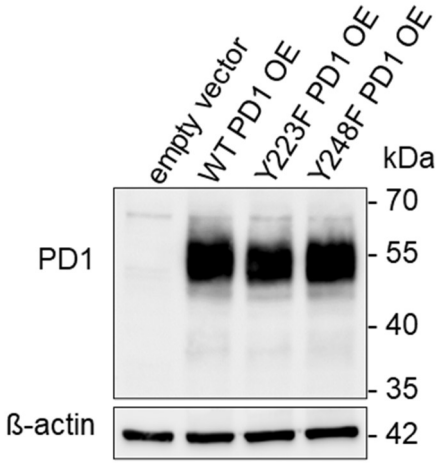

Figure 27 Stable expression of PD1 in U2OS cells confirmed by Western Blot.

5.4 PD1 is overexpressed both intra- and extracellularly.

Having confirmed PD1 overexpression in U2OS cells, we wanted to characterize PD1 expression more accurately in these cells. Therefore, we implemented flow cytometry analysis with extra- and intracellular staining. Our initial findings demonstrated that endogenous PD1 expression in U2OS cells is mostly restricted to the intracellular compartment. However, upon overexpression, PD1 is markedly overexpressed both extra- and intracellularly (**Figure 28**). Furthermore, PD1 mutations have no effect on either the level or localization of PD1. Thereby, implementation of these cells to study the PD1 interactome facilitated the identification of interactions with both membrane-bound and cytosolic proteins.

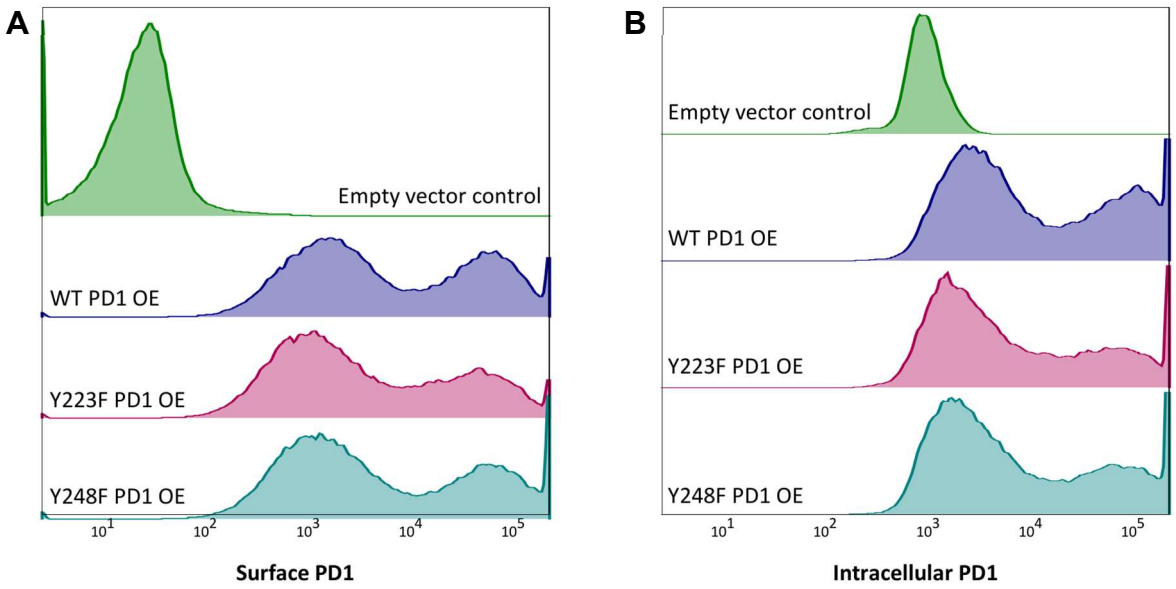

Figure 28 PD1 protein is expressed both extra- and intracellularly in U2OS PD1 overexpressing cells. A) surface and **B)** intracellular staining performed for flow cytometry analysis revealed that upon overexpression PD1 is expressed both extra- and intracellularly. Flow cytometry data was analysed with FlowJo v10.8.1 flow cytometry analysis software (BD Biosciences).

5.5 Identification of protein candidates interacting with PD1

Isolation of PD1 interacting proteins was performed during pull-down experiment using U2OS cells overexpressing PD1 protein fused with Twin-Strep-tag®. PD1 elution from the beads was performed by boiling samples under reducing conditions with SDS sample buffer. Subsequently, we implemented FASP (Filter Aided Sample Preparation) to generate tryptic peptides from the eluted proteins. Following desalting, drying and reconstitution of the samples, we performed LC-MS/MS analysis and data acquisition.

The data was searched against a protein database, quantified, and then subjected to the bioinformatic and statistical analyses, ultimately providing a list of protein identities and their fold changes. We initially ranked proteins by their adjusted p-values of fold changes, reflecting the significance of protein enrichment in the pull-down samples when compared to the control. To select the candidates for further validation, we applied several criteria. First, only the proteins with the adjusted p-value < 0.05 were considered. Then, we expected either a complete absence of the interacting candidate in the control conditions or at least threefold increase in protein abundance

expressed as fold change compared to the control. Detection and subsequent quantification of a protein in the control sample, where no bait protein was present, indicates unspecific binding to isolation beads, but we did not exclude such candidates. However, to avoid the selection of a false positive interacting partner, we arbitrary set a threshold of at least three-fold increase in protein abundance in samples with PD1 overexpression, effectively filtering out the unspecific binders.

To further increase the confidence, we only considered the hits with less than 75% missing values in the compared dataset. The missing percentage value refers directly to the missing data points in the mass spectrometry data files, which make the statistical analysis insignificant. In such case, implementation of biological model-driven imputation methods artificially but reasonably adds the missing values to the analysis, making the comparison more accurate and unbiased. This approach may seem relatively liberal, but it is standard for the pull-down samples, where the complete absence of many proteins in control conditions is expected. Nevertheless, stringent data filtering was implemented at multiple stages of the analysis, minimizing the risk of false discovery.

Having applied all the above criteria, we obtained a list of 52 interacting protein candidates for the WT PD1 and 79 proteins for each of the mutants (**Figure 29A**). Of those, 36 proteins were shared across all PD1 forms, while 8 proteins were unique for the WT PD1, implicating that these interactions require the functional phosphorylation of PD1 tyrosine residues (**Figure 29B, Tables 5 and 6**).

Yet, the known PD1 interacting partners such as PDL1, PTEN or SHP2 were not identified in our analysis (Bardhan, Anagnostou, and Boussiotis 2016; Patsoukis, Duke-Cohan, et al. 2020; Patsoukis et al. 2013). Despite high specificity and accuracy, LC-MS/MS data analysis is not free of potential biases due to high-throughput and complex nature of the analysis. The primary technical limitation affecting the quantitative analysis is the potential interference from peptides or peak groups generated in different transitions sets. Each peptide produced during tryptic digestion has predefined transitions from precursor ion to product ion. In certain cases, such as having a similar mass-to-charge-ratio or a similar fragmentation pattern, peptides

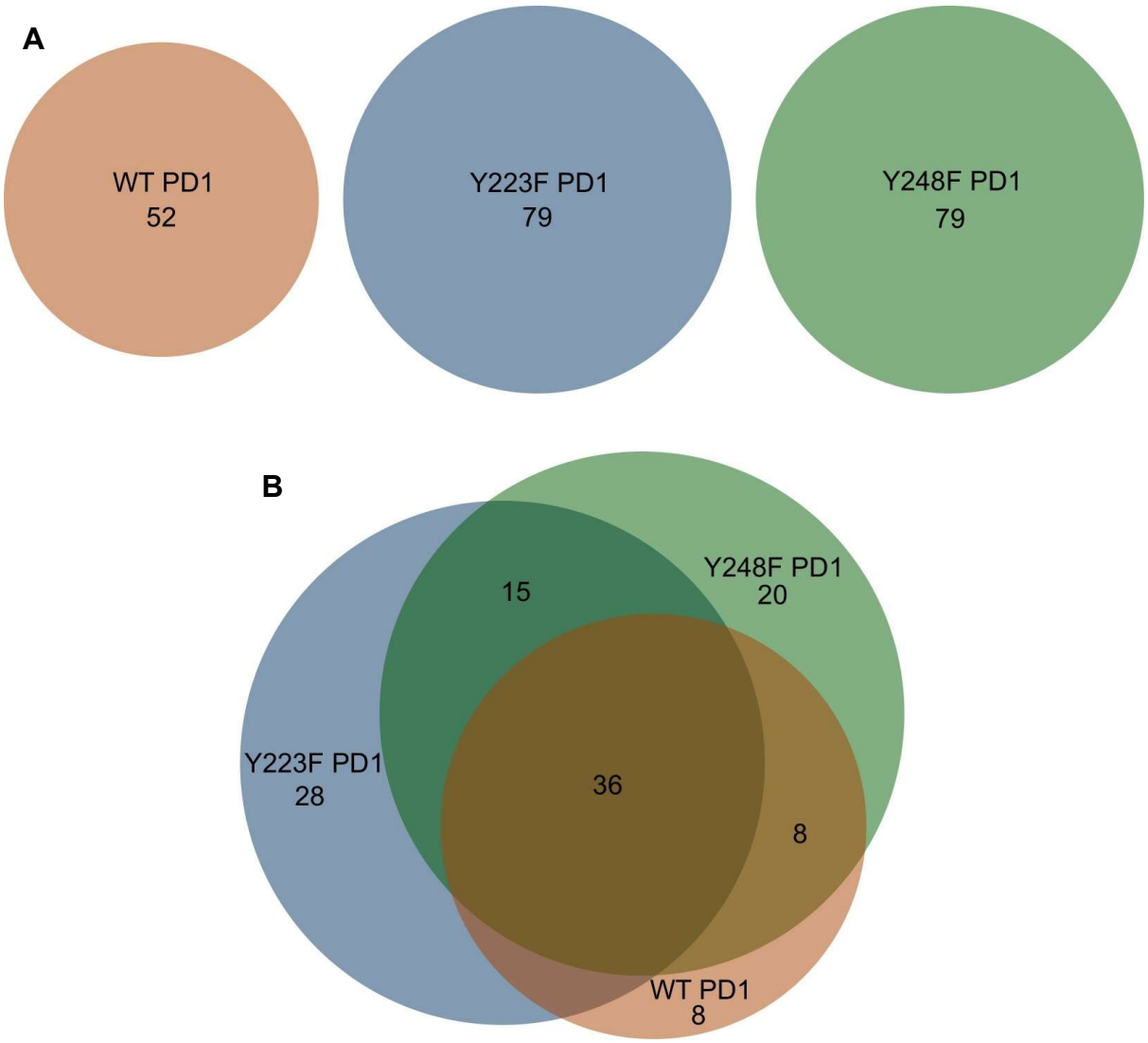

Figure 29 DeepVenn diagram illustrating **A)** the number of potential protein candidates for the interaction with PD1 in WT, Y223F and Y248F overexpressing U2OS cells, **B)** the distribution of shared and unique proteins identified in the WT and mutant PD1 overexpressing cells.

other than the target peptide might interfere with the quantification process. This biased measurement may be caused by co-elution of interfering peptides, similarities in the mass of peptides with varying sequences or the co-fragmentation of peptides sharing transition patterns.

When considering peak group interference, the cluster of transitions characteristic to a given peptide can be mimicked by peptides other than the target peptide or by the background signals. This type of interference often arises from overlapping transitions of distinct peptides or the co-elution of interfering compounds.

Table 5 Proteins identified by LC-MS/MS analysis as potential PD1 interacting candidates shared by all PD1 forms employed in the experiment, most likely through the mechanism independent of PD1 tyrosine phosphorylation.

		Proteins common for WT, Y223F and Y248F
No.	Protein	Full name
1	**ADT3**	ADP/ATP translocase 3
2	**AIFM1**	Apoptosis-inducing factor 1
3	**AUP1**	AUP1, lipid droplet regulating VLDL assembly factor
4	**BAIP2**	Brain-specific angiogenesis inhibitor 1-associated protein 2
5	**CEPT1**	Choline/ethanolaminephosphotransferase 1
6	**COQ5**	2-methoxy-6-polyprenyl-1,4-benzoquinol methylase
7	**COX15**	Cytochrome c oxidase assembly protein COX15 homolog
8	**DGLB**	Diacylglycerol lipase-beta
9	**F210A**	Protein FAM210A
10	**FAF2**	FAS-associated factor 2
11	**GCN1**	Stalled ribosome sensor GCN1
12	**HEAT6**	HEAT repeat-containing protein 6
13	**IMB1**	Importin subunit beta-1
14	**IPO9**	Importin-9
15	**M2OM**	Mitochondrial 2-oxoglutarate/malate carrier protein
16	**MAGT1**	Magnesium transporter protein 1
17	**MIC13**	MICOS complex subunit MIC13
18	**MOES**	Moesin
19	**MYCPP**	C-myc promoter-binding protein
20	**PEX3**	Peroxisomal biogenesis factor 3
21	**PLPL6**	Patatin-like phospholipase domain-containing protein 6
22	**PNKD**	Paroxysmal nonkinesiogenic dyskinesia protein
23	**RAB21**	Ras-related protein Rab-21
24	**RAB8A**	Ras-related protein Rab-8A
25	**RFC3**	Replication factor C subunit 3
26	**RNF5**	E3 ubiquitin-protein ligase RNF5
27	**S39AA**	Zinc transporter ZIP10
28	**SGPL1**	Sphinganine-1-phosphate aldolase
29	**SMIM4**	Small integral membrane protein 4
30	**SNG3**	Synaptogyrin-3
31	**STML2**	Stomatin-like protein 2, mitochondrial
32	**TI17A**	Mitochondrial import inner membrane translocase subunit Tim17-A
33	**TNPO1**	Transportin-1
34	**UFO**	Tyrosine-protein kinase receptor UFO
35	**VKOR1**	Vitamin K epoxide reductase complex subunit 1
36	**XPO2**	Exportin-2

Table 6 List of proteins identified by the LC-MS/MS analysis, which were unique for WT PD1 OE cells and were not identified in the mutants. Interactions between PD1 and the proteins listed below are most probably PD1 tyrosine phosphorylation dependent.

		Proteins unique for WT
No.	Protein	Full name
1	**DRG1**	Developmentally-regulated GTP-binding protein 1
2	**TM258**	Transmembrane protein 258
3	**RAB32**	Ras-related protein Rab-32
4	**NDUV1**	NADH dehydrogenase [ubiquinone] flavoprotein 1, mitochondrial
5	**SPAS1**	Spermatogenesis-associated serine-rich protein 1
6	**MICA3**	[F-actin]-monooxygenase MICAL3
7	**MIB1**	E3 ubiquitin-protein ligase MIB1
8	**APOL2**	Apolipoprotein L2

Strategies employed to mitigate the impact of peptide or peak group interference on quantitative analysis include the thorough selection of transitions for target peptides using software like Skyline, implementation of reference compounds as the internal standards and continuous monitoring of the results' quality at multiple stages throughout the analysis (J. Park et al. 2023).

Additional technical limitations which should be considered during LC-MS/MS analysis of complex biological samples involve the preferential detection of highly abundant proteins, like enzymes and structural components. In such cases, the interference of proteins present in large quantities in samples may hinder the detection of low abundance proteins due to their preferential ionisation and signal production over those with trace amount. To address this challenge, various methods reducing sample complexity, such fractionation or immunoaffinity chromatography, may be applied. To further improve detection of low abundance proteins advanced analytical techniques such as data-independent-acquisition (DIA), as utilized in our study, may be implemented to acquire accurate data across broad *m/z* range (Nakayasu et al. 2021).

Apart from that, it is crucial to consider the chemical structure of the peptides, as it can significantly influence their ionisation, subsequent fragmentation, and detection in the mass spectrometer. For example, peptides that incorporate charged amino acids, particularly those with basic residues like lysine or arginine, tend to exhibit

enhanced ionization efficiency. Equally important are factors such as protonation sites, which affect ion stability, the influence of hydrophobicity on chromatographic retention time, and the impact of secondary structure of peptides (Karpievitch et al. 2010; Dupree et al. 2020).

The above-mentioned factors may result in detection of proteins of limited relevance in the study. Therefore, for further validation steps, it was crucial to critically evaluate the potential interaction rationale within the context of novelty and the candidate's role in cancer through extensive review of the literature.

5.6 AXL is a novel cancer PD1 interacting partner.

From a pool of potential PD1 interacting candidates, the tyrosine kinase receptor UFO (AXL) emerged as a highly promising target. Nonetheless, prior to the validation, we analysed AXL peptide spectra in Skyline software, confirming its identity with two high-ranking ion products (**Figure 30 A and B**).

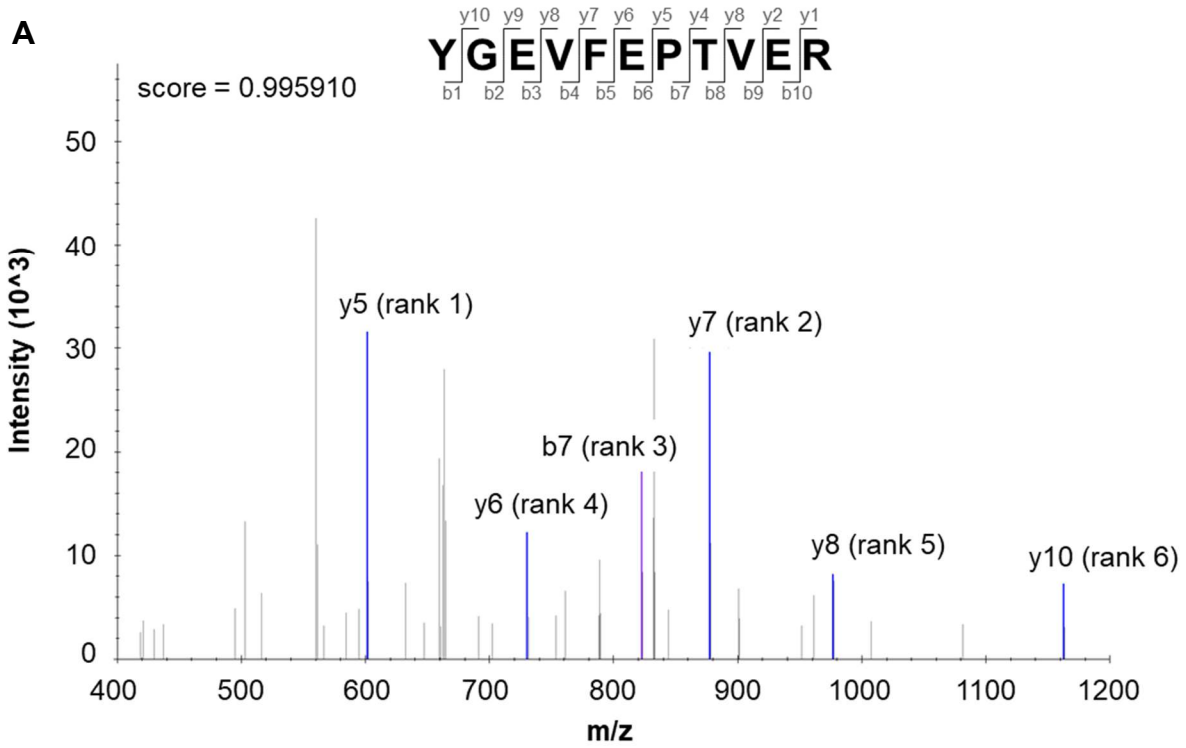

Figure 30 LC-MS/MS spectra of two (A and B) tryptic peptides ion products originating from AXL protein, which were used for protein quantification. Peptide sequence is shown on the top in bold; y ion products shown in blue, b in purple.

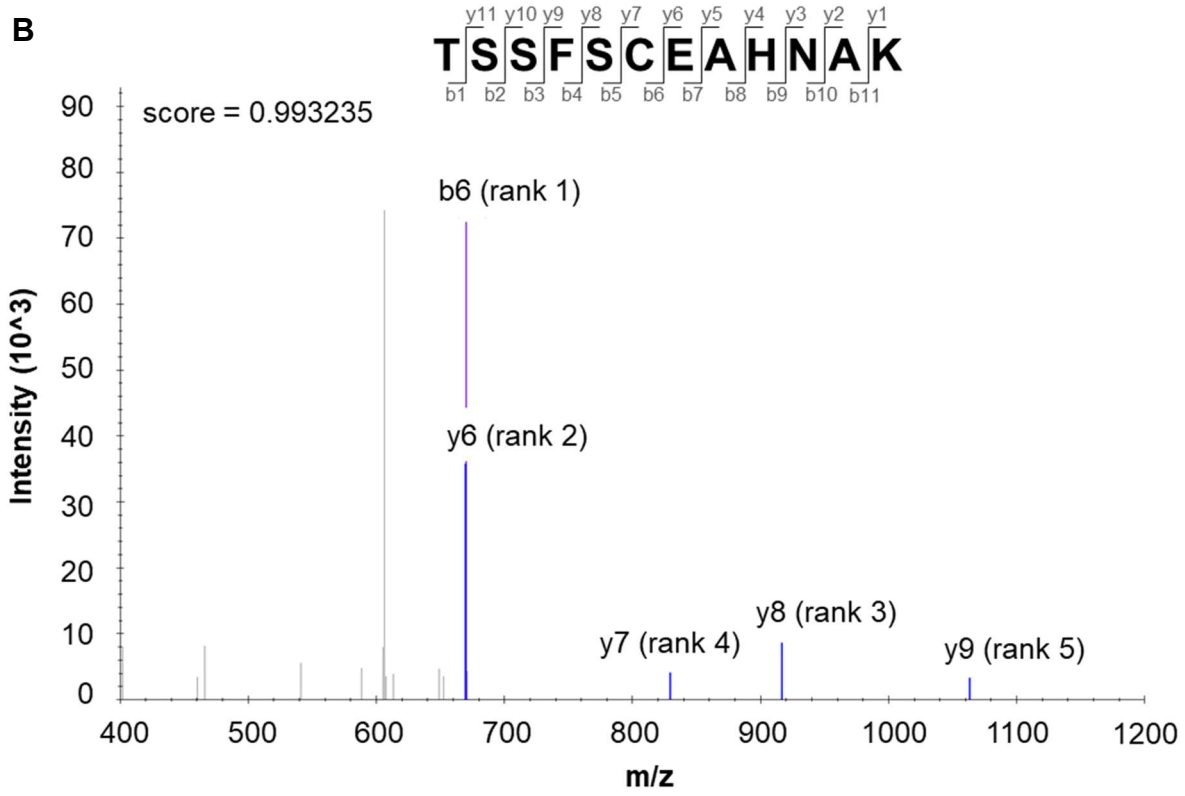

5.7 Validation of LC/MS findings confirm the PD1 - AXL interaction.

LC-MS/MS analysis provides high sensitivity and accuracy; however, it is strongly recommended to validate the data using alternative molecular biology methods. In our study, we employed immunoblotting to confirm the elution of AXL from PD1 the pull-down samples, thereby verifying the physical interaction between these proteins. Moreover, AXL was detected in the eluates of all samples with PD1 overexpression, including the Y223F and Y248F mutants. This indicates that the interaction does not require PD1 tyrosine phosphorylation and is consistent with our LC-MS/MS findings (**Figure 31**).

For additional validation of the interaction between PD1 and AXL, we conducted Proximity Ligation Assay (PLA) (Alam 2018). In brief, PLA enables the in situ detection of protein-protein interactions for targets in close proximity (~40nm). Such a small distance indicates protein-protein binding or association. Initially, the target proteins are labelled with specific primary antibodies, each raised in a different species. Subsequently, oligonucleotide labelled secondary antibodies (probes), specifically recognize the primary antibodies. If the oligonucleotides are close enough, the DNA

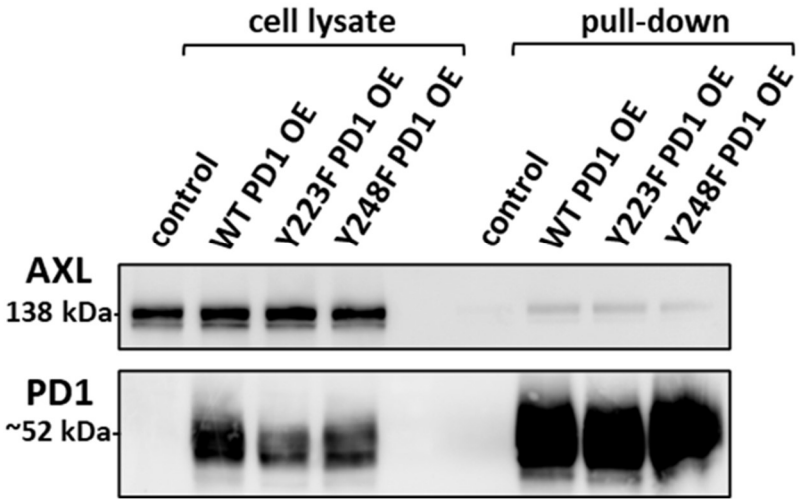

Figure 31 Immunoblotting of the pull-down samples confirms the interaction between PD1 and AXL. PD1 was used both as a loading control and positive control for the pull-down experiment.

ligase added in the next step, facilitates the formation of closed circular structures. These structures are then utilized as templates for DNA polymerase, which generates concatemeric sequences (amplicons) amplifying the signal by approximately 1000-fold. Simultaneously, the DNA repeats remain attached to the PLA probes, ensuring the in situ detection of the interaction. Lastly, the amplicons are hybridized with fluorescently labelled oligonucleotides, enabling signal detection. The interaction can be visualized by fluorescence microscopy and is observed as spots. Overall, PLA assay offers the in situ detection of protein-protein interactions with high specificity and sensitivity, making it a reliable approach to study protein interactions.

Prior to conducting the PLA, we performed standard immunofluorescent staining to optimize the experimental conditions. At that point, the dual staining of PD1 and AXL already indicated potential co-localization in a subset of cells, observed as the orange signal in channel merged images (**Figure 32**).

Then, the interaction between PD1 and AXL was confirmed by PLA (**Figure 33**). Consistently with the LC-MS and immunoblotting data, mutations in tyrosine phosphorylation sites did not abrogate the interaction between PD1 and AXL. Notably, the interaction was not detected in the empty vector control despite endogenous expression of both proteins in U2OS cells.

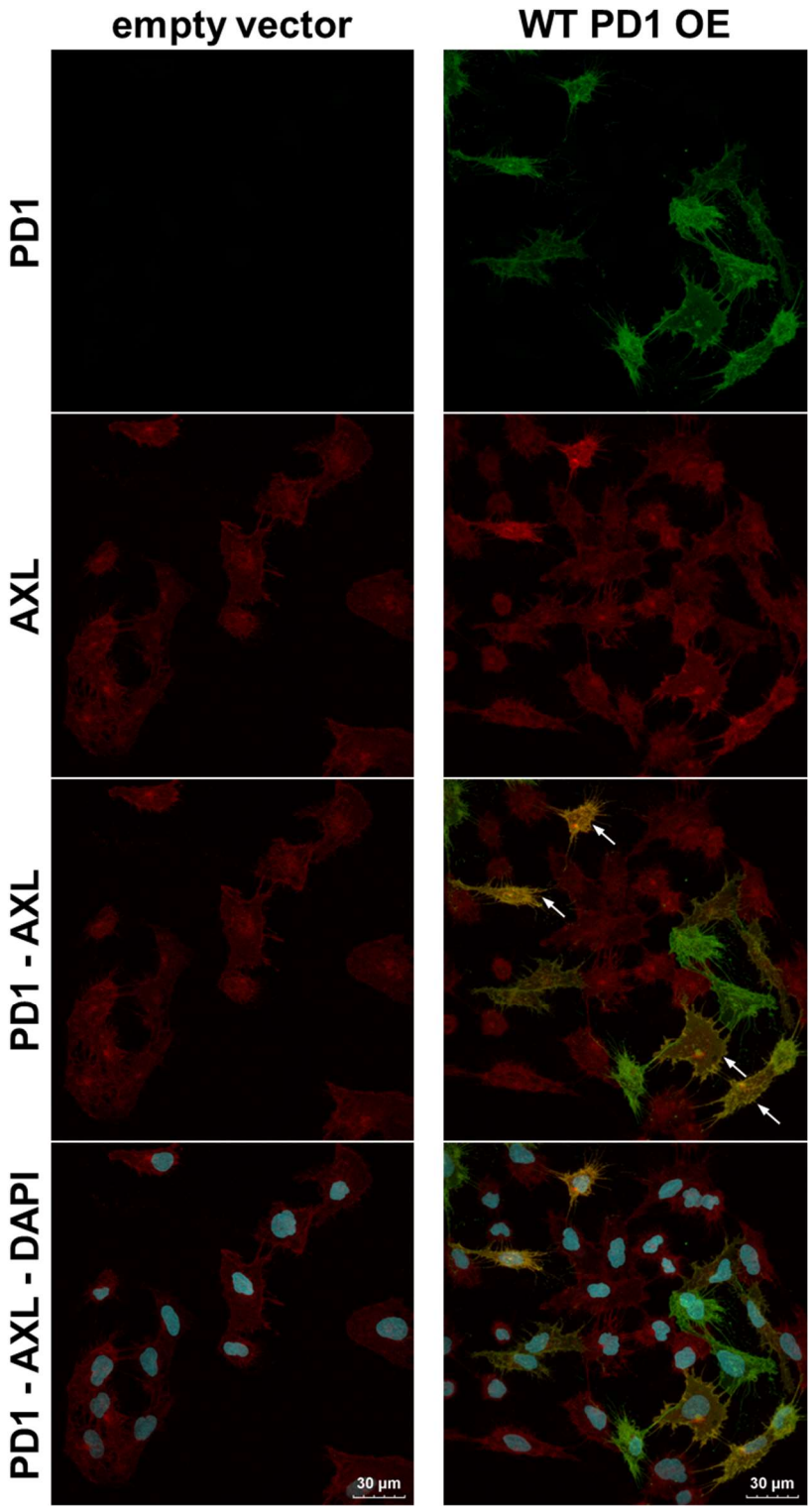

Figure 32 Immunofluorescent staining indicates co-localization of PD1 and AXL in a fraction of U2OS PD1 OE cells. Images were acquired with confocal microscopy. White arrows mark the cells with potential co-localization of PD1 and AXL. U2OS cells were stained with anti-PD1 and anti-AXL primary antibodies, followed by staining with Alexa Fluor™ 488 and Alexa Fluor™ 647 secondary antibodies, respectively. Cells were mounted with mounting medium with DAPI, which was used for nuclear staining. Specimens were visualized by confocal microscopy with 63X oil immersion lens, bar= 30µm.

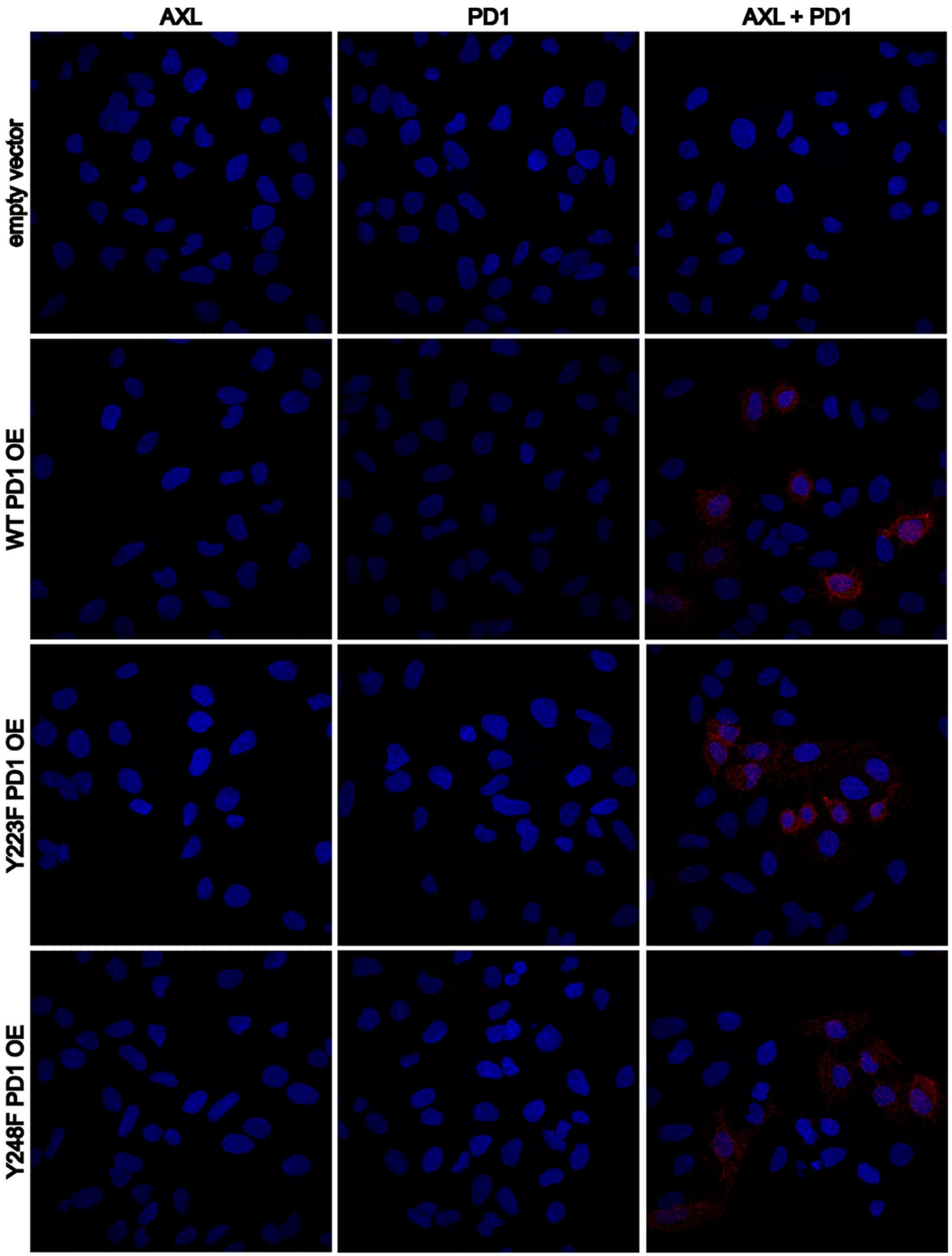

Figure 33 Proximity ligation assay confirms the interaction between PD1 and AXL (red), which is not disrupted by the mutations in PD1 phosphorylation sites. PLA was performed between PD1 and AXL, samples were mounted with mounting media with DAPI. The figure demonstrates representative images, specimens were visualized by confocal microscopy with 63X oil immersion lens.

While Figure 33 represents Z-stack images of the images acquired with a confocal microscope, the image of a single focal plane (one Z-stack) suggests that the interaction localizes to the cellular membrane (**Figure 34**).

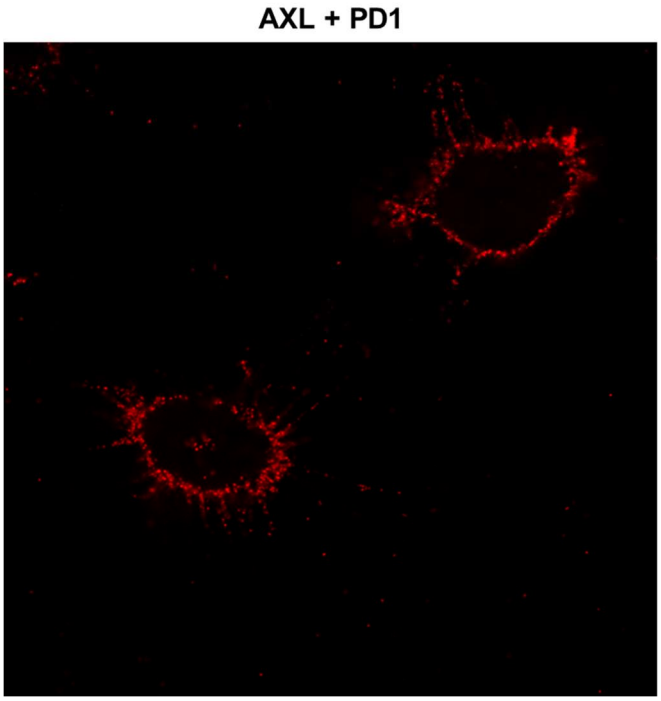

Figure 34 The interaction of PD1 and AXL takes place on the cellular membrane. A representative image of one focal plane illustrating the PLA (red) performed between PD1 and AXL in WT PD1 OE U2OS cells, samples were mounted with mounting media with DAPI and imaged by confocal microscopy at 120X magnification.

Our flow cytometry results indicated that only about 4% of U2OS express PD1 on the membrane, while the level of PD1 expression in U2OS cells is low as demonstrated by immunofluorescent staining. Conversely, nearly all U2OS transfected cells, overexpressing PD1, demonstrated strong surface expression of PD1 (see Figure 28 for reference), facilitating detection of the interaction. However, the membrane localization of the PD1-AXL interaction should be additionally validated with plasma membrane markers, for instance ezrin.

5.8 Molecular dynamics proposes the mechanism of PD1–AXL interaction.

Having confirmed the interaction between PD1 and AXL, we aimed at more in-depth characterization of its underlying mechanism. Collaborating with Dr Kiran Lockhante, who utilized our data to perform molecular modelling and molecular dynamics simulations (and who kindly provided the figures presented in this paragraph), we investigated the specific binding sites involved in this interaction. Moreover, the analysis included studies on the impact of mutations in PD1 tyrosine residues on the binding affinity between PD1 and AXL.

5.8.1 Stereochemical validation of modelled proteins

Except from the crystal structure of the extracellular domain of PD1 (PD1-ECD), which was retrieved from Protein Data Bank (PDB), the full crystal structures of neither PD1 nor AXL were available in PDB. To overcome this obstacle and study the structures of these proteins, input sequences for the intracellular domain of PD1 (PD1-ICD), the extracellular domain of AXL (AXL-ECD) and the intracellular domain of AXL (AXL-ICD) were obtained from UniProt database, and their structures were modelled using RoseTTAFold method. This approach allowed to obtain accurate and reliable structural models for AXL-ECD, AXL-ICD, and PD1-ICD, despite the unavailability of their full crystal structures. Moreover, the RoseTTAFold method provided insights into the structural characteristics and potential interactions between PD1 and AXL (Baek et al. 2021).

To assess the accuracy and reliability of the generated models, we performed a structure validation, which is a crucial step in protein structure prediction. For the AXL-ECD protein, 88.4% of its residues were found in the most favoured regions, indicating that the majority of residues adopted energetically favourable conformations. Additionally, 8.8% of the residues were in additional allowed regions, demonstrating that they were still within acceptable conformational space. A small portion, 0.6% of the residues, occupied the generously allowed regions, indicating slightly less favourable but still permissible conformations. However, 2.2% of the residues were classified in the disallowed regions, suggesting that these residues adopted unfavourable or non-physiological conformations.

Ramachandran plots, a widely used tool for evaluating the conformational quality, were used as graphical representation of the amino acid residues within different regions of conformational space. These regions include the favourable, allowed, and disallowed regions, which correspond to the ideal, acceptable, and unfavourable conformations of amino acids, respectively. The most reliable three-dimensional (3D) structures were selected for the further study (**Figure 35A**).

Similarly, for the AXL-ICD protein, the Ramachandran plot showed 91.4% of its residues in the most favoured regions, indicating a high-quality conformational distribution. Furthermore, 6.5% of the residues were in additional allowed regions, and 0.7% were in the generously allowed regions. These percentages suggest that the majority of residues adopted energetically favourable conformations with a smaller fraction slightly deviating from the ideal backbone angles. Only 1.4% of the residues were categorized as disallowed, implying a relatively low occurrence of unfavourable conformations (**Figure 35B**).

In the case of PD1-ICD, the Ramachandran plot analysis revealed that 84.7% of its residues were in the most favoured regions, indicating a substantial proportion of energetically favourable conformations. Additionally, 13.9% of the residues were in additional allowed regions, suggesting that they were still within acceptable conformational space but with a slightly higher deviation from the ideal angles. Furthermore, 1.4% of the residues occupied the generously allowed regions, indicating a relatively lower preference for these conformations. Notably, no residues were classified in the disallowed regions, indicating a lack of highly unfavourable conformations (**Figure 35C**).

A

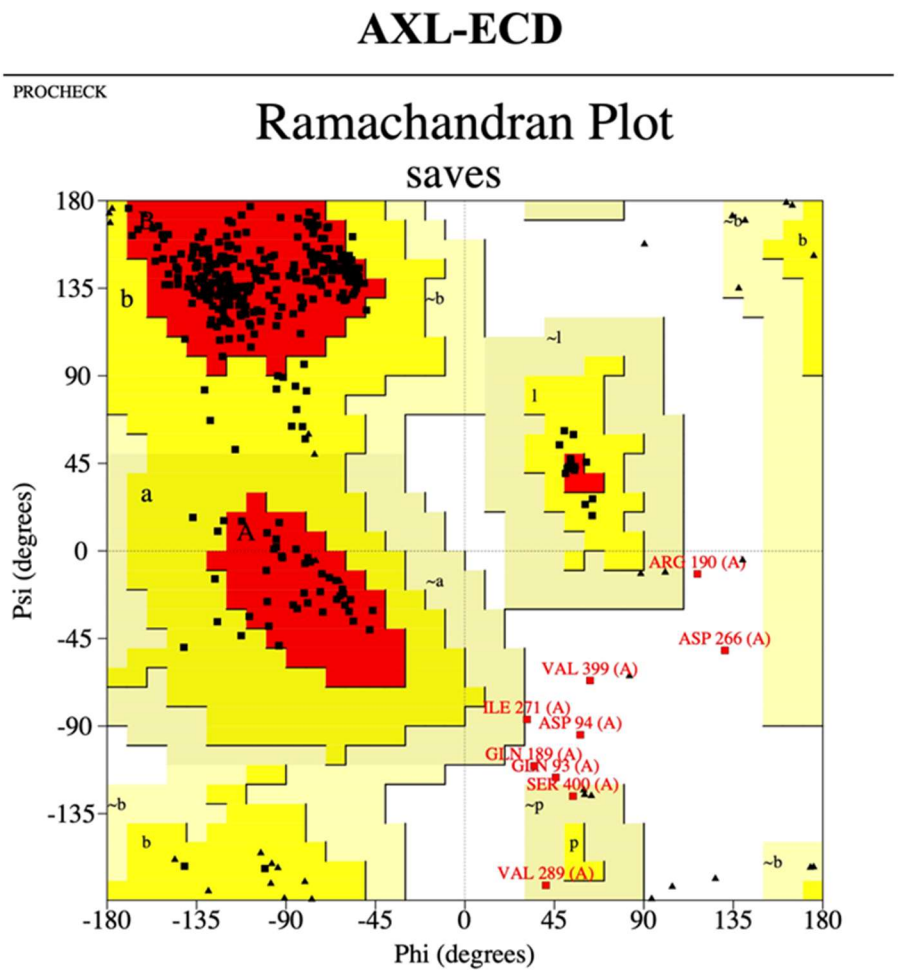

Plot statistics

Residues in most favoured regions [A,B,L]	282	88.4%
Residues in additional allowed regions [a,b,l,p]	28	8.8%
Residues in generously allowed regions [~a,~b,~1,~p]	2	0.6%
Residues in disallowed regions	7	2.2%
Number of non-glycine and non-proline residues	319	100%
Number of end-residues (excl. Gly and Pro)	2	
Number of glycine residues (shown as triangles)	37	
Number of proline residues	42	
Total number of residues	400	

Based on an analysis of 118 structures of resolution of at least 2.0 Angstroms and R-factor no greater than 20%, a good quality model would be expected to have over 90% in the most favoured regions

Figure 35 Ramchandran plots representing the quality assessment of the modelled A) AXL-ECD, B) AXL-ICD, and C) PD1-ICD protein structures. Robetta Models for, (A) AXL-ECD, (B) AXL-ICD, and (C) PD1-ICD. The majority of the residues in all three proteins were found in the most favoured

B

AXL-ICD

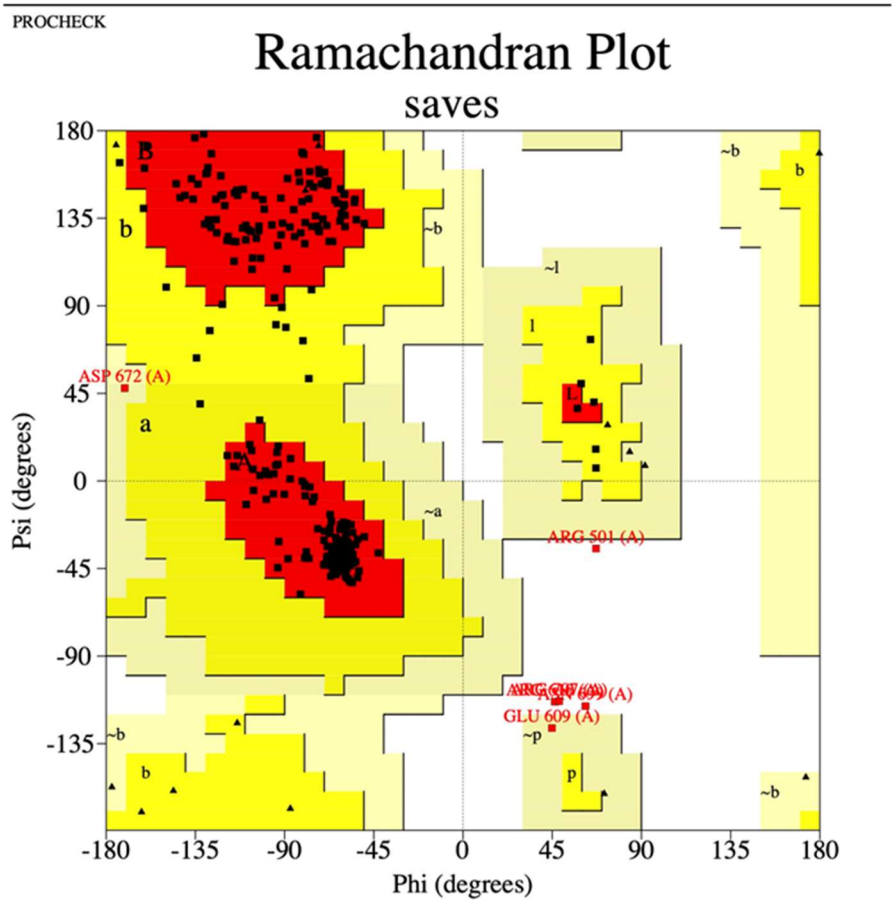

Plot statistics

Residues in most favoured regions [A,B,L]	255	91.4%
Residues in additional allowed regions [a,b,l,p]	18	6.5%
Residues in generously allowed regions [~a,~b,~1,~p]	2	0.7%
Residues in disallowed regions	4	1.4%
Number of non-glycine and non-proline residues	279	100%
Number of end-residues (excl. Gly and Pro)	1	
Number of glycine residues (shown as triangles)	19	
Number of proline residues	13	
Total number of residues	312	

Based on an analysis of 118 structures of resolution of at least 2.0 Angstroms and R-factor no greater than 20%, a good quality model would be expected to have over 90% in the most favoured regions

regions, indicating good overall quality and reliable backbone conformations. The presence of a small fraction of residues in the additional allowed and generously allowed regions suggests some deviations from the ideal conformations, although they are still within acceptable limits. The absence of residues

c

PD1-ICD

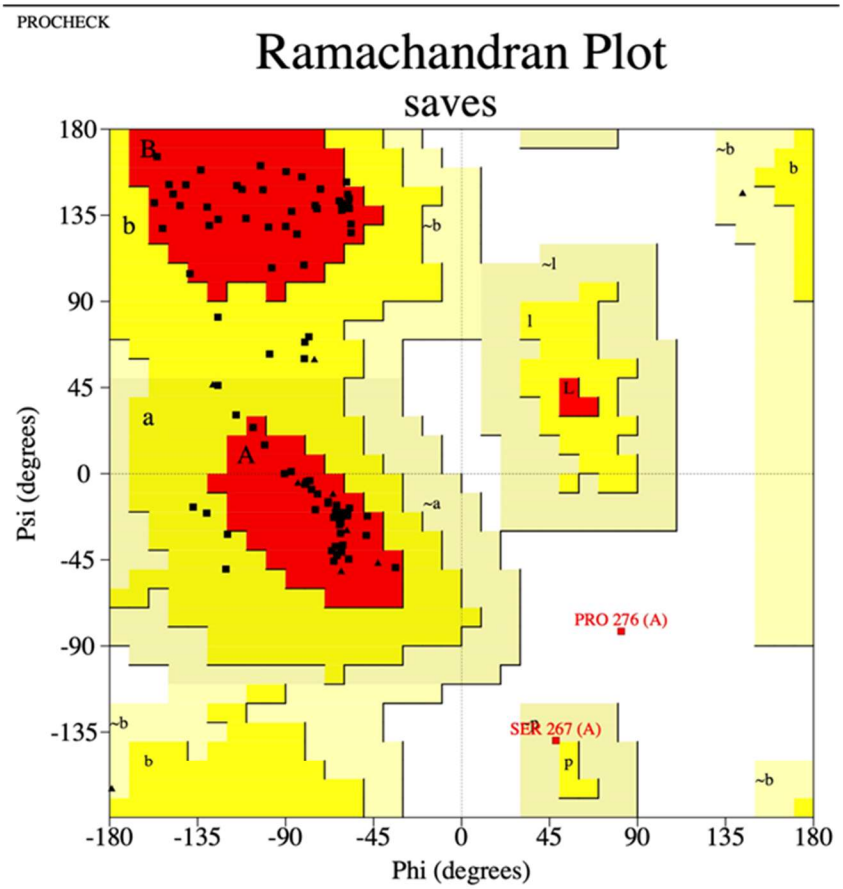

Plot statistics

Residues in most favoured regions [A,B,L]	61	84.7%
Residues in additional allowed regions [a,b,l,p]	10	13.9%
Residues in generously allowed regions [~a,~b,~1,~p]	1	1.4%
Residues in disallowed regions	0	0.0%
Number of non-glycine and non-proline residues	72	100%
Number of end-residues (excl. Gly and Pro)	2	
Number of glycine residues (shown as triangles)	9	
Number of proline residues	14	
Total number of residues	97	

Based on an analysis of 118 structures of resolution of at least 2.0 Angstroms and R-factor no greater than 20%, a good quality model would be expected to have over 90% in the most favoured regions

in the disallowed regions for PD1-ICD indicates a higher level of conformational quality compared to AXL-ECD and AXL-ICD. The Ramchandra plots were generated using SAVES V.6.0 server (https://saves.mbi.ucla.edu/).

5.8.2 Docking analysis of binding affinities between AXL and PD1

We performed macromolecular docking simulations using HDOCK online server to analyse the binding between AXL (ECD) and PD1 (ECD), as well as between AXL (ICD) and PD1 (ICD). Additionally, we examined the interactions between AXL (ICD) and WT PD1, Y223F and Y248F (ICD) PD1 mutant variants. These results were used to assess the potential interactions and binding strengths between AXL and PD1. Subsequently, the resulting protein-protein complexes were subjected to analysis of their intermolecular interaction patterns using the Schrodinger's Maestro software.

The docking results summarized in the **Table 7,** indicate the specific residues involved in the interaction between AXL and PD1 in the formation of AXL-PD1-ECD complex. The docking score suggests favourable binding affinity between the two proteins. A lower docking score indicates a stronger predicted binding affinity. The identified interactions, including hydrogen bonds and salt bridges, describe the nature of the intermolecular interactions and the potential stabilizing forces between AXL and PD1 in the complex. The bond distances mentioned represent the spatial proximity between the interacting residues.

Table 7 Detailed intermolecular interaction between AXL and PD1.

Complex Name	Docking Score (kcal/mol)	Interacting Residues		Bond Type	Bond Distance
		AXL	PD1		
AXL-PD1-ECD	-220.02	Glu167	Arg94	H-Bond	2.0
		Glu167	Arg94	Salt Bridge	4.8
		Tyr140	Gln91	H-Bond	2.1
		Glu136	Arg112	H-Bond	1.2
		Glu136	Arg112	Salt Bridge	4.8
		Gln114	Thr98	H-Bond	2.3
		Gln114	His107	H-Bond	1.8
AXL-PD1-ICD (WT)	-296.67	Pro811	Glu247	H-Blond	1.4
		Ser685	Trp230	H-Bond	1.1

AXL-PD1-ICD (Y223F)	-238.96	Tyr779	Trp230	Pi-Pi Stacking	4.8
		Asp776	Lys233	H-Bond	1.6
		Asp776	Lys233	Salt-Bridge	3.7
		Gln770	Lys233	H-Bond	2.3
		Lys769	Pro243	H-Bond	1.3
		Asp639	Arg264	Salt Bridge	3.0
AXL-PD1-ICD (Y248F)	-303.29	Pro811	Glu247	H-Bond	1.4
		Ser685	Trp230	H-Bond	1.2
		Asn683	Gln229	H-Bond	1.5
			Thr250	H-Bond	Tyr643

5.8.2.1 Docking results for AXL–PD1-ECD complex

The docking results for the AXL-PD1-ECD complex revealed that the complex obtained a docking score of -220.02kcal/mol, indicating a strong binding affinity. Among the interacting residues, Glu167 in the AXL protein formed hydrogen bonds and a salt bridge with Arg94 in PD1. These interactions were crucial for stabilizing the complex, with a hydrogen bond distance of 2.0Å and a salt bridge distance of 4.8Å. Another significant interaction occurred between Tyr140 in AXL and Gln91 in PD1, forming a hydrogen bond at a distance of 2.1Å. Furthermore, Glu136 in AXL established hydrogen bonds with Arg112 in PD1, contributing to the structural stability of the complex. The hydrogen bond distance between these residues was measured to be 1.2Å. Additionally, Glu136 and Arg112 also formed a salt bridge, further reinforcing the binding between the two proteins at a distance of 4.8Å. The analysis also revealed interactions between Gln114 in AXL and both Thr98 and His107 in PD1. These interactions involved hydrogen bonds with distances of 2.3Å and 1.8Å, respectively (**Figure 36**).

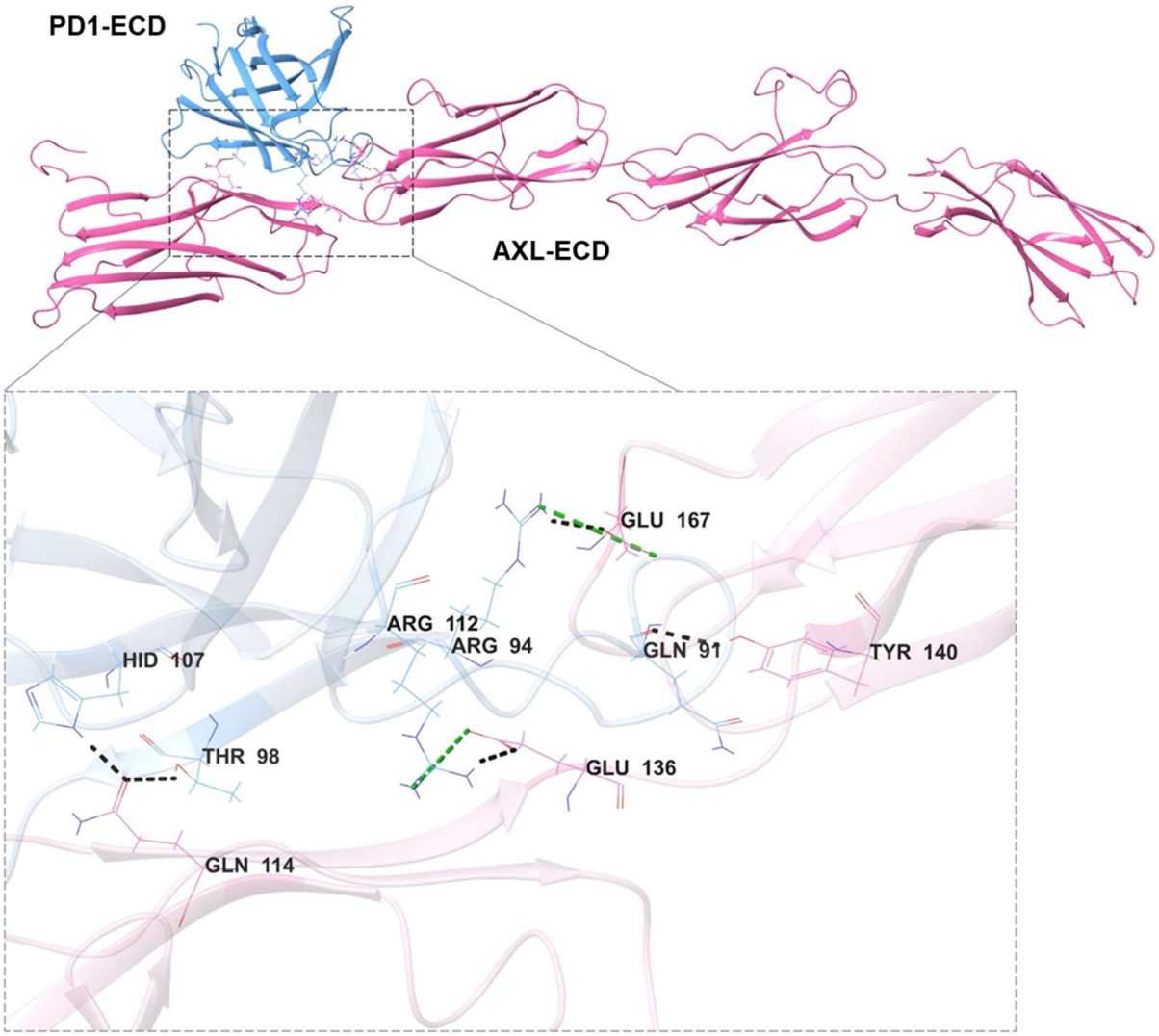

Figure 36 3D interaction diagram of docked AXL-ECD and PD1-ECD complex. Interacting residues (line representation) are depicted in zoomed out image. Interactions shown in dashed line with following colour scheme as applicable: H-bond (black), salt-bridge (green), pi-pi stacking (lime), and pi-cation (dark green).

5.8.2.2 Docking results for AXL – PD1-ICD (WT) complex

When compared to AXL-PD1-ECD complex (docking score of -220.02kcal/mol), the docking results for the AXL-PD1-ICD (WT) complex revealed additional interactions and a lower docking score of -296.67kcal/mol. This suggests a potentially higher affinity and stronger binding between the intracellular domains of AXL and PD1. The docking analysis identified specific interacting residues and bond types in the AXL-PD1-ICD (WT) complex. One important interaction involved Pro811 in AXL forming a hydrogen bond with Glu247 in PD1, with a bond distance of 1.4Å. This hydrogen bond contributes to the stability and binding between the two proteins.

Another significant interaction occurred between Ser685 in AXL and Trp230 in PD1, forming a hydrogen bond with a distance of 1.1Å. This interaction further enhances the binding between AXL and PD1 in the intracellular domain complex (**Figure 37**).

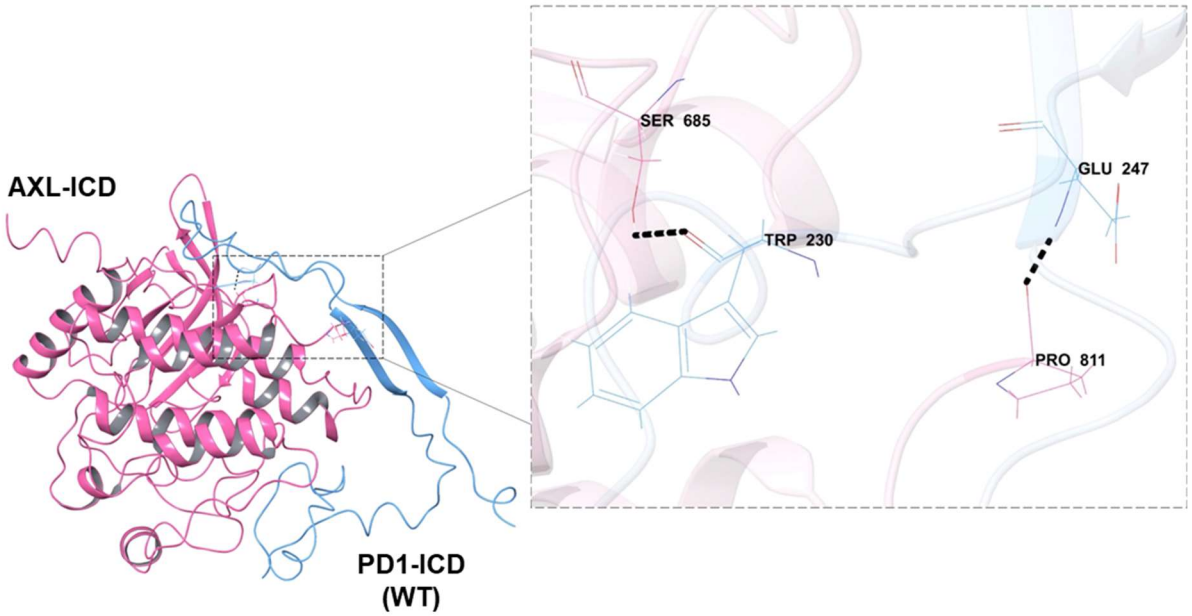

Figure 37 3D interaction diagram of docked AXL-ICD and PD1-ICD complex. Interacting residues (line representation) are depicted in zoomed out image. Interactions shown in dashed line with following colour scheme as applicable: H-bond (black), salt-bridge (green), pi-pi stacking (lime), and pi-cation (dark green).

It is evident that the AXL-PD1-ICD (WT) complex exhibited stronger binding than the AXL-PD1-ECD as indicated by the lower docking score. Additionally, the specific interacting residues and bond types differed between the two complexes, suggesting distinct molecular interactions and binding modes in the intracellular domain complex compared to the extracellular domain. It highlights the importance of considering various regions of the proteins and their specific interactions when investigating the AXL-PD1 complex, as the binding characteristics may vary depending on the domain being studied.

5.8.2.3 Docking results for AXL–PD1-ICD (Y223F) complex

The docking results for the AXL-PD1-ICD (Y223F) and AXL-PD1-ICD (Y248F) complexes demonstrated distinct interactions and docking scores than for PD1-ECD and PD1-ICD (WT), implying variations in the binding characteristics. The AXL-PD1-ICD (Y223F) complex achieved a docking score of -238.96kcal/mol, while the AXL-

PD1-ICD (Y248F) complex obtained a lower docking score of -303.29kcal/mol, indicating a potentially stronger binding affinity in the latter.

In the AXL-PD1-ICD (Y223F) complex, pi-pi stacking interactions were observed between Tyr779 in AXL and Trp230 in PD1 at a distance of 4.8Å, contributing to the stabilization of the complex. Additionally, Asp776 in AXL formed both a hydrogen bond (H-bond) and a salt bridge with Lys233 in PD1, with bond distances of 1.6Å and 3.7Å, respectively. Furthermore, Gln770 in AXL formed a hydrogen bond with Lys233 in PD1 at a distance of 2.3Å. Lys769 in AXL and Pro243 in PD1 also engaged in a hydrogen bond interaction with a distance of 1.3Å. Lastly, Asp639 in AXL and Arg264 in PD1 formed a salt bridge at a distance of 3.0Å (**Figure 38**).

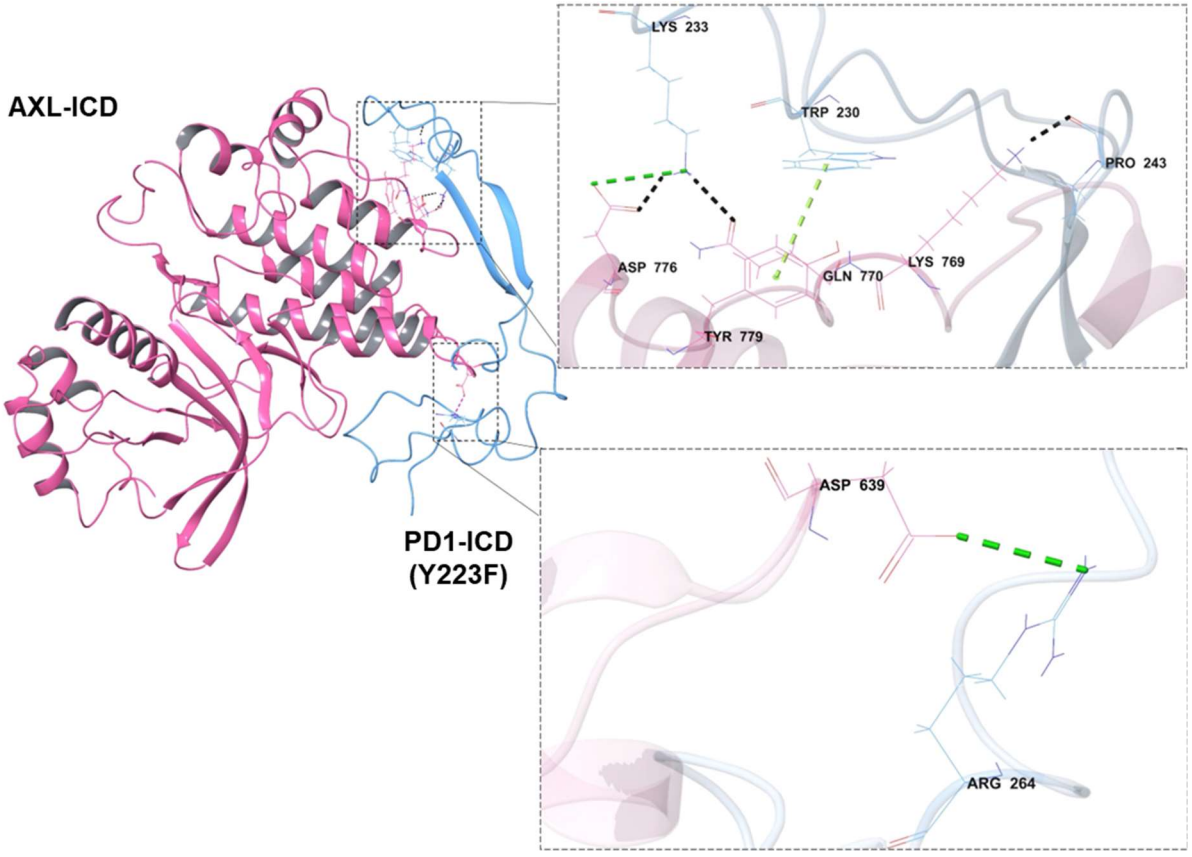

Figure 38 3D interaction diagram of docked AXL-ICD and PD1-ICD (Y223F) complex. Interacting residues (line representation) are depicted in zoomed out image. Interactions shown in dashed line with following colour scheme as applicable: H-bond (black), salt-bridge (green), pi-pi stacking (lime), and pi-cation (dark green).

5.8.2.4 Docking results for AXL–PD1-ICD (Y248F) complex

Lastly, we observed that in the AXL-PD1-ICD (Y248F) complex, Pro811 in AXL formed a hydrogen bond with Glu247 in PD1 at a distance of 1.4Å. Also, Ser685 in AXL and Trp230 in PD1 established a hydrogen bond with a distance of 1.2Å. Asn683 in AXL and Gln229 in PD1 exhibited a hydrogen bond interaction at a distance of 1.5Å. Additionally, Tyr643 in AXL formed a hydrogen bond with Thr250 in PD1, with a bond distance of 1.9Å (**Figure 39**).

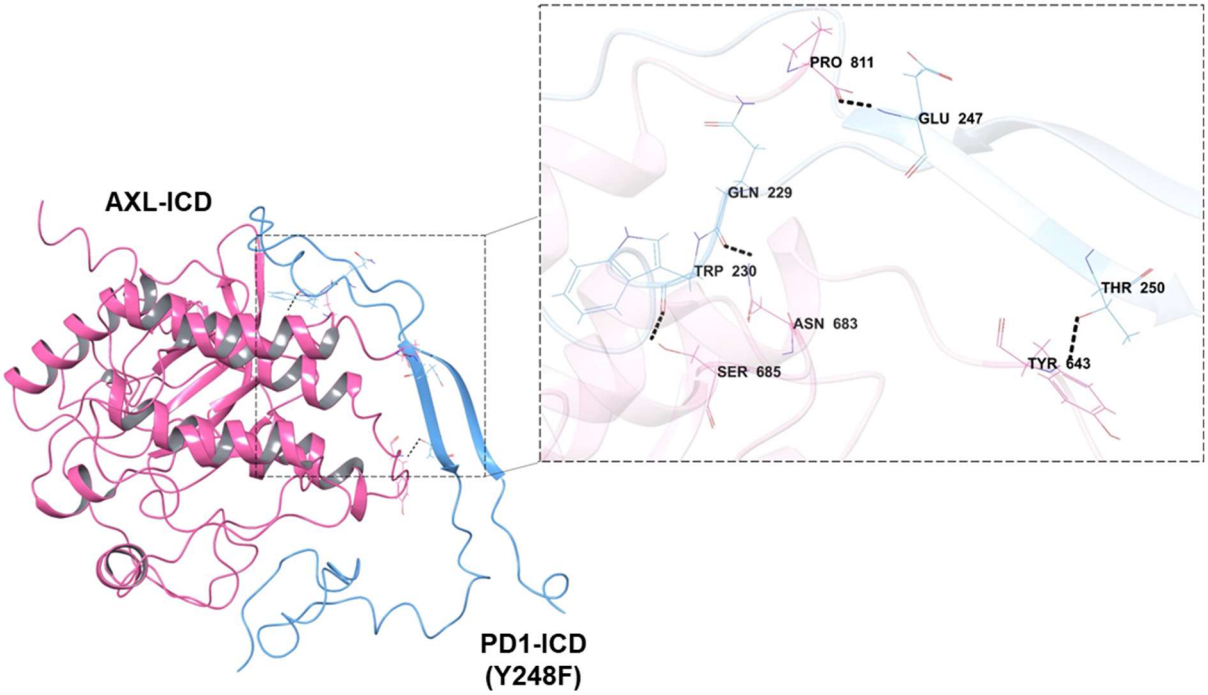

Figure 39 3D interaction diagram of docked AXL-ICD and PD1-ICD (Y248F) complex. Interacting residues (line representation) are depicted in zoomed out image. Interactions shown in dashed line with following colour scheme as applicable: H-bond (black), salt-bridge (green), pi-pi stacking (lime), and pi-cation (dark green).

The docking scores indicated that the AXL-PD1-ECD complex had the lowest binding affinity with a docking score of -220.02kcal/mol. The AXL-PD1-ICD (WT) complex had a slightly lower docking score of -296.67kcal/mol, demonstrating relatively higher binding compared to the AXL-PD1-ECD complex. The AXL-PD1-ICD (Y223F) complex exhibited a docking score of -238.96kcal/mol, suggesting a stronger binding affinity than the AXL-PD1-ECD complex but still not as strong as the AXL-PD1-ICD (WT) complex. Of those, the AXL–PD1-ICD (Y248F) complex demonstrated the lowest docking score of -303.29kcal/mol, indicating the highest binding affinity among the complexes analysed.

Considering the comparison between the complexes formed between AXL and intracellular domains of WT PD1 and Y223F and Y248F mutants, it is evident that mutations in the intracellular domain of PD1 led to variations in the specific interactions and docking scores. These alterations suggest different binding modes and potentially distinct effects on the stability and affinity of the AXL-PD1 complex. However, in Western Blot and PLA experiments, we did not observe significant difference in the efficiency of AXL-PD1 interactions, suggesting that tyrosine mutations do not abrogate the interaction between AXL and PD1. Nevertheless, differences in the binding mode between conditions could impact the functional role of the interaction, but it requires further variation.

5.8.3 Conformational analysis by long-scale MD simulations

The Macromolecular HDOCK docking protocol lacks the ability to account for flexibility in protein receptors and does not consider the dynamic motion of receptor structures during docking calculations. In order to investigate the dynamic behaviour of the AXL receptor upon binding of PD1, we conducted MD simulations for a total of four complexes, each simulated for a duration of 2μs. To compare the structural changes during the simulation, we calculated the RMSD (Root Mean Square Deviation) of AXL and PD1 proteins when they were complexed together. The RMSD value quantifies the average deviation between the positions of corresponding atoms in two structures. By calculating the RMSD, we assessed the extent of conformational changes that occur in the AXL receptor and PD1 during the simulation.

We investigated the interactions involving the extracellular domain (ECD) of AXL and the extracellular domain of PD1, as well as the interactions between the intracellular domains (ICD) of AXL and PD1, including wild-type and mutant forms of PD1 (PD1-Y223F and PD1-Y248F). The study design considered the following:

ECD - ECD interactions

We examined the interactions between the ECD of AXL and the ECD of PD1. These interactions occurred in two different scenarios.

A. When both AXL and PD1 were embedded within the same cell membrane, we explored the interactions between their respective ECDs (**Figure 40A**).

B. When AXL and PD1 were present in different cell membranes, we investigated the interactions between their ECDs in this separate cellular environment (**Figure 40B**).

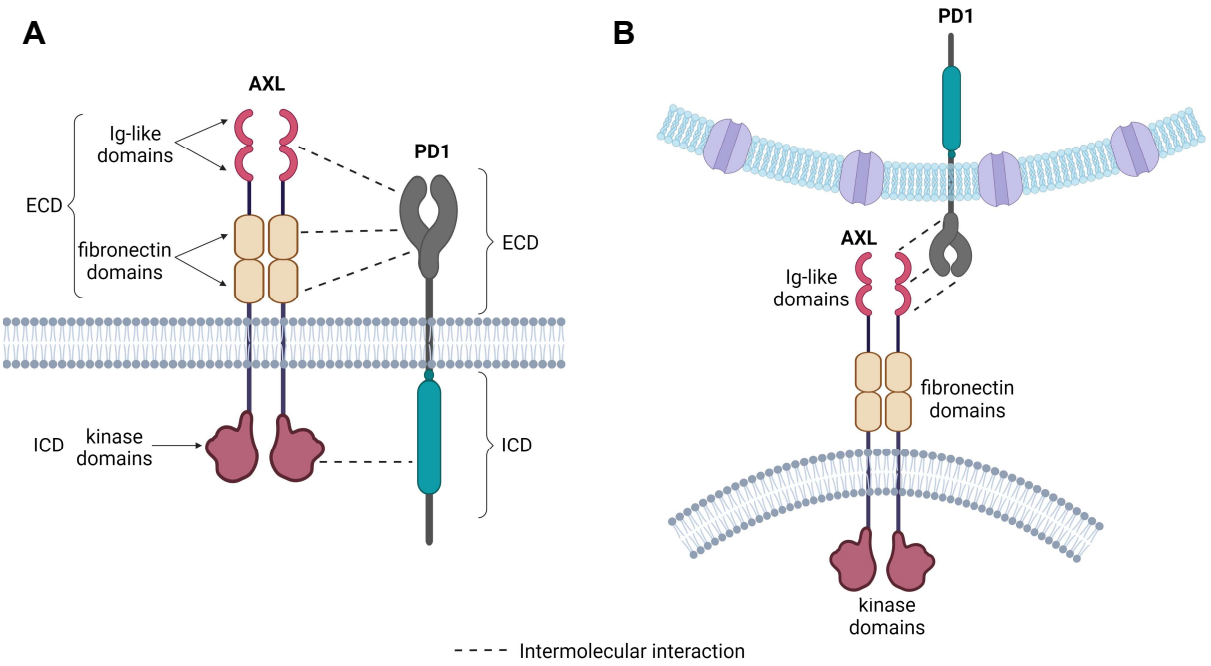

Figure 40 Schematic illustration of possible intermolecular interactions between AXL-PD1, specifically ECDs of AXL and PD1, and ICDs of AXL and PD1. A) both AXL and PD1 are embedded within the same cell membrane, **B)** AXL and PD1 are present in different cell membranes.

ICD - ICD interactions

In the case of AXL and PD1, their ICDs were able to interact only when they were embedded within similar cell membranes (**Figure 40A**). This means that for ICD-ICD interactions to occur, AXL and PD1 has to be located within the same cell membrane.

5.8.3.1 AXL-PD1-ECD complex

The RMSD calculated from the 2μs of simulation data for the AXL-PD1-ECD complex indicated that PD1 exhibited higher thermodynamic stability when it was complexed with AXL. The averaged RMSD value obtained was 3.45 ± 0.19Å throughout the simulation **(Figure 41A)**. This suggests that the complex formed between AXL and PD1 remained relatively stable during the simulation, with PD1 showing less structural deviation from its initial conformation when bound to AXL. The lower RMSD value indicates that PD1 maintained a more consistent and stable structure in the presence of AXL throughout the simulation time.

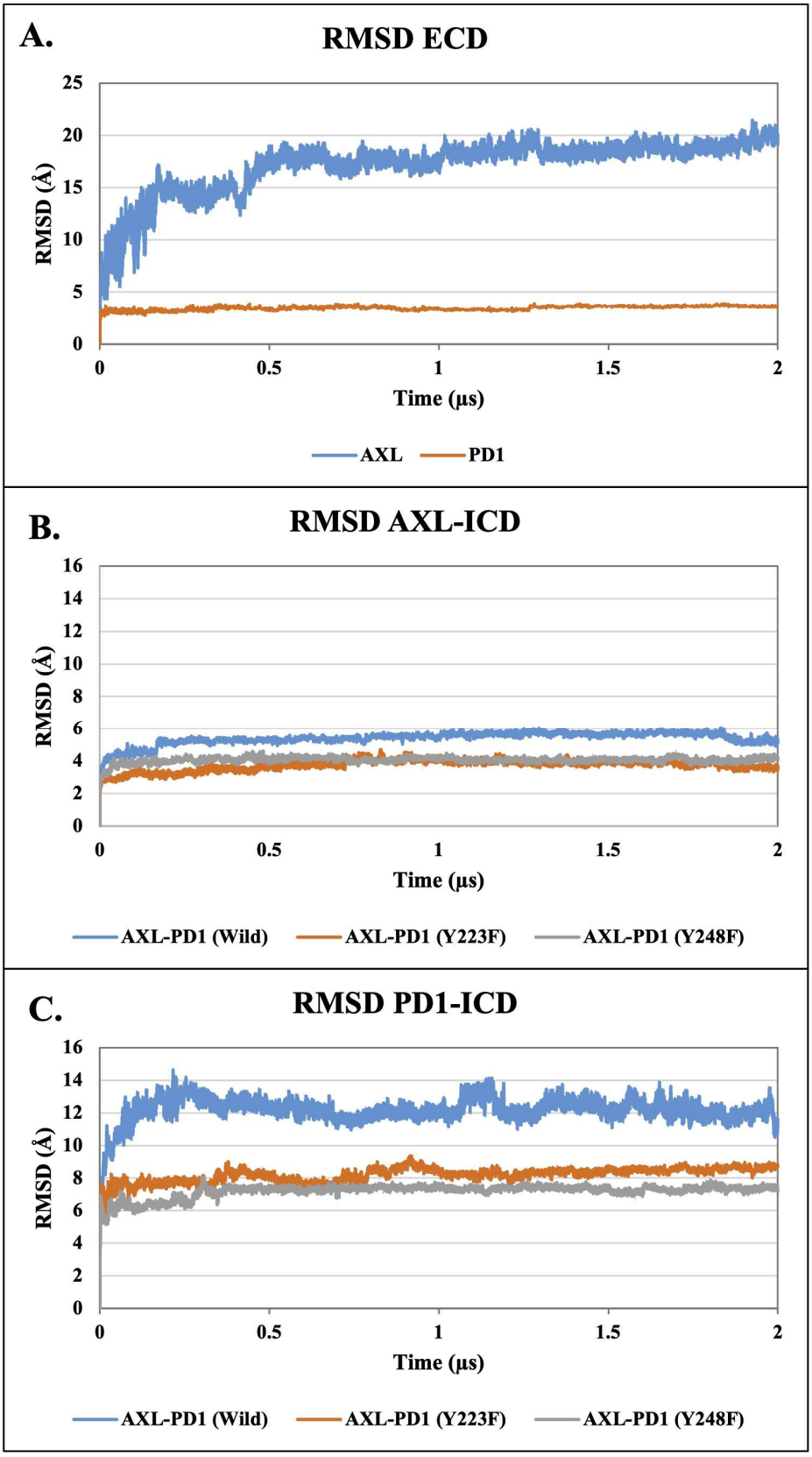

Figure 41 Root mean square deviation (RMSD) analysis throughout the MD simulation trajectories. A) AXL and PD1 ECDs, **B)** AXL ICD when interacting with PD1 ICDs (WT and mutants), **C)** PD1 ICDs (WT and mutants) when complexed with AXL ICD.

During the initial 500 ns of the MD simulation of AXL, there was a notable decrease in conformational stability, as evidenced by a deviation of up to 17Å in the RMSD. However, after this initial phase, the AXL structure stabilized, and its conformational stability was maintained throughout the remaining of the production run (up to 2μs), with an average RMSD of 17.12 ± 2.65Å (**Figure 41A**). The observed thermodynamic instability of the AXL structure during the initial phase could be attributed to the presence of a loop between the two immunoglobulin (Ig) domains and the two-fibronectin type III (FNIII) domains of AXL. This loop region likely undergoes significant conformational changes, leading to the observed higher RMSD values. Notably, during the simulation, the PD1 extracellular domain (ECD) remained complexed within the Ig domains of AXL.

Overall, these findings suggest that while the AXL structure exhibited instability during the initial phase of the simulation due to a loop region, it eventually reached a more stable conformation and remained relatively stable throughout the remaining simulation time. The presence of the PD1 ECD complexed within the Ig domains of AXL likely contributed to stabilizing the AXL structure after the initial phase.

5.8.3.2 Thermodynamics of AXL-ICD complexed with PD1-ICD

The RMSD plot, as illustrated in **Figure 41B**, provides compelling evidence indicating that the interaction between the AXL-ICD and PD1-ICD (WT) resulted in a conformational stability of the AXL-ICD, with an average RMSD value of 5.39 ± 0.40Å. Notably, when the AXL-ICD was bound to the mutant variants of PD1-ICD, the conformational stability of AXL-ICD further increased. This enhanced stability was evident from the averaged RMSD values of 3.73 ± 0.34Å and 4.05 ± 0.18Å, respectively.

Moreover, the conformational stability of AXL-ICD significantly increased when it was bound to PD1-ICD, regardless of PD1 mutations. In comparison to AXL-ECD (extracellular domain), the intracellular domain of AXL (AXL-ICD) exhibited remarkable thermodynamic stability throughout the 2 μs simulation (**Figure 41A and B**).

5.8.3.3 Thermodynamics of PD1-ICD complexed with AXL-ICD

The RMSD plot (**Figure 41C**) indicated that when WT PD1-ICD is bound to AXL-ICD, a higher degree of deviation was observed, with an average RMSD of 12.18 ± 0.77Å. This increased deviation was particularly prominent during the initial phase of the simulation, up to 400ns, where the RMSD ranged from 11 to 14Å. Subsequently, from 400ns to 1.1μs, the PD1-ICD gradually started to equilibrate within the 11 to 13Å RMSD range. Following that, from 1.3μs to 2μs, the PD1-ICD achieved a second equilibration phase, maintaining a stable RMSD range of 11 to 13Å.

In conclusion, WT PD1-ICD exhibited a higher deviation when bound to AXL-ICD, indicating a relatively less stable conformation. However, it gradually equilibrated within the range of 11 to 13Å over the course of the simulation. On the other hand, the mutant variants of PD1-ICD, Y223F and Y248F, demonstrated higher thermodynamic stability when bound to AXL-ICD. This suggests that these mutant variants adopted more stable conformations when interacting with AXL-ICD.

5.8.4 AXL: an emerging PD1 binder with growing importance in cancer

Having confirmed the novel interaction between PD1 and AXL, we aimed to understand the significance of this interaction. Therefore, we scrutinized the current scientific reports linking both proteins, which revealed the growing importance of AXL as therapeutic target in cancer treatment.

5.8.4.1 Function

AXL is an 894-amino acid protein, which belongs to the TAM (TYRO3-AXL-MERTK) receptor family classified as receptor tyrosine kinases (RTKs). It consists of an extracellular region with two immunoglobulin-like domains and two fibronectin III domains, a transmembrane domain, and a kinase domain in the intracellular region (Q. Lu and Lemke 2001). AXL is widely expressed in healthy tissues such muscles, lungs, gastrointestinal tract, brain, bone marrow and lymphoid organs (source: Protein Atlas, https://www.proteinatlas.org/ENSG00000167601-AXL/tissue, accessed on November 2, 2023).

Physiologically, TAM receptors are engaged in a variety of functions. For example, triple TYRO3-AXL-MERK knockout in mice is not lethal for the embryonic germline but leads to severe autoimmune response. It is manifested as massive splenomegaly, immune infiltrates of nearly all tissues and high levels of circulating antibodies, emphasizing the major role of TAM receptors in regulation of the immune response (Q. Lu and Lemke 2001). AXL itself, regulates cell survival, orchestrates phagocytic clearance of apoptotic cells, and regulates the innate immune system response by suppressing the function of NK cells and TLR-induced inflammation (Seitz et al. 2007; I. K. Park et al. 2009; Kreiner et al. 2020; G. Wu, M C Bride, and Zhang 2017). Additionally, AXL was implicated in central nervous system development, blood coagulation and vascular integrity (Weinger et al. 2011).

5.8.4.2 AXL signalling cascade

Like other tyrosine kinase receptors, AXL activation is ligand dependent and requires ligation with GAS6 (growth arrest-specific protein 6) (Tsou et al. 2014). Subsequently, AXL forms homodimers and undergoes transphosphorylation of tyrosine residues. The phosphorylation step is necessary for further recruitment of SH2 domain-containing proteins and adaptor molecules such as p85, PLC, SRC, LCK and GRB2

(Auyez et al. 2021). Ultimately, AXL activates several critical pathways such as, MEK/ERK, PI3K/AKT/mTOR, NF-κB, and JAK/STAT (Ruan and Kazlauskas 2012; Braunger et al. 1997; Elkabets et al. 2015; Konen et al. 2021). Notably, AXL signalling activation may occur non-canonically via transactivation of neighbouring cell-expressed AXL molecules or through receptor homodimerization within a single cell. Alternatively, several reports described AXL activation through the formation of heterodimers with other RTKs such as HER2 or EGFR. which was proposed to play significant role in drug resistance (Vouri et al. 2016; Yoshimura et al. 2023; Adam-Artigues et al. 2022; Goyette et al. 2018).

5.8.4.3 Role in cancer

In recent years, a growing body of evidence suggested the significance of the tyrosine kinase receptor AXL in various malignancies such as NSCLS, breast and prostate cancer or haematologic malignancies such as acute myeloid leukaemia (O'bryan et al. 1991; Tsukita et al. 2019; Terry et al. 2021). AXL was showed to modulate the tumour microenvironment, impact the immune response, and play a role in tumour intrinsic signalling. **Figure 42** summarizes the mechanisms underlying AXL signalling in cancer (Goyette et al. 2021; Sadahiro et al. 2018; C. Zhu, Wei, and Wei 2019).

Increased expression of AXL protein is considered a poor prognostic marker, promoting cancer progression and metastasis, therefore resulting in shorter overall survival (Onken et al. 2017). This occurs through AXL-driven activation of the PI3K/AKT/mTOR, RAS/RAF/MEK/ ERK, JAK/STAT pathways, directly facilitating cell proliferation (Ruan and Kazlauskas 2012). Additionally, AXL contributes to increased cell migration and invasion, but it also stimulates NF-κB signalling, supporting cell survival and evasion of apoptosis (Tai et al. 2008).

Furthermore, in a murine HER2+ breast cancer model, AXL was linked to EMT molecular signatures. Studies demonstrated that it has the capacity to facilitate all stages of metastasis including intravasation, extravasations and establishment of the metastatic niche, while tumour spread could be mitigated by implementation of AXL inhibitors (Goyette et al. 2018). Apart from the direct impact on the metastatic

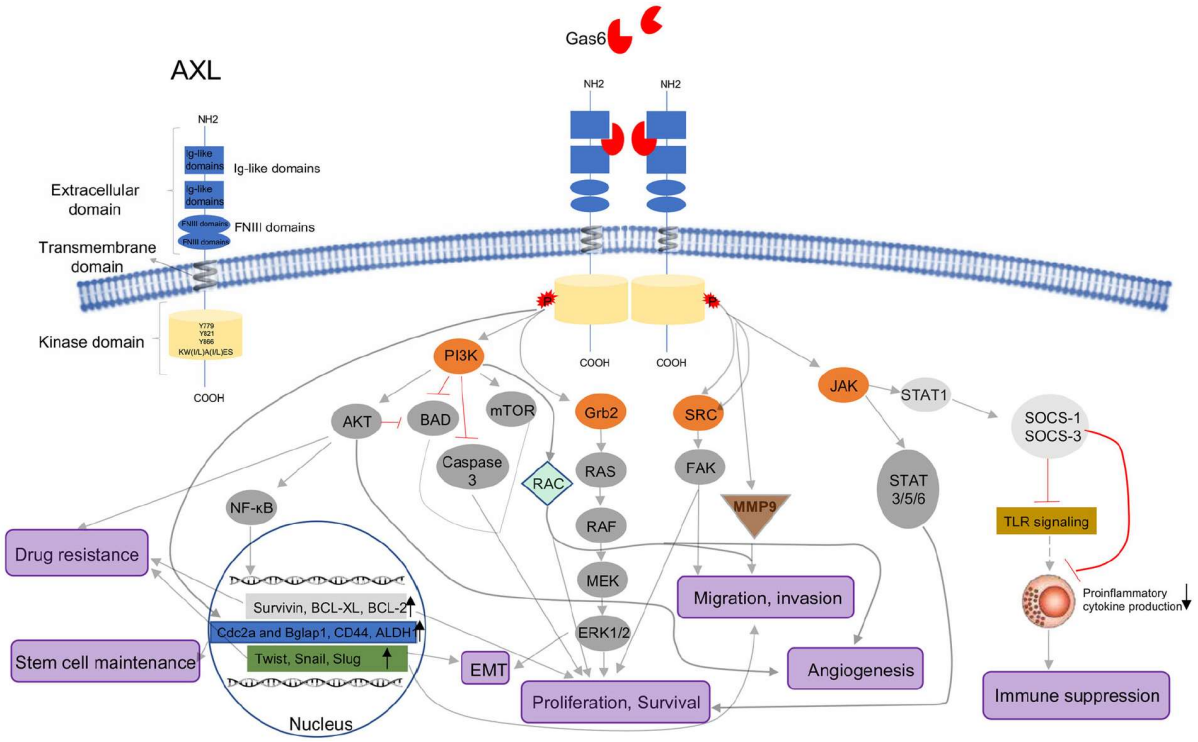

Figure 42 Structure, signalling pathways and activation of AXL. **A)** Schematic diagram the of the protein structure, **B)** AXL signalling networks upon classical GAS6-mediated activation. Figure adopted from Zhu, Chenjing, Yuquan Wei, and Xiawei Wei (2019); doi:10.1186/s12943-019-1090-3.

process, AXL has the potential to regulate angiogenesis. It was observed that AXL knockout supresses the release of angiogenic factors by tumour cell. Further *in vivo* validation confirmed that either AXL knockout or inhibition supresses tumour-induced angiogenesis. (Tanaka and Siemann 2019; Goyette et al. 2018)

In addition, AXL was associated with drug resistance, particularly in the course of molecular targeted therapy with RTK inhibitors targeting receptors such as HER2, EGFR, ERK or PI3K. It was observed that this type of treatment can lead to increased expression of AXL. Given its pro-survival, proliferative and EMT promoting capabilities, AXL has the potential to decrease the efficacy of such therapy and drive cancer progression (Tian et al. 2016; Elkabets et al. 2015). Alternatively, the mechanism of drug resistance can be mediated through the non-canonical activation of AXL by RTK receptors. In such case, the therapeutic RTK inhibition is circumvented by RTKs ability to activate AXL. Subsequently, AXL promotes cancer progression through downstream activation of PI3K/Akt/mTOR, RAS/RAF/MEK, or JAK/STAT

signalling, thereby supporting tumour growth and survival (Adam-Artigues et al. 2023; Gay, Balaji, and Byers 2017; Elkabets et al. 2015).

5.8.4.4 AXL as a therapeutic target

AXL plays an array of functions in cancer, including but not limited to the propagation of EMT, cancer-induced angiogenesis, metastasis, and drug resistance. Consequently, AXL has emerged as an attractive therapeutic target in combination with existing therapies. Thus far, AXL inhibitors demonstrated promising effects in preclinical studies in cancers such as melanoma, ovarian or renal cell carcinoma. In 2021 FDA approved the fast-track designation of an AXL inhibitor bemcentinib in combination with PD1 immunotherapy for treatment of NSCLS with STK11 mutations (Nyakas et al. 2022; Yeo et al. 2023; Synn et al. 2022; Veluswamy et al. 2023).

In fact, several underlying mechanisms were described linking AXL inhibition with improved response to immunotherapy. First, AXL expression strongly correlates with PDL1 expression by tumour cells. In turn, the increased PDL1 expression activates PD1 on T cells, the leading mechanism of immune evasion, underlying T cell exhaustion. Implementation of AXL inhibitors demonstrated to decrease PDL1 overexpression, improving the efficacy of immunotherapy (Terry et al. 2021).

An alternative mechanism underlying the improved response to immunotherapy in combination with AXL inhibition was reported in NSCLC patients with STK11 mutations (Veluswamy et al. 2023). The enhanced response to ICIs was linked to the increase in PD1+ CD8 T cells, a critical population of cells responding to immune checkpoint inhibition responsible for therapeutic effects. NSCLS patients with STK11 mutations lack this population of cells, while AXL inhibition increases the number of PD1+ CD8 T cells in TME. It happens by the increase in type I interferon production by DCs and leads to restored sensitivity to immunotherapy (Huiyu Li et al. 2022; Veluswamy et al. 2023).

Additionally, in a preclinical model, AXL inhibition was implicated in creating anti-tumorigenic and pro-inflammatory TME thorough modulation of Hif1α activity(Goyette

et al. 2021). The hypoxic stress is of the hallmarks of cancer and the mitigated hypoxic response observed in this study led to diminished EMT, decreased production of proinflammatory cytokines, therefore better control over tumour associated macrophages. Ultimately, AXL inhibitors resulted in more favourable environment for the tumour infiltrating lymphocytes, improving the conditions for better response to ICIs (Goyette et al. 2021).

By investigating the interaction between AXL and PD1, our findings may contribute to better understanding of the role these proteins play in cancer. Moreover, confirming the interaction between AXL and PD1 not only in cancer but also in immune cells will shed new light on the mechanism underlying the improved response to immunotherapy in patients treated with AXL inhibitors.

5.9 Discussion – identification of AXL as a novel PD1 interacting partner.

Our understanding of the PD1 interactome and the downstream effects of PD1 signalling stem from studies on PD1/PDL1 pathway in effector T cells (Topalian, Drake, and Pardoll 2012; Carter et al. 2002; Chatterjee et al. 2013). However, only scarce reports are available regarding this pathway in cancer cells. Considering the mutational burden and the distinct role of PD1 in immune cells, one can expect variations in the PD1 interactome and effector function between these two types of cells. Moreover, it has been demonstrated that cancer-intrinsic PD1 signalling effects differ depending on the tumour type, with PD1 acting either as a tumour suppressor or promoter (Ieranò et al. 2022; Yao et al. 2018; Du et al. 2018; Liotti et al. 2021; Pu et al. 2019; Harper et al. 2022; Gan et al. 2022). Therefore, PD1 interactome studies are essential to fully understand the mechanism of PD1 signalling in cancer cells and to find new druggable targets if necessary.

Here, we conducted a high-throughput PD1 interactome study employing LC-MS/MS appraoch to identify PD1 binding partners obtained through pull-down isolation. Our analysis encompassed the wild-type PD1 protein and PD1 tyrosine phosphorylation mutants Y223 and Y248, with Y248 previously reported as critical for the inhibitory function of PD1 in T cells (Bardhan et al. 2019; Bu et al. 2021).

Ultimately, we identified several PD1 binding candidates, demonstrating varying affinities dependent or independent of tyrosine residue mutations, emphasizing the significance of PD1 phosphorylation in some interactions. Among all proteins studied, we focused on AXL, a receptor tyrosine kinase with growing significance in cancer (Cao et al., n.d.; Gay, Balaji, and Byers 2017; Tanaka and Siemann 2019; Shao, Teramae, and Wells 2023). Using several independent methods, we confirmed that AXL interacts with PD1 receptor. Moreover, our findings indicate that AXL interacts with PD1 on the cellular membrane rather than the cytoplasmic pool, but this could be expected given that AXL is a membrane receptor.

The docking analysis revealed that the AXL-PD1-ECD complex exhibited strong binding affinity, with specific hydrogen bonds and salt bridges stabilizing the complex. However, AXL-PD1-ICD (WT) complex showed potentially stronger binding compared

to the extracellular domain complex, with distinct residues and bond types involved in the interaction. The mutant complexes, AXL-PD1-ICD (Y223F) and AXL-PD1-ICD (Y248F), demonstrated variations in interactions and docking scores, indicating altered but not abrogated protein-protein binding. The molecular dynamics simulation study of the conformational stability and dynamic behaviour demonstrated that the complex formed between AXL and PD1 exhibits higher thermodynamic stability, as evidenced by the lower RMSD values. Specifically, PD1 showed less structural deviation from its initial conformation when bound to AXL, indicating a stable interaction between the two proteins. (Lokhande, Shrivastava, and Singh 2023)

Notably, AXL has recently emerged as an attractive cancer therapeutic target and its blockade was reported to improve response to immunotherapy (Y. Tang et al. 2023; C. A. Liu et al. 2022; T. J. Chen et al. 2021). While previous studies have associated AXL overexpression to increased levels of PDL1 in cancer cells (Tsukita et al. 2019; Terry et al. 2021), the mechanistic link between PD1 and AXL has not been reported previously. Significantly, previous reports demonstrated that AXL could undergo noncanonical activation through heterodimerization with other receptors such as EGFR or HER2, resulting in mutual activation. This mechanism was proposed to promote AXL-driven resistance to HER or EGFR inhibitors by their alternative activation (Vouri et al. 2016; Adam-Artigues et al. 2023; 2022; Goyette et al. 2018). Although no such correlation was previously reported for PD1, it is tempting to speculate that the interaction between PD1 and AXL could cross-modulate activity of these proteins. Therefore, our studies may shed new light on the mechanism underlying more favourable outcomes of combined inhibition of PD1 and AXL. However, further studies are necessary to elucidate the functional role of this interaction.

6. Limitations

The limitations of our study stem primarily from the implementation of a cellular model of osteosarcoma without *in vivo* or clinical material validation of our findings. Nevertheless, the cellular model is indispensable for preliminary studies on the role of proteins and the discovery of protein interactions.

To determine the ultimate role of PD1 in osteosarcoma cells as a tumour suppressor would require the *in vivo* studies. However, to perform such experiments, cellular modifications ensuring stable silencing of PD1 protein in the cells would be necessary. siRNA technology utilized in our study had the limited silencing effect on PD1 protein and caused inconsistencies in cellular response. Perhaps, implementation of shRNA or CRISPR-Cas9 knockout would generate more efficient and long-lasting silencing effect. Additionally, replacing U2OS cells with a cell line exhibiting higher level of PD1 expression could enhance the clarity of the results and make the silencing effect more prominent.

Furthermore, the *PDCD1* gene knockdown demonstrated sometimes unclear results, what remained unsolved. This ambiguity included the origin of PD1 isoforms expressed in our model and the nature and role of PD1 equilibrium in cancer cells. Moreover, our study did not investigate if the intrinsic effects of PD1 signalling in osteosarcoma require ligation with PDL1 and whether or not could be modulated with PD1/PDL1 blocking antibodies. This part is critical for assessing the significance of cancer-intrinsic PD1 signalling in the outcomes of immunotherapy.

PD1 interaction studies identified AXL as a novel PD1 interacting partner, which binds independently of PD1 phosphorylation state. However, a potential concern arises regarding the functionality of both tyrosine residues, which may exhibit varying binding affinities but sufficient to exert the downstream effect of protein-protein interaction. To address this, implementing a double mutant (Y223/Y248) would be helpful in eliminating such risk. Moreover, it is vital to better understand the significance of the interaction between PD1 and AXL, as well as to validate proteomic data describing the molecular effects of PD1 signalling in osteosarcoma cells.

7. Summary

Recent years of cancer therapeutic approach brought an advent of PD1/PDL1 immunotherapy. Constant efforts are made to improve the success rate of immune checkpoint inhibitors majorly by combination with other cancer therapeutic targets. At the same time, more attention is paid to the role of cancer-intrinsic PD1 and its impact on the response to ICIs. Apart from re-evaluating the safety of current treatment in patients with tumour-expressed PD1, studies on cancer-intrinsic PD1 signalling pathway and molecular interactions may help to overcome limited response to ICIs in certain malignancies.

The aim of this work was to investigate if PD1 expression on the osteosarcoma could be the underlying mechanism for limited response of osteosarcoma to immunotherapy. To our knowledge, PD1 expression was not reported previously in osteosarcoma. Our studies strongly suggest that PD1 has the intrinsic effect on human osteosarcoma cells and might act as a tumour suppressor. Additionally, the proteomic analysis linked osteosarcoma-PD1 to cancer stem cell-like molecules and cell adhesion molecules, suggesting PD1 importance in processes such as cancer invasion and metastasis. The proteomic data was supported by the cellular experiments we performed, which indicated increased cell viability and ability to migrate upon siRNA mediated *PDCD1* knockdown.

Moreover, we identified a novel interaction between PD1 and AXL and we observed that it does not depend on PD1 phosphorylation but rather on an alternative mechanism, which we tried to understand by molecular modelling and molecular dynamics studies. The analysis clearly indicated that PD1 and AXL can interact, and the interaction takes place in their intracellular regions.

7.1 Future directions: canine model of PD1 signalling in osteosarcoma.

This project is funded by the Preludium research grant 2022/45/N/NZ1/02699, which I have been awarded by the National Science Centre for three years.

Relatively low prevalence of osteosarcoma in humans and difficulty in running clinical trials in children, resulted in no significant therapeutic advancement over the past decades (Ya Zhang et al. 2018). Thus, there is a need for novel treatment approaches, which are currently hampered by lack of spontaneous models of the disease (Maniscalco 2015; Schiffman and Breen 2015). Given the great success of PD1/PDL1 immunotherapy in certain cancer types, many clinical trials were started to evaluate its efficacy in other tumours including osteosarcoma (Le Cesne et al. 2019). Considering high levels of PDL1 expression in human osteosarcoma, yet its poor response to immune checkpoint blockade, suggests that PD1 intrinsic signalling may be one of the reasons why immunotherapy has failed in this type of cancer and should be further investigated.

However, low incidence of osteosarcoma in humans is a serious obstacle, which prevents research advancement, suggesting a need for an alternative model to study osteosarcoma (Bielack et al. 2016; Hytönen and Lohi 2016). Strikingly, this rare human disease is 27 times more frequently diagnosed in large dog breeds than in humans (Fenger, London, and Kisseberth 2014). Also, companion dogs develop osteosarcoma spontaneously and it was shown that human and canine osteosarcoma share many pathological, morphological, and genetic similarities (Simpson et al. 2017; Culp et al. 2020). In contrast to laboratory animals which are isolated from the external environment, companion dogs share similar environmental hazards to humans (Rowell, McCarthy, and Alvarez 2011; Alvarez 2014; Rotroff et al. 2013). Also, murine studies often exploit a patient's derived xenograft model, which requires animals with compromised immune system in order to carry out the experiments. Conversely, the canine model allows to study the disease in animals with an intact immune system and to monitor how its function changes over time and affects the tumour. Therefore, it all makes them a far more appropriate model to study cancer (J. S. Park et al. 2016).

At the same time, both canines and humans could benefit from development of the therapy. Considering the long way from discovery to approval of the actual therapy, translational studies in dogs may significantly accelerate human therapeutics approval and these are only some of many more benefits of using companion dogs with spontaneously occurring cancer as a model for human diseases. One must bear in mind, that while there is wide accessibility of samples for most types of cancer, then when it comes to rare diseases such as osteosarcoma, dogs could contribute to huge treatment advancement of rare disorders. Wider access to clinical samples would undoubtedly make such studies more robust (Shaffer 2019; Khanna et al. 2009).

Our human data strongly suggests the role of cancer-intrinsic PD1 signalling in cell invasion and metastasis. Therefore, there is a risk that it could be a mechanism of resistance to PD1 therapy in this type of cancer. Moreover, we provided comprehensive insights into PD1 pathway molecular interconnections and identified new PD1 interacting candidates. Considering that spontaneously occurring canine osteosarcoma shares many histopathological and molecular features of human osteosarcoma, we will perform a comparative analysis and validate how close canine and human PD1 signalling resembles one another. This will surely facilitate immunotherapy studies in both species in the future and perhaps contribute to identification of mechanisms responsible for immunotherapy ineffectiveness and hopefully help to finding druggable targets to overcome this obstacle.

We aim to determine the role of PD1 intrinsic signalling in canine osteosarcoma and to accomplish our goal, we will do the following.

1. Characterising the significance of cancer PD-1 expression in canine osteosarcoma cell lines on global proteomics to evaluate how it correlates to the human data.
2. Identifying the novel canine PD1 interacting partners to better clarify its role in canine cancer cells and how it corresponds to human data.
3. Implementing the Chick Chorioallantoic Membrane (CAM) assay to evaluate and compare the *in vivo* effect of cancer PD1 expression on the invasion and metastatic properties of human and canine osteosarcoma cell lines.

4. Assessing the effect of PD1 blocking antibodies on cancer cells growth in both models as an attempt to determine the safety of immunotherapy implementation in both species in the tumours with PD1 intrinsic signalling.

Figure 43 demonstrates the graphical summary of the research plan and methodology included in the project.

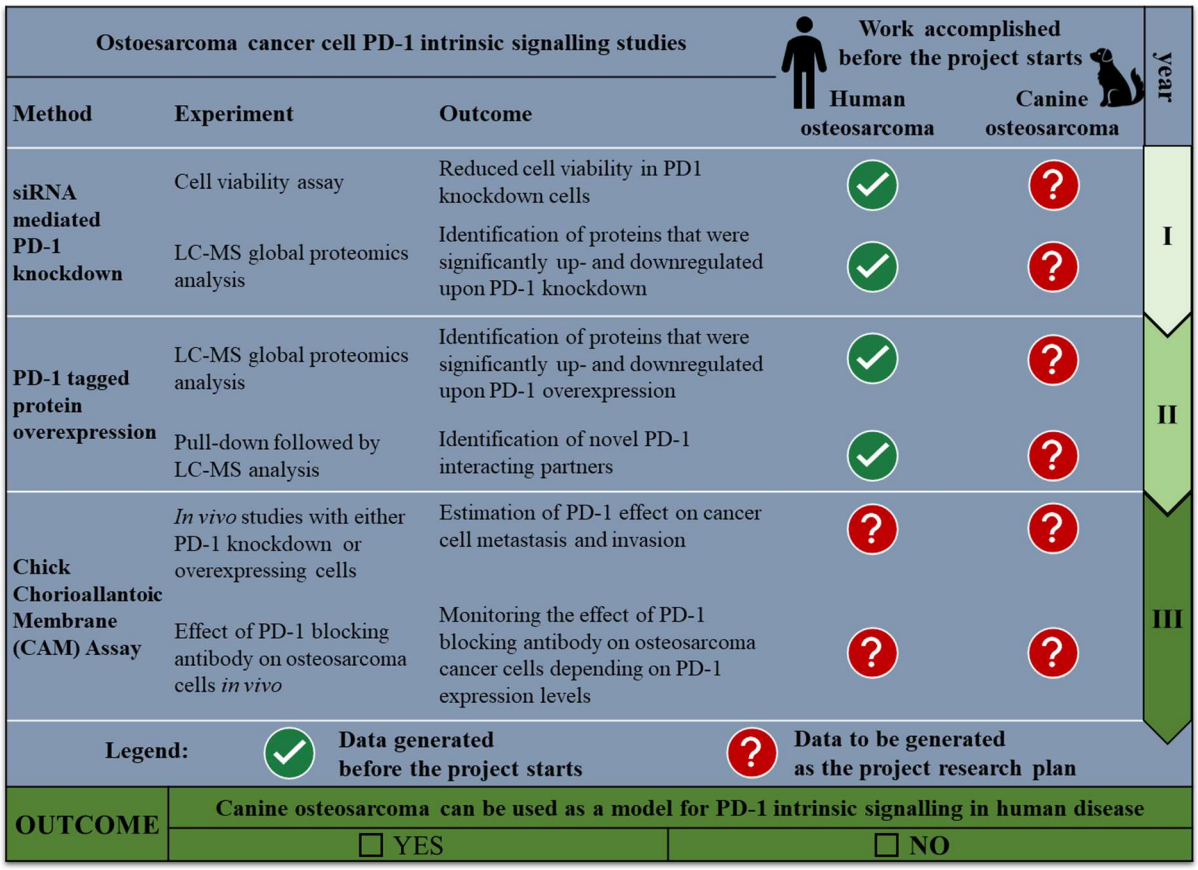

Figure 43 Graphical abstract demonstrating the research plan to determine if canine cancer-intrinsic PD1 signalling can be used as a model for human disease.

To execute the scientific plan, most of the experiments will utilize the methods and protocols implemented for studying the significance of cancer-intrinsic PD1 signalling in human osteosarcoma, including:

1. Investigation of changes in canine global proteome induced by PD1 knockdown using LC-MS/MS based proteomics and how it corresponds to the results presented in this thesis.

2. Monitoring changes in canine global proteome induced by PD1 overexpression. Similarly to the work plan introduced above, we will track the changes in global

proteome induced by PD1 overexpression to compare these results with human proteomics data. This data will be used to further support our comparative studies.

3. Identification of canine PD1 interacting partners by PD1 pull-down followed by LC-MS/MS analysis and validation by Proximity Ligation Assay. Similar analysis was performed for identification of PD1 interacting partners in human osteosarcoma. We will investigate if the interactions we have already identified in the human model occur in canine osteosarcoma and we will perform the pull-down experiment to identify unique PD1 binding partners in canine model.

4. In vivo studies evaluating cancer cell metastasis and invasion depending on PD1 silencing or overexpression with implementation of PD1 blocking antibodies.

Our preliminary data clearly indicated that cancer PD1 expression in human osteosarcoma affects the expression of proteins that facilitates cancer progression, metastasis, and cell invasion. However, to accurately demonstrate the ultimate effect and its impact on immunotherapy, it would be critical to monitor cellular behaviour *in vivo*. Therefore, we proposed to implement the Chick Chorioallantoic Membrane (CAM) Assay to evaluate the effect of cancer PD1 expression on the invasion and metastatic properties of human and canine osteosarcoma cell lines. CAM assay is a well-recognized, fast, and relatively inexpensive method widely used to study angiogenesis, regenerative medicine, tissue engineering or cancer research. Technically, engraftment of cancer cells requires cutting a small window into an eggshell, which exposes the chick chorioallantoic membrane. Interestingly, the cell mediated-immunity of the chick embryo starts to develop at day 14th, but the standard procedure optimised for CAM assay lasts up to 13 days, warranting no interference with the animal immune system. In these conditions cancer cells can grow freely, in the environment resembling natural tumour stroma, including the presence of fibroblasts and endothelial cells, while preserving the potential of cancer cells to metastasize to organs of the embryo. Ultimately, it offers a great chance for rapid estimation of tumour cells' aggressiveness and evaluation of new therapeutics if cancer cells’ inoculum contains a drug of interest (Walewska et al. 2017; Kunz et al. 2019; Lokman et al. 2012; Vu et al. 2018).

CAM assay is commonly used by our research partner at the Roslin Institute (University of Edinburgh), where I will perform this part of the study. The experiment will be performed with osteosarcoma cell lines with stable PD1 knockdown or overexpression to evaluate how PD-1 expression affects the outcome of immune checkpoint immunotherapy. In order to achieve this, we will add either human or canine PD1 blocking antibody to the cell suspension, which will be engrafted on the membrane and observe how it affects tumour growth and metastasis.

Therefore, the potential of this study is not only to conduct comparative research but also to determine the ultimate role of cancer-PD1 in osteosarcoma. It will bring us one step closer to determining whether it acts as a tumour suppressor or rather as the tumour promoter.

8. Supplementary materials

8.1 Intermolecular Interaction Patterns through Simulation

The binding strength between the extracellular and intracellular domains of AXL and PD1 was assessed by the intermolecular interactions between AXL and PD1 using a dataset comprising 20,000 frames obtained from a 2μs MD simulation trajectory. The simulation event analysis module in Schrodinger's Maestro was employed to generate an intermolecular interaction pattern based on the simulation data. These interactions are visualized **Figures 44-47**, demonstrating the presence and occurrence of intermolecular interactions between AXL and PD1, further supporting the existence of binding interactions between the ECD and ICD domains of AXL and PD1.

8.1.1 Intermolecular interaction profile of AXL - PD1-ECD complex

During the examination of intermolecular interactions between the ECDs of AXL and PD1, various types of interactions were observed, contributing to the stability of the complex. These interactions include hydrogen bonds, salt-bridges, pi-pi stacking, and pi-cation interactions. In the initial 600 ns of the MD simulation, irregular hydrogen bonds were detected between AXL-ECD and PD1-ECD, ranging from 2 to 25 hydrogen bonds. These interactions were not consistently present but occurred intermittently. Between 600ns and 1.25μs into the MD simulation, the number of hydrogen bonds increased, resulting in more stable interactions between AXL-ECD and PD1-ECD. The complex formed between 20 to 30 hydrogen bonds during this period, indicating a strengthening of the interactions. Subsequently, in the later stages of the simulation, irregular interactions continued to occur but with an overall increase in the number of hydrogen bonds. The interactions became more stable as the complex formed between 20 to 35 hydrogen bonds. Overall, the analysis demonstrates that hydrogen bonds play a crucial role in stabilizing the intermolecular interactions between the ECDs of AXL and PD1. The observed pattern suggests an initial stage of sporadic interactions, followed by an intermediate phase of increased hydrogen bonding and ultimately, stabilized interactions during the production stage (**Figure 44**).

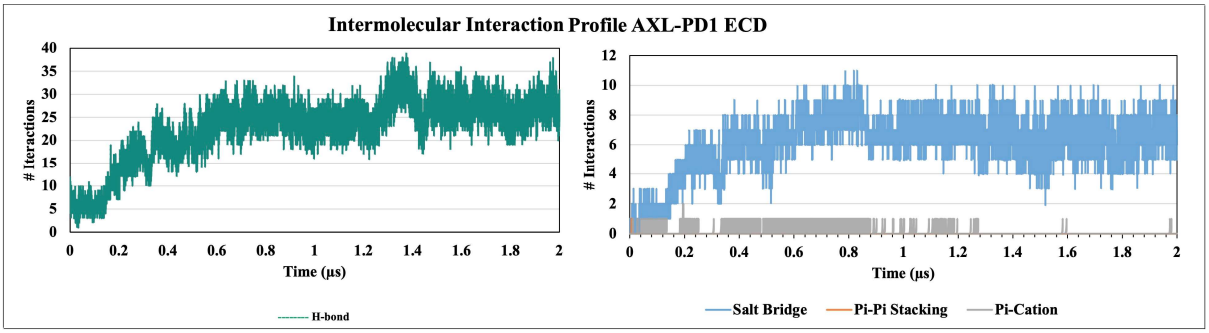

Figure 44 Intermolecular interactions measured throughout the simulation trajectories to assess binding stability between the AXL - PD1-ECD complex.

In addition to the hydrogen bonds, salt-bridges between the ECDs of AXL and PD1 were formed. The salt-bridges contribute to the stability of the complex. During the initial phase of the MD simulation (first 200ns), the complex formed a range of 1 to 4 salt-bridges between AXL-ECD and PD1-ECD. The number of salt-bridges gradually increased during this phase. From 200ns to 900ns of the MD simulation, the salt-bridges continued to increase but in an irregular pattern. The specific number of salt-bridges formed varied during this period, indicating some degree of fluctuation in the interactions. In the production stage of 1µs to 2µs, the complex achieved further stabilization as the number of salt-bridges formed between AXL-ECD and PD1-ECD ranged from 5 to 9. This indicates a strengthening of the interactions and a higher level of stability within the complex. The increasing salt-bridges formation throughout the simulation suggests their contribution to the overall stability of the AXL-ECD and PD1-ECD complex, alongside the hydrogen bonds.

During the analysis of the intermolecular interactions between the ECDs of AXL and PD1, several observations were made regarding salt-bridges and pi-cation interactions. In the first 350 ns of the simulation, the complex exhibited a range of 1 to 7 salt-bridges between the ECDs of AXL and PD1. Following this initial phase, the number of salt-bridges increased, ranging from 5 to 9 throughout the rest of the simulation. This indicates a strengthening and stabilization of the salt-bridges over time. Regarding the pi-cation interaction, an irregular single pi-cation interaction was observed between the ECDs of AXL and PD1 during the first 1.1µs of the simulation. However, this interaction disappeared afterwards, suggesting a transient or unstable nature of the pi-cation interaction in this context. In terms of pi-pi stacking, an initial observation of this interaction was made, but throughout

the entire simulation, the pi-pi stacking interaction was not detected (**Figure 44**). This suggests that pi-pi stacking may not play a significant role in the intermolecular interactions between the ECDs of AXL and PD1 in this particular context.

This analysis indicates that salt-bridges are the prominent intermolecular interactions between the ECDs of AXL and PD1, while the presence of pi-cation interactions is observed in the initial phase and subsequently diminishes. Pi-pi stacking, on the other hand, does not appear to be a significant interaction in this system throughout the simulation.

8.1.2 Intermolecular interaction profile of AXL - PD1-ICD (WT) complex

The analysis of intermolecular interactions between AXL-ICD and PD1-ICD (WT) indicated that in the initial 700ns of the MD simulation, a range of 10 to 25 hydrogen bonds were observed. This demonstrates a relatively high number of hydrogen bonds contributing to the interactions between the two domains. Following the initial phase, a stabilized interaction pattern emerged, where the ICDs maintained an average of 12 to 30 hydrogen bonds throughout the remaining 2μs of the MD simulation. This suggests a consistent and relatively strong binding between the ICDs of AXL and PD1 (WT).

Regarding salt-bridges, in the first 200ns, the complex exhibited 1 to 4 salt-bridges between the ICDs of AXL and PD1 (WT). This number increased to 3 to 6 salt-bridges between 200 ns and 600 ns, indicating a strengthening of the interactions during this period. Between 600ns and 1.7μs, the number of salt-bridges observed varied between 3 to 8, suggesting some fluctuation in the interactions. However, in the later phase of the MD simulation, the number of salt-bridges decreased to 6 (**Figure 45**). It demonstrates the presence of stable hydrogen bonds and salt-bridges between the ICDs of AXL and PD1 (WT) throughout the MD simulation. These interactions contribute to the stability and binding between the two domains, indicating their importance in the complex formation.

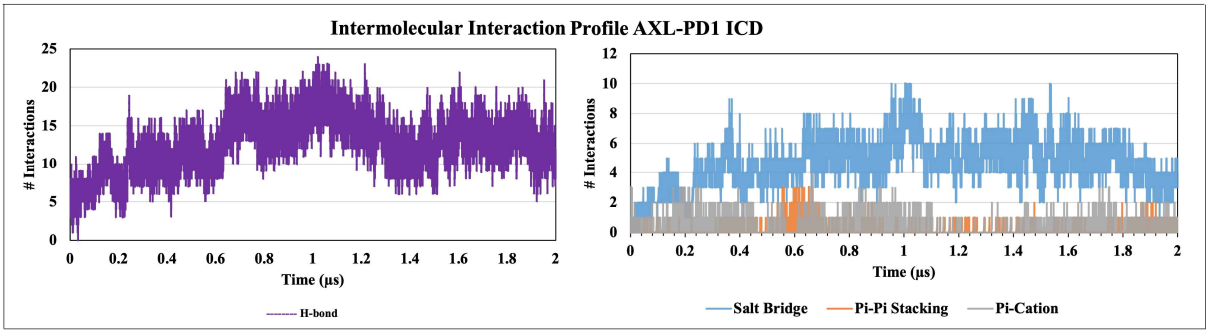

Figure 45 Intermolecular interactions measured throughout the simulation trajectories to assess binding stability between the AXL - PD1-ICD (WT) complex.

In addition to hydrogen bonds and salt-bridges, the analysis revealed the presence of pi-cation and pi-pi stacking interactions. Throughout the entire simulation, two pi-cation interactions were consistently observed between AXL-ICD and PD1-ICD (WT). These interactions involve the positive charge of a cation interacting with the pi-electron cloud of an aromatic ring. Furthermore, a single pi-pi stacking interaction was consistently present between the domains. This interaction occurs when two aromatic rings align and their pi-electron clouds overlap. During the simulation time between 300ns and 600ns, the pi-pi stacking interaction increased to a maximum of three interactions, indicating a transient strengthening of the pi-pi stacking interaction during this specific time period (**Figure 45**). These pi-cation and pi-pi stacking interactions contribute to the overall stability and binding between ICDs of AXL and PD1 (WT) throughout the simulation, along with the hydrogen bonds and salt-bridges.

8.1.3 Intermolecular interaction profile of AXL - PD1-ICD (Y223F) complex

In the case of the ICDs of AXL and PD1 (Y223F), the analysis revealed varying and irregular patterns of intermolecular interactions for hydrogen bonds, salt bridges, pi-cation interactions, and pi-pi stacking. During the first 1µs of the simulation, the number of hydrogen bonds formed between the AXL-ICD and PD1-ICD (Y223F) complex ranged from 12 to 35, displaying irregular variations. However, as the simulation progressed, the complex formed stabilized hydrogen bonds ranging from 18 to 35. This suggests a transition from irregular interactions to more consistent and stable hydrogen bonding throughout the simulation. In the initial half of the simulation (first 1µs), the number of salt bridges between AXL-ICD and PD1-ICD (Y223F) ranged from 1 to 6, indicating variability in the interactions. However,

beyond this point, the number of salt bridges increased to a range of 3 to 8, with occasional observations of 3 to 9 salt bridges (**Figure 46**). This trend suggests

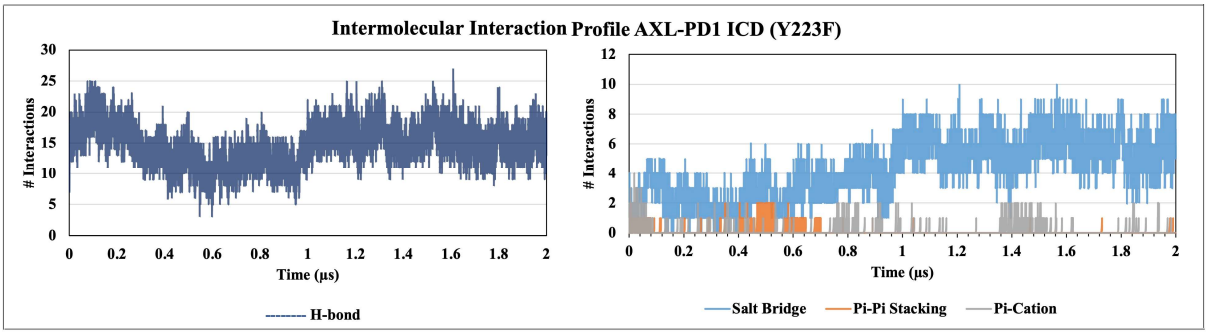

Figure 46 Intermolecular interactions measured throughout the simulation trajectories to assess binding stability between the AXL - PD1-ICD (Y223F) complex.

a progression towards a more stable and tightly bound complex between the ICDs. Interpreting pi-cation interactions, the initial 100 ns of the MD simulation exhibited up to three such interactions between AXL-ICD and PD1-ICD (Y223F). Subsequently, for the remaining duration of the simulation, the complex predominantly displayed 1 to 2 irregular pi-cation interactions. Observing pi-pi stacking, 1 to 2 such interactions were observed within the first 700ns of the simulation. However, after this point, pi-pi stacking was not detected until the end of the 1 µs MD simulation. Occasionally, a single pi-pi stacking interaction between AXL-ICD and PD1-ICD (Y223F) was observed, as depicted in **Figure 46**. This analysis highlights the varying and irregular nature of intermolecular interactions involving hydrogen bonds, salt bridges, pi-cation interactions, and pi-pi stacking in the complex formed by the ICDs of AXL and PD1 mutant (Y223F). However, the overall trend indicates a progression towards a stabilized and tightly bound complex as the simulation progresses.

8.1.4 Intermolecular interaction profile of AXL - PD1-ICD (Y248) complex

The analysis of the complex formed by the ICDs of AXL and PD1 mutant (Y248F) reveals distinct characteristics compared to other complexes. The complex formed by AXL-ICD and PD1-ICD (Y248F) exhibited a highly stable interaction, as evidenced by the consistent formation of hydrogen bonds throughout the 2µs MD simulation. The number of hydrogen bonds ranging from 15 to 34, indicating a strong and stable binding between the ICDs. Furthermore, the complex consistently formed 2 to 6 salt

bridges throughout the entire simulation (**Figure 47**). This suggests a persistent and stable interaction between the two domains, contributing to the overall stability of the complex.

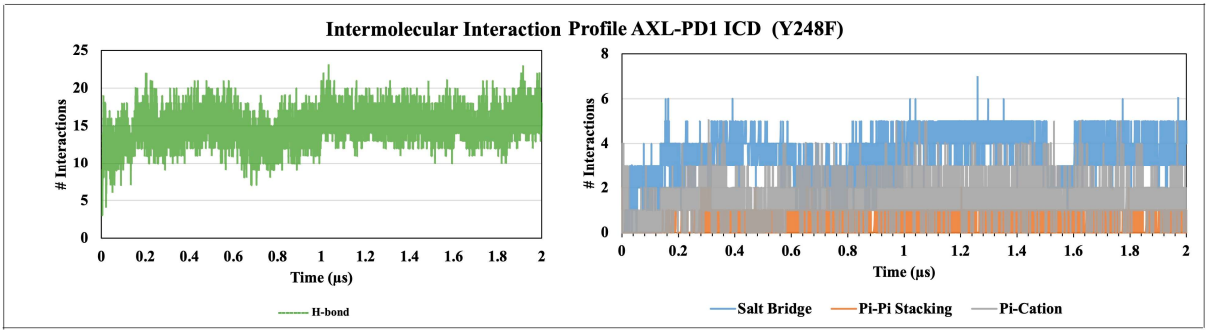

Figure 47 Intermolecular interactions measured throughout the simulation trajectories to assess binding stability between the AXL - PD1-ICD (Y248F) complex.

In addition, the analysis shows a notable presence of 3 pi-cation interactions throughout the MD simulation, indicating a consistent and favourable arrangement of positive cations with aromatic rings (**Figure 47**). Moreover, a single pi-pi stacking interaction is consistently observed during the entire simulation. The regularity of pi-pi stacking and the increased occurrence of pi-cation interactions in this complex are distinct characteristics not observed in the other complexes mentioned (ECDs of AXL and PD1, ICDs of AXL and PD1 wild type, and ICDs of AXL and PD1 mutant Y223F). These findings indicate that the complex formed by AXL-ICD and PD1-ICD mutant (Y248F) possesses unique and stable intermolecular interactions, including hydrogen bonds, salt bridges, pi-cation interactions, and pi-pi stacking. These interactions contribute to the overall stability and binding of the complex throughout the MD simulation.

Overall, hydrogen bonds and salt bridges play a crucial role in stabilizing the interactions between the ECDs and ICDs of AXL and PD1. The presence of pi-cation interactions and pi-pi stacking varies among the complexes, with the ICDs of AXL and PD1 mutant (Y248F) demonstrating the most stable and consistent interactions.

Acknowledgements

The authors would like to express their gratitude to the Shiv Nadar Institute of Excellence (IoE) for providing access to the high-performance computing resource

(HPC-magus02) used for conducting the extensive molecular dynamics simulations. Dr Kiran Bharat Lokhande extends heartfelt thanks to the Shiv Nadar IoE for the Post Doctoral Fellowship awarded to support this research. The authors also acknowledge the Indian Council of Medical Research, New Delhi, for awarding the Senior Research Fellowship to Mr. Ashish Shrivastava (Project ID: 2021-14351; File No.: BMI/11(100)/2022).

9. Bibliography

Adachi, Keishi, and Mark M. Davisa. 2011. 'T-Cell Receptor Ligation Induces Distinct Signaling Pathways in Naïve vs. Antigen-Experienced T Cells'. *Proceedings of the National Academy of Sciences of the United States of America* 108 (4): 1549–54. https://doi.org/10.1073/PNAS.1017340108/SUPPL_FILE/PNAS.201017340SI.PDF.

Adam-Artigues, Anna, Enrique J. Arenas, Joaquín Arribas, Aleix Prat, and Juan Miguel Cejalvo. 2023. 'AXL – a New Player in Resistance to HER2 Blockade'. *Cancer Treatment Reviews* 121 (December). https://doi.org/10.1016/J.CTRV.2023.102639.

Adam-Artigues, Anna, Enrique J. Arenas, Alex Martínez-Sabadell, Fara Brasó-Maristany, Raimundo Cervera, Eduardo Tormo, Cristina Hernando, et al. 2022. 'Targeting HER2-AXL Heterodimerization to Overcome Resistance to HER2 Blockade in Breast Cancer'. *Science Advances* 8 (20): 2746. https://doi.org/10.1126/SCIADV.ABK2746.

Agata, Yasutoshi, Akemi Kawasaki, Hiroyuki Nishimura, Yasumasa Ishida, Takeshi Tsubata, Hideo Yagita, and Tasuku Honjo. 1996. 'Expression of the PD-1 Antigen on the Surface of Stimulated Mouse T and B Lymphocytes'. *International Immunology* 8 (5): 765–72. https://academic.oup.com/intimm/article-abstract/8/5/765/693918.

Ahn, Eunseon, Koichi Araki, Masao Hashimoto, Weiyan Li, James L. Riley, Jeanne Cheung, Arlene H. Sharpe, Gordon J. Freeman, Bryan A. Irving, and Rafi Ahmed. 2018. 'Role of PD-1 during Effector CD8 T Cell Differentiation'. *Proceedings of the National Academy of Sciences of the United States of America* 115 (18): 4749–54. https://doi.org/10.1073/pnas.1718217115.

Akbay, Esra A., Shohei Koyama, Julian Carretero, Abigail Altabef, Jeremy H. Tchaicha, Camilla L. Christensen, Oliver R. Mikse, et al. 2013. 'Activation of the PD-1 Pathway Contributes to Immune Escape in EGFR-Driven Lung Tumors'. *Cancer Discovery* 3 (12): 1355–63. https://doi.org/10.1158/2159-8290.CD-13-0310.

Alam, Muhammad S. 2018. ‘Proximity Ligation Assay (PLA)’. *Current Protocols in Immunology* 123 (1). https://doi.org/10.1002/cpim.58.

Alexander, Gregory S., Joshua D. Palmer, Madalina Tuluc, Jianqing Lin, Adam P. Dicker, Voichita Bar-Ad, Larry A. Harshyne, et al. 2016. ‘Immune Biomarkers of Treatment Failure for a Patient on a Phase i Clinical Trial of Pembrolizumab plus Radiotherapy’. *Journal of Hematology and Oncology* 9 (1). https://doi.org/10.1186/s13045-016-0328-4.

Alvarez, Carlos E. 2014. ‘Naturally Occurring Cancers in Dogs: Insights for Translational Genetics and Medicine’. *ILAR Journal* 55 (1): 16–45. https://doi.org/10.1093/ilar/ilu010.

Álvarez-Viejo, María, Yolanda Menéndez-Menéndez, and Jesús Otero-Hernández. 2015. ‘CD271 as a Marker to Identify Mesenchymal Stem Cells from Diverse Sources before Culture’. *World Journal of Stem Cells* 7 (2): 470. https://doi.org/10.4252/WJSC.V7.I2.470.

Andersson, Patrik, Amorette Barber, Jie Xu, Fang J-y, Han Yao, Huanbin Wang, Chushu Li, and Jing-Yuan Fang. 2018. ‘Cancer Cell-Intrinsic PD-1 and Implications in Combinatorial Immunotherapy’. *Cancer Cell-Intrinsic PD-1 and Implications in Combinatorial Immunotherapy. Front. Immunol* 9: 1774. https://doi.org/10.3389/fimmu.2018.01774.

Anfosso, Francine, Nathalie Bardin, Eric Vivier, Florence Sabatier, José Sampol, and Franç Oise Dignat-George. 2000. ‘Outside-in Signaling Pathway Linked to CD146 Engagement in Human Endothelial Cells. https://doi.org/10.1074/jbc.M007065200.

Appleman, Leonard J., and Vassiliki A. Boussiotis. 2003. *T Cell Anergy and Costimulation*. *Immunological Reviews*. Vol. 192. https://doi.org/10.1034/j.1600-065X.2003.00009.x.

Arasanz, Hugo, Miren Zuazo, Ana Bocanegra, Luisa Chocarro, Ester Blanco, Maite Martínez, Idoia Morilla, et al. 2021. ‘Hyperprogressive Disease: Main Features and Key Controversies’. *International Journal of Molecular Sciences* 22 (7). https://doi.org/10.3390/IJMS22073736.

Araujo, Mariana E. de, Gertraud Erhart, Katharina Buck, Elisabeth Müller-Holzner, Michael Hubalek, Heidelinde Fiegl, Daniele Campa, et al. 2013. ‘Polymorphisms

in the Gene Regions of the Adaptor Complex LAMTOR2/LAMTOR3 and Their Association with Breast Cancer Risk'. *PLoS ONE* 8 (1). https://doi.org/10.1371/JOURNAL.PONE.0053768.

Artyomov, Maxim N., Mieszko Lis, Srinivas Devadas, Mark M. Davis, and Arup K. Chakraborty. 2010. 'CD4 and CD8 Binding to MHC Molecules Primarily Acts to Enhance Lck Delivery'. *Proceedings of the National Academy of Sciences of the United States of America* 107 (39): 16916–21. https://doi.org/10.1073/PNAS.1010568107/-/DCSUPPLEMENTAL.

Atsaves, Vasileios, Vasiliki Leventaki, George Z Rassidakis, and Francois X Claret. 2019. 'AP-1 Transcription Factors as Regulators of Immune Responses in Cancer'. *Cancers* 11 (1037). https://doi.org/10.3390/cancers11071037.

Attanasio, John, and E. John Wherry. 2016. 'Costimulatory and Coinhibitory Receptor Pathways in Infectious Disease'. *Immunity*. Cell Press. https://doi.org/10.1016/j.immuni.2016.04.022.

Auyez, Almira, A. Emre Sayan, Marina Kriajevska, and Eugene Tulchinsky. 2021. 'AXL Receptor in Cancer Metastasis and Drug Resistance: When Normal Functions Go Askew'. *Cancers 2021, Vol. 13, Page 4864* 13 (19): 4864. https://doi.org/10.3390/CANCERS13194864.

Azevedo, Judson Welber Veríssimo de, Thales Allyrio Araújo de Medeiros Fernandes, José Veríssimo Fernandes, Jenner Chrystian Veríssimo de Azevedo, Daniel Carlos Ferreira Lanza, Christiane Medeiros Bezerra, Vânia Sousa Andrade, Josélio Maria Galvão de Araújo, and José Veríssimo Fernandes. 2020. 'Biology and Pathogenesis of Human Osteosarcoma (Review)'. *Oncology Letters*. Spandidos Publications. https://doi.org/10.3892/ol.2019.11229.

Azuma, K., K. Ota, A. Kawahara, S. Hattori, E. Iwama, T. Harada, K. Matsumoto, et al. 2014. 'Association of PD-L1 Overexpression with Activating EGFR Mutations in Surgically Resected Nonsmall-Cell Lung Cancer'. *Annals of Oncology* 25 (10): 1935–40. https://doi.org/10.1093/annonc/mdu242.

Baek, Minkyung, Frank DiMaio, Ivan Anishchenko, Justas Dauparas, Sergey Ovchinnikov, Gyu Rie Lee, Jue Wang, et al. 2021. 'Accurate Prediction of Protein Structures and Interactions Using a Three-Track Neural Network'. *Science* 373 (6557): 871–76.

https://doi.org/10.1126/SCIENCE.ABJ8754/SUPPL_FILE/ABJ8754_MDAR_REPRODUCIBILITY_CHECKLIST.PDF.

Baldwin, Louise A., Nenad Bartonicek, Jessica Yang, Sunny Z. Wu, Niantao Deng, Daniel L. Roden, Chia Ling Chan, et al. 2022. 'DNA Barcoding Reveals Ongoing Immunoediting of Clonal Cancer Populations during Metastatic Progression and Immunotherapy Response'. *Nature Communications* 13 (1). https://doi.org/10.1038/s41467-022-34041-x.

Bardhan, Kankana, Halil Ibrahim Aksoylar, Thibault Le Bourgeois, Laura Strauss, Jessica D. Weaver, Bethany Delcuze, Alain Charest, Nikolaos Patsoukis, and Vassiliki A. Boussiotis. 2019. 'Phosphorylation of PD-1-Y248 Is a Marker of PD-1-Mediated Inhibitory Function in Human T Cells'. *Scientific Reports 2019 9:1* 9 (1): 1–9. https://doi.org/10.1038/s41598-019-53463-0.

Bardhan, Kankana, Theodora Anagnostou, and Vassiliki A. Boussiotis. 2016. 'The PD1: PD-L1/2 Pathway from Discovery to Clinical Implementation'. *Frontiers in Immunology* 7 (DEC). https://doi.org/10.3389/fimmu.2016.00550.

Barnes, Sarah E., Ying Wang, Luqiu Chen, Luciana L. Molinero, Thomas F. Gajewski, Cesar Evaristo, and Maria Luisa Alegre. 2015. 'T Cell-NF-KB Activation Is Required for Tumor Control in Vivo'. *Journal for ImmunoTherapy of Cancer* 3 (1). https://doi.org/10.1186/s40425-014-0045-x.

Barthel, Andreas, Steven T. Okino, Jinfang Liao, Kaname Nakatani, Jinping Li, James P. Whitlock, and Richard A. Roth. 1999. 'Regulation of GLUT1 Gene Transcription by the Serine/Threonine Kinase Akt1'. *Journal of Biological Chemistry* 274 (29): 20281–86. https://doi.org/10.1074/JBC.274.29.20281.

Bartholomew M. Shefton. 1998. 'Overview of Protein Phosphorylation'. *Current Protocols in Cell Biology* 14 (1): 1–3.

Bengsch, Bertram, Andy L. Johnson, Makoto Kurachi, Pamela M. Odorizzi, Kristen E. Pauken, John Attanasio, Erietta Stelekati, et al. 2016. 'Bioenergetic Insufficiencies Due to Metabolic Alterations Regulated by the Inhibitory Receptor PD-1 Are an Early Driver of CD8+ T Cell Exhaustion'. *Immunity* 45 (2): 358–73. https://doi.org/10.1016/j.immuni.2016.07.008.

Bie, Fenglong, He Tian, Nan Sun, Ruochuan Zang, Moyan Zhang, Peng Song, Lei Liu, et al. 2022. 'Research Progress of Anti-PD-1/PD-L1 Immunotherapy Related Mechanisms and Predictive Biomarkers in NSCLC'. *Frontiers in Oncology* 12 (February).
https://doi.org/10.3389/FONC.2022.769124.

Bielack, Stefan S., Stefanie Hecker-Nolting, Claudia Blattmann, and Leo Kager. 2016. 'Advances in the Management of Osteosarcoma'. *F1000Research*. Faculty of 1000 Ltd.
https://doi.org/10.12688/f1000research.9465.1.

Blank, Christian U., W. Nicholas Haining, Werner Held, Patrick G. Hogan, Axel Kallies, Enrico Lugli, Rachel C. Lynn, et al. 2019. 'Defining "T Cell Exhaustion"'. *Nature Reviews Immunology* 19 (11): 665–74.
https://doi.org/10.1038/s41577-019-0221-9.

Bonaventura, Paola, Tala Shekarian, Vincent Alcazer, Jenny Valladeau-Guilemond, Sandrine Valsesia-Wittmann, Sebastian Amigorena, Christophe Caux, and Stéphane Depil. 2019. 'Cold Tumors: A Therapeutic Challenge for Immunotherapy'. *Frontiers in Immunology*. Frontiers Media S.A. https://doi.org/10.3389/fimmu.2019.00168.

Bonnevier, Jody L., Ruan Zhang, and Daniel L. Mueller. 2005. 'E3 Ubiquitin Ligases and Their Control of T Cell Autoreactivity'. *Arthritis Research and Therapy*. https://doi.org/10.1186/ar1842.

Bouchal, Pavel, Theodoras Roumeliotis, Roman Hrstka, Rudolf Nenutil, Borivoj Vojtesek, and Spiros D. Garbis. 2009. 'Biomarker Discovery in Low-Grade Breast Cancer Using Isobaric Stable Isotope Tags and Two-Dimensional Liquid Chromatography-Tandem Mass Spectrometry (ITRAQ-2DLC-MS/MS) Based Quantitative Proteomic Analysis'. *Journal of Proteome Research* 8 (1): 362–73. https://doi.org/10.1021/PR800622B/SUPPL_FILE/PR800622B_SI_001.XLS.

Bowers, K J, D E Chow, H Xu, R O Dror, M P Eastwood, B A Gregersen, J L Klepeis, et al. 2006. 'Scalable Algorithms for Molecular Dynamics Simulations on Commodity Clusters'. In *SC '06: Proceedings of the 2006 ACM/IEEE Conference on Supercomputing*, 43.
https://doi.org/10.1109/SC.2006.54.

Boye, Kjetil, Alessandra Longhi, · Tormod Guren, Susanne Lorenz, · Stine Naess, Michela Pierini, Ingeborg Taksdal, et al. 2021. 'Pembrolizumab in Advanced Osteosarcoma: Results of a Single-Arm, Open-Label, Phase 2 Trial'. *Cancer Immunology, Immunotherapy : CII* 70 (9): 2617–24. https://pubmed.ncbi.nlm.nih.gov/33580363/.

Brahmer, Julie R., Scott S. Tykodi, Laura Q.M. Chow, Wen-Jen Hwu, Suzanne L. Topalian, Patrick Hwu, Charles G. Drake, et al. 2012. 'Safety and Activity of Anti–PD-L1 Antibody in Patients with Advanced Cancer'. *New England Journal of Medicine* 366 (26): 2455–65. https://doi.org/10.1056/nejmoa1200694.

Braunger, Jürgen, Lothar Schleithoff, Ansgar S. Schulz, Heidi Kessler, Reiner Lammers, Axel Ullrich, Claus R. Bartram, and Johannes W.G. Janssen. 1997. 'Intracellular Signaling of the Ufo/Axl Receptor Tyrosine Kinase Is Mediated Mainly by a Multi-Substrate Docking-Site'. *Oncogene* 14 (22): 2619–31. https://doi.org/10.1038/SJ.ONC.1201123.

Bretscher, Peter A. 1999. 'A Two-Step, Two-Signal Model for the Primary Activation of Precursor Helper T Cells' 96: 185–90. www.pnas.org.

Bretscher, Peter, and Melvin Cohn. 1970. 'A Theory of Self-Nonself Discrimination'. *New Series*. Vol. 169.

Brinkhof, Bas, Bo Zhang, Zhanfeng Cui, Hua Ye, and Hui Wang. 2020. 'ALCAM (CD166) as a Gene Expression Marker for Human Mesenchymal Stromal Cell Characterisation'. *Gene* 763 (December): 100031. https://doi.org/10.1016/J.GENE.2020.100031.

Brower, Vicki. 2016. 'Hyperprogressive Disease with Anti-PD-1 and Anti-PD-L1'. *The Lancet. Oncology*. https://doi.org/10.1016/S1470-2045(16)30590-3.

Brown, Keturah E., Gordon J. Freeman, E. John Wherry, and Arlene H. Sharpe. 2010. 'Role of PD-1 in Regulating Acute Infections'. *Current Opinion in Immunology*. Elsevier Ltd. https://doi.org/10.1016/j.coi.2010.03.007.

Bu, Xia, Vikram R. Juneja, Carol G. Reynolds, Kathleen M. Mahoney, Melissa T. Bu, Kathleen A. McGuire, Seth Maleri, et al. 2021. 'Monitoring PD-1 Phosphorylation

to Evaluate PD-1 Signaling during Antitumor Immune Responses'. *Cancer Immunology Research* 9 (12): 1465–75. https://doi.org/10.1158/2326-6066.CIR-21-0493.

Butte, Manish J., Mary E. Keir, Theresa B. Phamduy, Arlene H. Sharpe, and Gordon J. Freeman. 2007. 'Programmed Death-1 Ligand 1 Interacts Specifically with the B7-1 Costimulatory Molecule to Inhibit T Cell Responses'. *Immunity* 27 (1): 111–22. https://doi.org/10.1016/j.immuni.2007.05.016.

Callahan, Margaret K., and Jedd D. Wolchok. 2013. 'At the Bedside: CTLA-4- and PD-1-Blocking Antibodies in Cancer Immunotherapy'. *Journal of Leukocyte Biology* 94 (1): 41–53. https://doi.org/10.1189/jlb.1212631.

Camelliti, Simone, Valentino Le Noci, Francesca Bianchi, Claudia Moscheni, Francesca Arnaboldi, Nicoletta Gagliano, Andrea Balsari, et al. 2020. 'Mechanisms of Hyperprogressive Disease after Immune Checkpoint Inhibitor Therapy: What We (Don't) Know'. *Journal of Experimental and Clinical Cancer Research*. BioMed Central Ltd. https://doi.org/10.1186/s13046-020-01721-9.

Cao, Bihui, Manting Liu, Lu Wang, Kangshun Zhu, Mingyue Cai, Xiaopei Chen, Yunfei Feng, et al. n.d. 'Remodelling of Tumour Microenvironment by Microwave Ablation Potentiates Immu-Notherapy of AXL-Specific CAR T Cells against Non-Small Cell Lung Cancer'. Accessed 6 November 2023. https://doi.org/10.1038/s41467-022-33968-5.

Carter, Laura L., Lynette A. Fouser, Jason Jussif, Lori Fitz, Bija Deng, Clive R. Wood, Mary Collins, Tasuku Honjo, Gordon J. Freeman, and Beatriz M. Carreno. 2002. 'PD-1:PD-L Inhibitory Pathway Affects Both CD4+ and CD8+ T Cells and Is Overcome by IL-2'. *European Journal of Immunology* 32 (3): 634–43. https://doi.org/10.1002/1521-4141(200203)32:3<634::AID-IMMU634>3.0.CO;2-9.

Cesne, A Le, P Marec-Berard, J.-Y Blay, N Gaspar, F Bertucci, N Penel, E Bompas, et al. 2019. 'Programmed Cell Death 1 (PD-1) Targeting in Patients with

Advanced Osteosarcomas: Results from the PEMBROSARC Study'. https://doi.org/10.1016/j.ejca.2019.07.018.

Chan, Yee Teng, Heng Choon Cheong, Ting Fang Tang, Reena Rajasuriar, Kian Kai Cheng, Chung Yeng Looi, Won Fen Wong, and Adeeba Kamarulzaman. 2022. 'Immune Checkpoint Molecules and Glucose Metabolism in HIV-Induced T Cell Exhaustion'. *Biomedicines 2022, Vol. 10, Page 2809* 10 (11): 2809. https://doi.org/10.3390/BIOMEDICINES10112809.

Chan, Yung Chieh, Yu Chan Chang, Hsiang Hao Chuang, Yi Chieh Yang, Yuan Feng Lin, Ming Shyan Huang, Michael Hsiao, Chih Jen Yang, and Kuo Tai Hua. 2020. 'Overexpression of PSAT1 Promotes Metastasis of Lung Adenocarcinoma by Suppressing the IRF1-IFNγ Axis'. *Oncogene* 39 (12): 2509–22. https://doi.org/10.1038/s41388-020-1160-4.

Chang, F., J. T. Lee, P. M. Navolanic, L. S. Steelman, J. G. Shelton, W. L. Blalock, R. A. Franklin, and J. A. McCubrey. 2003. *Involvement of PI3K/Akt Pathway in Cell Cycle Progression, Apoptosis, and Neoplastic Transformation: A Target for Cancer Chemotherapy*. *Leukemia*. Vol. 17. Nature Publishing Group. https://doi.org/10.1038/sj.leu.2402824.

Chatterjee, Pranam, Nikolaos Patsoukis, Gordon J. Freeman, and Vassiliki A. Boussiotis. 2013. 'Distinct Roles Of PD-1 Itsm and ITIM In Regulating Interactions With SHP-2, ZAP-70 and Lck, and PD-1-Mediated Inhibitory Function'. *Blood* 122 (21): 191–191. https://doi.org/10.1182/blood.v122.21.191.191.

Chen, Gang, Yong Ho Kim, Hui Li, Hao Luo, Da-Lu Liu, Zhi-Jun Zhang, Mark Lay, et al. 2017. 'PD-L1 Inhibits Acute and Chronic Pain by Suppressing Nociceptive Neuron Activity via PD-1 HHS Public Access Author Manuscript'. *Nat Neurosci* 20 (7): 917–26. https://doi.org/10.1038/nn.4571.

Chen, Shixue, Zhibo Zhang, Xuan Zheng, Haitao Tao, Sujie Zhang, Junxun Ma, Zhefeng Liu, et al. 2021. 'Response Efficacy of PD-1 and PD-L1 Inhibitors in Clinical Trials: A Systematic Review and Meta-Analysis'. *Frontiers in Oncology* 11 (April). https://doi.org/10.3389/fonc.2021.562315.

Chen, Tony J., Piotr Mydel, Małgorzata Benedyk-Machaczka, Marta Kamińska, Urszula Kalucka, Magnus Blø, Jessica Furriol, et al. 2021. 'AXL Targeting by a Specific Small Molecule or Monoclonal Antibody Inhibits Renal Cell Carcinoma Progression in an Orthotopic Mice Model'. *Physiological Reports* 9 (23). https://doi.org/10.14814/phy2.15140.

Chen, Xin, Xiaomin Song, Kang Li, and Tong Zhang. 2019. 'FCλ-Binding Is an Important Functional Attribute for Immune Checkpoint Antibodies in Cancer Immunotheraphy'. *Frontiers in Immunology* 10 (FEB): 292. https://doi.org/10.3389/FIMMU.2019.00292/BIBTEX.

Chen, Yongjing, Zhenhua Hu, Qin Wang, Yan Ge, Lixiong Bai, Xuefeng Wang, and Xueguang Zhang. 2010. 'Generation and Characterization of Four Novel Monoclonal Antibodies against Human Programmed Death-1 Molecule'. *Hybridoma* 29 (2): 153–60. https://doi.org/10.1089/hyb.2009.0091.

Choi, Meena, Ching-Yun Chang, Timothy Clough, Daniel Broudy, Trevor Killeen, Brendan Maclean, and Olga Vitek. 2014. 'Systems Biology MSstats: An R Package for Statistical Analysis of Quantitative Mass Spectrometry-Based Proteomic Experiments' 30 (17): 2524–26. https://doi.org/10.1093/bioinformatics/btu305.

Choudhury, Rajarshi, Thomas Bonacci, Xianxi Wang, Andrew Truong, Anthony Arceci, Yanqiong Zhang, Christine A. Mills, Jennifer L. Kernan, Pengda Liu, and Michael J. Emanuele. 2017. 'The E3 Ubiquitin Ligase SCF (Cyclin F) Transmits AKT Signaling to the Cell-Cycle Machinery'. *Cell Reports* 20 (13): 3212–22. https://doi.org/10.1016/J.CELREP.2017.08.099.

Chubachi, Shotaro, Hiroyuki Yasuda, Hidehiro Irie, Koichi Fukunaga, Katsuhiko Naoki, Kenzo Soejima, and Tomoko Betsuyaku. 2016. 'A Case of Non-Small Cell Lung Cancer with Possible "Disease Flare" on Nivolumab Treatment'. *Case Reports in Oncological Medicine* 2016: 1–3. https://doi.org/10.1155/2016/1075641.

Concha-Benavente, Fernando, Raghvendra M. Srivastava, Sumita Trivedi, Yu Lei, Uma Chandran, Raja R. Seethala, Gordon J. Freeman, and Robert L. Ferris. 2016. 'Identification of the Cell-Intrinsic and -Extrinsic Pathways Downstream of

EGFR and IFNγ That Induce PD-L1 Expression in Head and Neck Cancer'. *Cancer Research* 76 (5): 1031–43. https://doi.org/10.1158/0008-5472.CAN-15-2001.

Courtney, Adam H., Wan Lin Lo, and Arthur Weiss. 2018. 'TCR Signaling: Mechanisms of Initiation and Propagation'. *Trends in Biochemical Sciences*. https://doi.org/10.1016/j.tibs.2017.11.008.

Culp, William T. N., Robert B. Rebhun, Elysia M. Alvarez, Marcio M. Malogolowkin, R. Lor Randall, and Steven W. Thorpe. 2020. 'Canine Osteosarcoma: Where Human and Canine Research Intersect'. *Annals of Joint* 5 (July): 30–30. https://doi.org/10.21037/aoj.2019.11.03.

Da, Lewis, and T Ly. 2021. 'Cell Cycle Entry Control in Naïve and Memory CD8 + T Cells'. *Cell Cycle Entry Control in Naïve and Memory CD8 + T Cells. Front. Cell Dev. Biol* 9: 727441. https://doi.org/10.3389/fcell.2021.727441.

Dahan, Rony, Emanuela Sega, John Engelhardt, Mark Selby, Alan J. Korman, and Jeffrey V. Ravetch. 2015. 'FcγRs Modulate the Anti-Tumor Activity of Antibodies Targeting the PD-1/PD-L1 Axis'. *Cancer Cell* 28 (3): 285–95. https://doi.org/10.1016/j.ccell.2015.08.004.

Danen, Erik H.J., and Arnoud Sonnenberg. 2003. 'Integrins in Regulation of Tissue Development and Function'. *The Journal of Pathology* 200 (4): 471–80. https://doi.org/10.1002/PATH.1416.

Daniel E Shumer, Natalie J Nokoff Norman P Spack. 2017. 'Significance of Talin in Cancer Progression and Metastasis Andreas'. *Physiology & Behavior* 176 (12): 139–48. https://doi.org/10.1016/B978-0-12-386039-2.00004-3.Significance.

Denis, Morgane, Michael Duruisseaux, Marie Brevet, and Charles Dumontet. 2020. 'How Can Immune Checkpoint Inhibitors Cause Hyperprogression in Solid Tumors?' *Frontiers in Immunology*. https://doi.org/10.3389/fimmu.2020.00492.

DeSouza, Nikhil, Jie Cui, Miroslav Dura, Thomas V. McDonald, and Andrew R. Marks. 2007. 'A Function for Tyrosine Phosphorylation of Type 1 Inositol 1,4,5-

Trisphosphate Receptor in Lymphocyte Activation'. *The Journal of Cell Biology* 179 (5): 923–34.
https://doi.org/10.1083/JCB.200708200.

Deutsch, Eric W., Luis Mendoza, David Shteynberg, Terry Farrah, Henry Lam, Natalie Tasman, Zhi Sun, et al. 2010. 'A Guided Tour of the Trans-Proteomic Pipeline'. *Proteomics* 10 (6): 1150–59.
https://doi.org/10.1002/PMIC.200900375.

Du, Shisuo, Neal McCall, Kyewon Park, Qing Guan, Paolo Fontina, Adam Ertel, Tingting Zhan, Adam P. Dicker, and Bo Lu. 2018. 'Blockade of Tumor-Expressed PD-1 Promotes Lung Cancer Growth'. *OncoImmunology* 7 (4).
https://doi.org/10.1080/2162402X.2017.1408747.

Dupree, Emmalyn J., Madhuri Jayathirtha, Hannah Yorkey, Marius Mihasan, Brindusa Alina Petre, and Costel C. Darie. 2020. 'A Critical Review of Bottom-Up Proteomics: The Good, the Bad, and the Future of This Field'. *Proteomes 2020, Vol. 8, Page 14* 8 (3): 14.
https://doi.org/10.3390/PROTEOMES8030014.

Elkabets, Moshe, Evangelos Pazarentzos, Dejan Juric, Qing Sheng, Raphael A. Pelossof, Samuel Brook, Ana Oaknin Benzaken, et al. 2015. 'AXL Mediates Resistance to PI3Kα Inhibition by Activating the EGFR/PKC/MTOR Axis in Head and Neck and Esophageal Squamous Cell Carcinomas'. *Cancer Cell* 27 (4): 533. https://doi.org/10.1016/J.CCELL.2015.03.010.

Fenger, Joelle M., Cheryl A. London, and William C. Kisseberth. 2014. 'Canine Osteosarcoma: A Naturally Occurring Disease to Inform Pediatric Oncology'. *ILAR Journal* 55 (1): 69–85.
https://doi.org/10.1093/ilar/ilu009.

Ferragut, Fátima, Vanina S Vachetta, María F Troncoso, Gabriel A Rabinovich, and María T Elola. 2021. 'ALCAM/CD166: A Pleiotropic Mediator of Cell Adhesion, Stemness and Cancer Progression'. *Cytokine and Growth Factor Reviews* 61: 27–37.
https://doi.org/10.1016/j.cytogfr.2021.07.001.

Fortner, Andra, Alexandra Chera, Antoanela Tanca, and Octavian Bucur. 2022. ‘Apoptosis Regulation by the Tyrosine-Protein Kinase CSK’. https://doi.org/10.3389/fcell.2022.1078180.

Francisco, Loise M., Peter T. Sage, and Arlene H. Sharpe. 2010. ‘The PD-1 Pathway in Tolerance and Autoimmunity’. *Immunological Reviews*. https://doi.org/10.1111/j.1600-065X.2010.00923.x.

Frauwirth, Kenneth A, James L Riley, Marian H Harris, Richard V Parry, Jeffrey C Rathmell, David R Plas, Rebecca L Elstrom, Carl H June, and Craig B Thompson. 2002. ‘The CD28 Signaling Pathway Regulates Glucose Metabolism Ability of Resting Cells to Take up and Utilize Nutrients at Levels Sufficient to Maintain Viability. *Immunity*. Vol. 16.

Frauwirth, Kenneth A, and Craig B Thompson. 2004. ‘Regulation of T Lymphocyte Metabolism’. *The Journal of Immunology* 172: 4661–65. http://journals.aai.org/jimmunol/article-pdf/172/8/4661/1177351/4661.pdf.

Galon, Jérôme, and Daniela Bruni. 2019. ‘Approaches to Treat Immune Hot, Altered and Cold Tumours with Combination Immunotherapies’. *Nature Reviews Drug Discovery*. Nature Publishing Group. https://doi.org/10.1038/s41573-018-0007-y.

Gan, Fanyi, Chuanfen Zhang, Liang Xia, and Senyi Deng. 2022. ‘Tumor-Endogenous PD-1 Promotes Cell Proliferation and Predicts Poor Survival in Non-Small Cell Lung Cancer’. *Translational Cancer Research* 11 (1): 3–13. https://doi.org/10.21037/TCR-21-1644/COIF).

Gao, Song, Anqi Ge, Shouping Xu, Zilong You, Shipeng Ning, Yashuang Zhao, and Da Pang. 2017. ‘PSAT1 Is Regulated by ATF4 and Enhances Cell Proliferation via the GSK3β/β-Catenin/Cyclin D1 Signaling Pathway in ER-Negative Breast Cancer’. *Journal of Experimental and Clinical Cancer Research* 36 (1). https://doi.org/10.1186/s13046-017-0648-4.

Garçon, Fabien, Daniel T Patton, Juliet L Emery, Emilio Hirsch, Robert Rottapel, Takehiko Sasaki, and Klaus Okkenhaug. 2008. ‘CD28 Provides T-Cell Costimulation and Enhances PI3K Activity at the Immune Synapse Independently of Its Capacity to Interact with the P85/P110 Heterodimer. https://doi.org/10.1182/blood.

Garon, Edward B., Naiyer A. Rizvi, Rina Hui, Natasha Leighl, Ani S. Balmanoukian, Joseph Paul Eder, Amita Patnaik, et al. 2015. 'Pembrolizumab for the Treatment of Non–Small-Cell Lung Cancer'. *New England Journal of Medicine* 372 (21): 2018–28. https://doi.org/10.1056/nejmoa1501824.

Gaud, Guillaume, Renaud Lesourne, and Paul E. Love. 2018. 'Regulatory Mechanisms in T Cell Receptor Signalling'. *Nature Reviews Immunology*. Nature Publishing Group. https://doi.org/10.1038/s41577-018-0020-8.

Gavali, Shubhangi, Jianing Liu, Xinyi Li, and Magdalena Paolino. 2021. 'Ubiquitination in T-Cell Activation and Checkpoint Inhibition: New Avenues for Targeted Cancer Immunotherapy'. *Molecular Sciences* 22. https://doi.org/10.3390/ijms221910800.

Gay, Carl M., Kavitha Balaji, and Lauren Averett Byers. 2017. 'Giving AXL the Axe: Targeting AXL in Human Malignancy'. *British Journal of Cancer 2017 116:4* 116 (4): 415–23. https://doi.org/10.1038/bjc.2016.428.

Gazon, Hélène, Benoit Barbeau, Jean Michel Mesnard, and Jean Marie Peloponese. 2018. 'Hijacking of the AP-1 Signaling Pathway during Development of ATL'. *Frontiers in Microbiology*. Frontiers Media S.A. https://doi.org/10.3389/fmicb.2017.02686.

Gong, Jun, Alexander Chehrazi-Raffle, Srikanth Reddi, and Ravi Salgia. 2018. 'Development of PD-1 and PD-L1 Inhibitors as a Form of Cancer Immunotherapy: A Comprehensive Review of Registration Trials and Future Considerations'. *Journal for ImmunoTherapy of Cancer*. https://doi.org/10.1186/s40425-018-0316-z.

Goyette, Marie Anne, Stéphanie Duhamel, Léo Aubert, Ariane Pelletier, Paul Savage, Marie Pier Thibault, Radia Marie Johnson, et al. 2018. 'The Receptor Tyrosine Kinase AXL Is Required at Multiple Steps of the Metastatic Cascade during HER2-Positive Breast Cancer Progression'. *Cell Reports* 23 (5): 1476–90. https://doi.org/10.1016/j.celrep.2018.04.019.

Goyette, Marie Anne, Islam E. Elkholi, Chloé Apcher, Hellen Kuasne, Carla V. Rothlin, William J. Muller, Darren E. Richard, Morag Park, Jean Philippe Gratton, and Jean François Côté. 2021. 'Targeting Axl Favors an Antitumorigenic Microenvironment That Enhances Immunotherapy Responses by Decreasing Hif-1α Levels'. *Proceedings of the National Academy of Sciences of the United States of America* 118 (29).
https://doi.org/10.1073/PNAS.2023868118/-/DCSUPPLEMENTAL.

Gregg, Randal K. 2021. 'Implications of Microgravity-Induced Cell Signaling Alterations upon Cancer Cell Growth, Invasiveness, Metastatic Potential, and Control by Host Immunity'. *International Review of Cell and Molecular Biology* 361 (January): 107–64.
https://doi.org/10.1016/bs.ircmb.2021.01.004.

Guo, Wenjun, and Filippo G. Giancotti. 2004. 'Integrin Signalling during Tumour Progression'. *Nature Reviews Molecular Cell Biology*. https://doi.org/10.1038/nrm1490.

Gutwillig, Amit, Nadine Santana-Magal, Leen Farhat-Younis, Diana Rasoulouniriana, Asaf Madi, Chen Luxenburg, Jonathan Cohen, et al. 2022. 'Transient Cell-in-Cell Formation Underlies Tumor Relapse and Resistance to Immunotherapy'. *ELife* 11.
https://doi.org/10.7554/ELIFE.80315.

Han, Dunxin, Mingming Wang, Zhongkai Yu, Long Yin, Changli Liu, Jianmin Wang, Yongjun Liu, Shengyang Jiang, Zhongwu Ren, and Jun Yin. 2019. 'FGF5 Promotes Osteosarcoma Cells Proliferation via Activating MAPK Signaling Pathway'. *Cancer Management and Research* 11: 6457–66.
https://doi.org/10.2147/CMAR.S200234.

Harper, Megan M., Miranda Lin, Michael J. Cavnar, Prakash K. Pandalai, Reema A. Patel, Mei Gao, and Joseph Kim. 2022. 'Interaction of Immune Checkpoint PD-1 and Chemokine Receptor 4 (CXCR4) Promotes a Malignant Phenotype in Pancreatic Cancer Cells'. *PloS One* 17 (7).
https://doi.org/10.1371/JOURNAL.PONE.0270832.

Hashimoto, Kazuhiko, Shunji Nishimura, and Masao Akagi. 2020. 'Characterization of PD-1/PD-L1 Immune Checkpoint Expression in Osteosarcoma'. *Diagnostics* 10 (8).
https://doi.org/10.3390/diagnostics10080528.

He, Shuai, Shirong Li, Jing Guo, Xiaozhu Zeng, Dandan Liang, Yongjie Zhu, Yi Li, Dong Yang, and Xudong Zhao. 2023. 'CD166-Specific CAR-T Cells Potently Target Colorectal Cancer Cells'. *Translational Oncology* 27: 1936–5233.
https://doi.org/10.1016/j.tranon.2022.101575.

Herbst, Roy S, Jean-Charles Soria, Marcin Kowanetz, Gregg D Fine, Omid Hamid, Michael S Gordon, Jeffery A Sosman, et al. 2014. 'Predictive Correlates of Response to the Anti-PD-L1 Antibody MPDL3280A in Cancer Patients HHS Public Access'. *Nature* 515 (7528): 563–67.
https://doi.org/10.1038/nature14011.

Herrero-Sánchez, M. Carmen, Concepción Rodríguez-Serrano, Julia Almeida, Laura San Segundo, Susana Inogés, Ángel Santos-Briz, Jesús García-Briñón, et al. 2016. 'Targeting of PI3K/AKT/MTOR Pathway to Inhibit T Cell Activation and Prevent Graft-versus-Host Disease Development'. *Journal of Hematology and Oncology* 9 (1).
https://doi.org/10.1186/s13045-016-0343-5.

Hinz, Andreas, Johanna Jedamzick, Valentina Herbring, Hanna Fischbach, Jessica Hartmann, David Parcej, Joachim Koch, and Robert Tampé. 2014. 'Assembly and Function of the Major Histocompatibility Complex (MHC) I Peptide-Loading Complex Are Conserved across Higher Vertebrates'. *Journal of Biological Chemistry* 289 (48): 33109–17.
https://doi.org/10.1074/jbc.M114.609263.

Hodi, F Stephen, Wen-Jen Hwu, Richard Kefford, Jeffrey S Weber, Adil Daud, Omid Hamid, Amita Patnaik, et al. 2016. 'JOURNAL OF CLINICAL ONCOLOGY Evaluation of Immune-Related Response Criteria and RECIST v1.1 in Patients With Advanced Melanoma Treated With Pembrolizumab.
https://doi.org/10.1200/JCO.2015.64.0391.

Hogan, Patrick G. 2017. ‘Calcium-NFAT Transcriptional Signalling in T Cell Activation and T Cell Exhaustion HHS Public Access’. *Cell Calcium* 63: 66–69. https://doi.org/10.1016/j.ceca.2017.01.014.

Huang, Weishan, and Avery August. 2015. ‘The Signaling Symphony: T Cell Receptor Tunes Cytokine-Mediated T Cell Differentiation’. *Journal of Leukocyte Biology* 97 (3): 477–85. https://doi.org/10.1189/jlb.1ri0614-293r.

Hudson, Katie, Neil Cross, Nicola Jordan-Mahy, and Rebecca Leyland. 2020. ‘The Extrinsic and Intrinsic Roles of PD-L1 and Its Receptor PD-1: Implications for Immunotherapy Treatment’. *Frontiers in Immunology* 11 (October): 568931. https://doi.org/10.3389/FIMMU.2020.568931.

Hui, Enfu, Jeanne Cheung, Jing Zhu, Xiaolei Su, Marcus J. Taylor, Heidi A. Wallweber, Dibyendu K. Sasmal, et al. 2017. ‘T Cell Costimulatory Receptor CD28 Is a Primary Target for PD-1-Mediated Inhibition’. *Science* 355 (6332): 1428–33. https://doi.org/10.1126/science.aaf1292.

Hulsen, Tim. 2022. ‘DeepVenn-a Web Application for the Creation of Area-Proportional Venn Diagrams Using the Deep Learning Framework Tensorflow.Js’. *ArXiv*. https://doi.org/https://doi.org/10.48550/arXiv.2210.04597.

Hytönen, Marjo K., and Hannes Lohi. 2016. ‘Canine Models of Human Rare Disorders’. *Rare Diseases* 4 (1): e1241362. https://doi.org/10.1080/21675511.2016.1241362.

Ieranò, Caterina, Dario Righelli, Crescenzo D’Alterio, Maria Napolitano, Luigi Portella, Giuseppina Rea, Federica Auletta, et al. 2022. ‘In PD-1+ Human Colon Cancer Cells NIVOLUMAB Promotes Survival and Could Protect Tumor Cells from Conventional Therapies’. *Journal for Immunotherapy of Cancer* 10 (3). https://doi.org/10.1136/JITC-2021-004032.

Ikemizu, Shinji, Robert J C Gilbert, Janet A Fennelly, Alison V Collins, Karl Harlos, ‡ E Yvonne Jones, and David I Stuart. 2000. ‘Structure and Dimerization of a Soluble Form of B7-1 Transfecting B7-1 into Murine Tumors (Chen et al or from Using Anti-CTLA-4 Antibodies to Block CTLA-4 Interactions with B7-1 And’. *Immunity* 12: 51–60.

Inoki, Ken, Yong Li, Tianquan Zhu, Jun Wu, and Kun Liang Guan. 2002. 'TSC2 Is Phosphorylated and Inhibited by Akt and Suppresses MTOR Signalling'. *Nature Cell Biology* 4 (9): 648–57. https://doi.org/10.1038/ncb839.

Ishida, Yasumasa, Yasutoshi Agata, Keiichi Shibahara, T. Honjo, and Tasuku Honjo1. 1992. 'Induced Expression of PD-1, a Novel Member of the Immunoglobulin Gene Superfamily, upon Programmed Cell Death'. *EMBO Journal* 11 (11): 3887–95. https://doi.org/10.1002/j.1460-2075.1992.tb05481.x.

Jemal, Ahmedin, Elizabeth M. Ward, Christopher J. Johnson, Kathleen A. Cronin, Jiemin Ma, A. Blythe Ryerson, Angela Mariotto, et al. 2017. 'Annual Report to the Nation on the Status of Cancer, 1975-2014, Featuring Survival'. *Journal of the National Cancer Institute*. Oxford University Press. https://doi.org/10.1093/jnci/djx030.

Jiang, L. Q., X. Feng, W. Zhou, P. G. Knyazev, A. Ullrich, and Z. Chen. 2006. 'Csk-Binding Protein (Cbp) Negatively Regulates Epidermal Growth Factor-Induced Cell Transformation by Controlling Src Activation'. *Oncogene* 25 (40): 5495–5506. https://doi.org/10.1038/SJ.ONC.1209554.

Kalantari, Elham, Tahereh Taheri, Saba Fata, Maryam Abolhasani, Mitra Mehrazma, Zahra Madjd, and Mojgan Asgari. 2022. 'Significant Co-Expression of Putative Cancer Stem Cell Markers, EpCAM and CD166, Correlates with Tumor Stage and Invasive Behavior in Colorectal Cancer'. *World Journal of Surgical Oncology* 20 (1): 1–11. https://doi.org/10.1186/S12957-021-02469-Y/TABLES/3.

Kamada, Takahiro, Yosuke Togashi, Christopher Tay, Danbee Ha, Akinori Sasaki, Yoshiaki Nakamura, Eiichi Sato, et al. 2019. 'PD-1+ Regulatory T Cells Amplified by PD-1 Blockade Promote Hyperprogression of Cancer'. *Proceedings of the National Academy of Sciences of the United States of America* 116 (20): 9999–10008. https://doi.org/10.1073/pnas.1822001116.

Kang, Da Hyun, Chaeuk Chung, Pureum Sun, Da Hye Lee, Song I. Lee, Dongil Park, Jeong Suk Koh, Yoonjoo Kim, Hyon Seung Yi, and Jeong Eun Lee. 2022. 'Circulating Regulatory T Cells Predict Efficacy and Atypical Responses in Lung

Cancer Patients Treated with PD-1/PD-L1 Inhibitors'. *Cancer Immunology, Immunotherapy* 71 (3): 579–88. https://doi.org/10.1007/s00262-021-03018-y.

Kao, Charlly, Kenneth J. Oestreich, Michael A. Paley, Alison Crawford, Jill M. Angelosanto, Mohammed Alkhatim A. Ali, Andrew M. Intlekofer, et al. 2011. 'Transcription Factor T-Bet Represses Expression of the Inhibitory Receptor PD-1 and Sustains Virus-Specific CD8+ T Cell Responses during Chronic Infection'. *Nature Immunology* 12 (7): 663–71. https://doi.org/10.1038/ni.2046.

Kappler, John W, Neal Roehm, and Philippa Marrack. 1987. 'T Cell Tolerance by Clonal Elimination in the Thymus'. *Cell*. Vol. 49.

Karpievitch, Yuliya V., Ashoka D. Polpitiya, Gordon A. Anderson, Richard D. Smith, and Alan R. Dabney. 2010. 'Liquid Chromatography Mass Spectrometry-Based Proteomics: Biological and Technological Aspects'. *The Annals of Applied Statistics* 4 (4): 1797. https://doi.org/10.1214/10-AOAS341.

Kato, Shumei, Aaron Goodman, Vighnesh Walavalkar, Donald A. Barkauskas, Andrew Sharabi, and Razelle Kurzrock. 2017. 'Hyperprogressors after Immunotherapy: Analysis of Genomic Alterations Associated with Accelerated Growth Rate'. *Clinical Cancer Research* 23 (15): 4242–50. https://doi.org/10.1158/1078-0432.CCR-16-3133.

Keller, Andrew, Alexey I. Nesvizhskii, Eugene Kolker, and Ruedi Aebersold. 2002. 'Empirical Statistical Model to Estimate the Accuracy of Peptide Identifications Made by MS/MS and Database Search'. *Analytical Chemistry* 74 (20): 5383–92. https://doi.org/10.1021/ac025747h.

Khanna, Chand, Cheryl London, David Vail, Christina Mazcko, and Steven Hirschfeld. 2009. 'Guiding the Optimal Translation of New Cancer Treatments from Canine to Human Cancer Patients'. *Clinical Cancer Research*. https://doi.org/10.1158/1078-0432.CCR-09-0719.

Kim, Dae Kyoung, Min Hee Ham, Seo Yul Lee, Min Joo Shin, Ye Eun Kim, Parkyong Song, Dong Soo Suh, and Jae Ho Kim. 2020. 'CD166 Promotes the Cancer Stem-

like Properties of Primary Epithelial Ovarian Cancer Cells'. *BMB Reports* 53 (12): 622–27.
https://doi.org/10.5483/BMBRep.2020.53.12.102.

Kim, Hojin, Gong-Rak Lee, Jiwon Kim, Jin Young Baek, You-Jin Jo, Seong-Eun Hong, Sung Hoon Kim, et al. 2015. 'Sulfiredoxin Inhibitor Induces Preferential Death of Cancer Cells through Reactive Oxygen Species-Mediated Mitochondrial Damage'.
https://doi.org/10.1016/j.freeradbiomed.2015.12.023.

Kleffel, Sonja, Christian Posch, Steven R Barthel, Arlene H Sharpe, Thomas S Kupper, and Tobias Schatton Correspondence. 2015. 'Melanoma Cell-Intrinsic PD-1 Receptor Functions Promote Tumor Growth'. *Cell* 162.
https://doi.org/10.1016/j.cell.2015.08.052.

Kocikowski, Mikolaj, Katarzyna Dziubek, and Maciej Parys. 2020. 'Hyperprogression Under Immune Checkpoint-Based Immunotherapy-Current Understanding, The Role of PD-1/PD-L1 Tumour-Intrinsic Signalling, Future Directions and a Potential Large Animal Model'. *Cancers* 12 (4).
https://doi.org/10.3390/CANCERS12040804.

Koirala, Pratistha, Michael E. Roth, Jonathan Gill, Sajida Piperdi, Jordan M. Chinai, David S. Geller, Bang H. Hoang, et al. 2016. 'Immune Infiltration and PD-L1 Expression in the Tumor Microenvironment Are Prognostic in Osteosarcoma'. *Scientific Reports* 6 (July).
https://doi.org/10.1038/srep30093.

Konen, Jessica M., B. Leticia Rodriguez, Aparna Padhye, Joshua K. Ochieng, Laura Gibson, Lixia Diao, Natalie W. Fowlkes, et al. 2021. 'Dual Inhibition of MEK and AXL Targets Tumor Cell Heterogeneity and Prevents Resistant Outgrowth Mediated by the Epithelial-to-Mesenchymal Transition in NSCLC'. *Cancer Research* 81 (5): 1398–1412.
https://doi.org/10.1158/0008-5472.CAN-20-1895.

Kreiner, Grzegorz, Ana Raquel Santiago, Sassan Hafizi, Shannon E Gilchrist, and Salman Goudarzi. 2020. 'Gas6 Inhibits Toll-Like Receptor-Mediated Inflammatory Pathways in Mouse Microglia via Axl and Mer Gas6 Inhibition of Inflammatory

Pathways'. *Frontiers in Cellular Neuroscience*. https://doi.org/10.3389/fncel.2020.576650.

Krummel, Matthew F., and James P. Allison. 1995. 'CD28 and CTLA-4 Have Opposing Effects on the Response of T Cells to Stimulation'. *The Journal of Experimental Medicine* 182 (2): 459. https://doi.org/10.1084/JEM.182.2.459.

Kunz, Pierre, Astrid Schenker, Heiner Sä hr, Burkhard Lehner, Jö ID rg Fellenberg, Heiner Sähr, Burkhard Lehner, and Jörg Fellenberg. 2019. 'Optimization of the Chicken Chorioallantoic Membrane Assay as Reliable in Vivo Model for the Analysis of Osteosarcoma'. *PLoS ONE* 14 (4): e0215312. https://doi.org/10.1371/journal.pone.0215312.

Lai, Ching Fang, Chih Ying Chen, and Lo Chun Au. 2013. 'Comparison between the Repression Potency of SiRNA Targeting the Coding Region and the 3′-Untranslated Region of MRNA'. *BioMed Research International* 2013. https://doi.org/10.1155/2013/637850.

Laird, Renee M., and Sandra M. Hayes. 2010. 'Roles of the Src Tyrosine Kinases Lck and Fyn in Regulating ΓδTCR Signal Strength'. *PLOS ONE* 5 (1): e8899. https://doi.org/10.1371/JOURNAL.PONE.0008899.

Lassman, Michael E., Derek L. Chappell, Thomas McAvoy, Amy Cheng, Dinesh P. de Alwis, Scott K. Pruitt, Omar F. Laterza, Claire Li, Aubrey Stoch, and Kapil Mayawala. 2021. 'Experimental Medicine Study to Measure Immune Checkpoint Receptors PD-1 and GITR Turnover Rates In Vivo in Humans'. *Clinical Pharmacology and Therapeutics* 109 (6): 1575–82. https://doi.org/10.1002/cpt.2129.

Lee, Jii Bum, Hye Ryun Kim, and Sang Jun Ha. 2022. 'Immune Checkpoint Inhibitors in 10 Years: Contribution of Basic Research and Clinical Application in Cancer Immunotherapy'. *Immune Network*. Korean Association of Immunologists. https://doi.org/10.4110/in.2022.22.e2.

Lehmann, Jurgen M, Gert Riethmuller, and Judith P Johnsont. 1989. 'MUC18, a Marker of Tumor Progression in Human Melanoma, Shows Sequence Similarity to the Neural Cell Adhesion Molecules of the Immunoglobulin Superfamily'. *Proc. Nati. Acad. Sci. USA* 86: 9891–95.

https://www.pnas.org.

Li, Chia Wei, Seung Oe Lim, Weiya Xia, Heng Huan Lee, Li Chuan Chan, Chu Wei Kuo, Kay Hooi Khoo, et al. 2016. 'Glycosylation and Stabilization of Programmed Death Ligand-1 Suppresses T-Cell Activity'. *Nature Communications* 7 (August). https://doi.org/10.1038/ncomms12632.

Li, Hanxiao, P. Anton van der Merwe, and Shivan Sivakumar. 2022. 'Biomarkers of Response to PD-1 Pathway Blockade'. *British Journal of Cancer 2022 126:12* 126 (12): 1663–75.
https://doi.org/10.1038/s41416-022-01743-4.

Li, Hui, Xiaoqiang Li, Shuang Liu, Lei Guo, Bo Zhang, Jubo Zhang, and Qinghai Ye. 2017. 'Programmed Cell Death-1 (PD-1) Checkpoint Blockade in Combination with a Mammalian Target of Rapamycin Inhibitor Restrains Hepatocellular Carcinoma Growth Induced by Hepatoma Cell–Intrinsic PD-1'. *Hepatology* 66 (6): 1920–33.
https://doi.org/10.1002/hep.29360.

Li, Huiyu, Zhida Liu, Longchao Liu, Hongyi Zhang, Chuanhui Han, Luc Girard, Hyunsil Park, et al. 2022. 'AXL Targeting Restores PD-1 Blockade Sensitivity of STK11/LKB1 Mutant NSCLC through Expansion of TCF1+ CD8 T Cells'. *Cell Reports Medicine* 3 (3).
https://doi.org/10.1016/J.XCRM.2022.100554.

Li, Yong, Michael N. Corradetti, Ken Inoki, and Kun Liang Guan. 2004. 'TSC2: Filling the GAP in the MTOR Signaling Pathway'. *Trends in Biochemical Sciences*.
https://doi.org/10.1016/j.tibs.2003.11.007.

Liang, Chun Chi, Ann Y. Park, and Jun Lin Guan. 2007. 'In Vitro Scratch Assay: A Convenient and Inexpensive Method for Analysis of Cell Migration in Vitro'. *Nature Protocols 2007 2:2* 2 (2): 329–33.
https://doi.org/10.1038/nprot.2007.30.

Liao, Kuang Ming, Tung Bo Chao, Yu Feng Tian, Ching Yih Lin, Sung Wei Lee, Hua Ying Chuang, Ti Chun Chan, et al. 2016. 'Overexpression of the PSAT1 Gene in Nasopharyngeal Carcinoma Is an Indicator of Poor Prognosis'. *Journal of Cancer* 7 (9): 1088–94.

https://doi.org/10.7150/jca.15258.

Liberti, Maria V, and Jason W Locasale. 2016. 'The Warburg Effect: How Does It Benefit Cancer Cells? HHS Public Access'. *Trends Biochem Sci* 41 (3): 211–18. https://doi.org/10.1016/j.tibs.2015.12.001.

Liotti, Federica, Narender Kumar, Nella Prevete, Maria Marotta, Daniela Sorriento, Caterina Ieranò, Andrea Ronchi, et al. 2021. 'PD-1 Blockade Delays Tumor Growth by Inhibiting an Intrinsic SHP2/Ras/MAPK Signalling in Thyroid Cancer Cells'. *Journal of Experimental & Clinical Cancer Research: CR* 40 (1). https://doi.org/10.1186/S13046-020-01818-1.

Lipson, Evan J., and Charles G. Drake. 2011. 'Ipilimumab: An Anti-CTLA-4 Antibody for Metastatic Melanoma'. *Clinical Cancer Research: An Official Journal of the American Association for Cancer Research* 17 (22): 6958. https://doi.org/10.1158/1078-0432.CCR-11-1595.

Liu, Chang, Xiaoyan Xu, Lei Han, Xiaopeng Wan, Lingming Zheng, Chunyang Li, Zhaohui Liao, et al. 2020. 'LRCH1 Deficiency Enhances LAT Signalosome Formation and CD8 + T Cell Responses against Tumors and Pathogens'. *Proceedings of the National Academy of Sciences* 117 (32): 19388–98. https://doi.org/10.1073/pnas.2000970117/-/DCSupplemental.

Liu, Ching Ann, Horng Jyh Harn, Kuan Pin Chen, Jui Hao Lee, Shinn Zong Lin, and Tsung Lang Chiu. 2022. 'Targeting the Axl and MTOR Pathway Synergizes Immunotherapy and Chemotherapy to Butylidenephthalide in a Recurrent GBM'. *Journal of Oncology* 2022. https://doi.org/10.1155/2022/3236058.

Liu, Fange, Imran Rehmani, Shingo Esaki, Rong Fu, Lirong Chen, Vesna De Serrano, and Aimin Liu. 2013. 'Pirin Is an Iron-Dependent Redox Regulator of NF-KB'. *Proceedings of the National Academy of Sciences of the United States of America* 110 (24): 9722–27. https://doi.org/10.1073/PNAS.1221743110/-/DCSUPPLEMENTAL/PNAS.201221743SI.PDF.

Liu, Jinhua, Zichao Chen, Yaqun Li, Wenjie Zhao, Ji Biao Wu, and Zhen Zhang. 2021. 'PD-1/PD-L1 Checkpoint Inhibitors in Tumor Immunotherapy'. *Frontiers in*

Pharmacology 12 (September): 2339. https://doi.org/10.3389/FPHAR.2021.731798/BIBTEX.

Lokhande, Kiran Bharat, Ashish Shrivastava, and Ashutosh Singh. 2023. 'In Silico Discovery of Potent Inhibitors against Monkeypox's Major Structural Proteins'. *Journal of Biomolecular Structure and Dynamics*, 1–16. https://doi.org/10.1080/07391102.2023.2183342.

Lokman, Noor A., Alison S.F. Elder, Carmela Ricciardelli, and Martin K. Oehler. 2012. 'Chick Chorioallantoic Membrane (CAM) Assay as an In Vivo Model to Study the Effect of Newly Identified Molecules on Ovarian Cancer Invasion and Metastasis'. *International Journal of Molecular Sciences* 13 (8): 9959. https://doi.org/10.3390/IJMS13089959.

Long, Yiru, Xiaolu Yu, Runqiu Chen, Yongliang Tong, and Likun Gong. 2022. 'Noncanonical PD-1/PD-L1 Axis in Relation to the Efficacy of Anti-PD Therapy'. *Frontiers in Immunology* 13 (May). https://doi.org/10.3389/FIMMU.2022.910704.

Lu, Fan, Liang Zhu, Thomas Bromberger, Jun Yang, Qiannan Yang, Jianmin Liu, Edward F Plow, Markus Moser, and Jun Qin. 2022. 'Mechanism of Integrin Activation by Talin and Its Cooperation with Kindlin'. *Nature Communications* 13 (2362). https://doi.org/10.1038/s41467-022-30117-w.

Lu, Qingxian, and Greg Lemke. 2001. 'Homeostatic Regulation of the Immune System by Receptor Tyrosine of the Tyro 3 Family'. *Science* 293: 306–11. https://doi.org/10.1126/science.1061663.

Lu, Yubao, Jiahe Zhang, Yutong Chen, Yuchen Kang, Zhipeng Liao, Yuanqi He, and Cangyu Zhang. 2022. 'Novel Immunotherapies for Osteosarcoma'. *Frontiers in Oncology* 12 (April): 1084. https://doi.org/10.3389/FONC.2022.830546/BIBTEX.

Majidpoor, Jamal, and Keywan Mortezaee. 2021. 'The Efficacy of PD-1/PD-L1 Blockade in Cold Cancers and Future Perspectives'. *Clinical Immunology* 226 (May): 108707. https://doi.org/10.1016/J.CLIM.2021.108707.

Maleki Vareki, Saman. 2018. ‘High and Low Mutational Burden Tumors versus Immunologically Hot and Cold Tumors and Response to Immune Checkpoint Inhibitors’. *Journal for ImmunoTherapy of Cancer*. https://doi.org/10.1186/s40425-018-0479-7.

Manifava, Maria, Matthew Smith, Sergio Rotondo, Simon Walker, Izabella Niewczas, Roberto Zoncu, Jonathan Clark, and Nicholas T Ktistakis. 2016. ‘Dynamics of MTORC1 Activation in Response to Amino Acids. https://doi.org/10.7554/eLife.19960.001.

Maniscalco, Lorella. 2015. ‘Canine Osteosarcoma: Understanding Its Variability to Improve Treatment’. *Veterinary Journal*. https://doi.org/10.1016/j.tvjl.2014.12.014.

Marasco, M., A. Berteotti, J. Weyershaeuser, N. Thorausch, J. Sikorska, J. Krausze, H. J. Brandt, et al. 2020. ‘Molecular Mechanism of SHP2 Activation by PD-1 Stimulation’. *Science Advances* 6 (5). https://doi.org/10.1126/SCIADV.AAY4458.

Mcgary, Eric C, Amy Heimberger, Lisa Mills, Kristy Weber, Gary W Thomas, Mikhail Shtivelband, Dina Chelouche Lev, and Menashe Bar-Eli. 2003. ‘A Fully Human Antimelanoma Cellular Adhesion Molecule/MUC18 Antibody Inhibits Spontaneous Pulmonary Metastasis of Osteosarcoma Cells In Vivo’. *Clinical Cancer Research* 9: 6560–66. http://aacrjournals.org/clincancerres/article-pdf/9/17/6560/2085359/zdf01703006560.pdf.

Megat, Salim, and Theodore J. Price. 2018. ‘Therapeutic Opportunities for Pain Medicines via Targeting of Specific Translation Signaling Mechanisms’. *Neurobiology of Pain*. Elsevier B.V. https://doi.org/10.1016/j.ynpai.2018.02.001.

Meng, Xiangbo, Xiwei Liu, Xingdong Guo, Shutan Jiang, Tingting Chen, Zhiqiang Hu, Haifeng Liu, et al. 2018. ‘FBXO38 Mediates PD-1 Ubiquitination and Regulates Anti-Tumour Immunity of T Cells’. *Nature* 564 (7734): 130–35. https://doi.org/10.1038/s41586-018-0756-0.

Mirzaei, Reza, Ashley Gordon, Franz J. Zemp, Mehul Kumar, Susobhan Sarkar, H. Artee Luchman, Anita C. Bellail, et al. 2021. ‘PD-1 Independent of PD-L1 Ligation

Promotes Glioblastoma Growth through the NFKB Pathway'. *Science Advances* 7 (45): 2148.
https://doi.org/10.1126/SCIADV.ABH2148.

Müller, Torsten, and Dominic Winter. 2017. 'Systematic Evaluation of Protein Reduction and Alkylation Reveals Massive Unspecific Side Effects by Iodine-Containing Reagents'. *Molecular & Cellular Proteomics : MCP* 16 (7): 1173.
https://doi.org/10.1074/MCP.M116.064048.

Na, Ki Yong, Youn Wha Kim, and Yong Koo Park. 2012. 'Mitogen-Activated Protein Kinase Pathway in Osteosarcoma'. *Pathology* 44 (6): 540–46.
https://doi.org/10.1097/PAT.0b013e32835803bc.

Nakayasu, Ernesto S., Marina Gritsenko, Paul D. Piehowski, Yuqian Gao, Daniel J. Orton, Athena A. Schepmoes, Thomas L. Fillmore, et al. 2021. 'Tutorial: Best Practices and Considerations for Mass-Spectrometry-Based Protein Biomarker Discovery and Validation'. *Nature Protocols*. Nature Research.
https://doi.org/10.1038/s41596-021-00566-6.

Nascimento, Emmani B.M., Marieke Snel, Bruno Guigas, Gerard C.M. van der Zon, Jan Kriek, J. Antonie Maassen, Ingrid M. Jazet, Michaela Diamant, and D. Margriet Ouwens. 2010. 'Phosphorylation of PRAS40 on Thr246 by PKB/AKT Facilitates Efficient Phosphorylation of Ser183 by MTORC1'. *Cellular Signalling* 22 (6): 961–67.
https://doi.org/10.1016/j.cellsig.2010.02.002.

Nielsen, Christian, Line Ohm-Laursen, Torben Barington, Steffen Husby, and Søren T. Lillevang. 2005. 'Alternative Splice Variants of the Human PD-1 Gene'. *Cellular Immunology* 235 (2): 109–16.
https://doi.org/10.1016/J.CELLIMM.2005.07.007.

Nishimura, Hiroyuki, Tasuku Honjo, and Nagahiro Minato. 2000. 'Facilitation of Selection and Modification of Positive Selection in the Thymus of PD-1-Deficient Mice'. *J. Exp. Med* 191 (5).
http://www.jem.org/cgi/current/full/191/5/891.

Nishimura, Hiroyuki, Masato Nose, Hiroshi Hiai, Nagahiro Minato, and Tasuku Honjo. 1999. 'Development of Lupus-like Autoimmune Diseases by Disruption of the PD-1 Gene Encoding an ITIM Motif-Carrying Immunoreceptor'. *Immunity*. Vol. 11.

Nurieva, Roza, Sunil Thomas, Thang Nguyen, Natalia Martin-Orozco, Ying Wang, Murali-Krishna Kaja, Xue-Zhong Yu, and Chen Dong. 2006. 'T-Cell Tolerance or Function Is Determined by Combinatorial Costimulatory Signals'. *The EMBO Journal* 25: 2623–33. https://doi.org/10.1038/sj.emboj.7601146.

Nyakas, Marta, Karianne Giller Fleten, Mads Haugland Haugen, Nikolai Engedal, Christina Sveen, Inger Nina Farstad, Vivi Ann Flørenes, Lina Prasmickaite, Gunhild Mari Maelandsmo, and Kotryna Seip. 2022. 'AXL Inhibition Improves BRAF-Targeted Treatment in Melanoma'. *Scientific Reports* 12 (5076). https://doi.org/10.1038/s41598-022-09078-z.

O'bryan, John P, Roy A Frye, Patricia C Cogswell, Andreas Neubauer, Barry Kitch, Carol Prokop, Rafael Espinosa Iii, Michelle M Le Beau, H Shelton Earp, and Edison T Liul. 1991. 'Axl, a Transforming Gene Isolated from Primary Human Myeloid Leukemia Cells, Encodes a Novel Receptor Tyrosine Kinase. *MOLECULAR AND CELLULAR BIOLOGY* 11 (10): 5016–31.

Oestreich, Kenneth J, Hyesuk Yoon, Rafi Ahmed, and Jeremy M Boss. 2008. 'NFATc1 Regulates Programmed Death-1 Expression Upon T Cell Activation 1'.

Okazaki, Taku, and Tasuku Honjo. 2007. 'PD-1 and PD-1 Ligands: From Discovery to Clinical Application'. *International Immunology*. https://doi.org/10.1093/intimm/dxm057.

Okazaki, Taku, Akito Maeda, Hiroyuki Nishimura, Tomohiro Kurosaki, and Tasuku Honjo. 2001. 'PD-1 Immunoreceptor Inhibits B Cell Receptor-Mediated Signaling by Recruiting Src Homology 2-Domain-Containing Tyrosine Phosphatase 2 to Phosphotyrosine'. *Proceedings of the National Academy of Sciences of the United States of America* 98 (24): 13866–71. https://doi.org/10.1073/PNAS.231486598/ASSET/6DCF43C9-7C9F-4E9D-93AD-CB8205AFD76F/ASSETS/GRAPHIC/PQ2314865005.JPEG.

Onken, Julia, Peter Vajkoczy, Robert Torka, Claudia Hempt, Victor Patsouris, Frank L Heppner, and Josefine Radke. 2017. 'Phospho-AXL Is Widely Expressed in Glioblastoma and Associated with Significant Shorter Overall Survival'. *Oncotarget*. Vol. 8. www.impactjournals.com/oncotarget/.

Pandey, Pratibha, Fahad Khan, Huda A. Qari, Tarun Kumar Upadhyay, Abdulhameed F. Alkhateeb, and Mohammad Oves. 2022. 'Revolutionization in Cancer Therapeutics via Targeting Major Immune Checkpoints PD-1, PD-L1 and CTLA-4'. *Pharmaceuticals* 15 (3): 1–16. https://doi.org/10.3390/ph15030335.

Park, Il Kyoo, Chiara Giovenzana, Tiffany L. Hughes, Jianhua Yu, Rossana Trotta, and Michael A. Caligiuri. 2009. 'The Axl/Gas6 Pathway Is Required for Optimal Cytokine Signaling during Human Natural Killer Cell Development'. *Blood* 113 (11): 2470–77. https://doi.org/10.1182/BLOOD-2008-05-157073.

Park, Jiwon S., Sita S. Withers, Jaime F. Modiano, Michael S. Kent, Mingyi Chen, Jesus I. Luna, William T.N. Culp, et al. 2016. 'Canine Cancer Immunotherapy Studies: Linking Mouse and Human'. *Journal for ImmunoTherapy of Cancer*. https://doi.org/10.1186/s40425-016-0200-7.

Park, Jungkap, Christopher Wilkins, Dmitry Avtonomov, Jiwon Hong, Seunghoon Back, Hokeun Kim, Nicholas Shulman, Brendan X. MacLean, Sang Won Lee, and Sangtae Kim. 2023. 'Targeted Proteomics Data Interpretation with DeepMRM'. *Cell Reports Methods* 3 (7). https://doi.org/10.1016/j.crmeth.2023.100521.

Parry, Richard V., Jens M. Chemnitz, Kenneth A. Frauwirth, Anthony R. Lanfranco, Inbal Braunstein, Sumire V. Kobayashi, Peter S. Linsley, Craig B. Thompson, and James L. Riley. 2005. 'CTLA-4 and PD-1 Receptors Inhibit T-Cell Activation by Distinct Mechanisms †'. *MOLECULAR AND CELLULAR BIOLOGY* 25 (21): 9543–53. https://doi.org/10.1128/MCB.25.21.9543-9553.2005.

Parsons, Sarah J., and J. Thomas Parsons. 2004. 'Src Family Kinases, Key Regulators of Signal Transduction'. *Oncogene*. https://doi.org/10.1038/sj.onc.1208160.

Patel, Rachna, Natacha Coppieters T'Wallant, Michael H. Herbert, Damian White, J. Greg Murison, and Glen Reid. 2009. 'The Potency of SiRNA-Mediated Growth Inhibition Following Silencing of Essential Genes Is Dependent on SiRNA Design

and Varies with Target Sequence'. *Oligonucleotides* 19 (4): 317–28. https://doi.org/10.1089/oli.2009.0207.

Patsoukis, Nikolaos, Kankana Bardhan, Pranam Chatterjee, Duygu Sari, Bianling Liu, Lauren N. Bell, Edward D. Karoly, et al. 2015. 'PD-1 Alters T-Cell Metabolic Reprogramming by Inhibiting Glycolysis and Promoting Lipolysis and Fatty Acid Oxidation'. *Nature Communications* 6. https://doi.org/10.1038/ncomms7692.

Patsoukis, Nikolaos, Julia Brown, Victoria Petkova, Fang Liu, Lequn Li, and Vassiliki A. Boussiotis. 2012. 'Selective Effects of PD-1 on Akt and Ras Pathways Regulate Molecular Components of the Cell Cycle and Inhibit T Cell Proliferation'. *Science Signaling* 5 (230). https://doi.org/10.1126/scisignal.2002796.

Patsoukis, Nikolaos, Jonathan S. Duke-Cohan, Apoorvi Chaudhri, Halil Ibrahim Aksoylar, Qi Wang, Asia Council, Anders Berg, Gordon J. Freeman, and Vassiliki A. Boussiotis. 2020. 'Interaction of SHP-2 SH2 Domains with PD-1 ITSM Induces PD-1 Dimerization and SHP-2 Activation'. *Communications Biology* 3 (1). https://doi.org/10.1038/s42003-020-0845-0.

Patsoukis, Nikolaos, Lequn Li, Duygu Sari, Victoria Petkova, and Vassiliki A Boussiotis. 2013. 'PD-1 Increases PTEN Phosphatase Activity While Decreasing PTEN Protein Stability by Inhibiting Casein Kinase 2. https://doi.org/10.1128/MCB.00319-13.

Patsoukis, Nikolaos, Duygu Sari, and Vassiliki A. Boussiotis. 2012. 'PD-1 Inhibits T Cell Proliferation by Upregulating P27 and P15 and Suppressing Cdc25A'. *Cell Cycle* 11 (23): 4305–9. https://doi.org/10.4161/CC.22135.

Patsoukis, Nikolaos, Qi Wang, Laura Strauss, and Vassiliki a Boussiotis. 2020. 'Revisiting the PD-1 Pathway'. *Sci. Adv* 6.

Pauken, Kristen E., and E. John Wherry. 2015. 'Overcoming T Cell Exhaustion in Infection and Cancer'. *Trends in Immunology*. https://doi.org/10.1016/j.it.2015.02.008.

Pearce, Erika L., Matthew C. Walsh, Pedro J. Cejas, Gretchen M. Harms, Hao Shen, Li San Wang, Russell G. Jones, and Yongwon Choi. 2009. 'Enhancing CD8 T-

Cell Memory by Modulating Fatty Acid Metabolism'. *Nature 2009 460:7251* 460 (7251): 103–7.
https://doi.org/10.1038/nature08097.

Peng, Weiyi, Jie Qing Chen, Chengwen Liu, Shruti Malu, Caitlin Creasy, Michael T. Tetzlaff, Chunyu Xu, et al. 2016. 'Loss of PTEN Promotes Resistance to T Cell–Mediated Immunotherapy'. *Cancer Discovery* 6 (2): 202–16.
https://doi.org/10.1158/2159-8290.CD-15-0283.

Pennington, K L, T Y Chan, • Mp Torres, and • Jl Andersen. 2018. 'The Dynamic and Stress-Adaptive Signaling Hub of 14-3-3: Emerging Mechanisms of Regulation and Context-Dependent Protein-Protein Interactions'. *Oncogene* 37: 5587–5604.
https://doi.org/10.1038/s41388-018-0348-3.

Perez-Dominguez, Francisco, Diego Carrillo-Beltrán, Rancés Blanco, Juan P Muñoz, Grettell León-Cruz, Alejandro H Corvalan, Ulises Urzúa, Gloria M Calaf, and Francisco Aguayo. 2021. 'Role of Pirin, an Oxidative Stress Sensor Protein, in Epithelial Carcinogenesis'. *Biology* 10 (116).
https://doi.org/10.3390/biology10020116.

Perillo, Bruno, Marzia Di Donato, Antonio Pezone, Erika Di Zazzo, Pia Giovannelli, Giovanni Galasso, Gabriella Castoria, and Antimo Migliaccio. 2020. 'ROS in Cancer Therapy: The Bright Side of the Moon'. *Experimental and Molecular Medicine*. Springer Nature.
https://doi.org/10.1038/s12276-020-0384-2.

Piperno-Neumann, Sophie, Marie Cécile Le Deley, Françoise Rédini, Hélène Pacquement, Perrine Marec-Bérard, Philippe Petit, Hervé Brisse, et al. 2016. 'Zoledronate in Combination with Chemotherapy and Surgery to Treat Osteosarcoma (OS2006): A Randomised, Multicentre, Open-Label, Phase 3 Trial'. *The Lancet Oncology* 17 (8): 1070–80.
https://doi.org/10.1016/S1470-2045(16)30096-1.

Ponce de León, Candelaria, Pedro Lorite, Miguel A´ngel López-Casado, Francisco Barro, Teresa Palomeque, and María Isabel Torres. 2021. 'Significance of PD1 Alternative Splicing in Celiac Disease as a Novel Source for Diagnostic and Therapeutic Target'. *Frontiers in Immunology* 12 (June).
https://doi.org/10.3389/fimmu.2021.678400.

Pu, Ning, Shanshan Gao, Hanlin Yin, Jian ang Li, Wenchuan Wu, Yuan Fang, Lei Zhang, et al. 2019. 'Cell-Intrinsic PD-1 Promotes Proliferation in Pancreatic Cancer by Targeting CYR61/CTGF via the Hippo Pathway'. *Cancer Letters* 460 (September): 42–53. https://doi.org/10.1016/j.canlet.2019.06.013.

Qian, Cheng, Yongsheng Xia, Yun Ren, Yan Yin, and Anmei Deng. 2017. 'Identification and Validation of PSAT1 as a Potential Prognostic Factor for Predicting Clinical Outcomes in Patients with Colorectal Carcinoma'. *Oncology Letters*. https://doi.org/10.3892/ol.2017.7211.

Rastogi, Sameer, Aditi Aggarwal, Akash Tiwari, and Vinod Sharma. 2018. 'Chemotherapy in Nonmetastatic Osteosarcoma: Recent Advances and Implications for Developing Countries'. *Journal of Global Oncology* 2018 (4). https://doi.org/10.1200/JGO.2016.007336.

Rathmell, Jeffrey C., Casey J. Fox, David R. Plas, Peter S. Hammerman, Ryan M. Cinalli, and Craig B. Thompson. 2003. 'Akt-Directed Glucose Metabolism Can Prevent Bax Conformation Change and Promote Growth Factor-Independent Survival'. *Molecular and Cellular Biology* 23 (20): 7315. https://doi.org/10.1128/MCB.23.20.7315-7328.2003.

Reiter, Lukas, Oliver Rinner, Paola Picotti, Ruth Hüttenhain, Martin Beck, Mi Youn Brusniak, Michael O. Hengartner, and Ruedi Aebersold. 2011. 'MProphet: Automated Data Processing and Statistical Validation for Large-Scale SRM Experiments'. *Nature Methods* 8 (5): 430–35. https://doi.org/10.1038/nmeth.1584.

Riley, James L. 2009. 'PD-1 Signaling in Primary T Cells'. *Immunological Reviews*. https://doi.org/10.1111/j.1600-065X.2009.00767.x.

Rogel, Anne, Jane E. Willoughby, Sarah L. Buchan, Henry J. Leonard, Stephen M. Thirdborough, and Aymen Al-Shamkhani. 2017. 'Akt Signaling Is Critical for Memory CD8+ T-Cell Development and Tumor Immune Surveillance'. *Proceedings of the National Academy of Sciences of the United States of America* 114 (7): E1178–87. https://doi.org/10.1073/pnas.1611299114.

Roncagalli, Romain, Michael Mingueneau, Claude Grégoire, Marie Malissen, and Bernard Malissen. 2010. 'LAT Signaling Pathology: An "Autoimmune" Condition without T Cell Self-Reactivity'. *Trends in Immunology*. https://doi.org/10.1016/j.it.2010.05.001.

Roose, Jeroen P., Marianne Mollenauer, Vikas A. Gupta, James Stone, and Arthur Weiss. 2005. 'A Diacylglycerol-Protein Kinase C-RasGRP1 Pathway Directs Ras Activation upon Antigen Receptor Stimulation of T Cells'. *Molecular and Cellular Biology* 25 (11): 4426–41. https://doi.org/10.1128/mcb.25.11.4426-4441.2005.

Rota, Giorgia, Charlène Niogret, Anh Thu Dang, Cristina Ramon Barros, Nicolas Pierre Fonta, Francesca Alfei, Leonor Morgado, et al. 2018. 'Shp-2 Is Dispensable for Establishing T Cell Exhaustion and for PD-1 Signaling In Vivo'. *Cell Reports* 23 (1): 39–49. https://doi.org/10.1016/j.celrep.2018.03.026.

Rotolo, Ramona, Valeria Leuci, Chiara Donini, Federica Galvagno, Annamaria Massa, Maria Chiara De Santis, Serena Peirone, et al. 2023. 'Novel Lymphocyte-Independent Antitumor Activity by PD-1 Blocking Antibody against PD-1+ Chemoresistant Lung Cancer Cells'. *Clinical Cancer Research: An Official Journal of the American Association for Cancer Research* 29 (3): 621–34. https://doi.org/10.1158/1078-0432.CCR-22-0761.

Rotroff, Daniel M., Rachael Thomas, Matthew Breen, and Alison A. Motsinger-Reif. 2013. 'Naturally Occuring Canine Cancers: Powerful Models for Stimulating Pharmacogenomic Advancement in Human Medicine'. *Pharmacogenomics* 14 (16): 1929–31. https://doi.org/10.2217/PGS.13.178/FORMAT/EPUB.

Rowell, Jennie L., Donna O. McCarthy, and Carlos E. Alvarez. 2011. 'Dog Models of Naturally Occurring Cancer'. *Trends in Molecular Medicine*. https://doi.org/10.1016/j.molmed.2011.02.004.

Rowshanravan, Behzad, Neil Halliday, and David M Sansom. 2018. 'Review Series THERAPEUTIC ANTIBODIES CTLA-4: A Moving Target in Immunotherapy'. Vol. 131. http://ashpublications.org/blood/article-pdf/131/1/58/1367947/blood741033.pdf.

Ruan, Guo Xiang, and Andrius Kazlauskas. 2012. 'Axl Is Essential for VEGF-A-Dependent Activation of PI3K/Akt'. *EMBO Journal* 31 (7): 1692–1703. https://doi.org/10.1038/emboj.2012.21.

Russo, Giuseppe Lo, Massimo Moro, Michele Sommariva, Valeria Cancila, Mattia Boeri, Giovanni Centonze, Simona Ferro, et al. 2019. 'Antibody-Fc/FcR Interaction on Macrophages as a Mechanism for Hyperprogressive Disease in Non-Small Cell Lung Cancer Subsequent to PD-1/PD-L1 Blockade'. *Clinical Cancer Research* 25 (3): 989–99. https://doi.org/10.1158/1078-0432.CCR-18-1390.

Sadahiro, Hirokazu, Kyung-Don Kang, Justin T Gibson, Mutsuko Minata, Hai Yu, Junfeng Shi, Rishi Chhipa, et al. 2018. 'Activation of the Receptor Tyrosine Kinase AXL Regulates the Immune Microenvironment in Glioblastoma HHS Public Access'. *Cancer Res* 78 (11): 3002–13. https://doi.org/10.1158/0008-5472.CAN-17-2433.

Safaeifard, Fateme, Bahram Goliaei, Amir R. Aref, Mohammad Hadi Foroughmand-Araabi, Sama Goliaei, Jochen Lorch, Russell W. Jenkins, David A. Barbie, Seyed Peyman Shariatpanahi, and Curzio Rüegg. 2022. 'Distinct Dynamics of Migratory Response to PD-1 and CTLA-4 Blockade Reveals New Mechanistic Insights for Potential T-Cell Reinvigoration Following Immune Checkpoint Blockade'. *Cells 2022, Vol. 11, Page 3534* 11 (22): 3534. https://doi.org/10.3390/CELLS11223534.

Sakthivel, Priya, Marcus Gereke, and Dunja Bruder. 2012. 'Therapeutic Intervention in Cancer and Chronic Viral Infections: Antibody Mediated Manipulation of PD-1/PD-L1 Interaction'. *Reviews on Recent Clinical Trials*. Vol. 7. http://globocan.iarc.fr/references.htm.

Sanlorenzo, Martina, Igor Vujic, Arianna Floris, Mauro Novelli, Loretta Gammaitoni, Lidia Giraudo, Marco Macagno, et al. 2018. 'BRAF and MEK Inhibitors Increase PD-1-Positive Melanoma Cells Leading to a Potential Lymphocyte-Independent Synergism with Anti–PD-1 Antibody'. *Clinical Cancer Research* 24 (14): 3377–85. https://doi.org/10.1158/1078-0432.CCR-17-1914/87477/AM/BRAF-AND-MEK-INHIBITORS-INCREASE-PD1-POSITIVE.

Sansom, D M. 2000. ‘CD28, CTLA-4 and Their Ligands: Who Does What and to Whom?’ *Immunology* 101: 169–77.

Saraf, A J, J M Fenger, and R D Roberts. 2017. ‘Osteosarcoma: Accelerating Progress Makes for a Hopeful Future’. *Front. Oncol* 8: 26. https://doi.org/10.3389/fonc.2018.00004.

Schatton, Tobias, George F. Murphy, Natasha Y. Frank, Kazuhiro Yamaura, Ana Maria Waaga-Gasser, Martin Gasser, Qian Zhan, et al. 2008. ‘Identification of Cells Initiating Human Melanomas’. *Nature* 451 (7176): 345–49. https://doi.org/10.1038/NATURE06489.

Schatton, Tobias, Ute Schütte, Natasha Y. Frank, Qian Zhan, André Hoerning, Susanne C. Robles, Jun Zhou, et al. 2010. ‘Modulation of T-Cell Activation by Malignant Melanoma Initiating Cells’. *Cancer Research* 70 (2): 697–708. https://doi.org/10.1158/0008-5472.CAN-09-1592.

Schiffman, Joshua D., and Matthew Breen. 2015. ‘Comparative Oncology: What Dogs and Other Species Can Teach Us about Humans with Cancer’. *Philosophical Transactions of the Royal Society B: Biological Sciences*. Royal Society of London. https://doi.org/10.1098/rstb.2014.0231.

Schönrich, Günther, and Martin J. Raftery. 2019. ‘The PD-1/PD-L1 Axis and Virus Infections: A Delicate Balance’. *Frontiers in Cellular and Infection Microbiology*. Frontiers Media S.A. https://doi.org/10.3389/fcimb.2019.00207.

Seidel, Judith A., Atsushi Otsuka, and Kenji Kabashima. 2018. ‘Anti-PD-1 and Anti-CTLA-4 Therapies in Cancer: Mechanisms of Action, Efficacy, and Limitations’. *Frontiers in Oncology*. Frontiers Media S.A. https://doi.org/10.3389/fonc.2018.00086.

Seitz, Heather M., Todd D. Camenisch, Greg Lemke, H. Shelton Earp, and Glenn K. Matsushima. 2007. ‘Macrophages and Dendritic Cells Use Different Axl/Mertk/Tyro3 Receptors in Clearance of Apoptotic Cells’. *The Journal of Immunology* 178 (9): 5635–42. https://doi.org/10.4049/JIMMUNOL.178.9.5635.

Serman, Taryn M, and Michaela U Gack. 2019. ‘FBXO38 Drives PD-1 to Destruction’. *Trends in Immunology* 40 (2): 81–83. https://doi.org/10.1016/j.it.2018.12.005.

Shaffer, Lisa G. 2019. ‘Special Issue on Canine Genetics: Animal Models for Human Disease and Gene Therapies, New Discoveries for Canine Inherited Diseases, and Standards and Guidelines for Clinical Genetic Testing for Domestic Dogs’. *Human Genetics 2019 138:5* 138 (5): 437–40. https://doi.org/10.1007/S00439-019-02025-5.

Shah, Kinjal, Amr Al-Haidari, Jianmin Sun, and Julhash U. Kazi. 2021. ‘T Cell Receptor (TCR) Signaling in Health and Disease’. *Signal Transduction and Targeted Therapy*. Springer Nature. https://doi.org/10.1038/s41392-021-00823-w.

Shao, Hanshuang, Diana Teramae, and Alan Wells. 2023. ‘Axl Contributes to Efficient Migration and Invasion of Melanoma Cells’. *PloS One* 18 (3). https://doi.org/10.1371/JOURNAL.PONE.0283749.

Shen, Jacson K., Gregory M. Cote, Edwin Choy, Pei Yang, David Harmon, Joseph Schwab, G. Petur Nielsen, et al. 2014. ‘Programmed Cell Death Ligand 1 Expression in Osteosarcoma’. *Cancer Immunology Research* 2 (7): 690–98. https://doi.org/10.1158/2326-6066.CIR-13-0224.

Shen, Pan, Liang Han, Xin Ba, Kai Qin, and Shenghao Tu. 2021. ‘Hyperprogressive Disease in Cancers Treated with Immune Checkpoint Inhibitors’. *Frontiers in Pharmacology*. Frontiers Media S.A. https://doi.org/10.3389/fphar.2021.678409.

Sheppard, Kelly Ann, Lori J. Fitz, Julie M. Lee, Christina Benander, Judith A. George, Joe Wooters, Yongchang Qiu, et al. 2004. ‘PD-1 Inhibits T-Cell Receptor Induced Phosphorylation of the ZAP70/CD3ζ Signalosome and Downstream Signaling to PKCθ’. *FEBS Letters* 574 (1–3): 37–41. https://doi.org/10.1016/J.FEBSLET.2004.07.083.

Shteynberg, David, Eric W Deutsch, Henry Lam, Jimmy K Eng, Zhi Sun, Natalie Tasman, Luis Mendoza, Robert L Moritz, Ruedi Aebersold, and Alexey I Nesvizhskii. 2011. ‘IProphet: Multi-Level Integrative Analysis of Shotgun Proteomic Data Improves Peptide and Protein Identification Rates and Error

Estimates* □ S Technological Innovation and Resources. https://doi.org/10.1074/mcp.M111.007690.

Shyer, Justin A., Richard A. Flavell, and Will Bailis. 2020. 'Metabolic Signaling in T Cells'. *Cell Research 2020 30:8* 30 (8): 649–59. https://doi.org/10.1038/s41422-020-0379-5.

Simpson, Siobhan, Mark David Dunning, Simone de Brot, Llorenç Grau-Roma, Nigel Patrick Mongan, and Catrin Sian Rutland. 2017. 'Comparative Review of Human and Canine Osteosarcoma: Morphology, Epidemiology, Prognosis, Treatment and Genetics'. *Acta Veterinaria Scandinavica* 59 (1): 71. https://doi.org/10.1186/s13028-017-0341-9.

Spruck, Charles H., and Heimo M. Strohmaier. 2002. 'Seek and Destroy: SCF Ubiquitin Ligases in Mammalian Cell Cycle Control.' *Cell Cycle (Georgetown, Tex.)*. https://doi.org/10.4161/cc.1.4.132.

Strazza, Marianne, Kieran Adam, Shalom Lerrer, Johanna Straube, Sabina Sandigursky, Beatrix Ueberheide, and Adam Mor. 2021. 'SHP2 Targets ITK Downstream of PD-1 to Inhibit T Cell Function'. *Inflammation* 44 (4): 1529–39. https://doi.org/10.1007/s10753-021-01437-8.

Sul, Joohee, Gideon M. Blumenthal, Xiaoping Jiang, Kun He, Patricia Keegan, and Richard Pazdur. 2016. 'FDA Approval Summary: Pembrolizumab for the Treatment of Patients with Metastatic Non-Small Cell Lung Cancer Whose Tumors Express Programmed Death-Ligand 1'. *The Oncologist* 21 (5): 643–50. https://doi.org/10.1634/THEONCOLOGIST.2015-0498/-/DC1.

Sun, Linlin, Chia-Wei Li, Ezra M Chung, Riyao Yang, Yong-Soo Kim, Andrew H Park, Yun-Ju Lai, et al. 2020. 'Targeting Glycosylated PD-1 Induces Potent Anti-Tumor Immunity HHS Public Access'. *Cancer Res* 80 (11): 2298–2310. https://doi.org/10.1158/0008-5472.CAN-19-3133.

Synn, Chun Bong, Sung Eun Kim, Hee Kyu Lee, Min Hwan Kim, Jae Hwan Kim, Ji Min Lee, Ha Ni Jo, et al. 2022. 'SKI-G-801, an AXL Kinase Inhibitor, Blocks Metastasis through Inducing Anti-Tumor Immune Responses and Potentiates Anti-PD-1 Therapy in Mouse Cancer Models'. *Clinical and Translational Immunology* 11 (1).

https://doi.org/10.1002/cti2.1364.

Szklarczyk, Damian, Andrea Franceschini, Stefan Wyder, Kristoffer Forslund, Davide Heller, Jaime Huerta-Cepas, Milan Simonovic, et al. 2014. 'STRING V10: Protein-Protein Interaction Networks, Integrated over the Tree of Life'. *Nucleic Acids Research* 43: 447–52.

https://doi.org/10.1093/nar/gku1003.

Tai, K. Y., Y. S. Shieh, C. S. Lee, S. G. Shiah, and C. W. Wu. 2008. 'Axl Promotes Cell Invasion by Inducing MMP-9 Activity through Activation of NF-KB and Brg-1'. *Oncogene* 27 (29): 4044–55.

https://doi.org/10.1038/onc.2008.57.

Takahara, Terunao, Yuna Amemiya, Risa Sugiyama, Masatoshi Maki, and Hideki Shibata. 2020. 'Amino Acid-Dependent Control of MTORC1 Signaling: A Variety of Regulatory Modes'. *Journal of Biomedical Science*.

https://doi.org/10.1186/s12929-020-00679-2.

Tanaka, Mai, and Dietmar W Siemann. 2019. 'Axl Signaling Is an Important Mediator of Tumor Angiogenesis'. *Oncotarget* 10 (30): 2887–98. www.oncotarget.com.

Tang, Pingtao, Chunzhang Cao, Min Xu, and Li Zhang. 2007. 'Cytoskeletal Protein Radixin Activates Integrin a M b 2 by Binding to Its Cytoplasmic Tail.

https://doi.org/10.1016/j.febslet.2007.02.013.

Tang, Yaoxiang, Hongjing Zang, Qiuyuan Wen, and Songqing Fan. 2023. 'AXL in Cancer: A Modulator of Drug Resistance and Therapeutic Target'. *Journal of Experimental & Clinical Cancer Research: CR* 42 (1).

https://doi.org/10.1186/S13046-023-02726-W.

Tawbi, Hussein A., Melissa Burgess, Vanessa Bolejack, Brian A. Van Tine, Scott M. Schuetze, James Hu, Sandra D'Angelo, et al. 2017. 'Pembrolizumab in Advanced Soft-Tissue Sarcoma and Bone Sarcoma (SARC028): A Multicentre, Two-Cohort, Single-Arm, Open-Label, Phase 2 Trial'. *The Lancet Oncology* 18 (11): 1493–1501.

https://doi.org/10.1016/S1470-2045(17)30624-1.

Terry, Stéphane, Cécile Dalban, Nathalie Rioux-Leclercq, Julien Adam, Maxime Meylan, Stéphanie Buart, Antoine Bougoüin, et al. 2021. 'Association of AXL and PD-L1 Expression with Clinical Outcomes in Patients with Advanced Renal Cell

Carcinoma Treated with PD-1 Blockade'. *Clinical Cancer Research: An Official Journal of the American Association for Cancer Research* 27 (24): 6749–60. https://doi.org/10.1158/1078-0432.CCR-21-0972.

Tian, Yaqiong, Zengli Zhang, Liyun Miao, Zhimin Yang, Jie Yang, Yinhua Wang, Danwen Qian, Hourong Cai, and Yongsheng Wang. 2016. 'Anexelekto (AXL) Increases Resistance to EGFR-TKI and Activation of AKT and ERK1/2 in Non-Small Cell Lung Cancer Cells'. *Oncology Research* 24 (5): 295–303. https://doi.org/10.3727/096504016X14648701447814.

Timmerbeul, Inke, Carrie M. Garrett-Engele, Uta Kossatz, Xueyan Chen, Eduardo Firpo, Viktor Grünwald, Kenji Kamino, et al. 2006. 'Testing the Importance of P27 Degradation by the SCFskp2 Pathway in Murine Models of Lung and Colon Cancer'. *Proceedings of the National Academy of Sciences of the United States of America* 103 (38): 14009–14. https://doi.org/10.1073/PNAS.0606316103/ASSET/4E843963-4968-4E82-AC55-F54A16B3105A/ASSETS/GRAPHIC/ZPQ0360634130004.JPEG.

Tivol, Elizabeth A, Frank Borriello, A Nicola Schweitzer, Wllllam P Lynch, Jeffrey A Bluestone, and Arlene H Sharpe. 1995. 'Loss of CTLA-4 Leads to Massive Lymphoproliferation and Fatal Multiorgan Tissue Destruction, Revealing a Critical Negative Regulatory Role of CTLA-4'. *Immunity* 3: 541–47.

Toomer, Kevin H. 2016. 'Related Content MTOR Complex 1 Signaling Regulates the Generation and Function of Central and Effector Foxp3 + Regulatory T Cells IL-6 and ICOS Antagonize Bim and Promote Regulatory T Cell Accrual with Age Requirement for CD28 in Effector Regulatory T Cell Differentiation, CCR6 Induction, and Skin Homing'. *J Immunol* 196 (9): 3665–76. https://doi.org/10.4049/jimmunol.1500595.

Topalian, Suzanne L., Charles G. Drake, and Drew M. Pardoll. 2012. 'Targeting the PD-1/B7-H1(PD-L1) Pathway to Activate Anti-Tumor Immunity'. *Current Opinion in Immunology*. https://doi.org/10.1016/j.coi.2011.12.009.

Torabi, Alireza, Clarissa N. Amaya, Frank H. Wians, and Brad A. Bryan. 2017. 'PD-1 and PD-L1 Expression in Bone and Soft Tissue Sarcomas'. *Pathology* 49 (5): 506–13.

https://doi.org/10.1016/j.pathol.2017.05.003.

Torres, Josema, and Rafael Pulido. 2001. 'The Tumor Suppressor PTEN Is Phosphorylated by the Protein Kinase CK2 at Its C Terminus. Implications for PTEN Stability to Proteasome-Mediated Degradation'. *Journal of Biological Chemistry* 276 (2): 993–98.

https://doi.org/10.1074/jbc.M009134200.

Trajanoski, Zlatko, Loredana Ruggeri, Manel Juan, Charles Dumontet, Morgane Denis, Michael Duruisseaux, and Marie Brevet. 2020. 'Article 492 (2020) How Can Immune Checkpoint Inhibitors Cause Hyperprogression in Solid Tumors?' *Front. Immunol* 11: 492.

https://doi.org/10.3389/fimmu.2020.00492.

Tsou, Wen-I, Khanh-Quynh N Nguyen, Daniel A Calarese, Scott J Garforth, Anita L Antes, Sergey V Smirnov, Steve C Almo, Raymond B Birge, and Sergei V Kotenko. 2014. 'Receptor Tyrosine Kinases, TYRO3, AXL, and MER, Demonstrate Distinct Patterns and Complex Regulation of Ligand-Induced Activation.

https://doi.org/10.1074/jbc.M114.569020.

Tsukita, Yoko, Naoya Fujino, Eisaku Miyauchi, Ryoko Saito, Fumiyoshi Fujishima, Koji Itakura, Yorihiko Kyogoku, et al. 2019. 'Axl Kinase Drives Immune Checkpoint and Chemokine Signalling Pathways in Lung Adenocarcinomas'. *Molecular Cancer* 18 (1).

https://doi.org/10.1186/s12943-019-0953-y.

Tsvetkov, Lyuben M., Kun Huei Yeh, Soo Jung Lee, Hong Sun, and Hui Zhang. 1999. 'P27(Kip1) Ubiquitination and Degradation Is Regulated by the SCF(Skp2) Complex through Phosphorylated Thr187 in P27'. *Current Biology* 9 (12): 661–64.

https://doi.org/10.1016/S0960-9822(99)80290-5.

Tumeh, Paul C., Christina L. Harview, Jennifer H. Yearley, I. Peter Shintaku, Emma J.M. Taylor, Lidia Robert, Bartosz Chmielowski, et al. 2014. 'PD-1 Blockade Induces Responses by Inhibiting Adaptive Immune Resistance'. *Nature* 515 (7528): 568–71.

https://doi.org/10.1038/nature13954.

Twomey, Julianne D., and Baolin Zhang. 2021. ‘Cancer Immunotherapy Update: FDA-Approved Checkpoint Inhibitors and Companion Diagnostics’. *AAPS Journal* 23 (2): 1–11. https://doi.org/10.1208/S12248-021-00574-0/FIGURES/2.

Vaupel, Peter, and Gabriele Multhoff. 2021. ‘Revisiting the Warburg Effect: Historical Dogma versus Current Understanding’. *Journal of Physiology*. https://doi.org/10.1113/JP278810.

Veluswamy, Rajwanth, Sheena Bhalla, Ranee Mehra, Marina Chiara Garassino, Oleg Gligich, Cristina Oliva, Claudia Gorcea-Carson, and Nigel William McCracken. 2023. ‘Phase 1b/2a Safety and Tolerability Study of Bemcentinib (BEM) with Pembrolizumab/Carboplatin/Pemetrexed in First Line (1L) Advanced or Metastatic Non-Squamous Non-Small Cell Lung Cancer (NSCLC) without/with a STK11 Mutation. *Https://Doi.Org/10.1200/JCO.2023.41.16_suppl.TPS9154* 41 (16_suppl): TPS9154–TPS9154. https://doi.org/10.1200/JCO.2023.41.16_SUPPL.TPS9154.

Vié, Nadia, Virginie Copois, Caroline Bascoul-Mollevi, Vincent Denis, Nicole Bec, Bruno Robert, Caroline Fraslon, et al. 2008. ‘Overexpression of Phosphoserine Aminotransferase PSAT1 Stimulates Cell Growth and Increases Chemoresistance of Colon Cancer Cells’. *Molecular Cancer* 7: 1–14. https://doi.org/10.1186/1476-4598-7-14.

Visekruna, Alexander, Anton Volkov, and Ulrich Steinhoff. 2012. ‘A Key Role for NF-KB Transcription Factor c-Rel in T-Lymphocyte-Differentiation and Effector Functions’. *Clinical and Developmental Immunology* 2012. https://doi.org/10.1155/2012/239368.

Vouri, M., D. R. Croucher, S. P. Kennedy, Q. An, G. J. Pilkington, and S. Hafizi. 2016. ‘Axl-EGFR Receptor Tyrosine Kinase Hetero-Interaction Provides EGFR with Access to pro-Invasive Signalling in Cancer Cells’. *Oncogenesis* 5 (10): e266. https://doi.org/10.1038/ONCSIS.2016.66.

Vu, Binh Thanh, Sophia Allaf Shahin, Jonas Croissant, Yevhen Fatieiev, Kotaro Matsumoto, Tan Le-Hoang Doan, Tammy Yik, et al. 2018. ‘Chick Chorioallantoic Membrane Assay as an in Vivo Model to Study the Effect of Nanoparticle-Based

Anticancer Drugs in Ovarian Cancer'. *Scientific Reports 2018 8:1* 8 (1): 1–10. https://doi.org/10.1038/s41598-018-25573-8.

Waickman, Adam T., and Jonathan D. Powell. 2012. 'Mammalian Target of Rapamycin Integrates Diverse Inputs to Guide the Outcome of Antigen Recognition in T Cells'. *The Journal of Immunology* 188 (10): 4721–29. https://doi.org/10.4049/jimmunol.1103143.

Walewska, Magdalena, Izabella Dolka, Anna Małek, Anna Wojtalewicz, Agata Wojtkowska, Artur Żbikowski, Roman Lechowski, and Katarzyna Zabielska-Koczywąs. 2017. 'Experimental Tumor Growth of Canine Osteosarcoma Cell Line on Chick Embryo Chorioallantoic Membrane (in Vivo Studies)'. *Acta Veterinaria Scandinavica* 59 (1): 30. https://doi.org/10.1186/s13028-017-0298-8.

Wang, Huijuan, Longzhen Cui, Dandan Li, Ming Fan, Zhangnan Liu, Chunqi Liu, Sijing Pan, Lei Zhang, Hailong Zhang, and Yinglan Zhao. 2020. 'Overexpression of PSAT1 Regulated by G9A Sustains Cell Proliferation in Colorectal Cancer'. *Signal Transduction and Targeted Therapy* 5 (1): 2019–21. https://doi.org/10.1038/s41392-020-0147-5.

Wang, Kaiyuan, Yun Gu, Yihan Liao, Sangsu Bang, Christopher R. Donnelly, Ouyang Chen, Xueshu Tao, Anthony J. Mirando, Matthew J. Hilton, and Ru Rong Ji. 2020. 'PD-1 Blockade Inhibits Osteoclast Formation and Murine Bone Cancer Pain'. *Journal of Clinical Investigation* 130 (7): 3603–20. https://doi.org/10.1172/JCI133334.

Wang, Xiaodong, Xiaohui Yang, Chang Zhang, Yang Wang, Tianyou Cheng, Liqiang Duan, Zhou Tong, et al. 2020. 'Tumor Cell-Intrinsic PD-1 Receptor Is a Tumor Suppressor and Mediates Resistance to PD-1 Blockade Therapy'. *Proceedings of the National Academy of Sciences of the United States of America* 117 (12): 6640–50. https://doi.org/10.1073/PNAS.1921445117/SUPPL_FILE/PNAS.1921445117.SAPP.PDF.

Wang, Yitian, Wei Yu, Jian Zhu, Junjie Wang, Kaishun Xia, Chengzhen Liang, and Huimin Tao. 2019. 'Anti-CD166/4-1BB Chimeric Antigen Receptor T Cell Therapy

for the Treatment of Osteosarcoma'. *Journal of Experimental & Clinical Cancer Research* 38 (168). https://doi.org/10.1186/s13046-019-1147-6.

Wang, Zenan, Zhan Wang, Binghao Li, Shengdong Wang, Tao Chen, and Zhaoming Ye. 2019. 'Innate Immune Cells: A Potential and Promising Cell Population for Treating Osteosarcoma'. *Frontiers in Immunology* 10 (MAY): 1114. https://doi.org/10.3389/FIMMU.2019.01114.

Wang, Zilong, Changyu Jiang, Qianru He, Megumi Matsuda, Qingjian Han, Kaiyuan Wang, Sangsu Bang, Huiping Ding, Mei Chuan Ko, and Ru Rong Ji. 2020. 'Anti-PD-1 Treatment Impairs Opioid Antinociception in Rodents and Nonhuman Primates'. *Science Translational Medicine* 12 (531). https://doi.org/10.1126/SCITRANSLMED.AAW6471.

Wartewig, Tim, Zsuzsanna Kurgyis, Selina Keppler, Konstanze Pechloff, Erik Hameister, Rupert Öllinger, Roman Maresch, et al. 2017. 'PD-1 Is a Haploinsufficient Suppressor of T Cell Lymphomagenesis'. *Nature* 552 (7683): 121–25. https://doi.org/10.1038/nature24649.

Wartewig, Tim, and Jürgen Ruland. 2019. 'PD-1 Tumor Suppressor Signaling in T Cell Lymphomas'. *Trends in Immunology*. https://doi.org/10.1016/j.it.2019.03.005.

Weber, Jeffrey S., Sandra P. D'Angelo, David Minor, F. Stephen Hodi, Ralf Gutzmer, Bart Neyns, Christoph Hoeller, et al. 2015. 'Nivolumab versus Chemotherapy in Patients with Advanced Melanoma Who Progressed after Anti-CTLA-4 Treatment (CheckMate 037): A Randomised, Controlled, Open-Label, Phase 3 Trial'. *The Lancet Oncology* 16 (4): 375–84. https://doi.org/10.1016/S1470-2045(15)70076-8.

Wei, Fang, Shi Zhong, Zhengyu Ma, Hong Kong, Andrew Medvec, Rafi Ahmed, Gordon J. Freeman, Michelle Krogsgaard, and James L. Riley. 2013. 'Strength of PD-1 Signaling Differentially Affects T-Cell Effector Functions'. *Proceedings of the National Academy of Sciences of the United States of America* 110 (27). https://doi.org/10.1073/pnas.1305394110.

Wei, Qiou, Hong Jiang, Connie P Matthews, and Nancy H Colburn. 2008. 'Sulfiredoxin Is an AP-1 Target Gene That Is Required for Transformation and Shows Elevated Expression in Human Skin Malignancies'. www.pnas.org/cgi/content/full/.

Weinberg, Robert A. 1995. 'The Retinoblastoma Protein and Cell Cycle Control'. *Cell* 81 (3): 323–30.
https://doi.org/10.1016/0092-8674(95)90385-2.

Weinger, Jason G, Celia F Brosnan, Olivier Loudig, Michael F Goldberg, Fernando Macian, Heather A Arnett, Anne L Prieto, Vladislav Tsiperson, and Bridget Shafit-Zagardo. 2011. 'Loss of the Receptor Tyrosine Kinase Axl Leads to Enhanced Inflammation in the CNS and Delayed Removal of Myelin Debris during Experimental Autoimmune Encephalomyelitis'. *Journal of Neuroinflammation* 8: 49.
https://doi.org/10.1186/1742-2094-8-49.

Wiśniewski, Jacek R., Alexandre Zougman, Nagarjuna Nagaraj, and Matthias Mann. 2009. 'Universal Sample Preparation Method for Proteome Analysis'. *Nature Methods* 6 (5): 359–62.
https://doi.org/10.1038/nmeth.1322.

Wiza, Claudia, Emmani B.M. Nascimento, and D. Margriet Ouwens. 2012. 'Role of PRAS40 in Akt and MTOR Signaling in Health and Disease'. *American Journal of Physiology. Endocrinology and Metabolism* 302 (12).
https://doi.org/10.1152/AJPENDO.00660.2011.

Wong, Gabriel K., James M. Heather, Sara Barmettler, and Mark Cobbold. 2017. 'Immune Dysregulation in Immunodeficiency Disorders: The Role of T-Cell Receptor Sequencing'. *Journal of Autoimmunity*. Academic Press.
https://doi.org/10.1016/j.jaut.2017.04.002.

Wu, Guangyong, Devin W M C Bride, and John H Zhang. 2017. 'Axl Activation Attenuates Neuroinflammation by Inhibiting the TLR/TRAF/ NF-KB Pathway after MCAO in Rats'.
https://doi.org/10.1016/j.nbd.2017.11.009.

Wu, Qing, Wei Qian, Xiaoli Sun, and Shaojie Jiang. 2022. 'Small-Molecule Inhibitors, Immune Checkpoint Inhibitors, and More: FDA-Approved Novel Therapeutic

Drugs for Solid Tumors from 1991 to 2021'. *Journal of Hematology & Oncology* 15 (1).
https://doi.org/10.1186/S13045-022-01362-9.

Wu, Tianzhi, Erqiang Hu, Shuangbin Xu, Meijun Chen, Pingfan Guo, Zehan Dai, Tingze Feng, et al. 2021. 'ClusterProfiler 4.0: A Universal Enrichment Tool for Interpreting Omics Data'. *The Innovation* 2 (3).
https://doi.org/10.1016/j.xinn.2021.100141.

Xia, An Liang, Jin Cheng Wang, Kun Yang, Dong Ji, Zheng Ming Huang, and Yong Xu. 2019. 'Genomic and Epigenomic Perspectives of T-Cell Exhaustion in Cancer'. *Briefings in Functional Genomics* 18 (2): 113–18.
https://doi.org/10.1093/bfgp/ely005.

Xiang, Xiaonan, Jianguo Wang, Di Lu, and Xiao Xu. 2021. 'Targeting Tumor-Associated Macrophages to Synergize Tumor Immunotherapy'. *Signal Transduction and Targeted Therapy*.
https://doi.org/10.1038/s41392-021-00484-9.

Yan, Yumeng, Huanyu Tao, Jiahua He, and Sheng You Huang. 2020. 'The HDOCK Server for Integrated Protein–Protein Docking'. *Nature Protocols 2020 15:5* 15 (5): 1829–52.
https://doi.org/10.1038/s41596-020-0312-x.

Yang, Fang, Jacqueline F. Wang, Yucai Wang, Baorui Liu, and Julian R. Molina. 2022. 'Comparative Analysis of Predictive Biomarkers for Pd-1/Pd-L1 Inhibitors in Cancers: Developments and Challenges'. *Cancers*. MDPI.
https://doi.org/10.3390/cancers14010109.

Yang, Yi, Jueheng Wu, Junchao Cai, Zhenjian He, Jie Yuan, Xun Zhu, Yanbing Li, Mengfeng Li, and Hongyu Guan. 2015. 'PSAT1 Regulates Cyclin D1 Degradation and Sustains Proliferation of Non-Small Cell Lung Cancer Cells'. *International Journal of Cancer* 136 (4): E39–50.
https://doi.org/10.1002/ijc.29150.

Yao, Han, Huanbin Wang, Chushu Li, Jing Yuan Fang, and Jie Xu. 2018. 'Cancer Cell-Intrinsic PD-1 and Implications in Combinatorial Immunotherapy'. *Frontiers in Immunology*. Frontiers Media S.A.
https://doi.org/10.3389/fimmu.2018.01774.

Yeo, Xun Hui, Vignesh Sundararajan, Zhengwei Wu, Zi Jin, Cheryl Phua, Yin Ying Ho, Kai Lay, et al. 2023. 'The Effect of Inhibition of Receptor Tyrosine Kinase AXL on DNA Damage Response in Ovarian Cancer'. *Communications Biology* 6 (660). https://doi.org/10.1038/s42003-023-05045-0.

Yoshimura, Akihiro, Tadaaki Yamada, Masakuni Serizawa, Hisanori Uehara, Keiko Tanimura, Yusuke Okuma, Akito Fukuda, et al. 2023. 'High Levels of AXL Expression in Untreated EGFR-Mutated Non-Small Cell Lung Cancer Negatively Impacts the Use of Osimertinib'. *Cancer Science* 114 (2): 606–18. https://doi.org/10.1111/CAS.15608.

Yukawa, Masashi, Sajjeev Jagannathan, Sushmitha Vallabh, Andrey V. Kartashov, Xiaoting Chen, Matthew T. Weirauch, and Artem Barski. 2020. 'AP-1 Activity Induced by Co-Stimulation Is Required for Chromatin Opening during T Cell Activation'. *Journal of Experimental Medicine* 217 (1). https://doi.org/10.1084/jem.20182009.

Zamani, Mohammad Reza, Saeed Aslani, Arash Salmaninejad, Mohammad Reza Javan, and Nima Rezaei. 2016. 'PD-1/PD-L and Autoimmunity: A Growing Relationship'. *Cellular Immunology*. https://doi.org/10.1016/j.cellimm.2016.09.009.

Zdzalik-Bielecka, Daria, Agata Poswiata, Kamila Kozik, Kamil Jastrzebski, Kay Oliver Schink, Marta Brewinska-Olchowik, Katarzyna Piwocka, Harald Stenmark, and Marta Miaczynska. 2021. 'The GAS6-AXL Signaling Pathway Triggers Actin Remodeling That Drives Membrane Ruffling, Macropinocytosis, and Cancer-Cell Invasion'. *Proceedings of the National Academy of Sciences of the United States of America* 118 (28). https://doi.org/10.1073/PNAS.2024596118/-/DCSUPPLEMENTAL.

Zha, Haoran, Ying Jiang, Xi Wang, Jin Shang, Ning Wang, Lei Yu, Wei Zhao, et al. 2021. 'Non-Canonical PD-1 Signaling in Cancer and Its Potential Implications in Clinic'. *Journal for ImmunoTherapy of Cancer* 9: 1230. https://doi.org/10.1136/jitc-2020-001230.

Zhang, Xuewu, Jean Claude D. Schwartz, Steven C. Almo, and Stanley G. Nathenson. 2003. 'Crystal Structure of the Receptor-Binding Domain of Human B7-2: Insights into Organization and Signaling. *Proceedings of the National Academy of*

Sciences of the United States of America 100 (5): 2586–91. https://doi.org/10.1073/PNAS.252771499.

Zhang, Ya, Jingqing Yang, Na Zhao, Cao Wang, Santosh Kamar, Yonghong Zhou, Zewei He, et al. 2018. 'Progress in the Chemotherapeutic Treatment of Osteosarcoma'. *Oncology Letters* 16 (5): 6228. https://doi.org/10.3892/OL.2018.9434.

Zhang, Yiqun, Jiajia Li, Xuhui Dong, Dan Meng, Xiuling Zhi, Lei Yuan, and Liangqing Yao. 2020. 'Psat1 Regulated Oxidation-Reduction Balance Affects the Growth and Prognosis of Epithelial Ovarian Cancer'. *OncoTargets and Therapy* 13: 5443–53. https://doi.org/10.2147/OTT.S250066.

Zhang, Yuting, Xianyong Chen, Hongmei Zheng, Yuting Zhan, Jiadi Luo, Yang Yang, Yue Ning, Haihua Wang, Weiyuan Wang, and Songqing Fan. 2021. 'Expression of Cancer Cell-Intrinsic PD-1 Associates with PD-L1 and p-S6 and Predicts a Good Prognosis in Nasopharyngeal Carcinoma'. *Journal of Cancer* 12 (20): 6118–25. https://doi.org/10.7150/JCA.60739.

Zhang, Zeng, Xin Tan, Zengxin Jiang, Hao Wang, and Hengfeng Yuan. 2022. 'Immune Checkpoint Inhibitors in Osteosarcoma: A Hopeful and Challenging Future'. *Frontiers in Pharmacology*. https://doi.org/10.3389/fphar.2022.1031527.

Zhao, Junli, Alexus Roberts, Zilong Wang, Justin Savage, and Ru Rong Ji. 2021. 'Emerging Role of PD-1 in the Central Nervous System and Brain Diseases'. *Neuroscience Bulletin* 37 (8): 1188–1202. https://doi.org/10.1007/S12264-021-00683-Y.

Zhao, Xin, Qirui Wu, Xiuqing Gong, Jinfeng Liu, and Yujie Ma. 2021. 'Osteosarcoma: A Review of Current and Future Therapeutic Approaches'. *BioMedical Engineering Online* 20 (1): 1–14. https://doi.org/10.1186/S12938-021-00860-0/FIGURES/1.

Zhao, Ye, Nikita Lykov, and Chimeng Tzeng. 2022. 'Talin-1 Interaction Network in Cellular Mechanotransduction (Review)'. *International Journal of Molecular Medicine*. Spandidos Publications.

https://doi.org/10.3892/ijmm.2022.5116.

Zhi, Jingtai, Jiaoyu Yi, Xiukun Hou, Wei Wang, Weiwei Yang, Linfei Hu, Jianfeng Huang, et al. 2022. ‘Targeting SHP2 Sensitizes Differentiated Thyroid Carcinoma to the MEK Inhibitor’. *American Journal of Cancer Research* 12 (1): 247. /pmc/articles/PMC8822290/.

Zhou, Jeff X., Chang Hoon Lee, Chen Feng Qi, Hongsheng Wang, Zohreh Naghashfar, Sadia Abbasi, and Herbert C. Morse. 2009. ‘IFN Regulatory Factor 8 Regulates MDM2 in Germinal Center B Cells’. *Journal of Immunology (Baltimore, Md.: 1950)* 183 (5): 3188–94. https://doi.org/10.4049/JIMMUNOL.0803693.

Zhu, Chenjing, Yuquan Wei, and Xiawei Wei. 2019. ‘AXL Receptor Tyrosine Kinase as a Promising Anti-Cancer Approach: Functions, Molecular Mechanisms and Clinical Applications’. *Molecular Cancer 2019 18:1* 18 (1): 1–22. https://doi.org/10.1186/S12943-019-1090-3.

Zhu, Shudong, Hui Wang, Kamakshi Ranjan, and Dianzheng Zhang. 2023. ‘Regulation, Targets and Functions of CSK. https://doi.org/10.3389/fcell.2023.1206539.